uOttawa

L'Université canadienne
Canada's university

FACULTÉ DES ÉTUDES SUPÉRIEURES ET POSTOCTORALES

uOttawa

L'Université canadienne
Canada's university

FACULTY OF GRADUATE AND POSDOCTORAL STUDIES

Dina Shafey

AUTEUR DE LA THÈSE / AUTHOR OF THESIS

Ph.D. (Cellular and Molecular Medicine)

GRADE / DEGREE

Department of Cellular and Molecular Medicine

FACULTÉ, ÉCOLE, DÉPARTEMENT / FACULTY, SCHOOL, DEPARTMENT

The Role of Smn on Moterneuron/muscle Unit Function and on Mouse Embryonic Development

TITRE DE LA THÈSE / TITLE OF THESIS

Rashmi Kothary

DIRECTEUR (DIRECTRICE) DE LA THÈSE / THESIS SUPERVISOR

CO-DIRECTEUR (CO-DIRECTRICE) DE LA THÈSE / THESIS CO-SUPERVISOR

EXAMINATEURS (EXAMINATRICES) DE LA THÈSE / THESIS EXAMINERS

Louise Simard

Jocelyn Côté

Dennis Bulman

Martin Holcik

Gary W. Slater

Le Doyen de la Faculté des études supérieures et postdoctorales / Dean of the Faculty of Graduate and Postdoctoral Studies

The role of Smn on motorneuron/muscle unit function and on mouse embryonic development.

Dina Shafey

Thesis submitted to the
Faculty of Graduate and Postgraduate Studies
In partial fulfillment of the requirements
For the Ph.D. degree in
Cellular and Molecular Medicine

Department of Cellular and Molecular Medicine
Faculty of Medicine
University of Ottawa

Your file Votre référence
ISBN: 978-0-494-41645-7
Our file Notre référence
ISBN: 978-0-494-41645-7

ABSTRACT

Spinal muscular atrophy (SMA) is a devastating childhood neurodegenerative disorder characterized by the degeneration of the alpha-motor neurons in the spinal cord. The loss of these neurons causes proximal, symmetrical limb and trunk muscle weakness that progresses to paralysis and ultimately to death. The disease causing protein in SMA is called survival motor neuron (SMN). SMA is a disease with ranging severity. Disease severity is inversely related to the amount of SMN a patient produces. Thus SMA is a dose-dependent disease.

To gain a better understanding of the pathogenesis of SMA and this dose-dependent effect, we have used short interference RNA (siRNA) to selectively reduce SMN expression in cell culture and transgenic mice. Knockdown of SMN protein levels affects properties of cells in culture and mice during embryonic development. We have observed decreased number of nuclear gems (gemini of coiled bodies), reduced proliferation with no increase in cell death, defects in myoblast fusion, and malformed myotubes in SMN depleted C2C12 cells.

In parallel, using shRNA vectors, we have developed knockdown mice. These intermediate SMA models, along with existing severe and mild SMA models, were used to assess neuronal development. We investigated the morphology and differentiation of neurosphere-derived neural stem cells (NSCs) generated from the brains of *Smn*$^{+/-}$ (mild) and *Smn*$^{-/-}$;*SMN2* (severe) SMA mice. Neurospheres from the severe mice produced NSCs with increased proliferation during growth and differentiation. These cells produced fewer TuJ1-positive neuronal cells, which displayed morphological alterations and had fewer and shorter neurites. In embryos

from the severe model, but not the mild model, we observed a significantly altered morphology of cranial nerves IX and X, which appeared to be partially fused.

Lastly, to better understand why Smn depletion preferentially affects neurons and muscle, we have used Tandem Affinity Purification to identify Smn complexes from muscle-like and neuronal-like cells. We have identified cell-specific and stage-specific Smn-interacting proteins, which will help us to better understand the diverse functions of Smn.

Altogether, our studies have helped identify the possibility of specific roles for SMN in different cell types; the function of these roles is dependent on the dosage of SMN; and this dosage requirement leads to roles for SMN during development and maintenance of neurons and muscle.

ACKNOWLEDGEMENTS

I would like to begin by thanking my supervisor, Dr. Rashmi Kothary. I feel very lucky to have had a supervisor who is so supportive and encouraging. Thanks for making me feel that I can accomplish anything.

Thanks must go to my supervisory committee members, Dr. Robin Parks, Dr. Jocelyn Côté and Dr. Chris Kennedy for their suggestions and advice throughout my graduate studies.

I would like to thank both current and past Kothary lab members for helpful discussions. More specifically, I'd like to thank Yves De Repentigny for taking care of my mice; Bruno Pinheiro for helping dissect my mice; and Hong Liu for lending me her wonderful thesis. I also thank Karen Lee, Bruno Pinheiro, Ariane Beauvais, Carrie Anderson, and Mélissa Bowerman for making these past few years in the lab a fun and enjoyable place to work.

I would like to thank Dr. Alex MacKenzie, Dan Kaplansky, Shannon Hayward-McClelland, Lucie Hyde, Lily Lin, Dr. Douglas Kerr, and Tara Martinez for collaborations. I would also like to thank Dr. Iain McKinnel for all of his advice and help with the tap-tag study.

Thanks must also be given to Dr. Robin Parks, Dr. Martin Holcik, Dr. Dennis Bulman, Dr. Valerie Wallace, Dr. Peter Humphries, and Dr. Lynn Megeney for critical reading of the manuscripts I've written over the years.

I would like to thank the Ontario Graduate Scholarship Program, Canadian Institutes of Health Research and Families of SMA for supporting me and my research through scholarships and grants. Lastly, I would like to thank my family and friends for their support. Most importantly, I would like to thank Naveed Gulzar, the love of my life, for always supporting me and listening to me vent when things weren't going well.

COPYRIGHT PERMISSIONS

Chapter 3 was reprinted from Shafey, D., Cote , P., De Repentigny, R. and Kothary, R. (2005). Hypomorphic Smn knockdown C2C12 myoblasts reveal intrinsic defects in myoblast fusion and myotube morphology. *Exp Cell Res.* 311 (1): 49-61, with permission from Elsevier.

Chapter 4 was reprinted in part from Shafey, D., MacKenzie, A., and Kothary, R. (2007). Neurodevelopmental abnormalities in neural stem cells and embryos from severe SMA mice. Accepted in *J Neurosci Res.*

TABLE OF CONTENTS

LIST OF ABBREVIATIONS

Δ7SMN: exon 7 alternatively spliced survival motor neuron

ALS: Amyotrophic lateral sclerosis

BAC: bacterial artificial chromosome

bFGF: basic fibroblast growth factor

bp: base pair

BrdU: 5-bromo-2-deoxyuridine

cDNA: complementary DNA

CTAP: c-terminal tandem affinity purification

DAB: 3,3 Diaminobenzidine

DMEM: Dulbecco's Modified Eagle's Medium

ds-RNA: double stranded RNA

ECL: enhanced chemiluminescence

EGF: epidermal growth factor

EM: electron microscopy

ERK: extracellular signal regulated kinase

ES: embryonic stem

ESE: exonic splice enhancer

FBS: fetal bovine serum

FL-SMN: full length survival motor neuron

Gems: gemini of coiled bodies

GFAP: glial fibrillary acidic protein

HS: horse serum

kDa: kiloDalton

LIF: leukemia inhibitory factor

MAPK: mitogen-activated protein kinase

MBP: myelin basic protein

MEFs: mouse embryonic fibroblasts

MEM: minimum essential medium

MHC: myosin heavy chain

MRLC: myosin regulatory light chain

NAIP: neuronal apoptosis inhibitory protein

NCAM: neural cell adhesion molecule

NGF: nerve growth factor

NMJ: neuromuscular junction

NSC: neural stem cell

NTAP: n-terminal tandem affinity purification

PCR: polymerase chain reaction

PFA: paraformaldehyde

PKR : protein kinase regulated by double-stranded RNA

PMSF: phenylmethylsulfonyl fluoride

ROCK: Rho kinase

RNAi: RNA interference

SEM: standard error of the mean

shRNA: short hairpin RNA

siRNA: short interference RNA

SLAP: sarcolemmal associated proteins

SMA: spinal muscular atrophy

SMN: survival motor neuron

snRNP: small nuclear ribonucleoprotein

TAP: tandem affinity purification

TEV: tobacco etch virus

WT: wild type

LIST OF FIGURES

LIST OF TABLES

1.0 INTRODUCTION

1.1 Spinal Muscular Atrophy: *the disease*

Proximal spinal muscular atrophy (SMA) is a clinically heterogeneous neuromuscular disease characterized by the degeneration of α-motor neurons and skeletal muscle atrophy, which results in progressive proximal weakness and paralysis. Ultimately death results from respiratory distress due to trunk deformity and paralysis. SMA is the second most common fatal autosomal recessive disorder after cystic fibrosis, with an estimated incidence of 1 in 10,000 live births, representing an overall carrier frequency of 1:40 (Pearn 1980). Diagnosis has been dependent upon clinical examination, muscle biopsy and electromyography, and more recently DNA testing.

The disease severity of SMA is highly variable, and can be subdivided into 5 clinical groups (type 0-IV) depending on the age of onset and achieved motor abilities (Table 1.1) (Munsat and Davies 1992; Munsat, Mancall et al. 1994; Zerres and Rudnik-Schoneborn 1995). Type 0 SMA (prenatal form) has very severe prenatal onset and early neonatal lethality. These patients only survive with respiratory assistance. Type I SMA (acute form, Werdnig-Hoffmann disease) patients display a severe form of the disease with generalized muscle weakness and hypotonia ("floppy infant") and a disease onset within the first 6 months of life. These children are never able to sit or walk and usually die within the first 2 years. Type II SMA (intermediate form) patients are able to sit but never able to walk unaided, usually present first symptoms after the first 6 months of life, and survive into their third decade. Type III SMA (juvenile form, Kugelberg-Welander

Table 1.1. Clinical classification of Spinal Muscular Atrophy.

Type	Onset	Maximum Motor Function Achieved	Life Expectancy
0	Prenatal	Needs respiratory support at birth	Fatal at birth without respirator
I	<6 months	Sits with support only	<2years
II	6-18 months	Sits independently when placed	10-40 years
III	>18 months	Walks unassisted	Indefinite
IV	>30 years	Walks normally	indefinite

disease) patients are able to sit and walk unassisted, and their lifespan is not reduced. Disease onset occurs after 2 years of age. Type IV (adult onset) SMA patients are comparatively mildly affected with an age of onset later than 30 years and they have a normal life expectancy. Presently, there are no available treatments for SMA. Clinical management consists of aggressive treatment of respiratory infections and prevention of trunk deformities.

1.2 *Survival motor neuron (SMN) – the SMA gene*

The SMA-determining gene was mapped by linkage analysis to a complex region of chromosome 5q11.2-q13.3 (Brzustowicz, Lehner et al. 1990; Gilliam, Brzustowicz et al. 1990; Melki, Abdelhak et al. 1990; Melki, Sheth et al. 1990; Simard, Vanasse et al. 1992; Wirth, Voosen et al. 1993; Burghes, Ingraham et al. 1994; MacKenzie, Jacob et al. 1994). This region contains a large inverted duplication of 500 kb (Lefebvre, Burglen et al. 1995). The smallest deletions involving the telomeric copy of the *Survival Motor Neuron* gene (*SMN1*) and the presence of intragenic mutations of *SMN1* in patients, including missense, non-sense or splice site mutations, have pinpointed *SMN1* as the gene mutated in SMA (Melki, Lefebvre et al. 1994; Bussaglia, Clermont et al. 1995; Lefebvre, Burglen et al. 1995; Brahe, Clermont et al. 1996; Parsons, McAndrew et al. 1996; Hahnen, Schonling et al. 1997). *SMN1* is duplicated with a highly homologous copy called *SMN2*. Although 5-10% of the normal population lacks the centromeric copy (*SMN2*), all patients with SMA retain at least one copy. *SMN1* and *SMN2* each span approximately 30 kb and contain nine exons (1, 2a, 2b-8) (Burglen, Lefebvre

et al. 1996; Chen, Baird et al. 1998). Only five nucleotides distinguish *SMN1* from *SMN2* without any effect on the amino acid sequence (Lefebvre, Burglen et al. 1995). Only one of these nucleotide differences is functionally important: a translationally silent "C" to "T" transition located at position 6 of exon 7. This change disrupts an ASF/SF2 exonic splice enhancer (ESE) in *SMN2*, which leads to frequent exon 7 skipping during splicing of *SMN2* derived transcripts (Lorson, Hahnen et al. 1999; Monani, Lorson et al. 1999). Consequently, although *SMN1* produces only full-length transcripts, *SMN2* produces predominantly an exon 7 alternatively spliced transcript (Fig.1.1). This exon 7 deleted transcript produces a truncated, unstable protein missing the last 16 amino acids of the protein encoded by exon 7. Although the low level of full-length protein produced by *SMN2* is unable to fully compensate for the homozygous loss of *SMN1*, it is clear from patient studies that *SMN2* copy number modifies disease severity in a dose dependent manner (Coovert, Le et al. 1997; Lefebvre, Burlet et al. 1997; Feldkotter, Schwarzer et al. 2002). The *SMN2* copy number varies in the population and in patients with SMA. Most patients with the most severe form of the disease, SMA type 0 or I, have 1 or 2 *SMN2* copie(s), most patients with type II SMA have 3 *SMN2* copies; and most patients with type III have 3 or 4 *SMN2* copies (Feldkotter, Schwarzer et al. 2002). It appears that some individuals with 5 or more copies of *SMN2* are very modestly affected or can be completely protected against developing disease manifestations (Prior, Swoboda et al. 2004; Wirth, Brichta et al. 2006). Thus, *SMN2* has been identified as a modifying gene

Fig. 1.1. Genetics of Spinal Muscular Atrophy. In unaffected individuals (control), most full-length SMN transcript and protein arises from the *SMN1* gene. Patients with SMA have homozygous mutations in *SMN1*, but retain at least one copy of the *SMN2* gene. During Splicing of *SMN2*, exon 7 is frequently skipped. Consequently, approximately of 90% of transcripts that arise from *SMN2* lack exon 7 and code for a truncated protein that is rapidly degraded, and approximately 10% of transcripts include exon 7 and code for the full-length protein. Rare transcripts exclude exon 5.

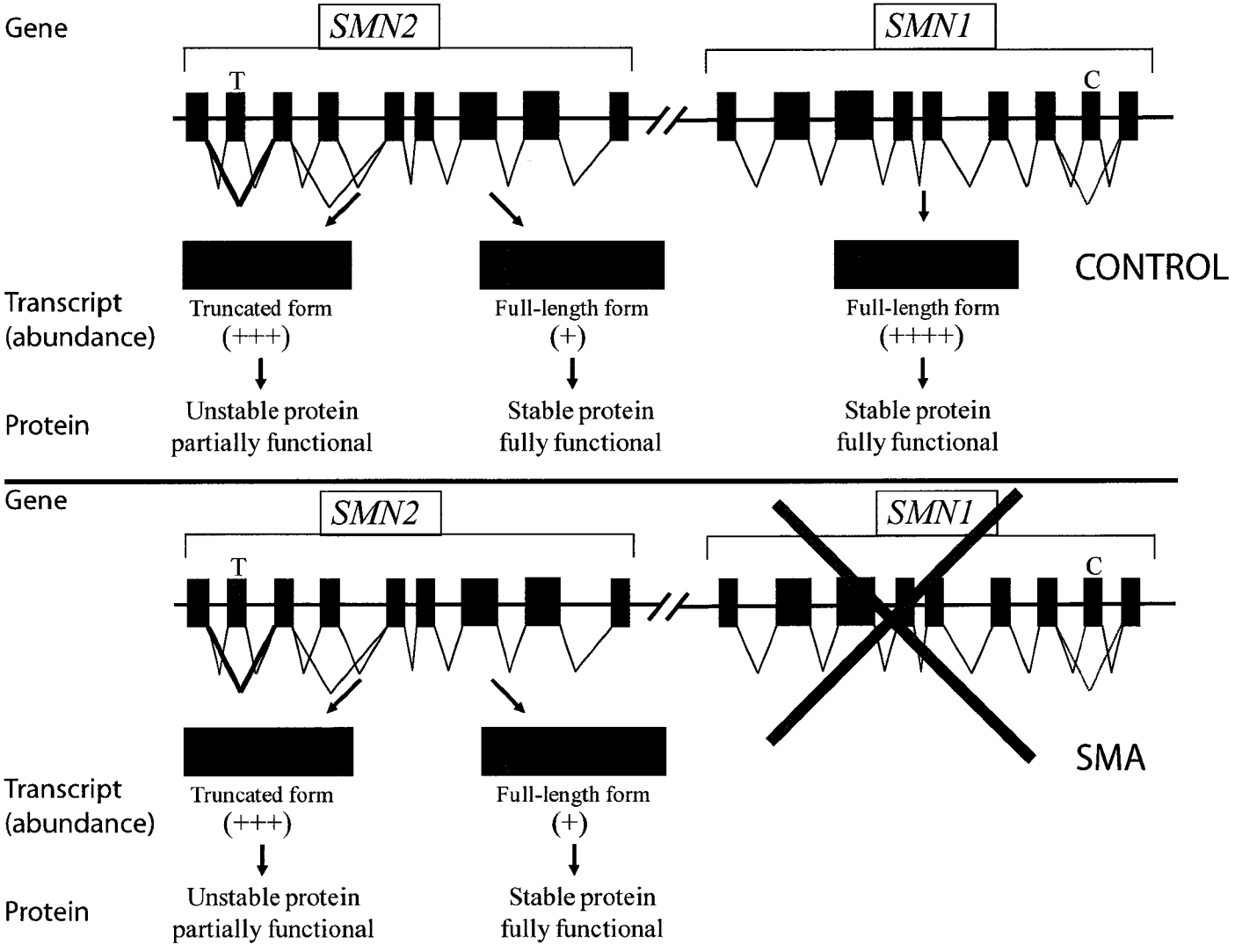
Gene
SMN2
SMN1
T
C
CONTROL
Transcript
(abundance)
Truncated form
(+++)
Full-length form
(+)
Full-length form
(++++)
Protein
Unstable protein
partially functional
Stable protein
fully functional
Stable protein
fully functional
Gene
SMN2
SMN1
T
C
SMA
Transcript
(abundance)
Truncated form
(+++)
Full-length form
(+)
Protein
Unstable protein
partially functional
Stable protein
fully functional

in SMA and as such, SMN protein level in SMA depends on *SMN2* copy number.

1.3 Survival Motor Neuron (SMN) – *the protein*

Full-length transcripts derived from both *SMN* copies encode identical full-length SMN protein composed of 294 amino acids. SMN is a ubiquitously expressed protein with a molecular weight of 38 kDa. SMN is highly expressed in brain, spinal cord, liver, and kidney, and moderately expressed in cardiac and skeletal muscle (Battaglia, Princivalle et al. 1997; Coovert, Le et al. 1997; Lefebvre, Burlet et al. 1997). The protein is expressed in high amounts during development then declines to a stable level throughout adulthood (Burlet, Huber et al. 1998; La Bella, Cisterni et al. 1998). SMN is present in both the cytoplasm and the nucleus. In the nucleus, it is concentrated in punctate structures called "gems" for "gemini of coiled bodies", termed as such due to their most often association with Cajal bodies (coiled bodies) (Liu and Dreyfuss 1996). Cajal bodies are nuclear structures that contain high levels of factors involved in transcription and processing of many types of nuclear RNAs and are known to be involved in RNA metabolism (Liu and Dreyfuss 1996). Gem number in cell lines and tissues from SMA patients correlates inversely with disease severity, with type I patients showing few or no gems (Patrizi, Tiziano et al. 1999).

The SMN protein has several identified motifs (Fig. 1.2), including a lysine-rich basic region encoded by exon 2, a Tudor motif (which may be important in RNA processing) encoded by exon 3, a polyproline region encoded by exons 4

Fig. 1.2. Schematic diagram of survival motor neuron coding regions. The locations of domains with known functions are indicated.

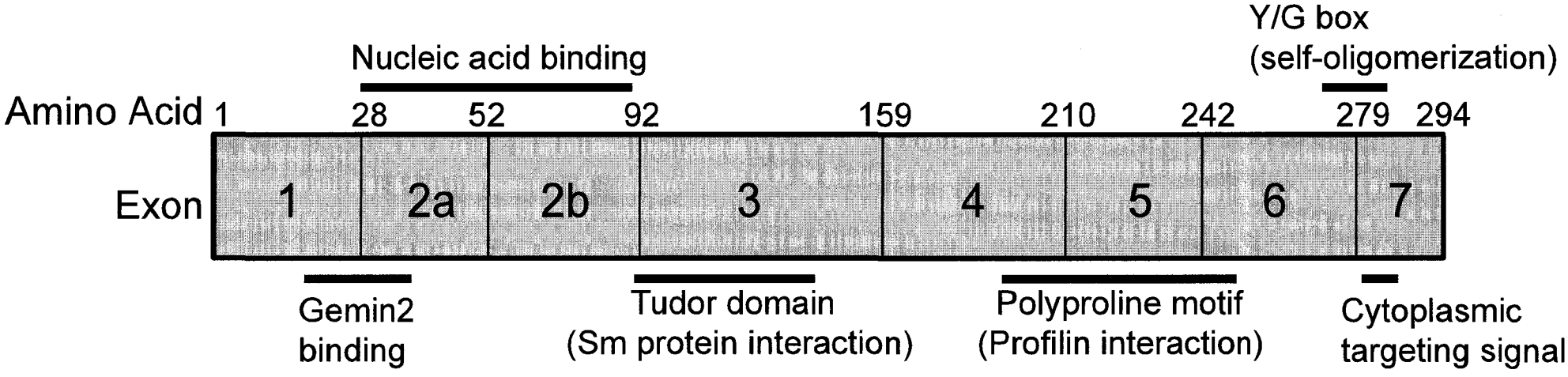
Y/G box
(self-oligomerization)
Nucleic acid binding
Amino Acid 1
28
52
92
159
210
242
279
294
Exon
1
2a
2b
3
4
5
6
7
Gemin2
binding
Tudor domain
(Sm protein interaction)
Polyproline motif
(Profilin interaction)
Cytoplasmic
targeting signal

and 5, and a region with several tyrosine-glycine (Y-G) pairs encoded by exon 6. Missense mutations have been identified in several of these regions, suggesting that each of these domains may be functionally important. SMN has been shown to oligomerize and form a stable multiprotein complex with Gemins 2-8 (Fig. 1.3) (Paushkin, Gubitz et al. 2002; Otter, Grimmler et al. 2007). These proteins are called Gemins because they display a subcellular distribution similar to that of SMN, including localization in Gems (Carissimi, Saieva et al. 2006). SMN interacts with Gemin2, Gemin3, Gemin5, and Gemin7, whereas Gemin4 and Gemin6 are brought to the SMN complex through their interactions with Gemin3 and Gemin7, respectively. Gemin8 binds the Gemin6-Gemin7 heterodimer as well as SMN, and mediates the association of Gemin6, Gemin7 and unrip with the SMN complex (Carissimi, Saieva et al. 2006; Carissimi, Saieva et al. 2006). This multiprotein complex performs SMN's major housekeeping function, the biogenesis of small nuclear ribonucleoproteins (snRNPs) (Fischer, Liu et al. 1997; Pellizzoni, Kataoka et al. 1998).

The best characterized function of the SMN complex is regulating the assembly of a specific class of RNA-protein complexes, the uridine-rich small nuclear ribonucleoproteins (UsnRNPs) (Yong, Golembe et al. 2004). The small nuclear ribonucleoproteins are a critical component of the spliceosome (Will, Schneider et al. 2001); a large RNA-protein complex that catalyzes pre-messenger RNA splicing. The SMN complex is essential and sufficient to mediate the ATP-dependent assembly of the seven-member ring of the common Sm proteins

Fig. 1.3. A schematic of the SMN complex. The survival motor neuron protein binds Gemin2, Gemin3, Gemin5, Gemin7, and Gemin8, whereas Gemin4 and Gemin6 associate with SMN through interactions with Gemin3 and Gemin7, respectively. The SMN protein oligomerizes, and as such is depicted in a dimeric form.

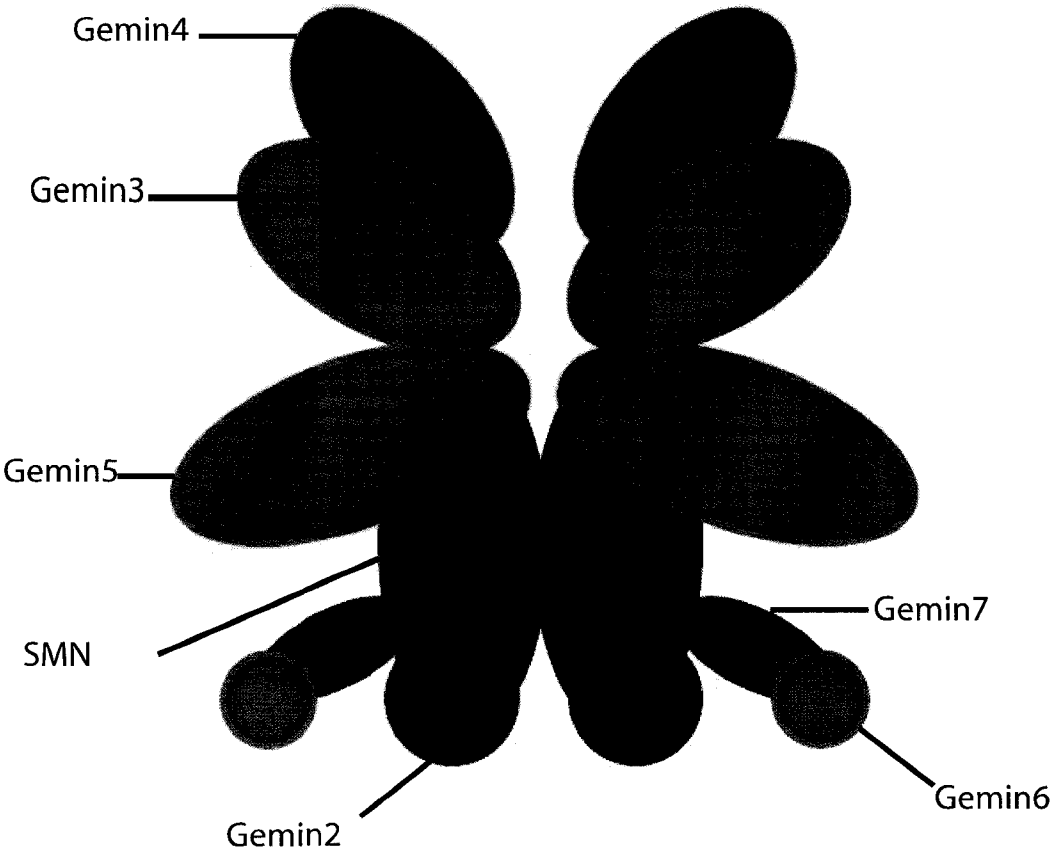
Gemin4
Gemin3
Gemin5
SMN
Gemin7
Gemin6
Gemin2

around a highly conserved sequence motif of less than 10 nucleotides, called the Sm site, present in most snRNAs. Moreover, the SMN complex was found to function as a specificity factor for this assembly process by ensuring that Sm cores are only formed on the correct RNA molecules (Pellizzoni, Yong et al. 2002). The ability of the SMN complex to facilitate and ensure accurate snRNP assembly is based on its capacity to bind both Sm proteins and also snRNAs. The SMN complex binds directly with high affinity and in a sequence specific manner to several snRNAs (Yong, Pellizzoni et al. 2002; Yong, Golembe et al. 2004). These observations suggest that the SMN complex brings the protein and RNA components together for snRNP assembly, thus serving as a genuine assemblyosome for Sm cores on snRNAs. Thus, the SMN complex is an essential mediator of snRNP assembly.

Despite the vast knowledge concerning SMN biochemistry, it remains unclear how impairment of snRNP biogenesis, which is a ubiquitous SMN function in all cell types, specifically causes alpha motor neuron degeneration and skeletal muscle atrophy. This dilemma raises the question whether SMN fulfils additional functions restricted to neurons and muscle. Interestingly, immunocytochemical studies have localized SMN in dendrites and axons and suggest a role in the transport of RNA along axons (Bechade, Rostaing et al. 1999; Pagliardini, Giavazzi et al. 2000). It has also been demonstrated that the SMN protein is localized in granules present in neurites and growth cones of cultured neuronal cells (Zhang, Pan et al. 2003). SMN granules exhibited rapid, bidirectional movements depending on both microtubules and microfilaments. Another major

finding that supports the idea of a neuron specific role of SMN in axonal mRNA transport is its interaction with hnRNP-R, a protein that binds to the 3' untranslated region of β-actin mRNA, as well as the identification of reduced levels of β-actin mRNA at distal axons and growth cones in motor neurons isolated from SMA-like transgenic mice (Rossoll, Jablonka et al. 2003). It has also been shown that SMN may have a specific role in muscle. It has been observed in *Drosophila* that SMN is a sarcomeric protein, implicating a muscle-specific function which when disrupted impacts on SMA pathogenesis (Rajendra, Gonsalvez et al. 2007). Finally, SMN has been found to interact with Bcl-2, p53, transactivator FUSE binding protein, profilins, zinc finger protein (ZPR1), RNA helicase A and RNA polymerase II (Iwahashi, Eguchi et al. 1997; Giesemann, Rathke-Hartlieb et al. 1999; Williams, Hamilton et al. 2000; Gangwani, Mikrut et al. 2001; Pellizzoni, Baccon et al. 2001; Pellizzoni, Charroux et al. 2001; Young, Day et al. 2002). It can be assumed from the various indirect and direct interactions of SMN with other various proteins that have been identified thus far, that SMN is involved in a large number of different pathways. Thus, a cascade of pathological events caused by the perturbation of multiple functions of SMN likely leads to SMA.

1.4 *Survival motor neuron - The mouse Smn gene*

The *SMN* genes are evolutionarily conserved. Orthologues have been identified in mice, zebrafish, *Drosophila*, nematodes, and yeast (DiDonato, Chen et al. 1997; Bertrandy, Burlet et al. 1999; Miguel-Aliaga, Culetto et al. 1999; Owen, Doe et al. 2000). To date, no natural mutations have been identified in these

organisms. Unlike in humans, the mouse *Smn* gene is present in a single copy. The mouse *Smn* gene maps to chromosome 13 within a conserved region that is syntenic to human chromosome 5q13 (Scharf, Damron et al. 1996; DiDonato, Chen et al. 1997; DiDonato, Ingraham et al. 1997; Viollet, Bertrandy et al. 1997). The entire Smn gene is 14,527 bp and has been subcloned and sequenced (DiDonato, Chen et al. 1997; DiDonato, Brun et al. 1999). This information has facilitated the construction of targeting vectors to create subtle alterations within the *Smn* gene.

The murine *Smn* gene produces a ubiquitously expressed 1.4 kb mRNA and unlike in humans, the mouse transcript does not undergo alternative splicing (DiDonato, Chen et al. 1997; Viollet, Bertrandy et al. 1997). This observation, coupled with studies from the human, suggest that only the full-length SMN protein is required for normal cellular function. Sequence comparison between murine and human SMN cDNAs indicates 83% nucleotide identity and 82% amino acid identity. The murine *Smn* gene resembles the human *SMN1* gene, as the conserved nucleotide at position 6 in exon 7 is maintained. Certain regions of the *SMN* gene are highly conserved in a number of species indicating their functional significance, as exemplified by the identification in the mouse Smn protein of the Gemin2 binding domain in exons 1-2a (Liu, Fischer et al. 1997), the Tudor domain in exon 3 (Talbot, Ponting et al. 1997), the Y-G box, the SMN self interaction domain and the Sm protein binding domain all in exon 6 (Liu, Fischer et al. 1997; Talbot, Ponting et al. 1997; Lorson, Strasswimmer et al. 1998).

1.5 Spinal Muscular Atrophy – *mouse models*

To get a better understanding of the various steps in the pathogenesis of SMA, different approaches have been employed to generate suitable mouse models (Fig. 1.4). The first strategy used homologous recombination to generate a knockout allele by creating an in-frame fusion between exon 2a of *Smn* and the *lacZ* gene (Schrank, Gotz et al. 1997). This abolished Smn expression in the targeted allele and placed *lacZ* under *Smn* transcriptional and translational control. Intercrosses that produce homozygous mutant embryos lacking a functional *Smn* gene ($Smn^{-/-}$) die at pre-implantation stages (Schrank, Gotz et al. 1997). Harmful effects start during the morula stage of development and coincide with the onset of embryonic transcription and depletion of maternal transcripts within the oocyte. These results also demonstrate the absolute cellular requirement for SMN within all cell types. Heterozygous $Smn^{+/-}$ mice undergo mild motor neuron degeneration but do not display overt signs of SMA (Jablonka, Schrank et al. 2000).

To more precisely recapitulate the genetic situation seen in SMA patients and test the hypothesis that human *SMN2* acts as a disease modifier due to small amount of functional SMN protein that each copy produces, two groups of researchers generated transgenic mice that contained the entire human *SMN2* locus (Hsieh-Li, Chang et al. 2000; Monani, Sendtner et al. 2000). The *SMN2* transgene from Monani et al., *SMN2(89Ahmb)*, contains only the genomic locus, whereas the *SMN2* transgene from Hsieh-Li et al., *SMN2(2Hung)*, contains *SMN2*, the *SERF1* gene, and a portion of the neuronal apoptosis inhibitory

Fig. 1.4 Mouse models of Spinal Muscular Atrophy. The left hand column depicts the mouse model generated, while the right hand column depicts the phenotype observed in the mouse model. $\Delta 7$, represents the deletion of exon 7 from the mouse *Smn* gene. *SMN2*, represents the transgenic addition of the human *SMN2* gene.

Mouse models of SMA

Genotype		Phenotype
• *Smn*$^{-/-}$ (null)	→	Embryonic lethality (E3.5)
• *Smn*$^{\Delta 7/\Delta 7}$	→	Embryonic lethality (E9.5)
• *Smn*$^{\Delta 7/\Delta 7}$ neuron-specific	→	Motor neuron deficit (P25)
• *Smn*$^{\Delta 7/\Delta 7}$ muscle-specific	→	Muscular dystrophy (1 month)
• *Smn*$^{-/-}$; *SMN2* (high copy)	→	Complete rescue (no abnormality)
• *Smn*$^{-/-}$; *SMN2* (low copy)	→	Severe SMA (peri-natal lethality)
• *Smn*$^{-/-}$; *SMN2; SMN*Δ7	→	Less severe SMA (P13)
• *Smn*$^{-/-}$; *SMN2;A2G*	→	Mild SMA phenoptype (8 months)
• *Smn*$^{+/-}$ (heterozygote)	→	Very mild late-onset

protein (*NAIP*) gene. Although there are minor differences between these transgenic models, the essential observations are the same. In both models, *SMN2* is able to rescue the embryonic lethality of $Smn^{-/-}$ mice. In both models, *SMN2* copy number correlates with a milder disease course and confirms family studies that show that *SMN2* modifies disease severity in a copy number-dependent manner (Coovert, Le et al. 1997; Lefebvre, Burlet et al. 1997; McAndrew, Parsons et al. 1997). Lastly, when enough *SMN2* copies are introduced into the mouse genome, the SMA phenotype is completely rescued. Taken together, these results confirm *SMN2* as a natural therapeutic target for the treatment of SMA.

Both the *SMN2(89Ahmb)* and *SMN2(2Hung)* transgenic mice display a disorder very similar to babies with severe type I SMA. These mice ($Smn^{-/-}$;$SMN2^{+/+}$) have 1 to 2 copies of the *SMN2* transgene on a mutant *Smn* background, produce low levels of SMN protein, and lack nuclear gem structures within their spinal motor neurons, an immunohistochemical hallmark of low SMN levels. These mice rapidly succumb to an SMN insufficiency and fail to thrive, becoming progressively smaller and weaker. They stop suckling and display severe muscular atrophy. Death occurs within days after birth. The phenotype of these mice varies depending on the background strain used. When in the FVB background, the phenotype is as stated above; however, when in the C57BL/6 background, these transgenic mice do not survive at birth, leading to the suggestion that there may be other modifying genes that modulate disease severity.

SMA mutant mice that die soon after or before birth (*Smn*$^{-/-}$;*SMN2*$^{+/+}$) do not allow for detailed analysis of pathogenic mechanisms and preclinical drug testing. However, this disease severity can be tempered to less severe phenotypes by adding additional transgenes that express various wild type isoforms of SMN (Monani, Pastore et al. 2003; Le, Pham et al. 2005). For a less severe mouse, a transgene expressing the SMNΔ7 cDNA on a severe mutant background (*Smn*$^{-/-}$;*SMN2*$^{+/+}$;*SMN*Δ*7*) increased the lifespan from approximately 5 days to 13 days (Le, Pham et al. 2005). At postnatal day 5, these mice are smaller and weigh less than their wild type littermates and they begin to have difficulty moving and righting themselves. When these mice walk, they display an abnormal gait and shakiness of their hind limbs (Le, Pham et al. 2005).

A mild SMA mouse was created by expressing a mild type III SMA mutation, A2G, as a hemizygous transgene on the severe SMA mouse background (*Smn*$^{-/-}$;*SMN2*$^{+/+}$;*SMNA2G*$^{+/-}$) (Monani, Pastore et al. 2003). In the absence of *SMN2*, the mild A2G transgenic mouse was not able to rescue the embryonic lethality of *Smn*$^{-/-}$ mice. However, in the presence of *SMN2,* the A2G mild mutant transgene delays onset of motor neuron loss and results in mice that are functionally normal with a mild phenotype and live to about 8 months of age.

To study the importance of *SMN* exon 7, which is the critical difference between *SMN1* and *SMN2* transcripts and protein, and to define cellular requirements of SMN expression, gene targeting coupled with the *Cre/loxP* technology was used to generate a conditional allele of *Smn* in which *LoxP* sites flank *Smn* exon7 (*Smn*^{F7}) (Frugier, Tiziano et al. 2000). This allows for conditional

excision of *Smn* exon 7 depending upon when and where CRE recombinase is expressed. Ubiquitous ablation of *Smn* exon 7 to generate the $Smn^{\Delta 7}$ allele results in SmnΔ7, a partially functional isoform, that in a homozygous state extends embryonic survival to E9.5 (Frugier, Tiziano et al. 2000; Hsieh-Li, Chang et al. 2000), compared with E3.5 for the $Smn^{-/-}$ embryos (Schrank, Gotz et al. 1997).

To study the cellular requirements of Smn in the motor unit, the conditional allele, Smn^{F7} was used to selectively delete *Smn* exon 7 in either neurons or skeletal muscle, the two cell types known to be affected in SMA. The "neuronal" mutant mice displayed rapid motor abnormalities and death at 25 days after birth (Frugier, Tiziano et al. 2000). These mice had improperly organized neuromuscular junctions, impaired axonal sprouting, massive accumulation of neurofilaments in terminal axons, and a significantly larger loss of motor axons compared with cell bodies. The converse experiment of deleting *Smn* exon 7 in skeletal muscle also had a pathologic effect. Mutant mice developed muscular dystrophy, muscle necrosis, and satellite cell depletion and died at about one month of age (Cifuentes-Diaz, Frugier et al. 2001).

The neuronal and muscle mutant mice do serve to illustrate once again, the essential nature of the Smn protein. However, whether they serve as useful models of SMA is questionable. In SMA, patients are homozygously deleted for *SMN1* and have only *SMN2* present, which produces a low amount of full-length SMN. Thus, every cell has at least residual full-length SMN protein available. In contrast, in the conditional "floxed" *Smn* mice, some cells have wild type Smn levels, whereas others have no Smn protein at all. The severe mice ($Smn^{-/-}$

;*SMN2*$^{+/+}$) and the modified versions of these mice serve as better SMA models that mimic the genetic complexity of SMA. However, these mice have given us very severe, less severe and a mild phenotype, but it would also be of benefit to generate mice with intermediate phenotypes.

1.6 Spinal Muscular Atrophy – *other animal models*

Model systems that are small, cheap, have short generation times, well-annotated genomes and can be easily manipulated for genetic and drug discovery experiments are useful in studying diseases. Model systems such as *Drosophila* and zebrafish have been used to study SMA pathogenesis.

Drosophila melanogaster have a single ortholog for SMN. This ortholog generates a transcript with a single exon, which is 828 nucleotides long, and encodes a 226 amino acid protein. Expression studies have suggested that SMN is expressed in both neuronal and muscle tissues and that both are required for rescue (Miguel-Aliaga, Chan et al. 2000; Chan, Miguel-Aliaga et al. 2003; Rajendra, Gonsalvez et al. 2007). The *Drosophila* SMA model has point mutations in Smn that are similar to those found in humans These mutations are located in a highly conserved region, the carboxy-terminal domain, containing the YXXG motif, of the encoded Smn protein and results in mis-sense mutations (Chan, Miguel-Aliaga et al. 2003). Similar mutations have been identified in SMN1 in SMA patients and they are thought to impair SMN oligomerization and/or binding of associated proteins (Lefebvre, Burglen et al. 1995; Lorson, Strasswimmer et al. 1998; Skordis, Dunckley et al. 2001). These *Drosophila* SMA models showed

defects in late developmental stages and a late larval lethality (Chan, Miguel-Aliaga et al. 2003). These flies show abnormal motor behavior and this phenotype is only alleviated when Smn is restored in both muscle and neurons (Chan, Miguel-Aliaga et al. 2003). This finding differs from what has been observed in the *Smn*$^{-/-}$*;SMN2* mice. In these mice, the expression of full-length SMN in neurons using the prion promoter rescues these mice, whereas expression of SMN in skeletal muscle does not (Gavrilina, McGovern et al. 2008). Thus, this suggests that the loss of Smn may affect neurons more in mice compared with muscle in *Drosophila.* Further analysis of the mutant flies demonstrated disorganized neuron boutons and a defect in neurotransmitter receptor subunit clustering (Chan, Miguel-Aliaga et al. 2003), thus suggesting a function for Smn at the neuromuscular junction. A hypomorphic allele of SMN in *Drosophila* produced viable hypomorphic SMN mutations in these flies (Rajendra, Gonsalvez et al. 2007). These flies have disorganized indirect flight muscles in the adult thorax and behavioural phenotypes that were fully penetrant. These flies were observed to be incapable of flying or jumping (Rajendra, Gonsalvez et al. 2007); thus, suggesting that the muscle defects in flies are more obvious than the neuronal defects.

The zebrafish has a rapid life cycle and external transparent embryonic development. This feature, coupled with a well-characterized stereotypical neuromuscular system at the cellular level, makes the zebrafish an ideal model system to study developing motor neurons and their axonal projections. Furthermore, because of their small size, low cost, and the ability to generate several hundred embryos in a single week, they are emerging as a powerful tool

for drug discovery (Rubinstein 2003; Zon and Peterson 2005). There are currently no known naturally or chemically induced mutations of the *SMN* gene in zebrafish. Thus, SMA has been modeled in this system by performing loss of function studies using a morpholino knockdown approach, which transiently suppresses protein levels (McWhorter, Monani et al. 2003). In this SMA zebrafish model, only motor axon-specific pathfinding defects were observed, and there were no effects on muscle development (McWhorter, Monani et al. 2003). These zebrafish did not show any movement deficits or paralysis, which are characteristics of the human SMA disease. However, these animals were only examined up until 3 days which are still embryonic stages. Thus, it is possible that movement deficits and muscle defects may show up later in development if Smn knockdown can be maintained.

Taken together, there are a range of phenotypes within the different SMA animal models, some involving neurons only and others involving both muscle and neurons. Therefore, whether SMA is a purely neurodegenerative disease or whether muscle also contributes in the pathogenesis remains controversial.

1.7 Spinal Muscular Atrophy – *therapy*

Current management of most SMA patients remains supportive only, with an emphasis in severe cases on respiratory function. Therefore, there is a need for developing therapeutics to treat SMA. As a result of progress in understanding the genetic basis and pathophysiology of SMA, potential approaches for the treatment of SMA have emerged (Table 1.2). Based on information gathered from the transgenic mouse models, one might predict that increased SMN protein levels

would correct SMA before symptoms are seen. In symptomatic SMA patients, increased SMN levels might help to preserve remaining motor neuron and muscle function. Several strategies are being actively investigated to increase full-length SMN protein levels, including activating *SMN2* gene expression, preventing *SMN2* exon skipping, and stabilizing SMN protein. Several academic and industrial groups have generated biological systems to develop high throughput screens for compounds that activate *SMN2* gene expression or prevent alternative splicing of *SMN2* exon 7. They have found that histone deacetylase inhibitors, such as sodium butyrate, valproic acid, 4-phenylbutyrate (Chang, Hsieh-Li et al. 2001; Brichta, Hofmann et al. 2003; Sumner, Huynh et al. 2003; Andreassi, Angelozzi et al. 2004; Kernochan, Russo et al. 2005), compounds that regulate DNA methylation of the *SMN2* gene promoter, such as valproic acid (Detich, Bovenzi et al. 2003), and other substances, such as interferon, indoprofen, and hydroxyurea (Baron-Delage, Abadie et al. 2000; Lunn, Root et al. 2004; Grzeschik, Ganta et al. 2005), transcriptionally activate the *SMN2* gene via its promoter. Others have found strategies to prevent the alternative splicing of the *SMN2* transcript. Some of these strategies involve the same drugs as above (valproic acid, sodium butyrate), but it has also been demonstrated that small antisense RNA molecules

Table 1.2 . Therapeutic strategies for Spinal Muscular Atrophy.

Rationale	Expected Results	Strategies
Genetic basis of SMA	Upregulation of*SMN2* gene Prevention of *SMN2* exon 7 skipping Stabilization of SMN Δ7 protein	High throughput screenings of compounds
Pathophysiology of SMA	Targeted therapeutics	SMN function, model characterization, gene therapy
Neurodegeneration	Non-targeted therapeutics (Neuroprotection)	Model Characterization, drug trials
Pluripotent cell capacity	Neuron or Muscle replacement	Hematopoietic stem cell transplantation in mouse models

can restore splicing of the *SMN2* pre-mRNA to include exon 7 (Lim and Hertel 2001; Cartegni and Krainer 2003; Skordis, Dunckley et al. 2003; Singh, Singh et al. 2006).

Other strategies that are being pursued for SMA therapeutics involve identifying drugs that might provide neuroprotection to motor neurons with low SMN levels. These include treatment with neurotrophic factors, such as cardiotrophin-1 (Lesbordes, Cifuentes-Diaz et al. 2003), neuroprotective compounds, such as Riluzol (Haddad, Cifuentes-Diaz et al. 2003) and regular exercise (Grondard, Biondi et al. 2005).

Lastly, there has been great interest in the possibility of repairing the nervous system or skeletal muscle by gene therapy or cell transplantation. Gene replacement strategies have been tested in cell culture and in mice and have shown promise (DiDonato, Parks et al. 2003; Azzouz, Le et al. 2004). The transplantation of cells that are able to divide, differentiate, and eventually replace those damaged or lost is of great interest. It has been demonstrated recently that bone marrow stem cells can differentiate into mature hepatocytes, skeletal muscle and cells with a neuronal phenotype (Ferrari, Cusella-De Angelis et al. 1998; Brazelton, Rossi et al. 2000; Krause, Theise et al. 2001). Whether these hematopoietic stem cells have the capacity to repair neuronal and muscle damage in the SMA mice is yet unknown, and further study must be undertaken to understand their therapeutic capacity fully.

Although a number of potential therapies are currently in clinical trials, their success may depend on identifying individuals as early as possible to begin

treatment before potentially irreversible neuronal loss and muscle damage. As well, it is clear from the animal and cell culture SMA models that SMN protein dosage determines severity of disease. Thus, regardless of which approach is used for the treatment of SMA, understanding the impact of SMN dosage on disease aetiology will be important in the decision of which strategy to employ.

1.8 Research Plan and Hypothesis

My hypothesis is that altering Smn dosage will result in changes in cellular properties and ultimately determine disease severity in SMA mouse models. Elucidating how the dosage of Smn impacts on overall development, as well as on neuronal development and function, will lead us to a better understanding of the pathogenesis of SMA. We propose the following specific aims to address this hypothesis:

Aim 1: To produce and characterize a hypomorphic series of Smn knockdown C2C12 cell lines.

Although motor neuron degeneration is generally accepted as the primary event in SMA, intrinsic muscle defects in this disease have not been ruled out. To gain a better understanding of the influence of SMN protein dosage in muscle, we have generated a hypomorphic series of myoblast (C2C12) stable cell lines with variable Smn knockdown. Establishing a hypomorphic series of Smn expressing cell lines in culture would allow us to dissect out the cell-specific roles of Smn and to determine the effect of Smn dosage on these roles.

Aim 2: To perform knockdown studies of mouse Smn *in vivo* to assess the effect on development.

Mutations in the *SMN1* gene are the causative agent of SMA. SMA is a disorder with ranging severity. The amount of SMN protein expressed in each individual is inversely correlated with the severity of SMA. Thus SMA can be considered to be a dose-dependent disorder. To gain a better understanding of the pathogenesis of SMA and this dose-dependent effect, we have used the short interference RNA (siRNA) approach to develop Smn hypomorphs in mice.

The *SMN* genes are evolutionarily conserved. Orthologues have been identified in mice, zebrafish, yeast, nematodes and *Drosophila*. Unlike the human gene, the mouse *Smn* gene is present as a single copy. Consequently, knocking out the gene through homologous recombination in embryonic stem cells and generating knock out mice causes early embryonic lethality. The null mouse is not informative in terms of understanding the SMA disease, thus developing mice with intermediate/mild phenotypes is critical for our ability to assess the pathogenesis of SMA.

Aim 3: To characterize the impact of Smn dosage on neuronal development and patterning in *Smn*$^{+/-}$ and *Smn*$^{-/-}$;*SMN2* mice.

Assessing two extreme SMA mouse models, *Smn*$^{+/-}$ (mild) and *Smn*$^{-/-}$;*SMN2* (severe), can help us understand how the dosage of Smn impacts on overall development, as well as on neuronal development and function, and will lead us to a better understanding of the pathogenesis of SMA.

Aim 4: To identify differences in the composition of Smn interacting proteins during different stages of C2C12 and PC12 differentiation.

Smn is thought to be part of diverse complexes. However, it is not yet known whether these complexes are dynamic or static in the context of specific cell types. Thus, examining whether Smn interacting partners change during different stages of growth and differentiation of both a muscle-like cell (C2C12) and a neuronal-like cell (PC12) will lead us to a better understanding of the diverse roles of Smn.

2.0 MATERIALS AND METHODS

2.1 Animals

All experimental protocols were performed in accordance with the University of Ottawa Animal Care Committee. Mild SMA mice were generated from males and females of the genotype *Smn*$^{+/-}$ in the C57BL/6 background. Severe SMA mice were generated from males and females of the genotype *Smn*$^{+/-}$;SMN2$^{+/+}$ in the C57BL/6 background. The description of these mice as severe and mild are our terms and may differ from the definitions of others. Wild type littermates were used as controls.

2.1.1 Generation of transgenic Smn knockdown founder embryos

The sh_Smn_519 and sh_Smn_866 shRNA constructs, described below, were microinjected by Yves De Repentigny (Kothary laboratory) into mouse embryos at the one-cell stage, embryos transferred to pseudopregnant mothers, and embryos were recovered and examined for morphological changes at E11.5. Photographs of embryos were taken on a Leica M29 dissecting scope using a Nikon coolpix 4500 digital camera.

2.1.2 Generation of transgenic Smn knockdown lines by DNA microinjection

The sh_Smn_519 and sh_Smn_866 constructs, described below, were microinjected by Yves De Repentigny separately or together with sh_Smn_249 into one-cell mouse embryos. Positive founder mice were identified by PCR genotyping. Although several founder mice were obtained, one was chosen from

sh_Smn_519 (845), two from sh_Smn_866 (426 and 428), and four from the combined sh_Smn_249, sh_Smn_519 and sh_Smn_866 (959, 977, 982, 983) injections for further breeding with C57BL6 mice to establish transgenic lines. Once transgenic lines were established, they were bred into the $Smn^{+/-}$ background for further analysis.

2.1.3 Generation of transgenic Smn knockdown lines by blastocyst injection

Embryonic stem cells cultured from the $Smn^{+/-}$;SMN2 mouse (Monani, 2000) were transfected with the sh_Smn_519 construct, described below, using Amaxa nucleofection (Amaxa Biosystems) following the manufacturer's protocol. These cells were subjected to drug selection using 50 μg/ml hygromycin (Specialty Media) for 8 days, and individual colonies selected and grown for an additional 7 days. Lysates were then taken for immunoblot analysis. Smn expression levels were quantified using FujiFilm Image Quant to measure band intensity normalized to β-tubulin 1 as the internal control. These Smn knockdown ES cell clones were provided by Tara Martinez and Doug Kerr (Johns Hopkins). These ES cell clones were then used to produce chimeras by blastocyst injections. The blastocyst injections were performed by Yves De Repentigny. Of several mice born, one was deemed to be chimeric based on coat colour mosaicism. This mouse was bred to wild type FVB mice and we were able to establish germline transmission of the shRNA transgene. The chimera and subsequent litters were crossed to wild type mice in the FVB background to remove the two copies of the SMN2 gene to attain a greater Smn knockdown.

2.14 Genotyping of the transgenic Smn knockdown mice

Genotyping for the shRNA Smn knockdown, $Smn^{+/-}$ and the $Smn^{-/-}$;SMN2 mice was performed by PCR on total genomic DNA extracted from embryonic tissue or tail samples. The shRNA Smn knockdown primers for genotyping are: 5' CCT GCA GGG TAC ACT GTG GAA TGT GTG 3' and 5' AGT CAA CAC GTG CTG ATC AGA TCC GA 3', with amplification of a 610 bp band. The primers for genotyping the $Smn^{+/-}$ mice are: 5' TTG GCC TGA ACT GCC AGC TGG CGC AGG 3' and 5' TCC CGC AGC GCA GAC CGT TTT CGC TCG 3', with amplification of a band of 417 bp. The primers for genotyping the $Smn^{-/-}$;SMN2 mice are: 5' CTT GGG TGG AGA GGC TAT TC 3', 5' AGG TGA GAT GAC AGG AGA TC 3', 5' TTT TCT CCC TCT TCA GAG TGA T 3', and 5' CTG TTT CAA GGG AGT TGT GGC 3'. In this multiplex reaction, a single band at 420 bp indicates the mouse is $Smn^{+/+}$;SMN2, a single band at 280 bp indicates the mouse is $Smn^{-/-}$;SMN2, and two bands (420 bp and 280 bp) indicates that the mouse is $Smn^{+/-}$;SMN2. The primers for genotyping the SMN2 gene are 5' GCG ATA GAG TGA GAC TCC ATC T 3' and 5' GAC ATA GAG GTC TGA TCT TTA GCT 3', with amplification of a band of 530 bp.

2.2 Immunoblotting

Cell culture or tissue lysates used for immunoblotting were collected in ice-cold lysis buffer (50 mM Tris–HCl [pH 7.4], 150 mM NaCl, 1 mM EDTA, 1% Nonidet P-40 [NP-40], and 1% glycerol) containing 10 mM Na_2VO_4, 1 mM

phenylmethylsulfonyl fluoride (PMSF), 0.01 mg/ml aprotinin, 0.01 mg/ml pepstatin, and 0.01 mg/ml leupeptin on ice. Lysates were resolved on 10% SDS-PAGE and transferred to a PVDF membrane (Millipore). The separated proteins were analyzed by western blot using one of the following antibodies: Smn (1:5000) (Transduction Laboratories, USA), Actin (1:1000) (Research Diagnostics), Gemin2 (1:1000) (Abcam), Myosin Regulatory Light Chain (1:1000) (Abcam), Nucleolin (1:1000) (Abcam), Profilin-1 (1:1000) (Abcam), Annexin-II (Abcam), MLC2 (1:200) (Santa Cruz Biotechnology), Annexin II (1:1000) (Santa Cruz Biotechnology), and GFP (1:1000) (Invitrogen) detected by the enhanced chemiluminescence (ECL) system (GE Healthcare).

2.3 DNA constructs and vector construction

2.3.1 Generation of Smn shRNA constructs

We have used the murine *Smn* cDNA sequence [DiDonato, 1999] (accession: NM_011420) to select the target regions for shRNA gene silencing (Fig. 2.1). The target sequences were selected using Ambion's siRNA Target Finder (www.ambion.com). The criteria used to choose the sequences were: length of 21 nucleotides, begins with AA, 30–50% GC content, avoid stretches of >4Ts or As. Sequence analysis using the BLAST algorithm (NCBI) gave no significant match to other targets. Double-stranded DNA oligonucleotides were

Fig. 2.1. siRNA targets for the mouse *Smn* gene. Mouse *Smn* gene is shown with the sequences selected using Ambion's siRNA Target Finder (www.ambion.com). The criteria used to choose the sequences were: length of 21 nucleotides, begins with AA, 30-50% GC content, avoid stretches of >4T's or A's. Sequence analysis using the BLAST algorithm (NCBI) gave no significant match to other targets.

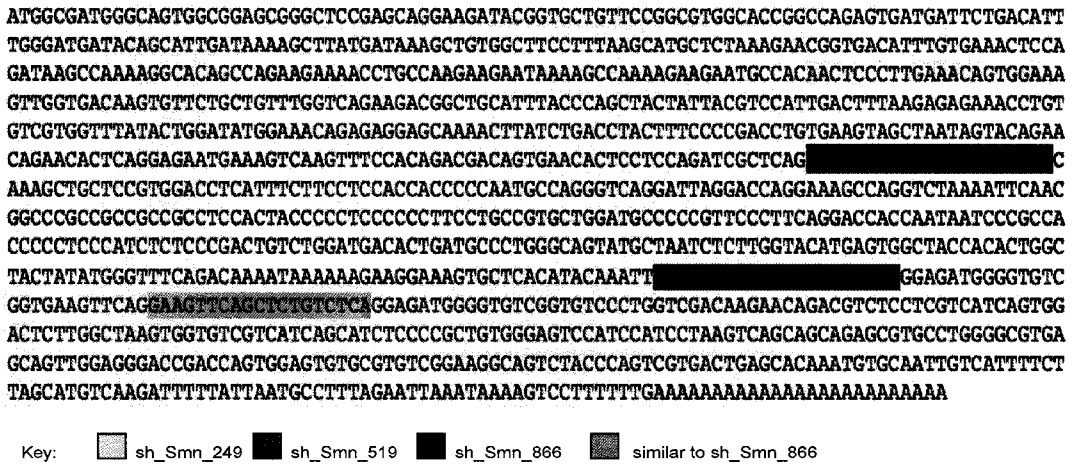
ATGGCGATGGGCAGTGGCGGAGCGGGCTCCGAGCAGGAAGATACGGTGCTGTTCCGGCGTGGCACCGGCCAGAGTGATGATTCTGACATT
TGGGATGATACAGCATTGATAAAAGCTTATGATAAAGCTGTGGCTTCCTTTAAGCATGCTCTAAAGAACGGTGACATTTGTGAAACTCCA
GATAAGCCAAAAGGCACAGCCAGAAGAAAACCTGCCAAGAAGAATAAAAGCCAAAAGAAGAATGCCACAACTCCCTTGAAACAGTGGAAA
GTTGGTGACAAGTGTTCTGCTGTTTGGTCAGAAGACGGCTGCATTTACCCAGCTACTATTACGTCCATTGACTTTAAGAGAGAAACCTGT
GTCGTGGTTTATACTGGATATGGAAACAGAGAGGAGCAAAACTTATCTGACCTACTTTCCCCGACCTGTGAAGTAGCTAATAGTACAGAA
CAGAACACTCAGGAGAATGAAAGTCAAGTTTCCACAGACGACAGTGAACACTCCTCCAGATCGCTCAG
AAAGCTGCTCCGTGGACCTCATTTCTTCCTCCACCACCCCCAATGCCAGGGTCAGGATTAGGACCAGGAAAGCCAGGTCTAAAATTCAAC
GGCCCGCCGCCGCCGCCTCCACTACCCCCTCCCCCCTTCCTGCCGTGCTGGATGCCCCCGTTCCCTTCAGGACCACCAATAATCCCGCCA
CCCCCTCCCATCTCTCCCGACTGTCTGGATGACACTGATGCCCTGGGCAGTATGCTAATCTCTTGGTACATGAGTGGCTACCACACTGGC
TACTATATGGGTTTCAGACAAAATAAAAAAGAAGGAAAGTGCTCACATACAAATT
GGAGATGGGGTGTC
GGTGAAGTTCAGGAAGTTCAGCTCTGTCTCAGGAGATGGGGTGTCGGTGTCCCTGGTCGACAAGAACAGACGTCTCCTCGTCATCAGTGG
ACTCTTGGCTAAGTGGTGTCGTCATCAGCATCTCCCCGCTGTGGGAGTCCATCCATCCTAAGTCAGCAGCAGAGCGTGCCTGGGGCGTGA
GCAGTTGGAGGGACCGACCAGTGGAGTGTGCGTGTCGGAAGGCAGTCTACCCAGTCGTGACTGAGCACAAATGTGCAATTGTCATTTTCT
TAGCATGTCAAGATTTTTATTAATGCCTTTAGAATTAAATAAAAGTCCTTTTTTGAAAAAAAAAAAAAAAAAAAAAAAAA
Key:
sh_Smn_249
sh_Smn_519
sh_Smn_866
similar to sh_Smn_866

ligated into the *Bbs*I sites of the psiRNA-hH1neo vector (Invivogen). The oligonucleotide sequence used to construct sh_Smn_249 was: 5′ TCC CAA ACT CCC TTG AAA CAG TGG AAT TCA AGA GAT TCC ACT GTT TCA AGG GAG TTT T 3′. The oligonucleotide sequence used to construct sh_Smn_519 was: 5′ TCC CAA AGT AAA GCA CAC AGC AAG TCT TCA AGA GAG ACT TGC TGT GTG CTT TAC TTT T 3′. The oligonucleotide sequence used to construct sh_Smn_866 was: 5′ TCC CAA AGA AGT TCA GCT CTG TCT GAT TCA AGA GAT GAG ACA GAG CTG AAC TTC TTT T 3′. The oligonucleotide sequence used to construct the control sh_LacZ_1348, which targets *LacZ*, was: 5′ TCC CAA ATC GTC TGA CCG ATG ATC CGT TCA AGA GAC GGA TCA TCG GTC AGA CGA TTT T 3′ and was a kind gift from Dr. Robin Parks (Ottawa Health Research Institute). The constructs were named as suggested in a recent paper (Huppi, Martin et al. 2005). The plasmid clones derived from each shRNA construct were verified by DNA sequencing with the OL381 and OL178 primers (Invivogen). See Fig. 2.2 for a schematic of the shRNA process.

2.3.2 Generation of NTAP-SMN and CTAP-SMN constructs

The retroviral expression constructs pBRIT-LoxP-CTAP HIS-FLAG and pBRIT-LoxP-NTAP FLAG-HIS were originally designed by Dr. Greenblatt and subsequently modified and generously supplied to us by Dr. Iain McKinnell and Dr. Michael Rudnicki (McKinnell, Ishibashi et al. 2007). The coding sequence for Human SMN was PCR amplified for insertion into the NTAP construct with 5'-GGA GAA TTC ATG GCG ATG AGC AGC GGC GGC AGT-3' (forward primer) and 5'-GGA CTC GAG ATT CCT TAC ACT CGT GGA AGG AAG AAA-3'

Fig. 2.2 The shRNA silencing process. RNAi can regulate endogenous gene expression. When long double stranded RNAs (dsRNAs) enter the cell, they are recognized and cleaved by Dicer. Dicer is a member of the RNAse III family of dsRNA-specific endonucleases. Cleavage by Dicer creates short dsRNAs, which are characterised by 2 nucleotide long 3' overhangs. These are called small interfering RNAs (siRNAs). siRNAs can form a ribonucleoprotein complex called RISC (RNAi silencing complex). This complex includes 'Slicer', an aregonaute protein with an RNAse H-like domain. RISC mediates the unwinding of the siRNA duplex. A single stranded siRNA that is coupled to RISC, then binds to a target mRNA in a sequence-specific manner. The binding mediates target mRNA cleavage by Slicer. The cleaved mRNA is recognized by the cell as being aberrant and is then destroyed. This prevents translation from occurring, thus silencing Smn expression.

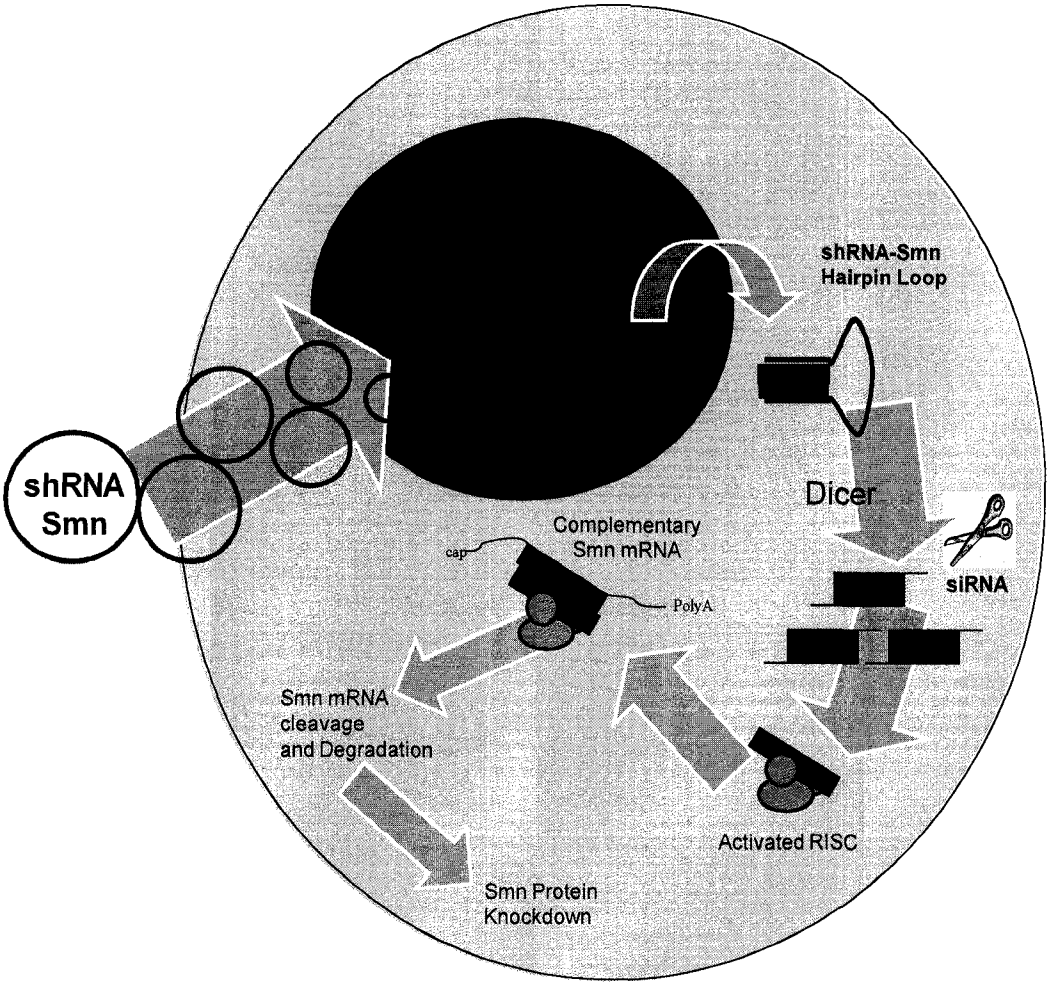
shRNA-Smn
Hairpin Loop
shRNA
Smn
Dicer
siRNA
Complementary
Smn mRNA
cap
PolyA
Smn mRNA
cleavage
and Degradation
Activated RISC
Smn Protein
Knockdown

(reverse primer) and with 5'-GGA GAA TTC GCC GCC ATG ATG GCG ATG AGC AGC GGC GGC AGT-3' (forward primer) and 5'-GGA CTC GAG ATT CCT TAC ACT CGT GGA AGG AAG AAA-3' (reverse primer) for insertion into the CTAP construct. The amplified SMN cDNA was gel purified and digested with the restriction enzymes EcoRI and XhoI. The pBRIT-LoxP-CTAP HIS-FLAG and pBRIT-LoxP-NTAP FLAG-HIS vectors were also digested with EcoRI and XhoI. The appropriate amplified SMN cDNA was ligated to the appropriate vector to generate our NTAP-SMN and CTAP-SMN constructs.

2.4 Cell culture

C2C12 myoblast cells were cultured in DMEM (Wisent) supplemented with 10% heat-inactivated fetal bovine serum (FBS) (Sigma) and 1% antibiotic/antimycotic solution (Invitrogen). For differentiation of C2C12 cells, the growth media was replaced with low-serum media (2% horse serum) (Invitrogen). PC12 cell lines were maintained in DMEM (Wisent) supplemented with 10% horse serum, 5% FBS, 1% antibiotic/antimycotic solution and 1% MEM non-essential amino acids solution (Invitrogen). For differentiation, PC12 cells were grown in DMEM supplemented with 1% FBS, 1% antibiotic/antimycotic solution and 50 ng/ml NGF (Chemicon). The retroviral packaging cell line, Phoenix-eco was maintained in DMEM supplemented with 5% FBS, and 1% penicillin/streptomycin (Invitrogen). For the experiments in Chapter 3, cells were plated on glass coverslips at a density of 25,000 cells per well in a 12-well plate. In the proliferation and same density myogenic differentiation experiments, the growth media was

replaced with low-serum media (2% horse serum) after 24 h. In the confluency myogenic differentiation experiments, the cells were allowed to grow to confluency before the growth media was replaced with low-serum media.

2.4.1 Establishment of stable cell lines expressing the Smn shRNA constructs

The sh_Smn_249, sh_Smn_519, sh_Smn_866, and sh_LacZ_1348 constructs were transfected into C2C12 cells using Lipofectamine Plus reagent (Invitrogen) to obtain stable lines with differing extents of Smn knockdown. These cells were subjected to drug selection with 1 mg/ml G418 (Invitrogen), plated at low density, and clonal colonies were isolated. Several drug-resistant C2C12 cell lines were established for all constructs, and their levels of Smn protein were determined by immunoblotting. The software program Image J, developed by Wayne Rasband at the National Institutes of Health, was used to quantify the intensity of bands to determine relative Smn knockdown in each of the cell lines.

2.4.2 Establishment of stable cell lines expressing the NTAP-SMN and CTAP-SMN constructs

High titer infectious retrovirus stocks were generated by transfecting the NTAP-SMN and CTAP-SMN constructs into Phoenix-eco cells using Lipofectamine 2000 (Invitrogen). Polybrene-enhanced retroviral infection of the above stocks into C2C12 and PC12 cells was used to obtain stable lines with NTAP-SMN or CTAP-SMN expression similar to endogenous levels. These cells were subjected to drug

selection with 2 μg/ml puromycin (Invitrogen), plated at low density, and clonal colonies were isolated. Several drug-resistant C2C12 and PC12 cell lines were established for both constructs, and their Smn protein levels determined by immunoblotting. Cell culture lysates used for immunoblotting were collected in ice-cold lysis buffer (50 mM Tris–HCl [pH 7.4], 150 mM NaCl, 1 mM EDTA, 1% Nonidet P-40 [NP-40], and 1% glycerol) containing 10 mM Na_2VO_4, 1 mM phenylmethylsulfonyl fluoride (PMSF), 0.01 mg/ml aprotinin, 0.01 mg/ml pepstatin, and 0.01 mg/ml leupeptin on ice. Lysates were resolved on 10% SDS-PAGE and transferred to a PVDF membrane (Millipore). Smn protein levels were determined by probing with a monoclonal Smn antibody (Transduction Laboratories, USA), and an actin-antibody (Research Diagnostics) was used to ensure equal protein loading. Bands were detected using the enhanced chemiluminescence (ECL) system (GE Healthcare).

2.4.3 Primary neurosphere culture

The striatum of E14.5 embryos was dissected, cells dissociated by light trituration with a fire-polished glass pipette, and cultured at 1 x 10^6 cells/ml. Neurospheres were grown in Neurocult basal media (Stem Cell Technologies) supplemented with Neurocult proliferation supplement (Stem Cell Technologies) and bFGF (10 μg/ml) (Invitrogen). After 7 days of culture, neurospheres were plated onto poly-L-lysine-coated coverslips, and diameters of 50-100 randomly chosen spheres were measured within 20 minutes after plating using the Axiovision 4.6 program.

2.4.4 Embryonic Stem Cell Culture

DR4 primary mouse embryonic fibroblasts (PMEFs) (Open Biosystems) were cultured in DMEM (Gibco) supplemented with 10% heat-inactivated fetal bovine serum (FBS) (Sigma), 1% glutamax (Gibco) and 1% penicillin/streptomycin (invitrogen). ES cells were cultured on PMEFS with DMEM (Specialty media) supplemented with 15% FBS (invitrogen), 1% glutamax (Gibco), 1% penicillin/streptomycin (invitrogen), 1% non essential amino acids (Gibco), 1% nucleosides (Specialty Media), 0.0007% β-mercaptoethanol and 1 μl/ml recombinant mouse Leukemia Inhibitory Factor (LIF) (Chemicon International). Prior to blastocyst injection, ES cells were removed from PMEFS.

2.5 Immunocytochemistry

2.5.1 Smn and Gemin2 localization by immunofluorescence

Cells grown on coverslips were rinsed in PBS and fixed in ice-cold 100% methanol for 5 min at −20°C and then air-dried for 30 min. The coverslips were blocked with PBS containing 3% bovine serum albumin (BSA) for 30 min at room temperature. Smn antibody (Transduction Laboratories, USA) and Gemin2 antibody (Santa Cruz) were diluted 1:100 and 1:50, respectively, in blocking solution, and applied to the coverslips, and incubated overnight at 4°C. The coverslips were washed 4 times, 5 min each in PBS, and incubated for 1 h in the dark with an Alexa Fluor 488-conjugated donkey anti-goat antibody (Molecular Probes) and an Alexa Fluor 555-conjugated donkey anti-mouse antibody

(Molecular Probes) that had been diluted in blocking solution. Hoechst staining of nuclei was also performed in parallel. Fluorescent images were photographed on a Zeiss Axiophot microscope equipped with a UV source and Cy-3, FITC and Hoechst detection filters.

2.5.2 Annexin II and MRLC localization by immunofluorescence

Cells grown on coverslips were rinsed in PBS and fixed in ice-cold 100% methanol for 5 min at −20°C and then air-dried for 30 min. The coverslips were blocked with PBS containing 10% horse serum for 30 min at room temperature. Smn (1:100) (Transduction Laboratories, USA), Annexin II (1:50) (Santa Cruz Biotechnology), and MLC2 (1:20) (Santa Cruz Biotechnology) were diluted in blocking solution and applied to the coverslips and incubated overnight at 4°C. The coverslips were washed 4 times, 5 min each in PBS, and incubated for 1 h in the dark with an Alexa Fluor 488-conjugated donkey anti-rabbit antibody (Molecular Probes) or an Alexa Fluor 555-conjugated donkey anti-mouse antibody (Molecular Probes) that had been diluted in blocking solution. Hoechst staining of nuclei was also performed in parallel. Fluorescent images were photographed on a Zeiss Axiophot microscope.

2.5.3 Proliferation assays

To assess the growth rate of wild type (WT), control, and Smn shRNA C2C12 cell lines, 5-bromo-2-deoxyuridine (BrdU) incorporation assays were performed. Cells in growth media for 24, 48, or 72 h or in differentiation media for

24, 48, or 72 h were exposed to BrdU (Roche) at a final concentration of 10 μM for a period of 24 h and then processed for immunofluorescence. Cells grown on coverslips were rinsed in PBS and fixed in 70% ethanol for 10 min at room temperature. After rinsing in PBS 3 times, the cells were incubated in 2 N HCl for 20 min at 37°C. HCl was then removed, and cells were incubated in 0.1 M Tris-Cl pH 8.4 for 10 min at room temperature. After washing 3 times in PBST (PBS and 0.1% Tween20), the cells were blocked in 5% milk in PBS for 30 min at 37°C. BrdU antibody (BD Biosciences) diluted 1:100 in 5% milk in PBS was added to the cells for 1 h. After washing, cells were incubated with an Alexa Fluor 488-conjugated goat anti-mouse antibody. Hoechst staining of nuclei was also performed in parallel. For the neurosphere proliferation experiments, assays were performed as above in growth media or differentiation media for 72 h or 120 h. Fluorescent images were photographed on a Zeiss Axiophot microscope equipped with a UV source and FITC and Hoechst detection filters. In stress-induced cell death experiments, cells were treated with 2 μM staurosporine, a potent inducer of apoptosis, for 3 h. The extent of nuclear DNA breaks characteristic of cells undergoing apoptosis was measured using the TUNEL labeling kit (Roche). Cell viability was measured using the LIVE/DEAD kit (Molecular Probes).

2.5.4 Differentiation assays of C2C12 cells

To assess the differentiation potential of wild type (WT) and Smn shRNA C2C12 cell lines, two different approaches were taken. In the 'same density' experiment, the cells were incubated in growth media for 24 h, then exposed to

differentiation media for 24 or 72 h. Cells were fixed at 24 h growth and 24 and 72 h differentiation. In the 'confluency experiment,' the cells were incubated in growth media until they reached 80% confluency then exposed to differentiation media for 24 or 72 h. Cells were then fixed at confluency in growth media and at 24 and 72 h differentiation. The cultures were fixed with 4% paraformaldehyde for 15 min, washed in PBS, permeabilized with 0.1% Triton X-100 in PBS for 5 min, and then blocked in 3% BSA for 30 min at room temperature. Cells were immunostained for two different myogenic markers: myosin heavy chain (MHC) using the MF20 antibody (Developmental Studies Hybridoma Bank, IA, USA) and NCAM using the H28–123 antibody (Abcam). After washing, cells were incubated with a Cy3-conjugated goat anti-mouse antibody or an Alexa Fluor 555-conjugated goat anti-Rat antibody. Hoechst staining of nuclei was also performed in parallel. Fluorescent images were captured on a Zeiss Axiophot microscope equipped with a UV source and Cy3 and Hoechst detection filters. The differentiation potential of the cultures was determined by counting the nuclei from MF20 or NCAM-positive cells and expressing this number as a percentage of the total number of nuclei counted. At least 200 nuclei from several random fields were counted for each time point and group (wild type and each of the C2C12 shRNA cell lines). The fusion potential of myocytes from wild type and each of the C2C12 shRNA cell lines was also calculated by determining the prevalence of myotubes as well as the relative proportions of myotubes containing 2 or more nuclei. The fusion index was calculated as the percent ratio of the number of nuclei in myotubes over the total number of myogenic nuclei in one field (number of nuclei in myotubes/total number

of myogenic nuclei) × 100%. In this case, myotubes were counted if they contained 2 or more nuclei.

2.5.5 Differentiation assays of the primary neurosphere cultures

Primary neurospheres were harvested after 7 days in culture, dissociated into single cells using the Neurocult dissociation kit (Stem Cell Technologies). Single cells (1 x 10^6 cells per well) were plated on cover glasses coated with 10 μg/ml poly-D-lysine (Sigma) and 5 μg/ml human laminin (Sigma) in growth culture medium for 24 h. After 24 h, the media was removed and replaced with media without mitogens and differentiated for 3 or 5 days. Cells were then processed for immunofluorescence. Cells were fixed in 4% paraformaldehyde for 30 min. After rinsing in PBS 3 times, the cells were incubated in 0.3% Triton X-100 for 10 min at room temperature, and then blocked in 10% horse serum for 30 min. Nestin (1:200) (Chemicon), GFAP (1:200) (Stem Cell Technologies), MBP (1:200) (Stem Cell Technologies), and Tuj1 (1:200) (Stem Cell Technologies) antibodies in 10% horse serum in PBS were added to the cells for 2 h at 37°C. After washing, cells were incubated with an Alexa Fluor 488-conjugated goat anti-mouse antibody. Hoechst staining of nuclei was also performed in parallel. Fluorescent images were photographed on a Zeiss Axiophot microscope equipped with a UV source and FITC and Hoechst detection filters. The numbers of neurites were measured from TuJ1-labeled differentiated cells plated as a single-cell suspension and the longest neurite of the TuJ1-labeled differentiating neuron was traced and measured using the Axiovision 4.6 program.

2.6 Immunohistochemistry

2.6.1 Neurofilament staining

For whole-mount neurofilament staining, embryos were fixed in 4% paraformaldehyde (PFA) at 4°C overnight, dehydrated in graded methanol and stored at -20°C. For staining, embryos were rehydrated, bleached with 6% H_2O_2 in PBST (PBS containing 0.01% Tween-20), treated with proteinase K dissolved in PBST (1 mg/ml) for 10 minutes, washed in PBST containing 10 mg/ml glycine, and rewashed three times in PBST. Embryos were then refixed in 4% PFA/0.2% glutaraldehyde dissolved in PBST for 20 minutes followed by three washes in PBST. For whole-mount staining of neurofilaments, embryos were blocked with 10% horse serum in PBST overnight at 4°C and then incubated with the first antibody (concentrate IgG clone 2H3 from Developmental Studies Hybridoma Bank of Iowa, DSHB) diluted 1:900 in 10% horse serum in PBST. After incubation, embryos were washed five times for 1 hour each with 10% horse serum in PBST and then overnight in PBST alone. After washing, cells were incubated with an HRP-conjugated goat anti-mouse antibody diluted 1:200 in 10% horse serum in PBST overnight at 4°C. After incubation, embryos were washed five times for 1 hour each with 10% horse serum in PBST and then overnight in PBST alone. The colour development of the embryos was performed by incubating embryos in 0.3 mg/ml DAB in PBS for 20 min at room temperature in the dark, then adding 0.03% H_2O_2 for ten minutes. Photographs of embryos were then taken on a Leica M29 dissecting scope using a Nikon coolpix 4500 digital camera.

2.6.2 Staining for neuronal markers on paraffin sections

Embryos were fixed in 4% paraformaldehyde (PFA) at 4°C overnight, dehydrated in a graded ethanol series, treated with xylene alone, followed by a 1:1 mixture of xylene and paraffin wax, and then embedded in paraffin wax. Paraffin blocks were cut at 6 μm and sections collected on glass slides. Each slide was photographed to select sections of the identical anteroposterior level from different embryos. Paired sections were then used for immunofluorescence staining with two monoclonal mouse antibodies. Slides were dewaxed and sections treated with heated 0.1 M citric acid buffer pH 6.0 (0.24% citric acid, 2.5% sodium citrate, pH6.0) for antigen unmasking. Sections were then washed in water and incubated in 0.3% in Triton-X100 for 10 min, and blocked in 10% horse serum in PBS for 30 min. The antibody was applied overnight at 4°C. The slides were washed 3 times in PBS. After washing, cells were incubated with a FITC-conjugated goat anti-mouse antibody for 1 hour. Hoechst staining of nuclei was also performed. Mouse monoclonal antibodies against Isl1 (clone 2D6) (1:100) (DSHB), Lim1 (1:100) (DSHB), HB9 (1:500) (Abcam), and Nestin (Chemicon) were used. Fluorescent images were photographed on a Zeiss Axiophot microscope equipped with a UV source.

2.6.3 Staining for neuromuscular junctions

Paraformaldehyde (4%) fixed diaphragm and gastrocnemius muscle from E18.5 embryos were embedded in 30% sucrose and OCT and frozen on liquid nitrogen. Cryosections (10 μm) were collected on coated glass slides and dried at room temperature for 2 hours. Sections were then stained for dystrophin (1:20) (mAb NCL-DYS2) (Novacastra Labs) following the M.O.M immunodetection kit protocol (Vector Laboratories, Inc.). Before mounting, sections were stained with Alexa fluor 566 conjugated α-bungarotoxin (1:500) (Molecular Probes) in PBS for 15 min. Fluorescent images were photographed on a Zeiss Axiophot microscope.

2.7 Morphological assessment

2.7.1 Morphological analysis and quantification of motor neurons

The L4 segment of the lumbar spinal cord, the brainstem and the gastrocnemius muscle were dissected and fixed in 4% paraformaldehyde. Samples were given to the University of Ottawa Histology department for paraffin embedding and serial sectioning. Sections were then stained with hematoxylin and eosin and examined by light microscopy using a Zeiss Axioplan microscope. Motorneurons in a defined area were counted in every fifth section of the L4 segment of the spinal cord and of the brainstem.

2.7.2 Electron microscopy

Diaphragm and gastrocnemius muscle from E18.5 embryos were dissected and fixed in 1.6% glutaraldehyde, and 0.2 M sodium cacodylate, pH7.2. Thin

sections were cut, stained with uranyl acetate and lead citrate, and analyzed by electron microscopy by Peter Rippstein at the University of Ottawa Heart Institute.

2.8 Tandem affinity purification

Approximately 1 g of cells was collected at growth, one, three, five, and seven days of differentiation from both the C2C12 and PC12 cell clones. Cells were flash frozen and lysed in 1.3 volume (ml/g of cell pellet) of Buffer A (10 mM Tris-HCl pH 7.9, 0.1 M NaCl, 1.5 mM $MgCl_2$, 0.18% NP40) supplemented with protease inhibitors (2.4 μg/ml chymostatin, 1.5 μg/ml pepstatin A, 88 μg/ml PMSF, 0.5 μg/ml leupeptin, 17 μg/ml aprotinin, 310 μg/ml benzamidine). Once the cells had been homogenized in Buffer A, one volume of Buffer B (50 mM Tris-HCl pH 7.9, 0.6 M NaCl, 1.5 mM $MgCl_2$, 25% glycerol) was added and cells were homogenized again. This was followed by addition of 1 μl of benzonase nuclease (Novogen) and the homogenate was rotated at 4°C for 30 minutes. The homogenate was then spun at 40,000g for one hour in an ultracentrifuge and the supernatant dialyzed with Slide-A-Lyzer Dialysis Cassette (PIERCE) for 3 hours in dialysis buffer (10 mM Tris-HCl pH 7.9, 0.1 M NaCl, 10.1 mM EDTA, 10% glycerol). Once dialyzed, the extract was spun at 14,000 g for 20 minutes and the supernatant was removed and placed into a Low Retention Microcentrifuge Tube (Fisher Scientific). At this point, the process of purification depended on the TAP construct being recovered. CTAP-SMN fusion protein and its associated components were recovered from extracts by affinity selection on anti-Flag M2 agarose beads (Sigma). M2-agarose beads (50 μl/sample) were washed twice with AFC Buffer (10 mM Tris-HCl pH 7.9, 100 mM NaCl, 0.1% NP40), then

resuspended in equal volume of AFC buffer. The 50 μl of beads (100 μl of slurry) were added to the extract and rotated overnight at 4°C. The beads were then washed three times in AFC buffer and twice in TEV buffer (20 mM Tris-HCl pH 7.9, 100 mM NaCl, 0.1 mM EDTA, 0.1% NP40). Beads were resuspended in 100 μl of TEV buffer, 2 mg/ml acTEV protease (Invitrogen) and 2 mg/ml Flag peptide (Sigma) and rotated for 30 minutes at 4°C. The beads were pelleted and the supernatant was kept for later use. The beads were resuspended again in 100 μl of TEV buffer, 2 mg/ml acTEV protease and 2 mg/ml Flag peptide. This process was repeated three times, each time the supernatant was kept for later use. Ni-NTA agarose beads (Qiagen) (60 μl/sample) were washed twice in Ni-NTA wash buffer (20 mM Tris-HCl pH 7.9, 100 mM NaCl, 0.1 mM EDTA, 5 mM imidazole) and then resuspended in an equal volume of Ni-NTA wash buffer. The Ni-NTA beads were then added to the TEV cleavage supernatant and rotated overnight at 4°C. The beads were then washed three times in Ni-NTA wash buffer and eluted with 4 x 100 μl Ni-NTA elution buffer (20 mM Tris-HCl pH 7.9, 100 mM NH_4HCO_3, 0.1 mM EDTA, 0.4 M imidazole). The recovery of NTAP-SMN fusion protein and its associated components was similar to the CTAP-SMN recovery; however, the order of purification was different. For the NTAP-SMN purification, the complex was first bound to the Ni-NTA beads. Following elution and TEV cleavage, the complex was bound to the M2 agarose beads. The final purified complex was eluted in 4 x 100 μl AFC buffer with 2 mg/ml Flag peptide. See Fig. 2.3 for a schematic of the different Tandem Affinity Purification process.

2.8.1 Sample preparation for mass spectrometry

The protein complexes recovered from the TAP-tag purification were concentrated using Microcon Centrifugal Filter device for protein concentration (Millipore). The concentrated purified complexes were resolved on a 12% SDS-PAGE gel. The gel was stained in a non-fixing silver stain, fixed in 50% ethanol, 5% acetic acid solution for 30 minutes, washed in 50% ethanol for 10 minutes, than washed in water twice for 10 minutes, sensitized for 2 minutes in 0.02% sodium thiosulphate, washed twice for 5 minutes, stained with chilled 0.1% silver nitrate for 30 minutes, and then washed in water for 2 minutes. After this, a small amount of developer (0.04% formalin, 2% sodium carbonate) was added to the water and swirled briefly to remove excess silver. The water was replaced with developer and the gel was shaken slowly until bands appeared. Once the bands appeared, the developer was discarded and a stop solution (5% acetic acid) was added to the gel for at least 5 minutes. The gel was then stored in 1% acetic acid. Unknown proteins were excised from the gel and stored in 1% acetic acid.

2.8.2 Mass spectrometric analysis

In gel digestion was performed using trypsin, and LTQ linear ion trap mass spectrometry was used to identify the unknown peptide products. The ions score cut-off was set at >40 and the number of peptides that matched to are identified protein was >3. Mass spectrometric analysis was done at the Ottawa Institute of Systems Biology.

Fig. 2.3. Tagged Affinity Purification (TAP) method. (A) General schematic of the tap-tag purification process. (B) Schematic of CTAP-SMN and detailed method of the purification process. (C) Schematic of NTAP-SMN and detailed method of the purification process.

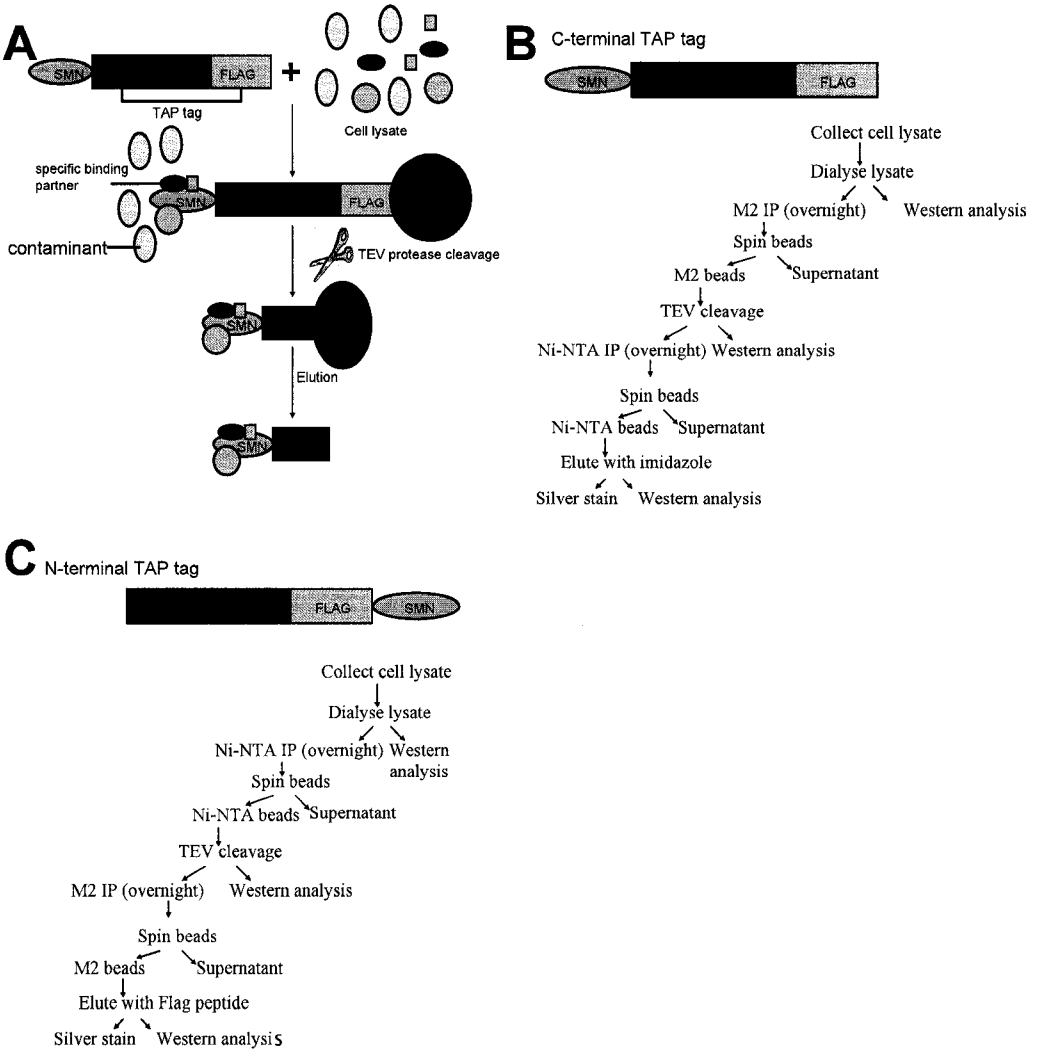
A
SMN
FLAG
TAP tag
Cell lysate
specific binding partner
contaminant
TEV protease cleavage
Elution
B
C-terminal TAP tag
Collect cell lysate
Dialyse lysate
M2 IP (overnight)
Western analysis
Spin beads
M2 beads
Supernatant
TEV cleavage
Ni-NTA IP (overnight) Western analysis
Spin beads
Ni-NTA beads
Supernatant
Elute with imidazole
Silver stain
Western analysis
C
N-terminal TAP tag
Collect cell lysate
Dialyse lysate
Ni-NTA IP (overnight) Western analysis
Spin beads
Ni-NTA beads
Supernatant
TEV cleavage
M2 IP (overnight)
Western analysis
Spin beads
M2 beads
Supernatant
Elute with Flag peptide
Silver stain
Western analysis

2.8.3 Immunoprecipitation

Wild type C2C12 and PC12 cells at growth, and 1, 3, 5 and 7 days of differentiation were lysed in NP-40 buffer (50 mM Tris-HCl, pH 7.4, 150 mM NaCl, 1% NP-40, 1 mM Na_2VO_4, 1 mM PMSF, 10 μg/ml pepstatin A, 30 μg/ml aprotinin, 20 mM leupeptin). Cell lysates were incubated overnight at 4°C with protein A or protein G sepharose beads (Amersham Biosciences), and with Smn (Transduction Laboratories), Gemin2 (Abcam), MRLC (Abcam), Nucleolin (Abcam), Profilin-1 (Abcam), or Annexin-II (Abcam) antibodies. Following incubation and after extensive washing, bound fractions were solubilized in 2X Laemmli SDS sample buffer and separated on a 10% SDS polyacrylamide gel. The separated proteins were analyzed by immunoblot analysis using one of the following antibodies: Smn (1:5000), Gemin2 (1:1000), MRLC (1:1000), Nucleolin (1:1000), Profilin-1 (1:1000), and Annexin-II (1:1000) and detected by ECL (GE Healthcare).

2.9 Statistical Analysis

All cell culture and animal experiments were at an $n > 3$. Data are expressed as the mean ± SEM. Differences in measured variables between experimental and control groups were assessed using the t-test assuming unequal variances. Statistical difference was accepted at $p < 0.05$.

3.0 Hypomorphic Smn knockdown C2C12 myoblasts reveal intrinsic defects in myoblast fusion and myotube morphology

Dosage of the survival motor neuron (SMN) protein has been directly correlated with the severity of disease in patients diagnosed with spinal muscular atrophy. It is also clear that SMA is a neurodegenerative disorder characterized by the degeneration of the α-motor neurons in the anterior horn of the spinal cord and atrophy of the associated skeletal muscle. What is more controversial is whether neuronal and/or muscle-cell-autonomous defects are responsible for the disease *per se*. Although motor neuron degeneration is generally accepted as the primary event in SMA, intrinsic muscle defects in this disease have not been ruled out. To gain a better understanding of the influence of SMN protein dosage in muscle, we have generated a hypomorphic series of myoblast (C2C12) stable cell lines with variable Smn knockdown. We show that depletion of Smn in these cells resulted in a decrease in the number of nuclear 'gems' (gemini of coiled bodies), reduced proliferation with no increase in cell death, defects in myoblast fusion, and malformed myotubes. Importantly, the severity of these abnormalities is directly correlated with the decrease in Smn dosage. Taken together, our work supports the view that there is an intrinsic defect in skeletal muscle cells of SMA patients and that this defect contributes to the overall pathogenesis in this devastating disease.

3.1 RESULTS

3.1.1 Establishment of stable cell lines expressing the Smn shRNA constructs

Three separate shRNA constructs targeting different regions of *Smn* were used in our experiments (see Chapter 2). The constructs were transfected into C2C12 cells to obtain stable cell lines with differing extents of Smn knockdown. Several drug-resistant C2C12 cell lines, herein referred to as Smn shRNA C2C12 cells, were established for all constructs, and their levels of Smn protein were determined by immunoblotting (Fig. 3.1). The range of Smn knockdown was from as low as 10% to as much as 90% when compared to wild type cells (Figs. 3.1A–C). Several of the sh_Smn_519 Smn shRNA C2C12 cell lines (2A2, 2B2, 2B3, and 2B5) were chosen for further study. In addition, we have utilized an shRNA targeted to a non-eukaryotic gene as a control for specificity (sh_LacZ_1348). As expected, the sh_LacZ_1348 clones did not show any depletion of Smn (Fig. 3.1D).

3.1.2 Sub-cellular localization of Smn

In the nucleus, SMN is involved in transcription and pre-mRNA splicing, where it is concentrated in structures called 'gems' (gemini of coiled bodies) (Liu and Dreyfuss 1996). In cells and tissues from SMA patients, the expression of SMN and the number of gems are greatly reduced (Coovert, Le et al. 1997). We therefore wanted to determine whether the reduction in Smn protein in C2C12

Fig. 3.1. Immunoblot analysis. C2C12 muscle cells were transfected with the (A) sh_Smn_249, (B) sh_Smn_519, (C) sh_Smn_866, or (D) sh_LacZ_1348 (control) shRNA constructs, selected with G418, plated at low density, and clonal colonies isolated. Lysates from stable C2C12 cell clones were resolved on 10% SDS-PAGE and transferred to a PVDF membrane. Smn levels were determined by blotting with an anti-Smn antibody (lower band), and anti-actin (upper band) was used as a loading control. WT = wild-type (non-transfected) C2C12 cells.

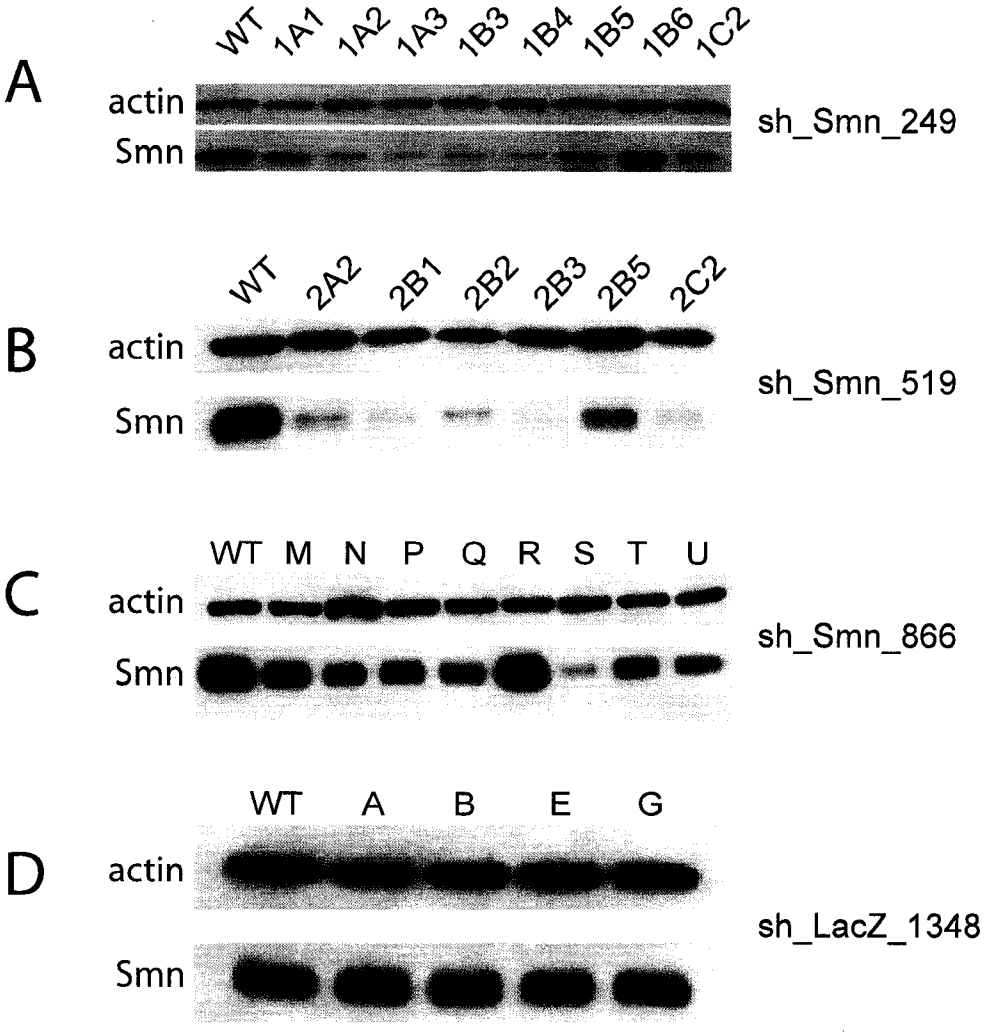
A
WT 1A1 1A2 1A3 1B3 1B4 1B5 1B6 1C2
actin
Smn
sh_Smn_249
B
WT 2A2 2B1 2B2 2B3 2B5 2C2
actin
Smn
sh_Smn_519
C
WT M N P Q R S T U
actin
Smn
sh_Smn_866
D
WT A B E G
actin
Smn
sh_LacZ_1348

cells had an effect on the number of gems in these cells. The range of Smn reduction varied from 55% (clone 2B5) to 90% (clone 2B3) in the cell lines being analyzed (Fig. 3.1B). Using immunofluorescence microscopy, we first determined the sub-cellular localization of Smn in normal C2C12 cells. As shown in Fig. 3.2A, Smn was present in the cytoplasm and in nuclear gems. To conclusively identify the nuclear structures labelled with the Smn antibody as gems, we have counterstained the cells for Gemin2 and Gemin3, known members of the Smn complex. Our observations indicated that nuclear Smn was always co-localized with these two Gemins (data for Gemin2 shown in Fig. 3.2). Similar analysis was performed with Smn shRNA C2C12 cell lines 2B5, 2A2, 2B2, and 2B3 (Fig. 3.2). These cells displayed fewer Smn staining gems. We have quantified the gem numbers in all four cell lines and in the parental C2C12 cell line (Fig. 3.2P). An inverse correlation between the amount of Smn knockdown and the number of gems is observed, with the 2B3 line showing the most Smn knockdown and the least number of gems. We have extended our analysis to determine whether the Smn knockdown also affected the absolute number of gems per cell. As expected, wild type C2C12 cells had more incidents of nuclei with 2-6 gems than did the Smn shRNA C2C12 cell lines (summarized in Table 3.1). As the dosage of Smn decreased, so did the number of cells with gems greater than 1.

3.1.3 Smn knockdown decreases C2C12 cell proliferation

Cell proliferation under conditions of growth and differentiation was investigated in wild type C2C12 cells and in control *LacZ* shRNA and Smn

Fig. 3.2. Immunocytochemical analysis of wild-type (WT) C2C12 and Smn shRNA C2C12 cell lines (2B5, 2A2, 2B2, 2B3). (A, F, K) WT C2C12 cells (arrows indicate gems within nuclei), (B, G, L) 2B5 (55% knockdown), (C, H, M) 2A2 (65% knockdown), (D, I, N) 2B2 (75% knockdown), and (E, J, O) 2B3 (90% knockdown) cells. Cells were stained for Smn protein (A–E) and for Gemin2 (F–J), two known members of the Smn complex that are present in nuclear gems. Merged images, including counterstain for Hoechst dye to identify the nucleus, are shown (K–O). Smn staining in the nucleus was always accompanied by staining for Gemin2, indicating that these structures were indeed gems. Loss of gems was observed in Smn knockdown cells, particularly in clone 2B3. (P) Quantification of the loss of gems. Cells were immunostained for Smn and Gemin2, counterstained with Hoechst dye to identify the nucleus, and images analyzed for the presence of gems. Smn knockdown was assessed by immunoblot as in Fig. 1. At least 200 cells were counted for each cell line, and the number of nuclear gems per 200 cells is depicted. An inverse correlation between the amount of Smn knockdown and the number of gems is observed (*$P < 0.01$ for WT vs. 2B5; $P < 0.0005$ for WT vs. 2A2, 2B2, and 2B3). Scale bar, 50 μm.

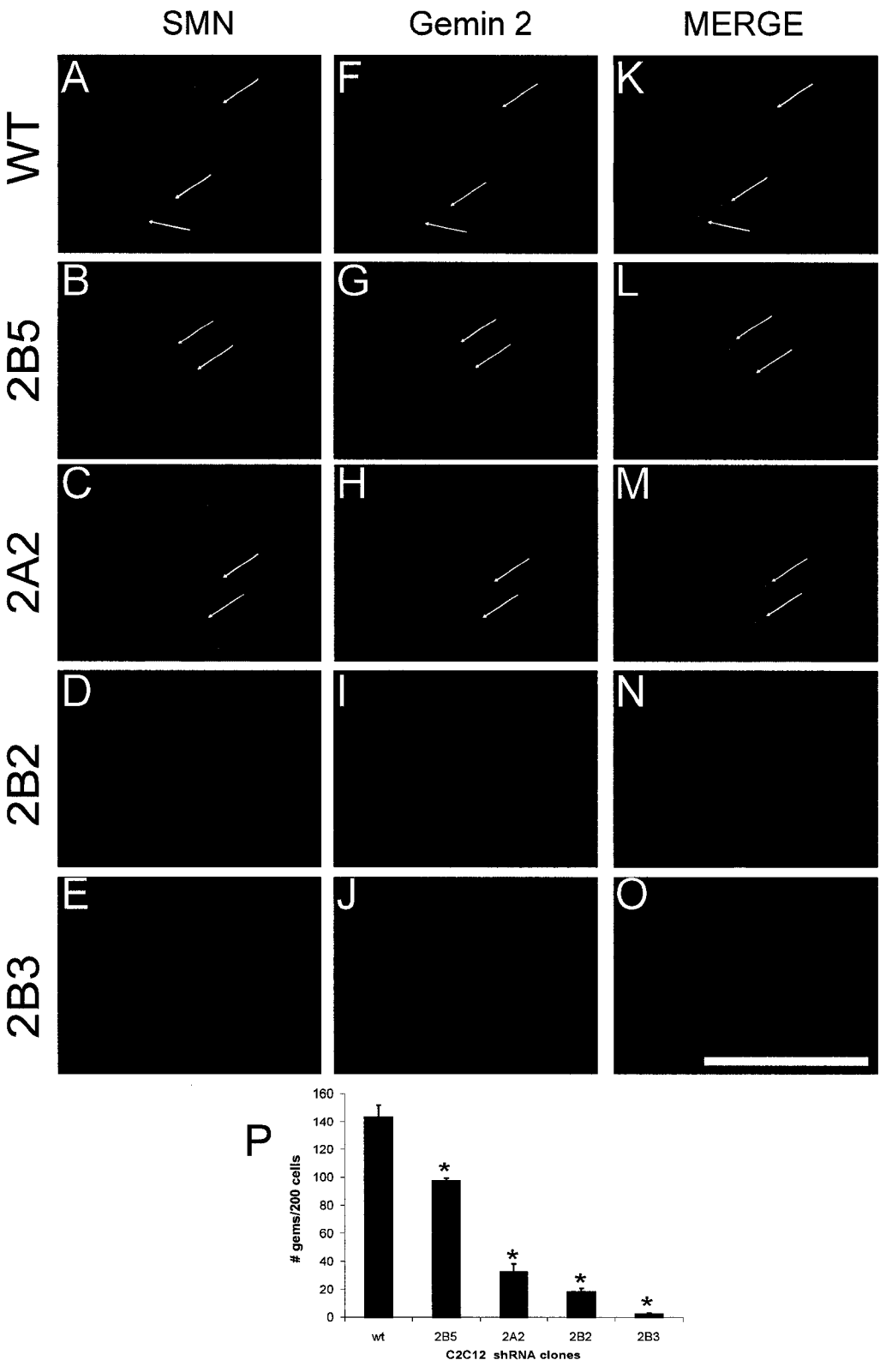
SMN
Gemin 2
MERGE
WT
2B5
2A2
2B2
2B3
A
F
K
B
G
L
C
H
M
D
I
N
E
J
O
P
gems/200 cells
160
140
120
100
80
60
40
20
0
wt
2B5
2A2
2B2
2B3
C2C12 shRNA clones

Table 3.1. Quantification of the number of times 'n' gems per cell were observed in 200 cells in Smn shRNA C2C12 stable cell lines.

Cell Line	Amount of Smn Knockdown	# times n gems/cell seen in 200 cells					
		6 gems	5 gems	4 gems	3 gems	2 gems	1 gems
WT (C2C12)	0%	2	2	4	5	4	127
2B5	55%	0	0	2	4	5	87
2A2	65%	0	0	0	1	4	30
2B2	75%	0	0	0	1	4	14
2B3	90%	0	0	0	0	0	2

shRNA C2C12 cell lines by subjecting them to 5-bromo-2′-deoxyuridine (BrdU) incorporation assays. Cells in growth media for 24, 48, or 72 h or in differentiation media for 24, 48, or 72 h were exposed to BrdU for a period of 24 h prior to fixation. Using immunofluorescence microscopy, we determined the extent of proliferation of wild type C2C12 and control and Smn shRNA C2C12 cell lines (Figs. 3.3A–L). The wild type C2C12 cells have a much higher rate of proliferation then the Smn shRNA C2C12 cell lines [24 h ($P < 0.0005$ for wild type vs. 2A2, 2B2, and 2B3); 48 h ($P < 0.05$ for wild type vs. 2A2, 2B2, and 2B3); and 72 h ($P < 0.05$ for wild type vs. 2A2, 2B2, and 2B3)] (Fig. 3.3M). The lower proliferation is especially dramatic in clone 2B3, which also has the most severe Smn knockdown. The wild type and control *LacZ* shRNA C2C12 cell lines have the same proliferation rate. Thus, the difference in proliferation rate between the Smn shRNA cell lines and wild type is due to the decrease in Smn protein levels and not due to the G418 selection procedure. Upon exposure to low-serum media (to initiate the differentiation) for 24, 48, or 72 h, BrdU incorporation decreased for wild type C2C12 and the Smn shRNA C2C12 cell lines (Fig. 3.3N), and there was no significant difference between the two.

To assess whether the decreased growth properties of the Smn knockdown shRNA C2C12 cell lines could be due to an increase in apoptosis, we measured the incidence of cell death using TUNEL assay, as well as by assessing cell viability. Our analysis of the clones showed no increase in cell death or loss of cell viability compared to wild type C2C12 cells (Fig. 3.4). Although there was no inherent increase in apoptosis in the Smn knockdown

Fig. 3.3. Growth potential of wild-type (WT) C2C12, control, and the Smn shRNA C2C12 cell lines (2B5, 2A2, 2B2, 2B3). Immunodetection of BrdU and Hoechst labeling of nuclei from (A, G) WT C2C12, (B, H) control sh_LacZ, (C, I) 2B5 (55% knockdown), (D, J) 2A2 (65% knockdown), (E, K) 2B2 (75% knockdown), (F, L) sh_Smn_519 clone 2B3 (90% knockdown) in growth medium for 24 h. (M) Quantitative analysis of BrdU incorporation in the wild-type C2C12, control, and the Smn C2C12 shRNA cell lines cultured in growth medium for 24 h ($P < 0.0005$ for WT vs. 2A2, 2B2, and 2B3), 48 h ($P < 0.05$ for WT vs. 2A2, 2B2, and 2B3), or 72 h ($P < 0.05$ for WT vs. 2A2, 2B2, and 2B3). Note the drop in proliferation is especially dramatic in clone 2B3, which has the highest Smn depletion. (N) Quantitative analysis of BrdU incorporation in the various cell lines in differentiation medium for 24 h, 48 h, and 72 h. No significant difference was noted in this case. Scale bar, 50 μm.

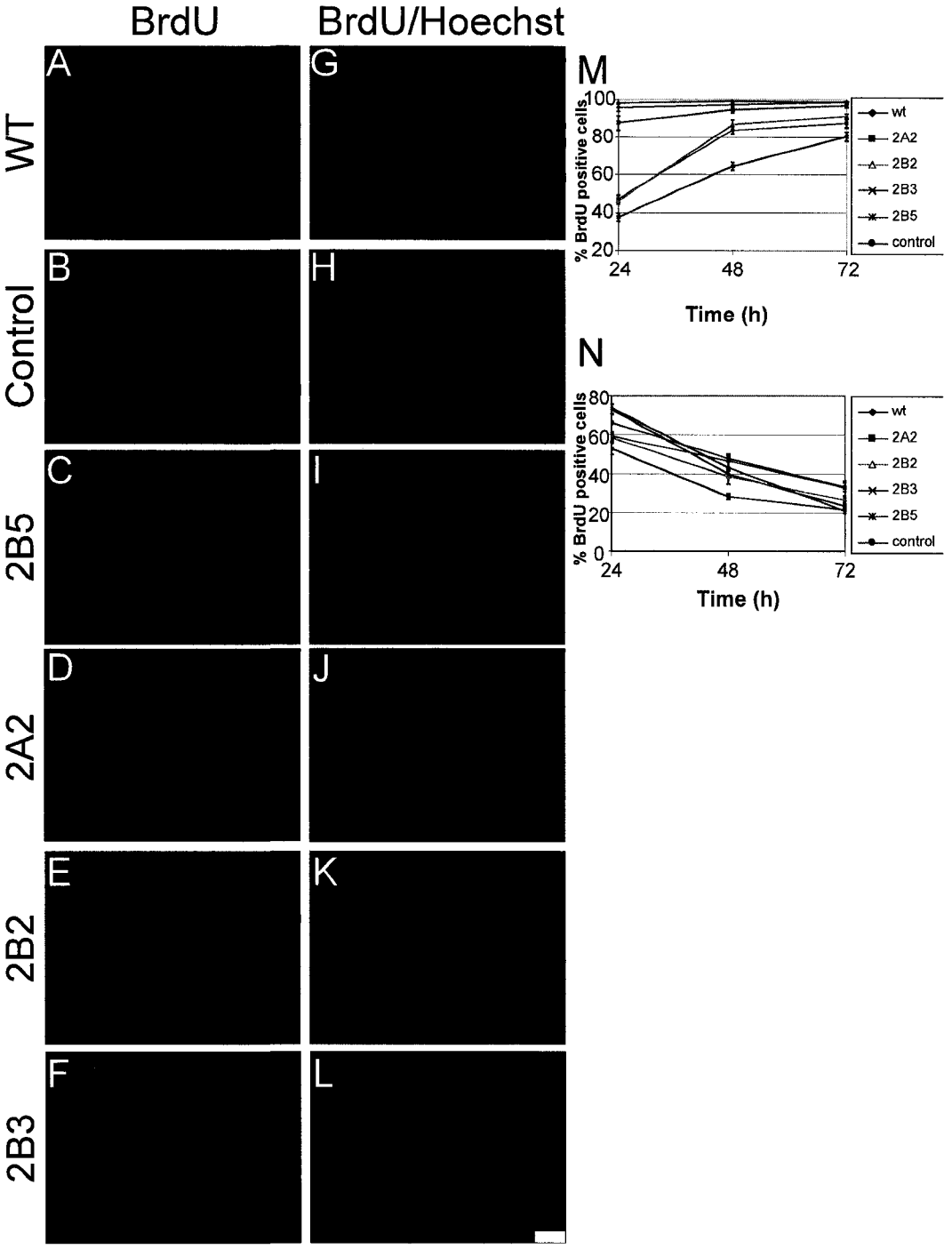
BrdU
BrdU/Hoechst
A
G
WT
B
H
Control
C
I
2B5
D
J
2A2
E
K
2B2
F
L
2B3
M
% BrdU positive cells
100
80
60
40
20
24
48
72
Time (h)
wt
2A2
2B2
2B3
2B5
control
N
% BrdU positive cells
80
60
40
20
0
24
48
72
Time (h)
wt
2A2
2B2
2B3
2B5
control

Fig. 3.4. Quantification of cell viability and incidence of cell death of WT C2C12 and the Smn shRNA C2C12 cell lines (LacZ, 2B5, 2A2, 2B2, 2B3). (A) Percentage of viable cells determined by LIVE/DEAD assay. (B) Percentage of TUNEL positive cells under normal conditions. (C) Percentage of TUNEL positive cells under stress conditions. For this assay, cells were treated with 2 μM staurosporine, a potent inducer of apoptosis, for 3 h. The extent of nuclear DNA breaks, characteristic of cells undergoing apoptosis, was measured using the TUNEL labeling assay. Smn-depleted cells did not display an increase in susceptibility to stress-induced apoptosis. DNase I-treated cells were the positive control for incidence of cells undergoing apoptosis.

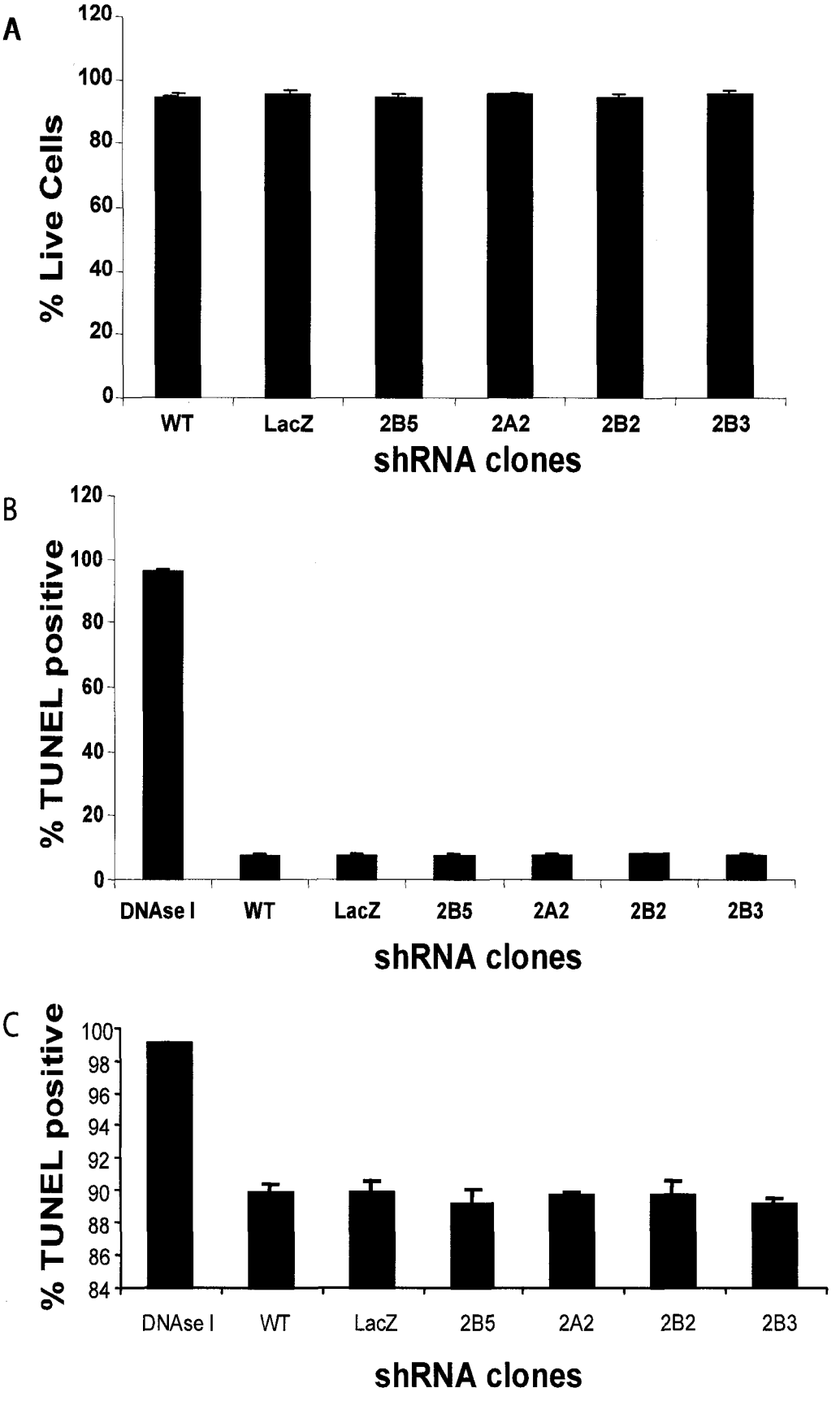
A
120
100
80
60
40
20
0
% Live Cells
WT
LacZ
2B5
2A2
2B2
2B3
shRNA clones
B
120
100
80
60
40
20
0
% TUNEL positive
DNAse I
WT
LacZ
2B5
2A2
2B2
2B3
shRNA clones
C
100
98
96
94
92
90
88
86
84
% TUNEL positive
DNAse I
WT
LacZ
2B5
2A2
2B2
2B3
shRNA clones

cells, it is possible that they may have a higher susceptibility to apoptosis following a stress-causing insult. We therefore treated the cells with staurosporine which is known to induce apoptosis in C2C12 cells. Our results showed similar numbers of TUNEL-positive cells in the Smn knockdown cells as compared to the *LacZ* and wild type cells after staurosporine treatment (Fig. 3.4).

3.1.4 Myotube formation and normal morphology is Smn-dependent

The extent of myogenic differentiation of wild type and SMN C2C12 shRNA cell lines at different time points in growth and differentiation media was determined by monitoring expression of myosin heavy chain (MHC), a marker of myogenic differentiation (Fig. 3.5). Although the Smn shRNA C2C12 cell lines appear to be expressing roughly the same number of MHC-positive cells, the morphology of the myotubes in these clones is not the same. Wild type myotubes show the expected elongated and multinucleated morphology (Figs. 3.5A, F). In contrast, there is an increase in the number of myotubes with single nuclei and in the presence of abnormal myotubes in the Smn shRNA C2C12 cell lines. This is particularly obvious as we examine the clone with the highest Smn knockdown, 2B3, in which myotubes appear small and have a 'bumpy' phenotype (Figs. 3.5E, J).

To quantify the differentiation potential of wild type and Smn C2C12 shRNA cell lines, cells were plated at 25,000 cells per well and then incubated in growth media for 24 h after which they were exposed to differentiation media for

Fig. 3.5. Differentiation potential of wild-type (WT) C2C12 and the Smn shRNA C2C12 cell lines (2B5, 2A2, 2B2, 2B3). Immunodetection of myosin heavy chain (MHC) and Hoechst labeling of cells from (A, F) WT C2C12, (B, G) 2B5 (55% knockdown), (C, H) 2A2 (65% knockdown), (D, I) 2B2 (75% knockdown), (E, J) and 2B3 (90% knockdown) that were confluent prior to exposure to low-serum media for 72 h. Note the abnormal morphology of myotubes, especially in clone 2B3, which has the highest Smn depletion. Scale bar, 50 μm.

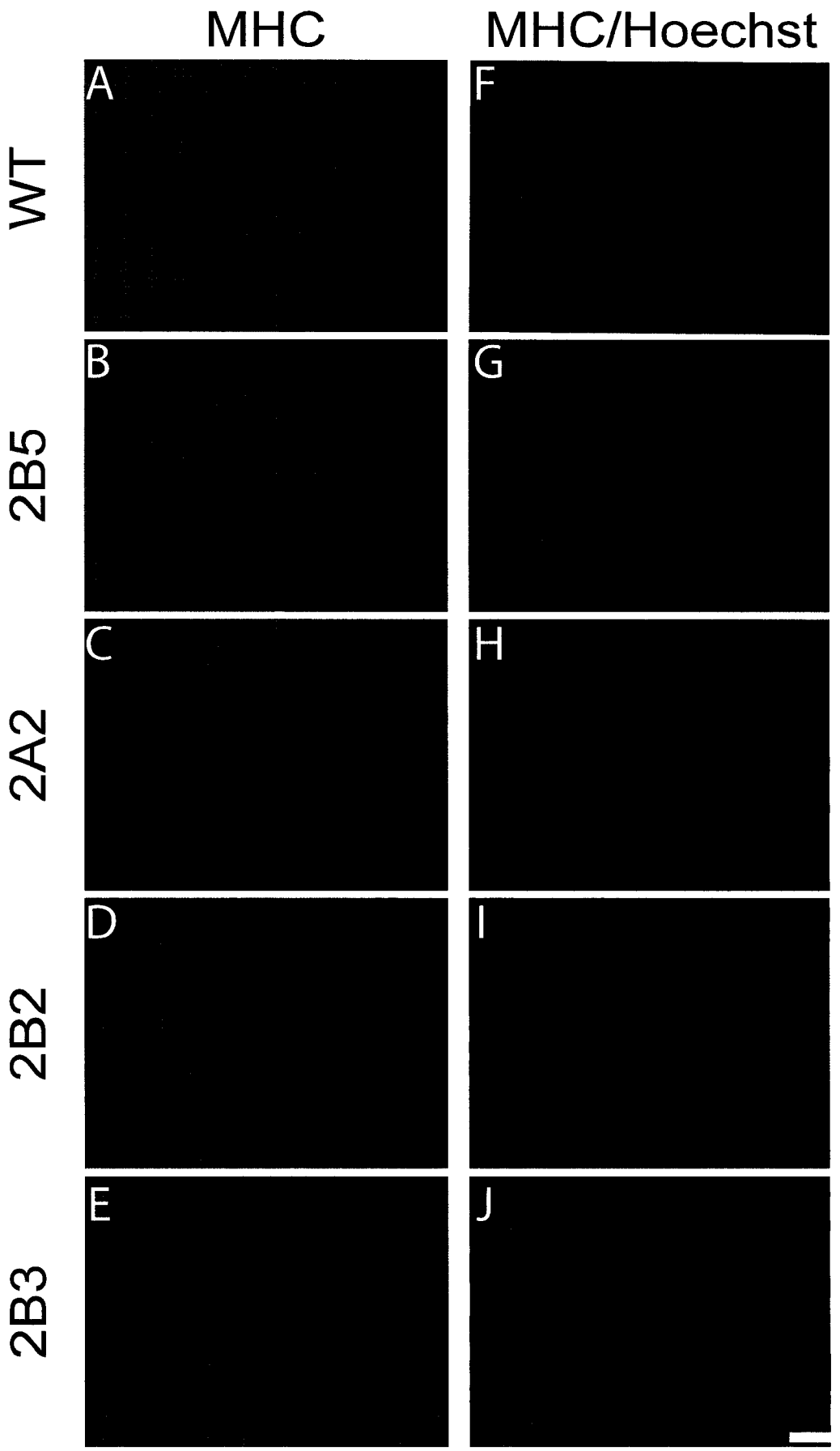
MHC
MHC/Hoechst
WT
2B5
2A2
2B2
2B3
A
B
C
D
E
F
G
H
I
J

24 or 72 h. Cells were then fixed at 24 h growth, 24 and 72 h differentiation, and immunostained for MHC. No MHC-positive cells were observed in wild type or the SMN C2C12 shRNA cell lines in growth conditions. After 24 h of exposure to low-serum media, wild type cells showed approximately 19% MHC-positive cells, whereas the Smn shRNA C2C12 cell lines showed a range of 10–17% MHC-positive cells (Fig. 3.6A). At this stage of the differentiation process, there was a significant reduction in the level of MHC-positive cells for clones 2B2 and 2B3, which had the most Smn knockdown. However, after 72 h of exposure to low-serum conditions, there was a general increase in the level of terminal differentiation, and there was no longer a significant difference among the various clones (Fig. 3.6A).

As mentioned above, the morphology of the myotubes was abnormal in the Smn shRNA cell lines. There was a reduction in the appearance of elongated and multinucleated myotubes in these cells. The severity of this phenotype increases with decreased levels of Smn and as differentiation progressed from 24 h (Fig. 3.6B) to 72 h (Fig. 3.6C). The extent of abnormality is especially dramatic in clone 2B3, which has the most severe Smn knockdown. The above experiments were repeated with NCAM, another myogenic marker, which is, expressed in low levels in myoblasts, and its expression increases approximately 4- to 5-fold in differentiating myoblasts. As with the MHC marker, similar results were obtained with NCAM (Figs. 3.7 and 3.8).

Fig. 3.6. Quantitative analysis of the differentiation potential of WT C2C12 and the Smn shRNA C2C12 cell lines (2B5, 2A2, 2B2, 2B3). Cells were plated at the same density and then exposed to low-serum media 24 h later. (A) Quantification of the number of MHC-positive cells at 24 h (*$P < 0.05$ for WT vs. 2B2 and 2B3) or 72 h differentiation. (B, C) Quantification of the frequency of normal versus abnormal myotubes at (B) 24 h or (C) 72 h differentiation (*$P < 0.05$ for WT vs. 2B5, 2A2, 2B2, and 2B3, indicated for normal myotubes; **$P < 0.05$ for WT vs. 2A2, 2B2, and 2B3, indicated for abnormal myotubes).

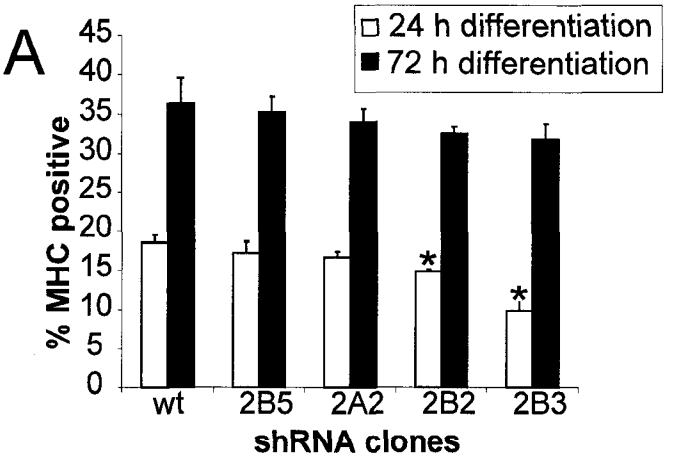
A
24 h differentiation
72 h differentiation
% MHC positive
45
40
35
30
25
20
15
10
5
0
wt
2B5
2A2
2B2
2B3
shRNA clones

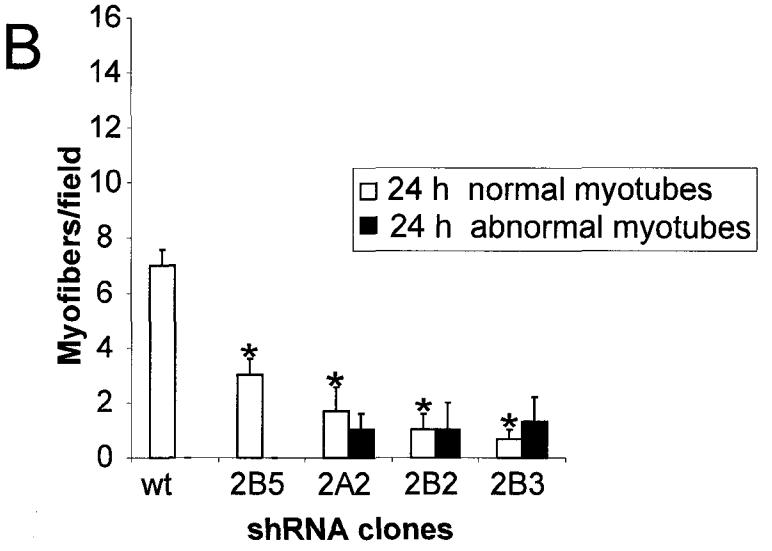
B
24 h normal myotubes
24 h abnormal myotubes
Myofibers/field
16
14
12
10
8
6
4
2
0
wt
2B5
2A2
2B2
2B3
shRNA clones

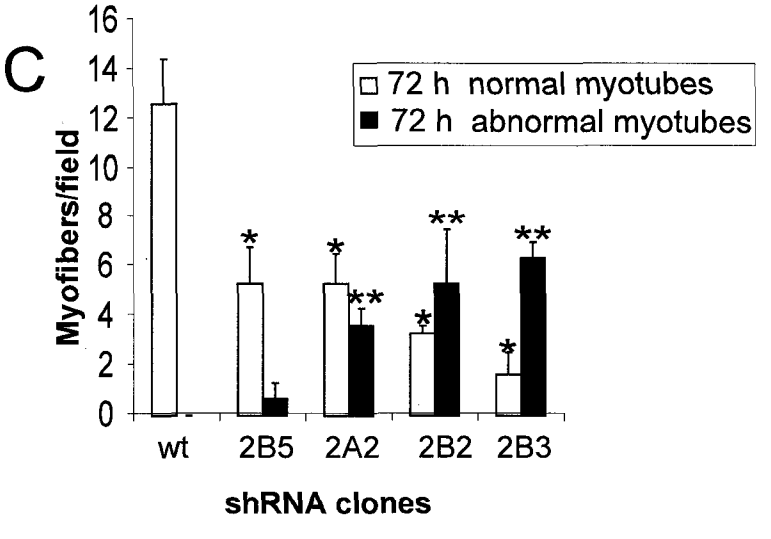
C
72 h normal myotubes
72 h abnormal myotubes
Myofibers/field
16
14
12
10
8
6
4
2
0
wt
2B5
2A2
2B2
2B3
shRNA clones

Fig. 3.7. Differentiation potential of wild-type (WT) C2C12 and the Smn shRNA C2C12 cell lines (2B5, 2A2, 2B2, 2B3). Immunodetection of NCAM and Hoechst labeling of cells from (A, F) WT C2C12, (B,G) LacZ (0% knockdown), (C, H) 2B5 (55% knockdown), (D, I) 2A2 (65% knockdown), (E, J) 2B2 (75% knockdown), and (F, K) 2B3 (90% knockdown) that were confluent prior to exposure to low-serum media for 72 h. Note the abnormal morphology of myotubes, especially in clone 2B3, which has the highest Smn depletion. Scale bar, 50 μm.

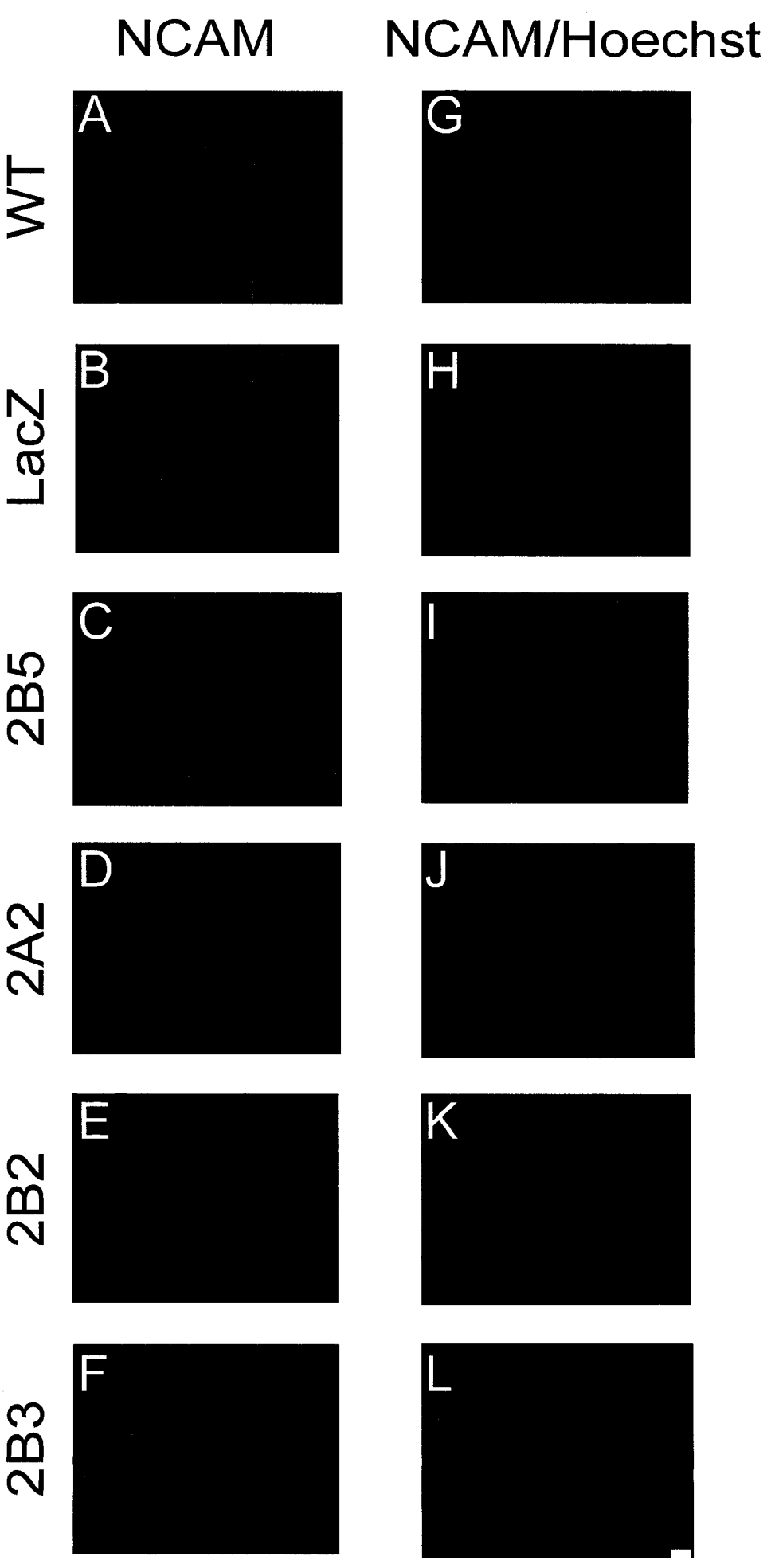
NCAM
NCAM/Hoechst
WT
LacZ
2B5
2A2
2B2
2B3
A
B
C
D
E
F
G
H
I
J
K
L

Fig. 3.8. Quantitative analysis of the differentiation potential of WT C2C12, LacZ shRNA C2C12, and the Smn shRNA C2C12 cell lines (2B5, 2A2, 2B2, 2B3). Cells were plated at the same density and then exposed to low-serum media 24 h later. (A) Quantification of the number of NCAM-positive cells at 24 h or 72 h differentiation. (B, C) Quantification of the frequency of normal versus abnormal myotubes at (B) 24 h or (C) 72 h differentiation (*$P < 0.05$ for WT vs. 2B5, 2A2, 2B2, and 2B3, indicated for normal myotubes; **$P < 0.05$ for WT vs. 2A2, 2B2, and 2B3, indicated for abnormal myotubes).

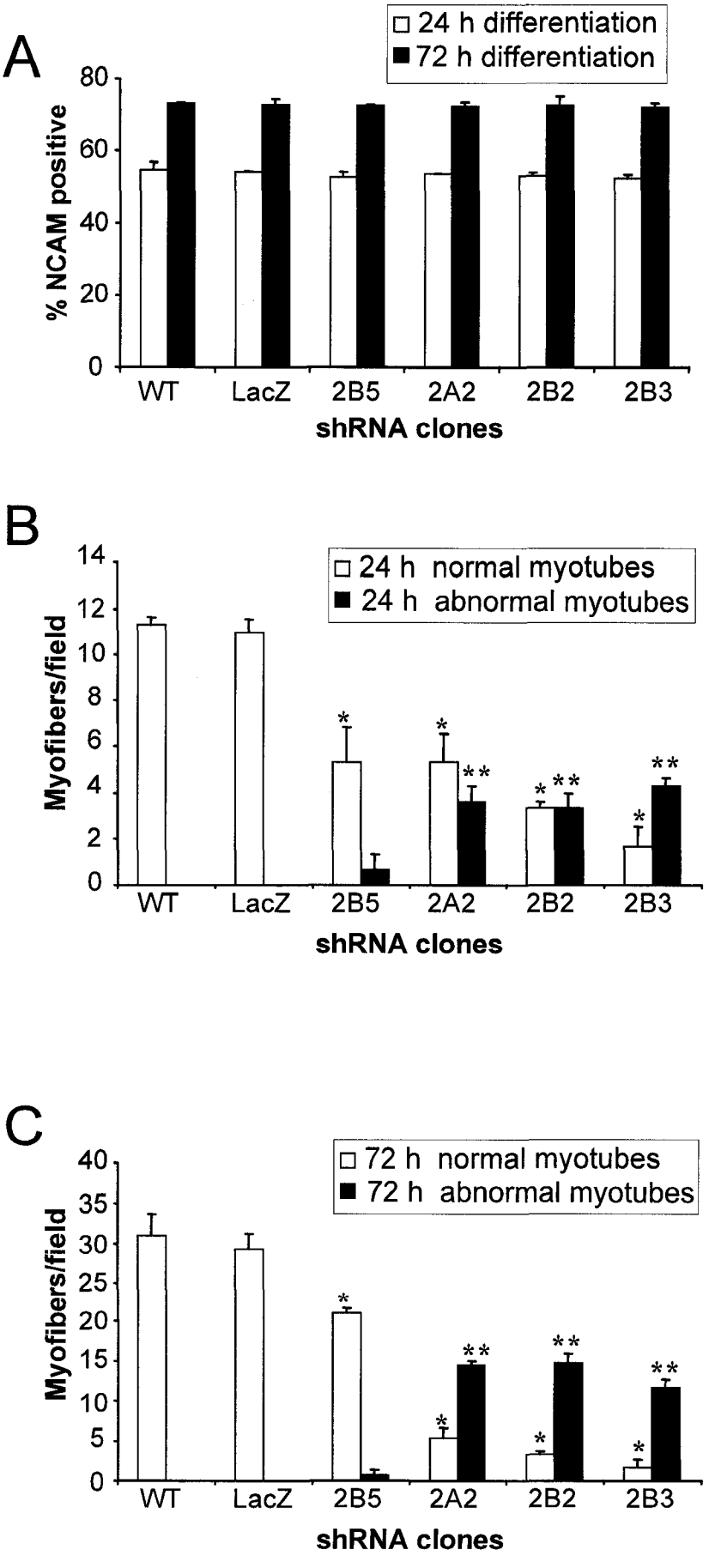
A
□ 24 h differentiation
■ 72 h differentiation
% NCAM positive
0
20
40
60
80
WT
LacZ
2B5
2A2
2B2
2B3
shRNA clones
B
□ 24 h normal myotubes
■ 24 h abnormal myotubes
Myofibers/field
0
2
4
6
8
10
12
14
WT
LacZ
2B5
2A2
2B2
2B3
shRNA clones
C
□ 72 h normal myotubes
■ 72 h abnormal myotubes
Myofibers/field
0
5
10
15
20
25
30
35
40
WT
LacZ
2B5
2A2
2B2
2B3
shRNA clones

3.1.5 Smn knockdown affects myoblast fusion

The fusion potential of myocytes was determined by counting the average number of nuclei per fiber and determining the prevalence of myocytes with ≥2 nuclei. At 24 h differentiation, the average number of nuclei per fiber was 3 for wild type cells and for the 2B5 cells and 1 for the 2A2, 2B2, and 2B3 cells (Fig. 3.9A). At 72 h differentiation, the average number of nuclei per fiber increased for wild type to 4 nuclei but does not increase for the Smn shRNA C2C12 cell lines (Fig. 3.9A). Only wild type and 2B5 cultures showed any myotubes with 2 or more nuclei at 24 h differentiation (Fig. 3.9B). At 72 h differentiation, the prevalence of myotubes with 2 or more nuclei increases, but Smn shRNA C2C12 cell lines still predominantly show myofibers with 1 nuclei (Fig. 3.9C). The fusion index was also calculated for these cultures. The fusion index for wild type C2C12 cells was 97 ± 1%, whereas the fusion index for the Smn shRNA C2C12 cell lines decreased and was 92 ± 1%, 56 ± 2%, 31 ± 1%, and 19 ± 1% for 2B5, 2A2, 2B2, and 2B3, respectively. Our results suggest that the knockdown of Smn disrupts myotube fusion and formation. To rule out the possibility that the observed defects are due to differences in cell confluency prior to exposure to low serum, we repeated the experiments, but this time we allowed all cells to grow to confluency prior to inducing differentiation. This change in the experimental approach did not improve the fusion defect or correct the abnormal morphology of the myotubes (Fig. 3.10 and Fig. 3.11). The fusion index was calculated and for wild type cells was 97 ± 1%, and, for the Smn shRNA C2C12

Fig. 3.9. Quantitative analysis of the fusion potential of WT C2C12 and Smn shRNA C2C12 cell lines (2B5, 2A2, 2B2, 2B3). Cells were plated at the same density and then exposed to low-serum media 24 h later. (A) Calculation of the average number of nuclei contained in the myotubes (MHC-positive) at 24 h or 72 h differentiation (*$P < 0.05$ for WT vs. 2A2, 2B2, and 2B3). (B, C) Prevalence of myofibers containing 2 or more nuclei when cells were exposed to low-serum media for (B) 24 h or (C) 72 h. Note the higher prevalence of myofibers with 2 nuclei or a single nucleus in the Smn shRNA cell lines.

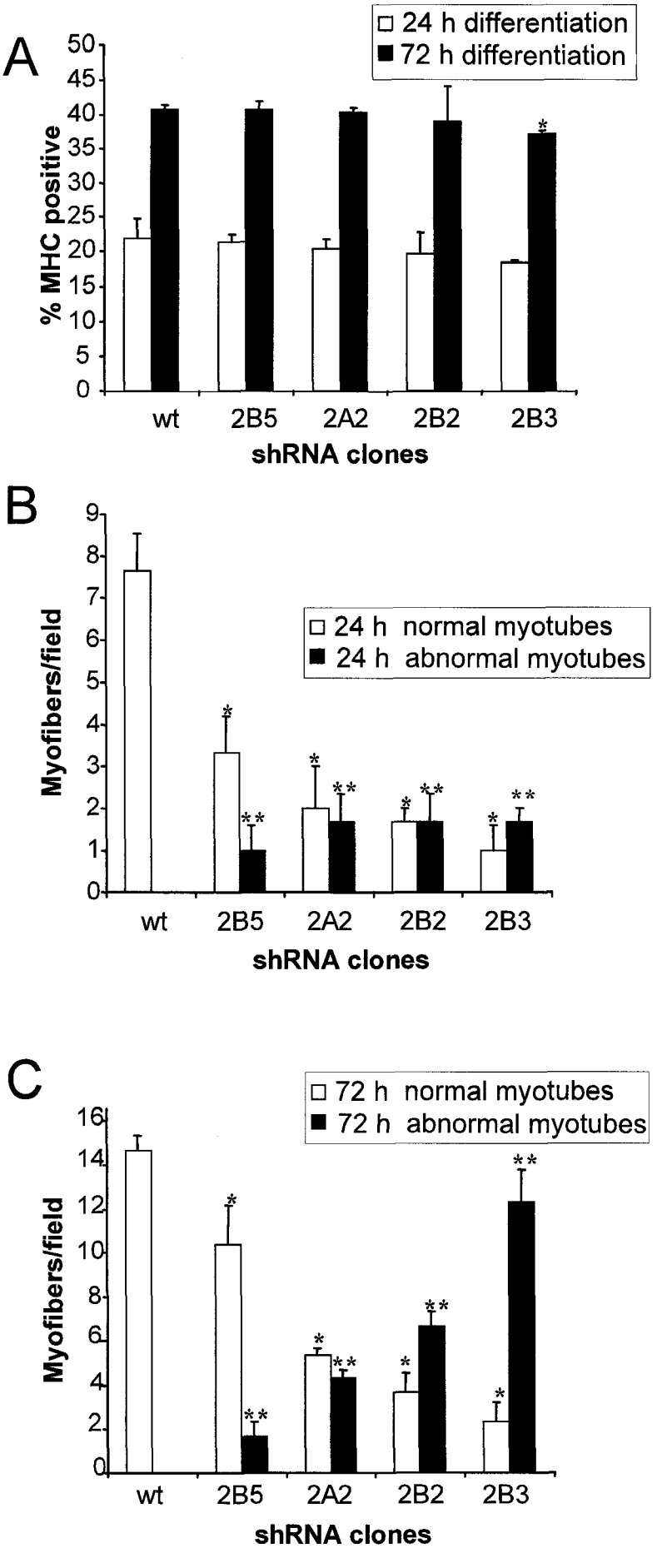
A
□ 24 h differentiation
■ 72 h differentiation
% MHC positive
50
45
40
35
30
25
20
15
10
5
0
wt
2B5
2A2
2B2
2B3
shRNA clones
B
Myofibers/field
9
8
7
6
5
4
3
2
1
0
□ 24 h normal myotubes
■ 24 h abnormal myotubes
wt
2B5
2A2
2B2
2B3
shRNA clones
C
Myofibers/field
16
14
12
10
8
6
4
2
0
□ 72 h normal myotubes
■ 72 h abnormal myotubes
wt
2B5
2A2
2B2
2B3
shRNA clones

Fig. 3.10. Quantitative analysis of the differentiation potential of WT C2C12 and the Smn shRNA C2C12 cell lines (2B5, 2A2, 2B2, 2B3) under confluent conditions. Cells were allowed to grow to confluency and then exposed to low-serum media 24 h later. (A) Quantification of the number of MHC-positive cells at 24 h or 72 h differentiation (*$P < 0.05$ for WT vs. 2B3). (B, C) Quantification of the frequency of normal versus abnormal myotubes at (B) 24 h or (C) 72 h differentiation (*$P < 0.05$ for WT vs. 2B5, 2A2, 2B2, and 2B3, indicated for normal myotubes; **$P < 0.05$ for WT vs. 2B5, 2A2, 2B2, and 2B3, indicated for abnormal myotubes).

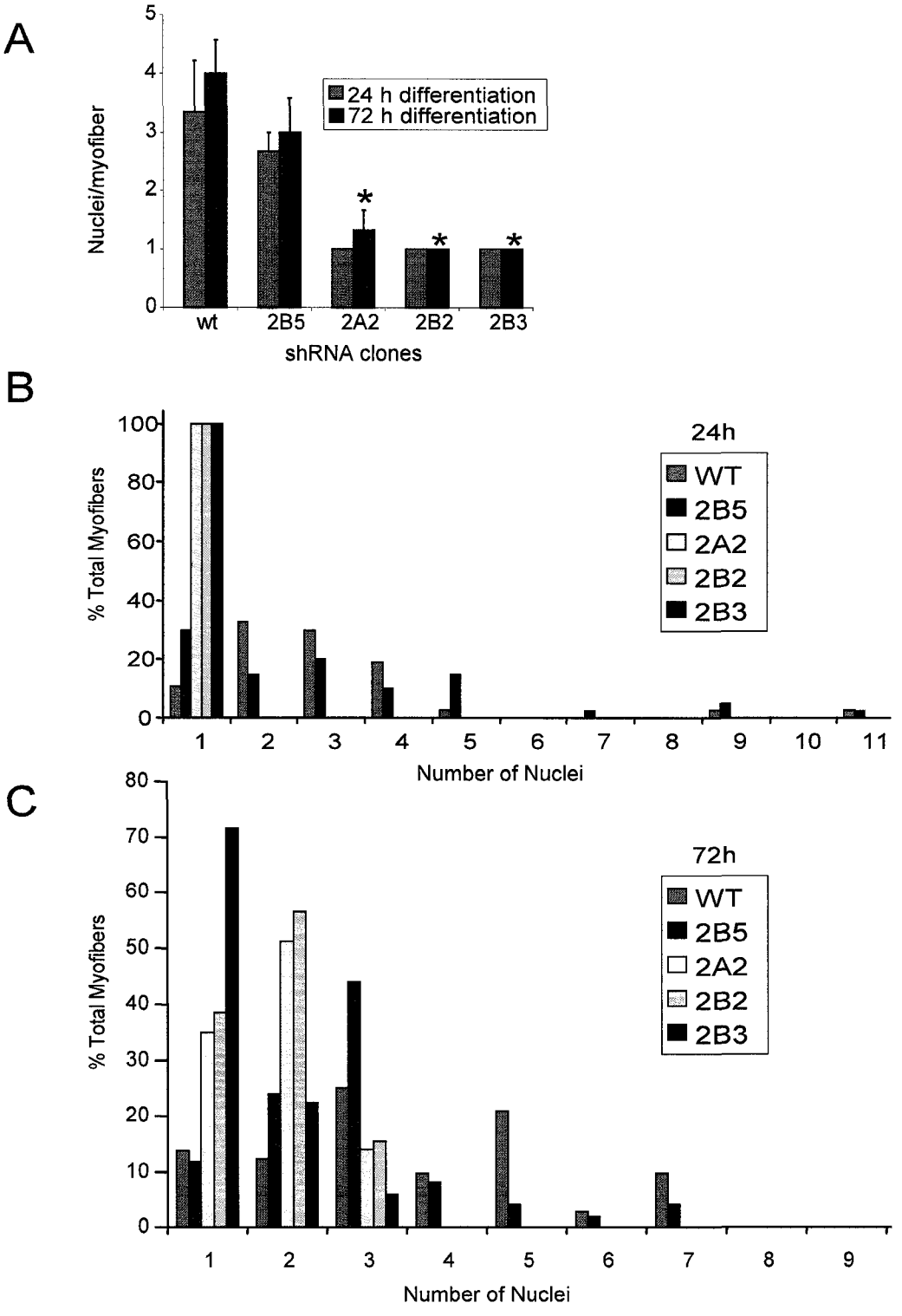
A
Nuclei/myofiber
24 h differentiation
72 h differentiation
wt
2B5
2A2
2B2
2B3
shRNA clones
B
% Total Myofibers
24h
WT
2B5
2A2
2B2
2B3
Number of Nuclei
C
% Total Myofibers
72h
WT
2B5
2A2
2B2
2B3
Number of Nuclei

Fig. 3.11. Quantitative analysis of the fusion potential of WT C2C12 and Smn shRNA C2C12 cell lines (2B5, 2A2, 2B2, 2B3) under confluent conditions. Cells were allowed to grow to confluency and then exposed to low-serum media 24 h later. (A) Calculation of the average number of nuclei contained in the myotubes (MHC-positive) at 24 h differentiation (*$P < 0.05$ for WT vs. 2A2, 2B2, and 2B3) or 72 h differentiation (**$P < 0.05$ for WT vs. 2B5, 2A2, 2B2, and 2B3). (B, C) Prevalence of myofibers containing 2 or more nuclei when cells were exposed to low-serum media for (B) 24 h or (C) 72 h. Note the higher prevalence of myofibers with 2 nuclei or a single nucleus in the Smn shRNA cell lines.

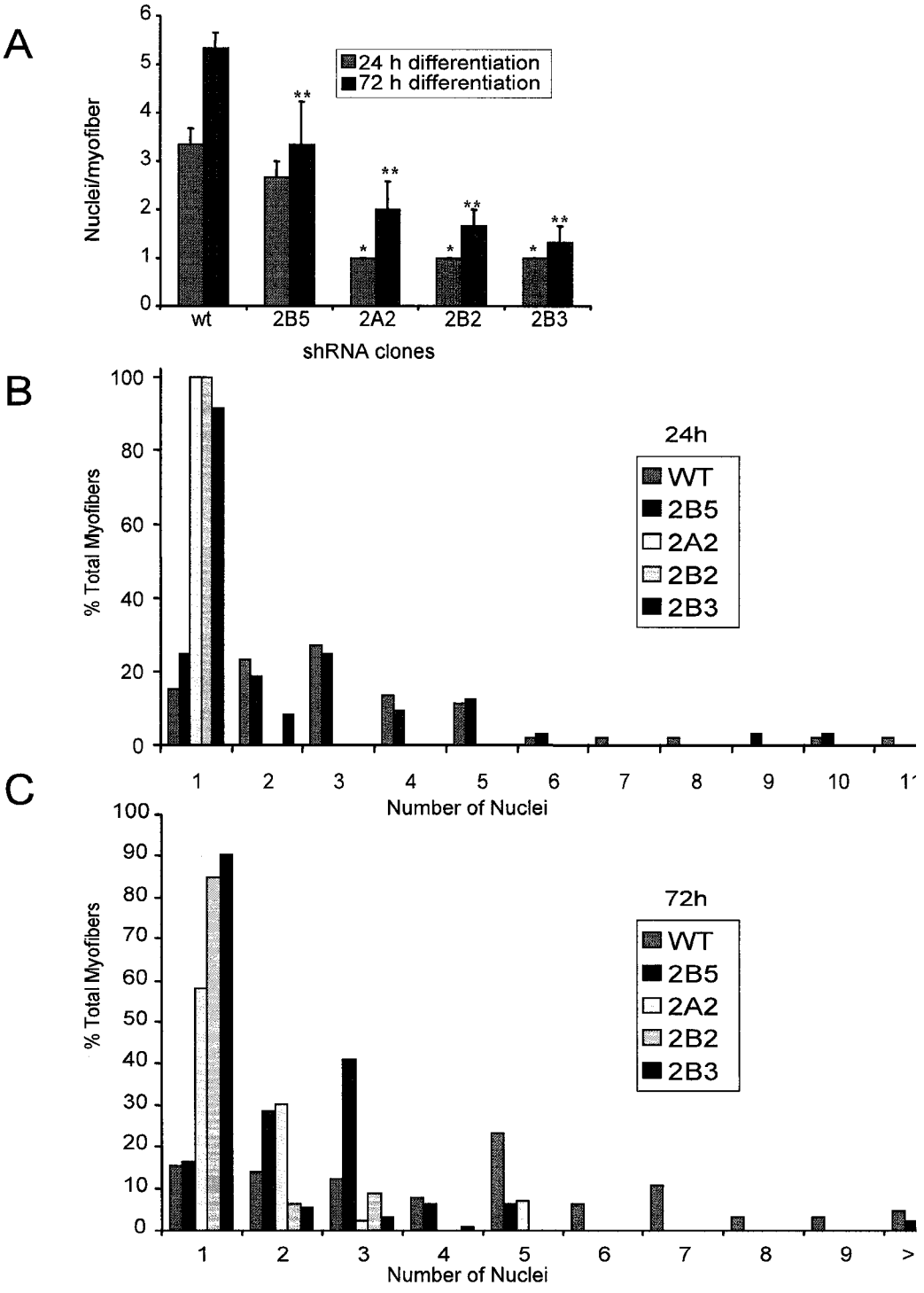
A
24 h differentiation
72 h differentiation
Nuclei/myofiber
0
1
2
3
4
5
6
wt
2B5
2A2
2B2
2B3
shRNA clones
B
24h
WT
2B5
2A2
2B2
2B3
% Total Myofibers
0
20
40
60
80
100
1
2
3
4
5
6
7
8
9
10
Number of Nuclei
C
72h
WT
2B5
2A2
2B2
2B3
% Total Myofibers
0
10
20
30
40
50
60
70
80
90
100
1
2
3
4
5
6
7
8
9
>
Number of Nuclei

cell lines, it decreased to 94 ± 1%, 57 ± 3%, 33 ± 1%, and 20 ± 1% for 2B5, 2A2, 2B2, and 2B3, respectively. Thus, these results demonstrate that the lack of fusion and the presence of abnormal myotubes are not due to differences in cell number but rather to the depletion of Smn itself. These experiments were also repeated with the NCAM antibody, and similar results were obtained (Fig. 3.12). The fusion index was calculated as above, and similar results were obtained.

Fig. 3.12. Quantitative analysis of the fusion potential of WT C2C12, LacZ shRNA C2C12, and Smn shRNA C2C12 cell lines (2B5, 2A2, 2B2, 2B3). Cells were plated at the same density and then exposed to low-serum media 24 h later. (A) Calculation of the average number of nuclei contained in the myotubes (NCAM-positive) at 24 h (*$P < 0.05$ for WT vs. 2B5, 2A2, 2B2, and 2B3) or 72 h differentiation (**$P < 0.05$ for WT vs. 2B5, 2A2, 2B2, and 2B3). (B, C) Prevalence of myofibers containing 2 or more nuclei when cells were exposed to low-serum media for (B) 24 h or (C) 72 h. Note the higher prevalence of myofibers with 2 nuclei or a single nucleus in the Smn shRNA cell lines.

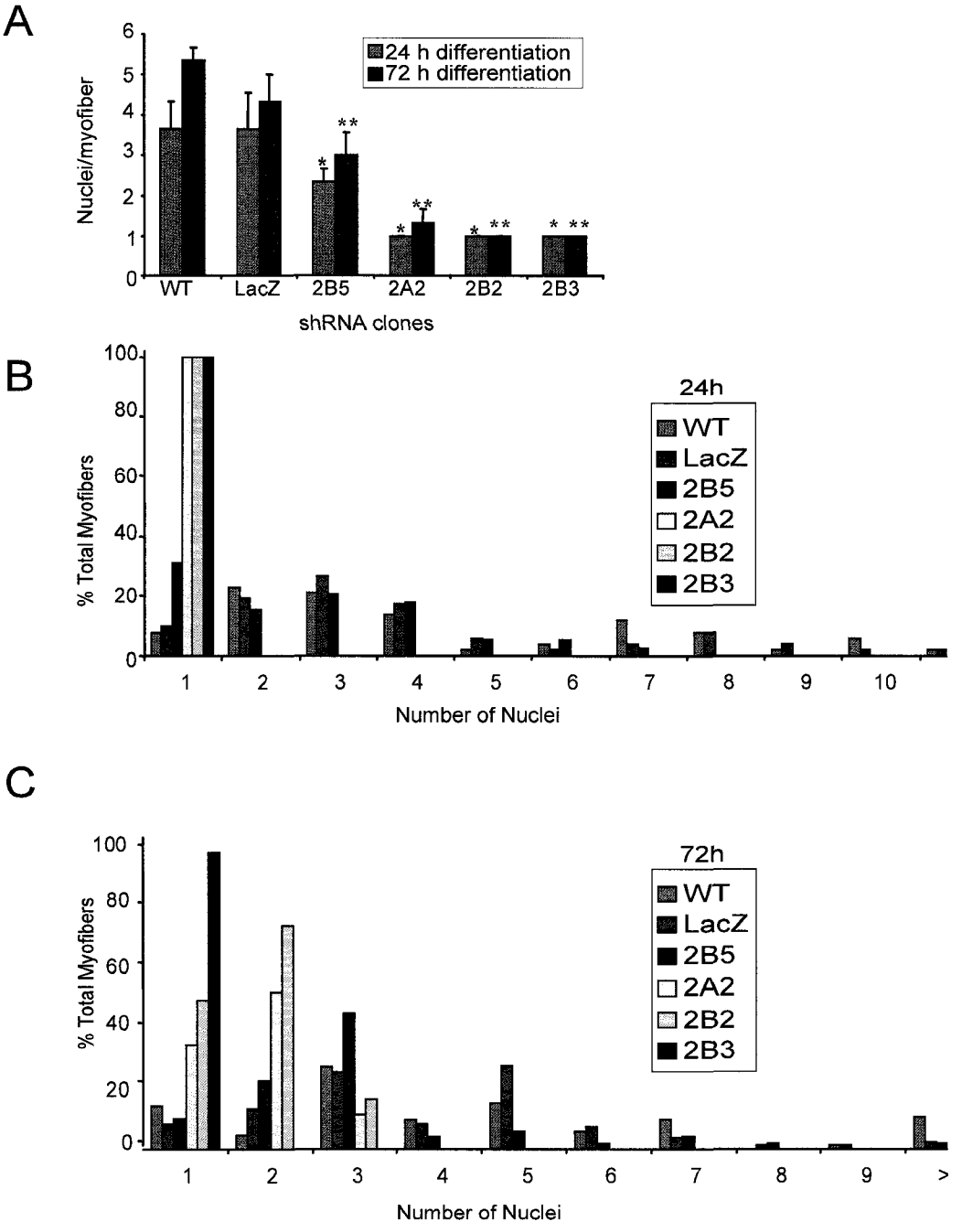
A
24 h differentiation
72 h differentiation
Nuclei/myofiber
0
1
2
3
4
5
6
WT
LacZ
2B5
2A2
2B2
2B3
shRNA clones
B
24h
WT
LacZ
2B5
2A2
2B2
2B3
% Total Myofibers
0
20
40
60
80
100
1
2
3
4
5
6
7
8
9
10
Number of Nuclei
C
72h
WT
LacZ
2B5
2A2
2B2
2B3
% Total Myofibers
0
20
40
60
80
100
1
2
3
4
5
6
7
8
9
>
Number of Nuclei

3.2 DISCUSSION

Previous work has demonstrated that Smn is an essential protein and complete loss of function alleles in mice is pre-implantation lethal (Schrank, Gotz et al. 1997). However, in SMA, patients have residual SMN protein from the *SMN2* gene, and this is sufficient to allow for proper development of the embryo and fetus to term. Specific cell types are more sensitive to the decrease in SMN, and this leads to onset of disease pathogenesis late during gestation and after birth. The debate as to which cell types contribute to SMA pathogenesis is ongoing, but it is clear that both motor neurons and skeletal muscle cells are implicated (Hsieh-Li, Chang et al. 2000; Monani, Sendtner et al. 2000; Cifuentes-Diaz, Frugier et al. 2001; Cifuentes-Diaz, Nicole et al. 2002). In this study, we have used the short hairpin RNA approach to selectively reduce Smn expression in C2C12 myoblasts. Our goal was to create muscle cell lines with different levels of Smn protein knockdown to allow us to study the importance of Smn dosage in muscle cell behaviour in the absence of any neuronal input. We have succeeded in establishing stable lines of C2C12 muscle cells with varying degrees of Smn protein knockdown. The range of Smn depletion was from as low as 10% to as high as 90%. This range of Smn expression is also found in patients who suffer from SMA (Coovert, Le et al. 1997; Lefebvre, Burlet et al. 1997). As a result, we have generated a hypomorphic series which represents a cell culture model of SMA, thereby replicating the human situation where decrease in SMN dosage has been directly correlated with disease severity (Lefebvre, Burlet et al. 1997).

Although the mouse models for SMA that have been generated (Braun, Croizat et al. 1995; Hsieh-Li, Chang et al. 2000; Monani, Sendtner et al. 2000; Cifuentes-Diaz, Nicole et al. 2002) are useful for elucidating the pathology of SMA, our cell culture model provides us with an opportunity to study the function of SMN directly in a specific cell type.

3.2.1 An inverse correlation between Smn levels and gem formation

In the nucleus, SMN is concentrated in structures called gems where it has been predicted to be involved in transcription and pre-mRNA splicing (Liu and Dreyfuss 1996). In cells and tissues from SMA patients, the expression of SMN and the number of gems are greatly reduced (Coovert, Le et al. 1997). We have shown that knockdown of Smn in C2C12 cells also results in a corresponding decrease in gem number. We have demonstrated a striking inverse correlation between the amount of Smn knockdown and the number of gems observed. Thus, the shRNA approach has proven to be useful in mimicking the human condition at the cellular level.

3.2.2 Decrease in Smn affects myoblast proliferation and myotube formation

The rates of myoblast proliferation in wild type and control (*LacZ*) shRNA cells were much higher than in the Smn knockdown shRNA C2C12 cell lines 2A2, 2B2, and 2B3. However, cell line 2B5, which has a knockdown of Smn of only 55%, had roughly the same proliferation rate as for the wild type and control cells. Thus, this result demonstrates that cells expressing low levels of Smn exhibit slow

growth properties proportional to the amount of Smn they harbor. This is reminiscent of what has previously been reported for a chicken pre-B lymphoma cell line (DT-40) in which the endogenous *Smn* gene has been disrupted by homologous recombination (Wang and Dreyfuss 2001). Smn has been restored in these cells using a tetracycline-repressible promoter system driving a chicken *Smn* cDNA. Upon treatment with tetracycline, there is a depletion of Smn protein and a concomitant decrease in growth rate (Wang and Dreyfuss 2001). However, in contrast to the latter study, we have not observed an increase in the incidence of cell death under normal and stress-induced conditions in Smn-depleted C2C12 cells.

Myoblast differentiation and fusion are essential for proper muscle development, regeneration, and maintenance. Our experiments have shown that depletion of Smn does not appear to have a major impact on the ability of C2C12 cells to differentiate down the myogenic lineage after serum withdrawal. Indeed, the number of differentiated cells was roughly the same between wild type and the Smn shRNA C2C12 cell lines as measured by the number of MHC- and NCAM-positive cells. This is not surprising since muscle differentiation has occurred in SMA patients and in mouse models where Smn has been completely removed in a muscle-specific manner (Cifuentes-Diaz, Frugier et al. 2001). However, what was striking was our observation of malformed myotubes and altered fusion potential in the Smn shRNA cell lines. We have noted single nuclei myotubes and abnormal myotubes that are small and have a 'bumpy' phenotype. The severity of this phenotype increases with increased Smn depletion and as differentiation

progresses from 24 h to 72 h (Fig. 3.9). The extent of abnormality is especially dramatic in clone 2B3, which has the most severe Smn knockdown. These abnormalities do not differ whether the cells were confluent prior to exposure to low-serum media or not. Thus, Smn depletion in C2C12 cells results in their inability to fuse correctly to form multinuclear myotubes. Of course, this observation would have to be validated in primary myoblasts, but it is noteworthy that our data correlate well with a recent study showing that cultured skeletal muscle cells from SMA patients have fusion abnormalities (Arnold, Gueye et al. 2004). As well, in a separate study, it was shown that muscle satellite cells from SMA patients were unable to fuse into myotubes, but when these cells are co-cultured with normal muscle satellite cells prior to inducing fusion, these mixed cultures can fuse and form heteromyotubes (Guettier-Sigrist, Coupin et al. 1998). These heteromyotubes were then innervated by rat spinal cord explants without degeneration (Guettier-Sigrist, Coupin et al. 1998). Thus, SMN dosage in muscle is important, and the survival of both muscle and nerve may depend on an exchange of signals between muscle and nerves. Therefore, our model can now be used to study the possible signals that are occurring between muscle and nerve and to examine how Smn dosage affects these signals.

Another possible explanation for the abnormal myoblast fusion and the altered myotube morphology is that there are factors involved in myotube formation that may be absent in the Smn-depleted C2C12 cells either due to defects in mRNA splicing or to transcriptional repression. Both of these possibilities have a foundation since the SMN heteromeric complex is essential for

spliceosomal snRNP biogenesis in the cytoplasm and for pre-mRNA splicing in the nucleus (Fischer, Liu et al. 1997; Pellizzoni, Kataoka et al. 1998; Buhler, Raker et al. 1999; Pellizzoni, Charroux et al. 2001; Selenko, Sprangers et al. 2001). As well, SMN has also been shown to interact with proteins like Bcl-2, p53, transactivator FUSE binding protein, profilins, zinc finger protein ZPR1, RNA helicase A, and RNA polymerase II (Iwahashi, Eguchi et al. 1997; Giesemann, Rathke-Hartlieb et al. 1999; Williams, Hamilton et al. 2000; Gangwani, Mikrut et al. 2001; Pellizzoni, Baccon et al. 2001; Pellizzoni, Charroux et al. 2001; Young, Day et al. 2002), suggesting a possible role in apoptosis, transcription, and other cellular processes. It should be noted, however, that the molecular pathways underpinning these functions for SMN remain to be elucidated. Through any one of these pathways, Smn reduction may affect factors such as the sarcolemmal-associated proteins (SLAPs), which get alternatively spliced (Wielowieyski, Sevinc et al. 2000) and are involved in myotube formation (Guzzo, Wigle et al. 2004). It has been shown that the deregulation of SLAPs in myoblasts results in inhibition of fusion without affecting the expression of muscle-specific genes (Guzzo, Wigle et al. 2004). Thus, deregulation of factors like the SLAPs in Smn-depleted C2C12 cells may be the reason why there is a problem in myoblast fusion and why myotube morphology is compromised.

In conclusion, we have created a hypomorphic series of Smn knockdown C2C12 cells that provides us with a muscle cell culture model for spinal muscular atrophy. The characterization of these cells has led us to a better understanding of the impact of Smn dosage on muscle cell behaviour and in particular points to

defects in myotube maturation. These studies add support to the view that, in addition to a primary defect in motor neurons, SMA patients have intrinsic abnormalities in their muscle cells that contribute to the overall disease pathogenesis. Future studies will be directed to the characterization of molecular changes that result from Smn knockdown to different levels in our C2C12 cell culture model. In the long term, this cell culture model will reveal important steps in the pathophysiology of SMA and help to identify targets for therapy.

4.0 Creating Smn knockdown mice using shRNA

Unlike the human gene, the mouse *Smn* gene is present as a single copy. Consequently, knocking out the gene through homologous recombination in embryonic stem cells causes early embryonic lethality. The null mouse is not informative in terms of understanding SMA disease pathology and etiology. Since SMA is a disorder with ranging severity and the amount of SMN protein expressed in each individual is inversely correlated with the severity of SMA, SMA can be considered to be a dose-dependent disorder. Thus developing mice with intermediate/mild phenotypes is critical for our ability to assess the pathogenesis of SMA. As discussed in the Introduction, there are SMA mouse models that resemble the more severe and milder types of human SMA, but it would be beneficial to generate mice with intermediate phenotypes. To gain a better understanding of the pathogenesis of SMA and this dose-dependent effect, we have used the short interference RNA (siRNA) approach to develop Smn hypomorphs in mice. We used the shRNA constructs against SMN from our previous study (see Chapter 3) to generate knockdown mice by a transgenic approach (microinjection into one-cell stage mouse embryos), as well as by generating stable embryonic stem cell clones with varying Smn knockdown, and producing mouse chimeras by blastocyst injections. These various mouse models were assessed in this study.

4.1 RESULTS

4.1.1 Generation of transgenic Smn knockdown founder embryos

To generate Smn-depleted embryos, the sh_Smn_519 and sh_Smn_866 shRNA constructs were microinjected into one-cell stage mouse embryos. Initially we analyzed founder embryos at E11.5 for morphological defects and for protein knockdown. Several of the embryos were identified as being transgenic by PCR genotyping and some of these were morphologically abnormal or developmentally retarded (Fig. 4.1). The morphological abnormalities these transgenic mice displayed included twisted spinal cords, brain haemorrhaging and smaller size. As well, Smn protein levels were reduced in the embryos with morphological abnormalities (Fig. 4.2). Transgenic embryos with little to no Smn reduction did not show any apparent abnormalities.

We further assessed whether Smn may have a role in specifying cranial nerve patterning and axonal growth by analyzing axonal tracts in the wild type and transgenic founder embryos from different founder litters from above by whole mount immunostaining at E10.5 with anti-neurofilament antibodies (2H3) (Fig. 4.3). Although most cranial nerves appear unaffected in the wild type, some of the transgenic embryos displayed abnormal patterning of the glossopharyngeal nerve (IX) and the vagus nerve (X) such that these nerves appeared to be partially fused in 34 out of 47 transgenic embryos. The wild type and some of the transgenic embryos did not show the merging of nerves IX and X, and maintained a gap between these two nerves. Those transgenic embryos

Fig. 4.1. sh_Smn_519 and sh_Smn_866 transgenic embryos show morphological abnormalities. Morphological assessment of sh_Smn_519 and sh_Smn_866 transgenic embryos (E11.5). sh_Smn_519 transgenic embryos (A,B) show delayed growth and/or craniofacial deformities next to a wild type embryo (WT) from the same litter. sh_Smn_866 transgenic embryos (C) show a twisted spinal cord and delayed growth.

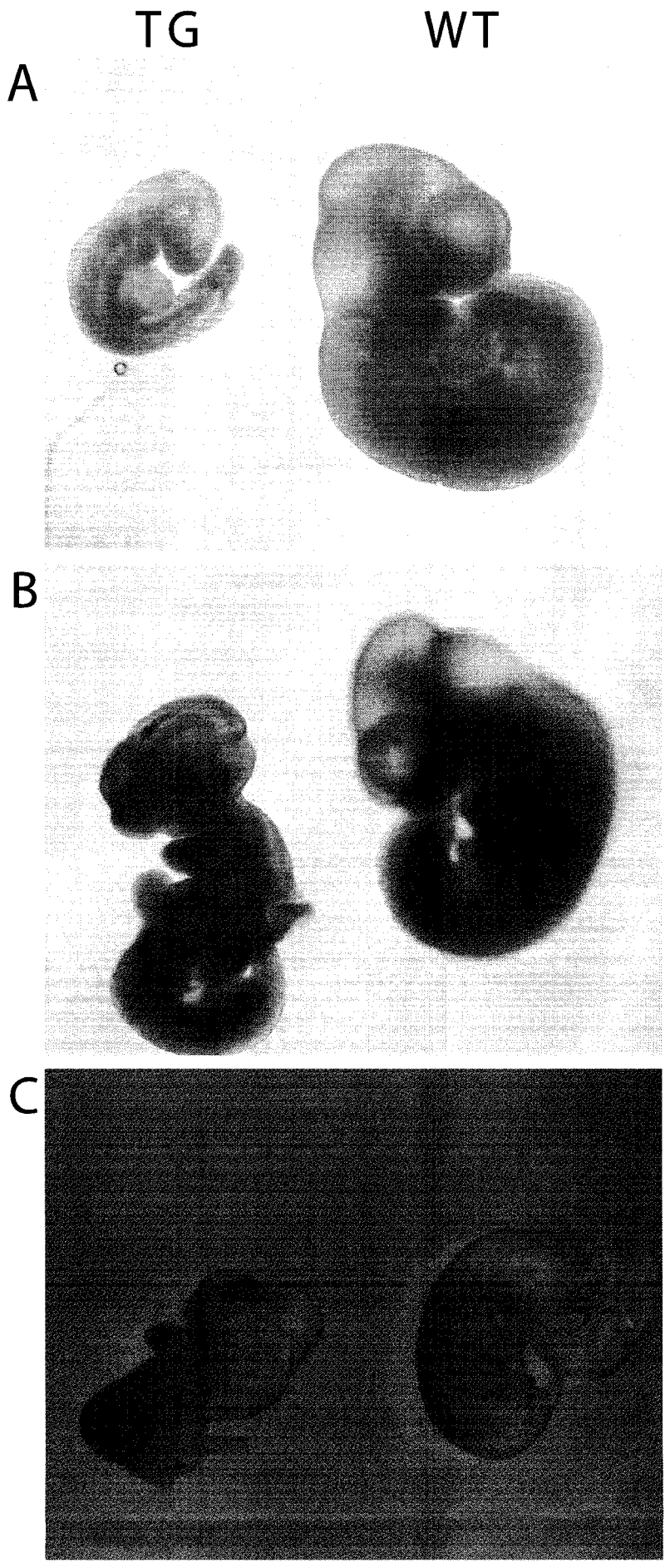
TG
WT
A
B
C

Fig. 4.2. Decreased Smn expression in sh_Smn_519 and sh_Smn_866 transgenic embryos. Western blot analysis of sh_Smn_519 (A) and sh_Smn_866 (B) transgenic mouse embryo tissue lysates were resolved on 10% SDS-PAGE. Smn levels were determined by blotting with an anti-Smn antibody (lower band); anti-actin (upper band) was used as a loading control. The knockdown of Smn in these embryos ranged from 5-75%. Asterisks indicate the embryos that have shown abnormalities.

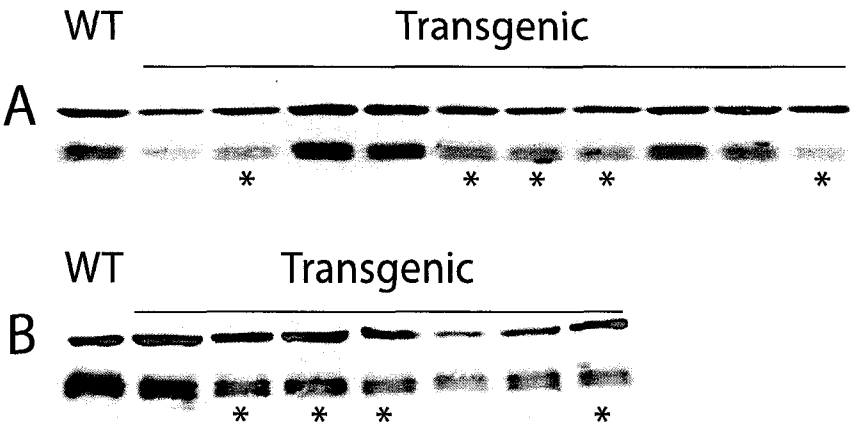
WT
Transgenic
A
*
*
*
*
*
WT
Transgenic
B
*
*
*
*

Fig. 4.3. Whole mount neurofilament immunostaining of sh_Smn_519 and sh_Smn_866 transgenic embryos at E10.5 shows abnormal nerve patterning. (A) WT embryo. Cranial nerves IX, X, and XI are indicated; (B, C) sh_Smn_519 transgenic embryos. Insets highlight merging of cranial nerves IX and X (indicated by an *); (D) sh_Smn_866 transgenic embryo. Abnormal cranial nerve patterning is shown in the inset (arrow).

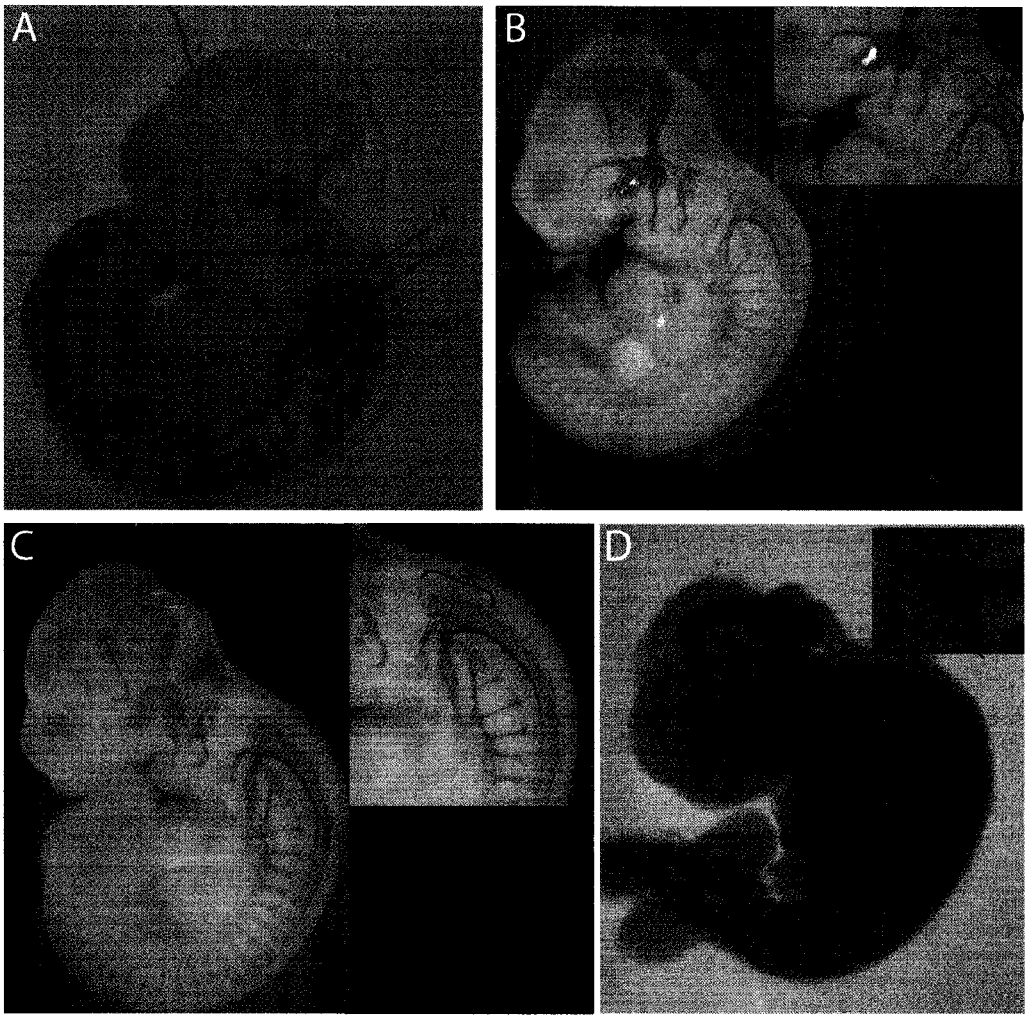
A
B
C
D

whose cranial nerves appear unaffected may not have had a high knockdown of Smn protein levels. These observations indicate that the reduction of Smn affects the normal formation of some cranial nerves, most notably those containing axons of the branchiomotor neurons subtype. Furthermore, these defects were much more apparent in embryos with severe depletion of Smn. These experiments have demonstrated the feasibility of the shRNA approach to derive Smn hypomorphs in mice and prompted us to establish transgenic lines with the shRNA constructs.

4.1.2 Developing and assessing sh_Smn_519 and sh_Smn_866 transgenic mouse lines

Our aim was to establish transgenic mouse lines that have the Smn protein knocked down to different levels (low, medium, and high). These lines would be useful in our studies to understand how the dosage of Smn impacts on overall development as well as on neuronal development and function. We developed transgenic lines with the sh_Smn_519 and sh_Smn_866 shRNA constructs. The sh_Smn_519 and sh_Smn_866 constructs were microinjected separately into one-cell mouse embryos. Positive founders were identified by PCR genotyping. Although several founder mice were obtained, we chose one from sh_Smn_519 (845), and 2 from sh_Smn_866 (426 and 428) for further study. Smn protein expression in several tissues (brain, liver, spinal cord) was assessed by immunoblot (Fig. 4.4). As is apparent by the results, none of these transgenic lines displayed significant knockdown of Smn in any of the tissues

Fig. 4.4. The sh_Smn_519 line 845 and sh_Smn_866, lines 426, 428 show a slight decrease in Smn levels. sh_Smn_519 line 845 (A) and sh_Smn_866, lines 426 (B), 428 (C) tissue lysates of spinal cord, brain and liver from one month old mice were resolved on 10% SDS-PAGE. Smn levels were determined by blotting with an anti-Smn antibody (lower band); anti-actin (upper band) was used as a loading control. Note mice carrying the shRNA transgene show only a slight decrease in Smn levels. Abbreviations: WT, wildtype; TG, transgenic mice carrying the shRNA transgene.

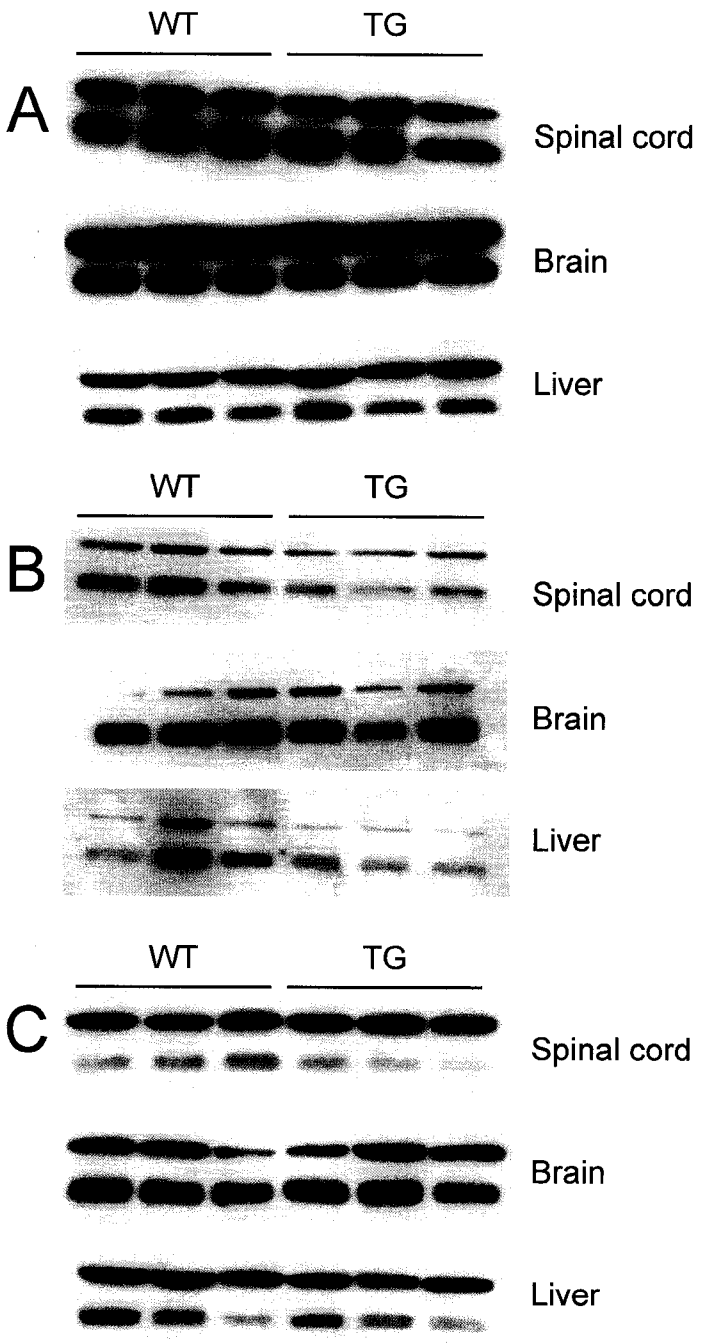
WT
TG
A
Spinal cord
Brain
Liver
WT
TG
B
Spinal cord
Brain
Liver
WT
TG
C
Spinal cord
Brain
Liver

examined. To uncover a functional effect of any Smn knockdown in these lines, we crossed the transgenic mice with the *Smn*$^{+/-}$ mice where the starting Smn dosage would be at 50% (Fig. 4.5). When line 428 is crossed onto the *Smn*$^{+/-}$ background, the Smn knockdown observed is variable in the tissues, whereas lines 845 and 426 on the *Smn*$^{+/-}$ background show approximately 60% Smn knockdown compared with normal. Interestingly, even with an overall Smn knockdown to 40% of normal levels within the heterozygous mice, we were not able to detect any overt phenotypes, suggesting that these levels were still sufficient for normal development and for maintenance of neuronal integrity in young mice. Coincidently, these results fit well with our more recent work demonstrating that a small increase of Smn has a dramatic impact on survival of SMA mice, essentially resulting in completely normal outcomes (unpublished data from the laboratory). Thus, depletion of Smn to 40% levels is well tolerated by the mice.

The *Smn*$^{+/-}$ mice eventually suffer from motor neuron degeneration at approximately 6 months of age (Jablonka, Schrank et al. 2000). To assess whether our mice would show slower progression of an SMA phenotype, similar to the *Smn*$^{+/-}$, we allowed the mice to age until six months at which time we analyzed protein expression again (Fig. 4.6). Smn protein levels at six months were similar to those at one month. We then wanted to determine whether the Smn knockdown (down to approximately 40% normal levels) in the *Smn*$^{+/-}$;sh_Smn_519 or *Smn*$^{+/-}$;sh_Smn_866 mice compared to the *Smn*$^{+/-}$ mice would have an additional effect on motor neuron degeneration. The L4 segment of the

Fig. 4.5. The sh_Smn_519 line 845 and sh_Smn_866, lines 426, 428 in the $Smn^{+/-}$ background show a slight decrease in Smn levels at one month. sh_Smn_519, line 845 (A) and sh_Smn_866 , lines 426 (B), 428 (C) in the $Smn^{+/-}$ background tissue lysates of spinal cord, brain and liver from one month old mice were resolved on 10% SDS-PAGE. Smn levels were determined by blotting with an anti-Smn antibody (lower band); anti-actin (upper band) was used as a loading control. Note that the mice carrying the shRNA in the $Smn^{+/-}$ background in line 845 and line 426 show a fairly consistent knockdown, while line 428 shows a variable knockdown. Abbreviations: WT, wildtype; TG, transgenic mice carrying the shRNA.

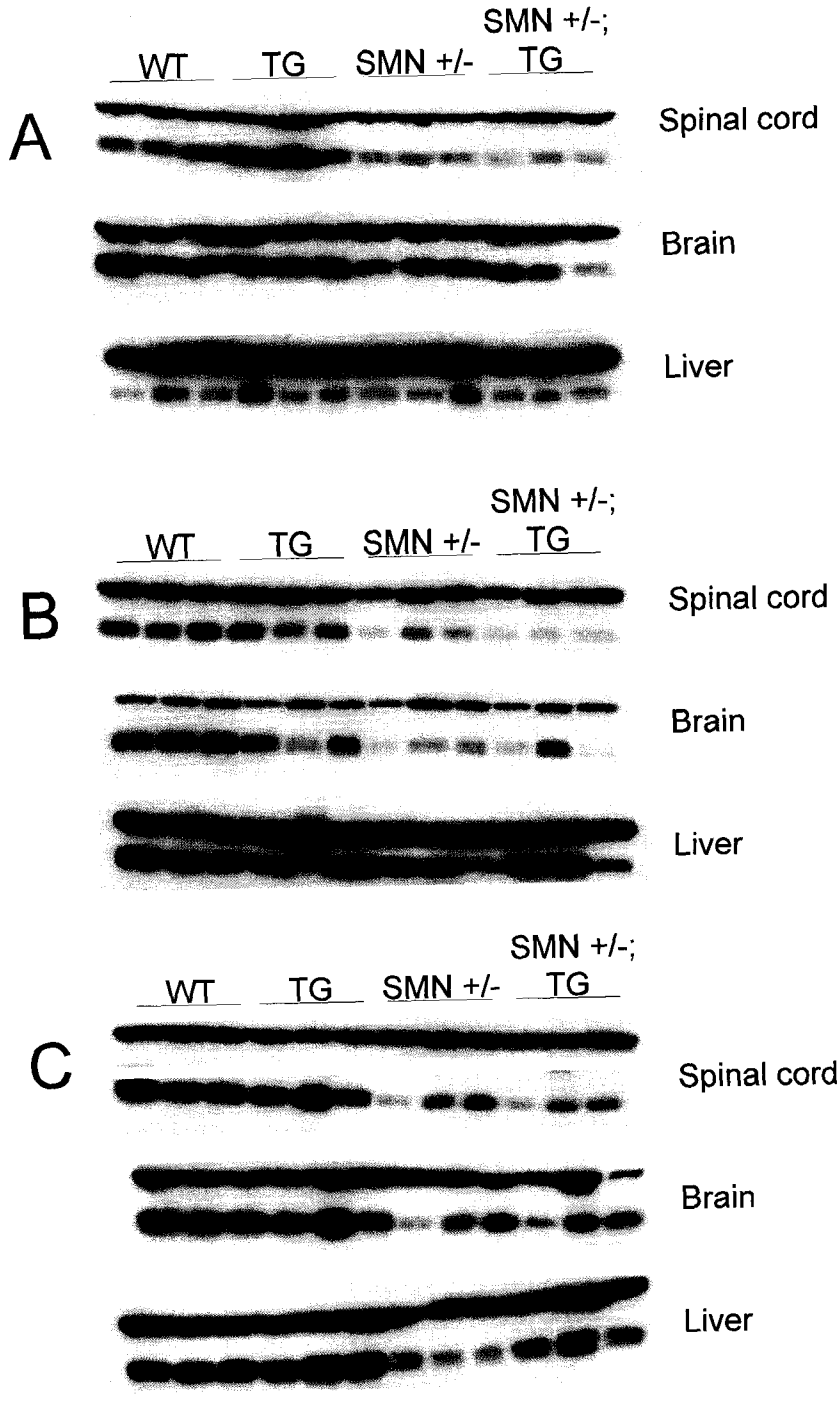
A
WT
TG
SMN +/-
SMN +/-; TG
Spinal cord
Brain
Liver
B
WT
TG
SMN +/-
SMN +/-; TG
Spinal cord
Brain
Liver
C
WT
TG
SMN +/-
SMN +/-; TG
Spinal cord
Brain
Liver

Fig. 4.6. The sh_Smn_519 line 845 and sh_Smn_866, lines 426, 428 in the $Smn^{+/-}$ background show a slight decrease in Smn levels at six months. sh_Smn_519, line 845 (A) and sh_Smn_866 , lines 426 (B), 428 (C) in the $Smn^{+/-}$ background tissue lysates of spinal cord, brain and liver from six month old mice were resolved on 10% SDS-PAGE. Smn levels were determined by blotting with an anti-Smn antibody (lower band); anti-actin (upper band) was used as a loading control. Note that the mice carrying the shRNA in the $Smn^{+/-}$ background in line 845 and line 426 show a fairly consistent knockdown. Abbreviations: WT, wildtype; TG, transgenic mice carrying the shRNA.

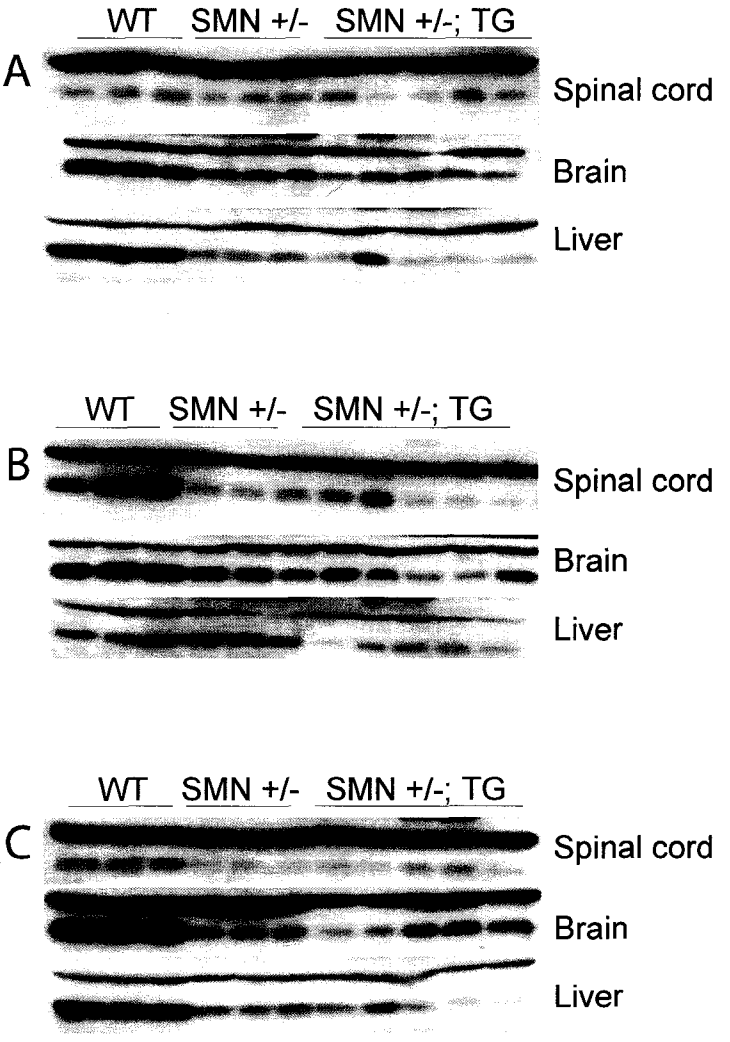
WT
SMN +/-
SMN +/-; TG
A
Spinal cord
Brain
Liver
WT
SMN +/-
SMN +/-; TG
B
Spinal cord
Brain
Liver
WT
SMN +/-
SMN +/-; TG
C
Spinal cord
Brain
Liver

spinal cord and the brainstem of wild type and *Smn*$^{+/-}$, *Smn*$^{+/-}$;sh_Smn_519 (line 845) or *Smn*$^{+/-}$;sh_Smn_866 (lines 426, 428) were serially sectioned and stained for hematoxylin and eosin. The number of motor neurons present per defined area per section was counted for each genotype. The number of motor neurons counted in the spinal cord per defined area per section was 38 ± 2, 25 ± 1, 25 ± 2, 24 ± 3 and 23 ± 2 for wildtype, Smn$^{+/-}$, *Smn*$^{+/-}$;sh_Smn_519 (845), *Smn*$^{+/-}$;sh_Smn_866 (426), and *Smn*$^{+/-}$;sh_Smn_866 (428), respectively (Fig. 4.7). The number of motor neurons counted in the brainstem per defined area per section was 34 ± 2, 21 ± 1, 21 ± 1, 23 ± 2 and 19 ± 1 for wildtype, Smn$^{+/-}$, *Smn*$^{+/-}$;sh_Smn_519 (845), *Smn*$^{+/-}$;sh_Smn_866 (426), and *Smn*$^{+/-}$;sh_Smn_866 (428), respectively (Fig. 4.8). As evident from these results, there was no significant difference in protein expression or motor neuron number between the *Smn*$^{+/-}$ mice and the *Smn*$^{+/-}$ mice expressing either sh_Smn_519 or sh_Smn_866. The gastrocnemius muscle of wild type, *Smn*$^{+/-}$, *Smn*$^{+/-}$;sh_Smn_519 (845), *Smn*$^{+/-}$;sh_Smn_866 (426, 428) were stained with hematoxylin and eosin and examined for any morphological differences (Fig. 4.9). No differences in muscle histology were observed.

4.1.3 Developing and assessing sh_Smn_249, sh_Smn_519 and sh_Smn_866 transgenic mouse lines

In a second approach, all three shRNA constructs (sh_Smn_249, sh_Smn_519 and sh_Smn_866) were microinjected together with the idea that this would result in mice that express all three constructs at the same time, and

Fig. 4.7. No significant difference in motor neuron number in the brainstem between the sh_Smn_519 and sh_Smn_866 transgenic mouse lines and the $Smn^{+/-}$ mice. Sections of the brainstem of WT(A), $Smn^{+/-}$(B), $Smn^{+/-}$;sh_Smn_519 (line 845)(C), $Smn^{+/-}$;sh_Smn_866 (line 426)(D), and $Smn^{+/-}$-;sh_Smn_866 (line 428)(E) were stained with hemotoxylin and eosin. The number of motor neurons per defined area for $Smn^{+/-}$;sh_Smn_519 (line 845)(F), $Smn^{+/-}$;sh_Smn_866 (line 426)(G), and $Smn^{+/-}$-;sh_Smn_866 (line 428)(H) were counted and compared to their WT and $Smn^{+/-}$ littermates. *, indicates $p<0.05$ as compared to WT.

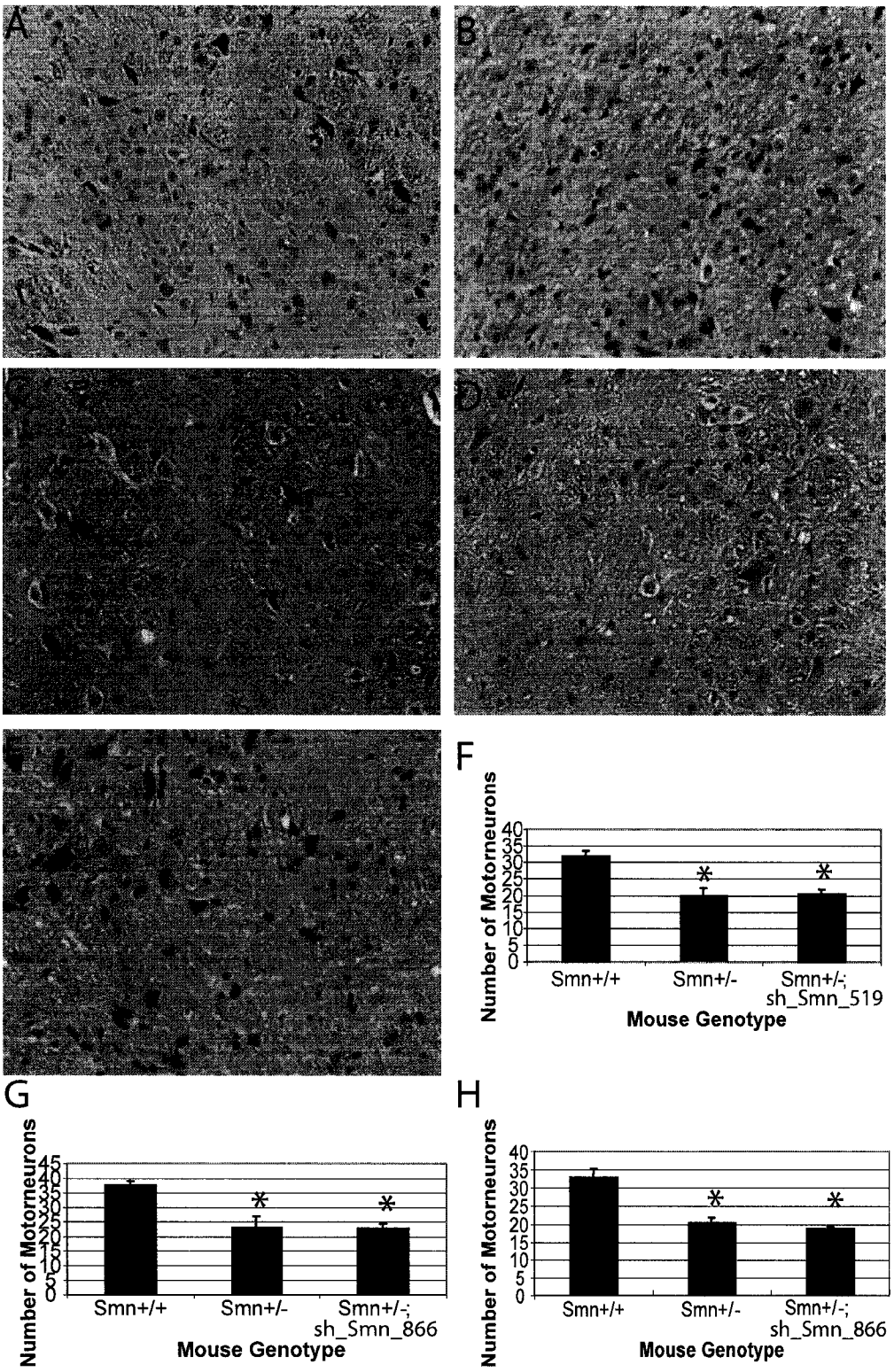
A
B
C
D
E
F
Number of Motorneurons
40
35
30
25
20
15
10
5
0
Smn+/+
Smn+/-
Smn+/-;
sh_Smn_519
Mouse Genotype
G
Number of Motorneurons
45
40
35
30
25
20
15
10
5
0
Smn+/+
Smn+/-
Smn+/-;
sh_Smn_866
Mouse Genotype
H
Number of Motorneurons
40
35
30
25
20
15
10
5
0
Smn+/+
Smn+/-
Smn+/-;
sh_Smn_866
Mouse Genotype

Fig. 4.8. No significant difference in motor neuron number in the spinal cord between the sh_Smn_519 and sh_Smn_866 transgenic mouse lines and the $Smn^{+/-}$ mice. Sections of the spinal cord of WT(A), $Smn^{+/-}$(B), $Smn^{+/-}$;sh_Smn_519 (line 845)(C), $Smn^{+/-}$;sh_Smn_866 (line 426)(D), and $Smn^{+/-}$;sh_Smn_866 (line 428)(E) were stained with hemotoxylin and eosin. The number of motor neurons in a defined area for $Smn^{+/-}$;sh_Smn_519 (line 845)(F), $Smn^{+/-}$;sh_Smn_866 (line 426)(G), and $Smn^{+/-}$;sh_Smn_866 (line 428)(H) were counted and compared to their WT and $Smn^{+/-}$ littermates. *, indicates $p<0.05$ as compared to WT.

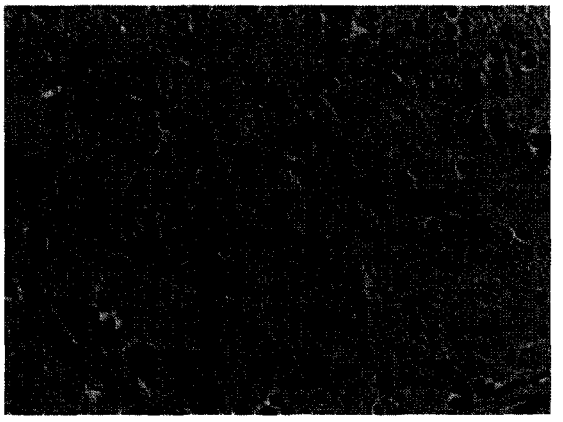

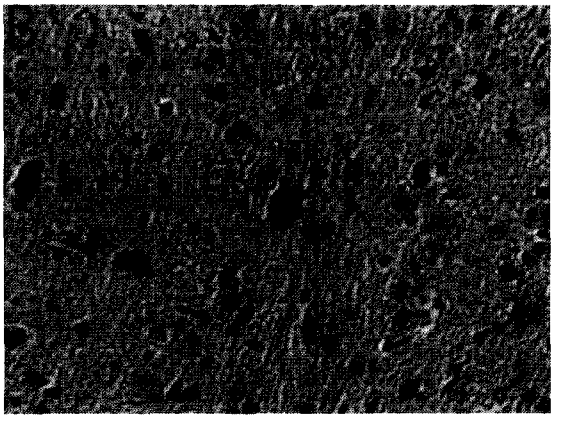

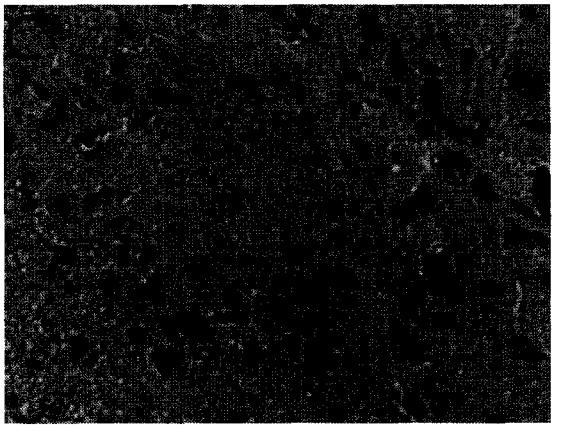

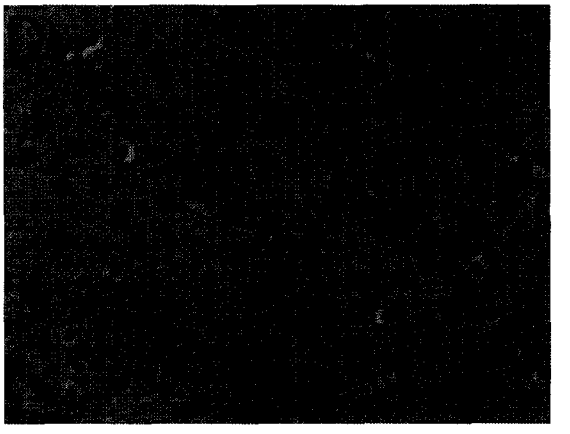

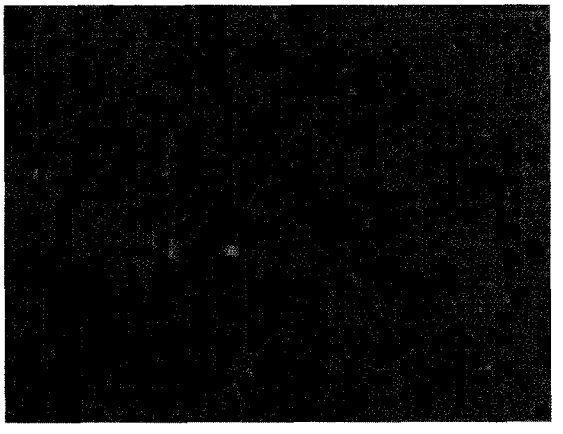

F

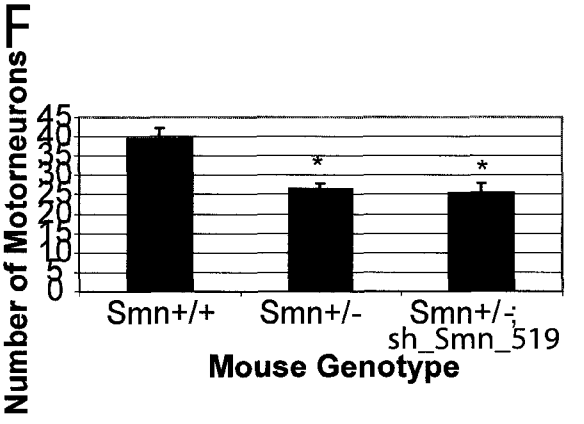
Number of Motorneurons
45
40
35
30
25
20
15
10
5
0
*
*
Smn+/+
Smn+/-
Smn+/-;
sh_Smn_519
Mouse Genotype

G

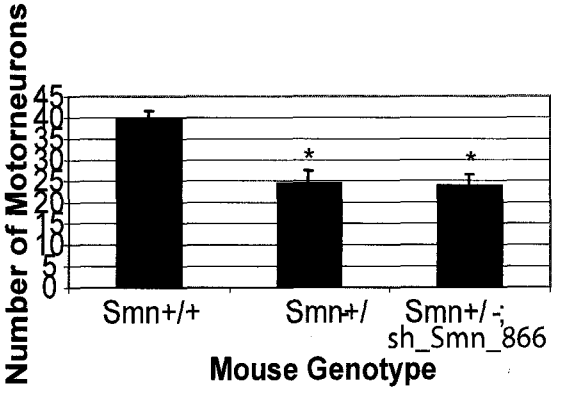
Number of Motorneurons
45
40
35
30
25
20
15
10
5
0
*
*
Smn+/+
Smn+/
Smn+/-;
sh_Smn_866
Mouse Genotype

H

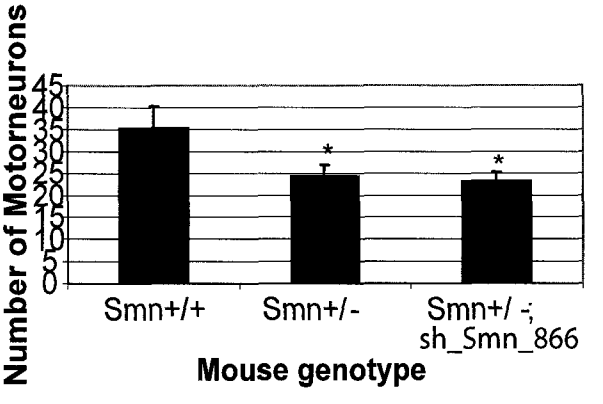
Number of Motorneurons
45
40
35
30
25
20
15
10
5
0
*
*
Smn+/+
Smn+/-
Smn+/-;
sh_Smn_866
Mouse genotype

Fig. 4.9. No morphological differences in gastrocnemius muscle of sh_Smn_519 and sh_Smn_866 transgenic mouse lines compared to wildtype and $Smn^{+/-}$. Sections of the gastrocnemius muscle of WT (A), $Smn^{+/-}$ (B), $Smn^{+/-}$;sh_Smn_519 (line 845)(C), $Smn^{+/-}$;sh_Smn_866 (line 426)(D), and $Smn^{+/-}$;sh_Smn_866 (line 428)(E) were stained with hemotoxylin and eosin. Note: There were no apparent differences between WT, $Smn^{+/-}$ and the sh_Smn_519 and sh_Smn_866 transgenic mouse lines.

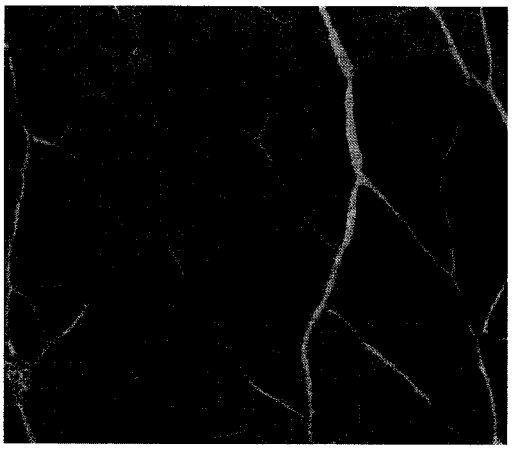

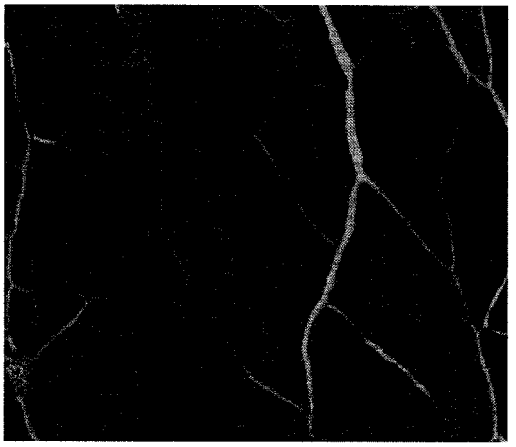

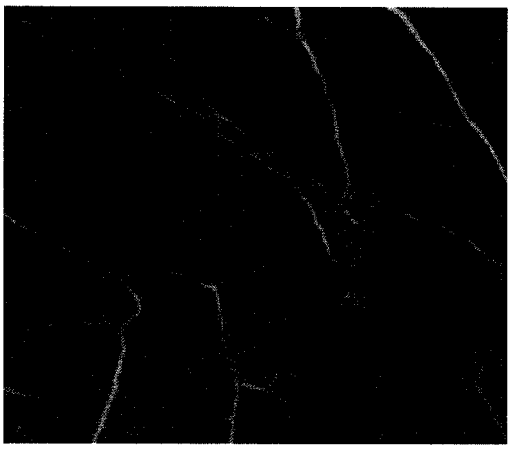

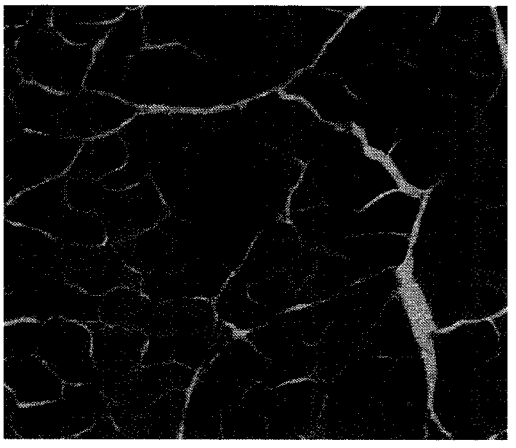

would therefore produce a more noticeable knockdown of Smn and mice with overt phenotypes. Four transgenic lines (959, 977, 982, 983) were generated with the combined pool of shRNA constructs. All four lines were analyzed by western blot and once again there was not a large difference in protein expression between wild type mice and mice carrying the shRNA transgenes (Fig. 4.10). Thus, despite the large number of transgenic lines analyzed, none demonstrated significant enough depletion of Smn to result in an intermediate phenotype. One possible reason for this is that Smn knockdown in the early embryo might be lethal and the only transgenic mice that survive are the low expressers of the shRNA. In effect, we may have been selecting against the high expressers of the shRNA.

4.1.4 Generation of transgenic Smn knockdown lines by blastocyst injection

Our last approach in attempting to develop Smn hypomorphs in mice using shRNA was done in collaboration with Tara Martinez and Dr. Doug Kerr (Johns Hopkins) where we used the shRNA constructs to knockdown Smn in ES cells prior to generating chimeric mice and establishing lines. The rationale behind this approach was that if we targeted the Smn gene in ES cells first, then we may be able to perform a pre-screen and only use clones with significant knockdown for the chimera experiments. The Smn shRNA constructs were used to develop Smn knockdown mouse embryonic stem (ES) cells with a range of Smn knockdown (50-90%) (Fig. 4.11A). The ES cell clones were karyotyped and

Fig. 4.10. No significant decrease in Smn levels in transgenic mice microinjected with three shRNA constructs (sh_Smn_249, sh_Smn_519, and sh_Smn_866). Western blot analysis of transgenic embryos microinjected with three shRNA constructs (sh_Smn_249, sh_Smn_519, and sh_Smn_866) line 959 (A), line 977 (B), line 982 (C), and line 983 (D) tissue lysates of spinal cord, brain and liver from one month old mice were resolved on 10% SDS-PAGE. Smn levels were determined by blotting with an anti-Smn antibody (lower band); anti-actin (upper band) was used as a loading control. Note mice carrying the shRNA transgene show only a slight decrease in Smn levels. Abbreviations: WT, wildtype; TG, transgenic mice carrying the shRNA transgene.

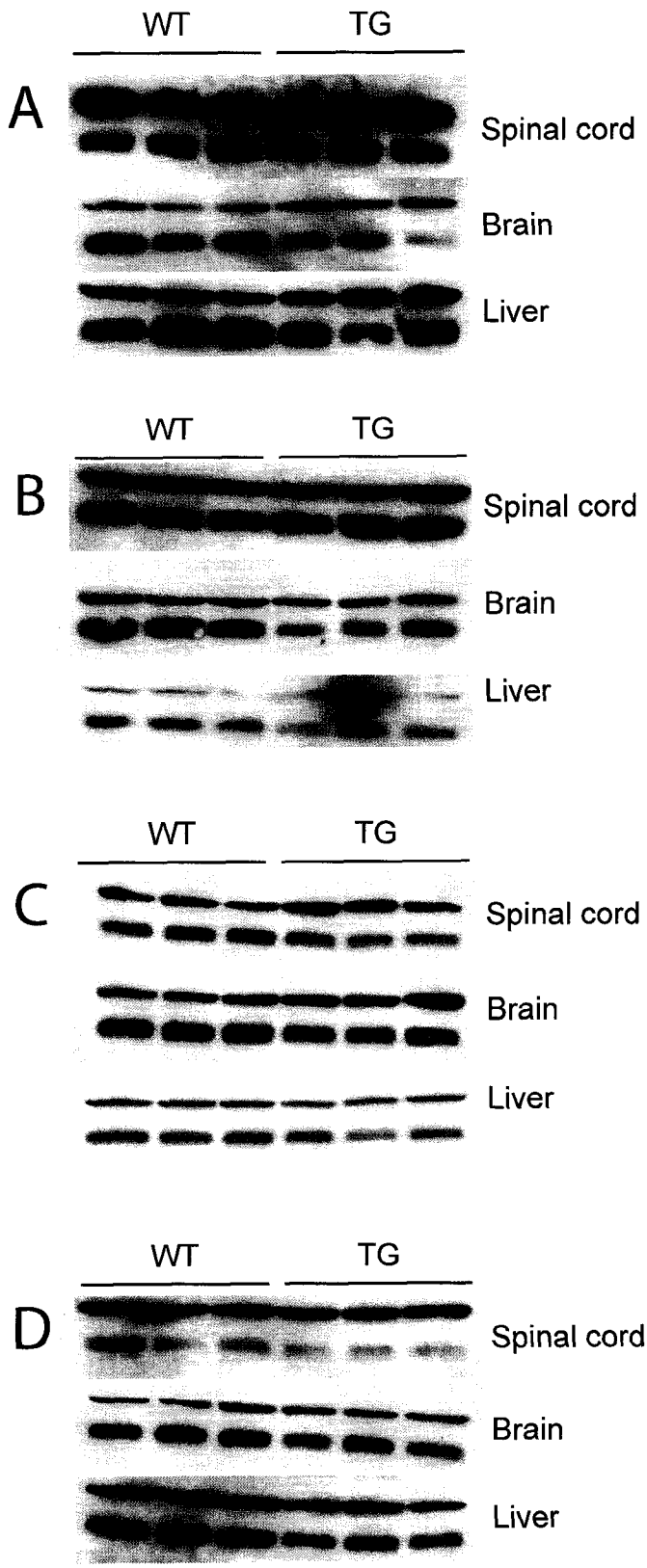
WT
TG
A
Spinal cord
Brain
Liver
WT
TG
B
Spinal cord
Brain
Liver
WT
TG
C
Spinal cord
Brain
Liver
WT
TG
D
Spinal cord
Brain
Liver

Fig. 4.11. No significant difference in sh_Smn_519 transgenic mice created by blastocyst injection. ES cells expressing $Smn^{+/-}$; SMN2; sh_Smn_519 (A) show 50-90% knockdown compared to wildtype ES cells. Smn expression levels were quantified using FujiFilm Image Quant to measure band intensity normalized to the β-Tubulin 1 loading control. *, indicates the only ES cell clone that contained the right number of chromosomes and was used for blastocyst injections. This ES cell clone expresses 40-50% of wildtype levels of Smn (B) Tissue lysates of spinal cord, brain and liver from one month old mice carrying the sh_Smn_519 were resolved on 10% SDS-PAGE. Smn levels were determined by blotting with an anti-Smn antibody (lower band); anti-actin (upper band) was used as a loading control. Note mice carrying the shRNA transgene show only a slight decrease in Smn levels. Abbreviations: WT, wildtype; TG, transgenic mice carrying the shRNA transgene. Figure 4.11A was provided by Tara Martinez from the Douglas Kerr Laboratory at John Hopkins Univeristy.

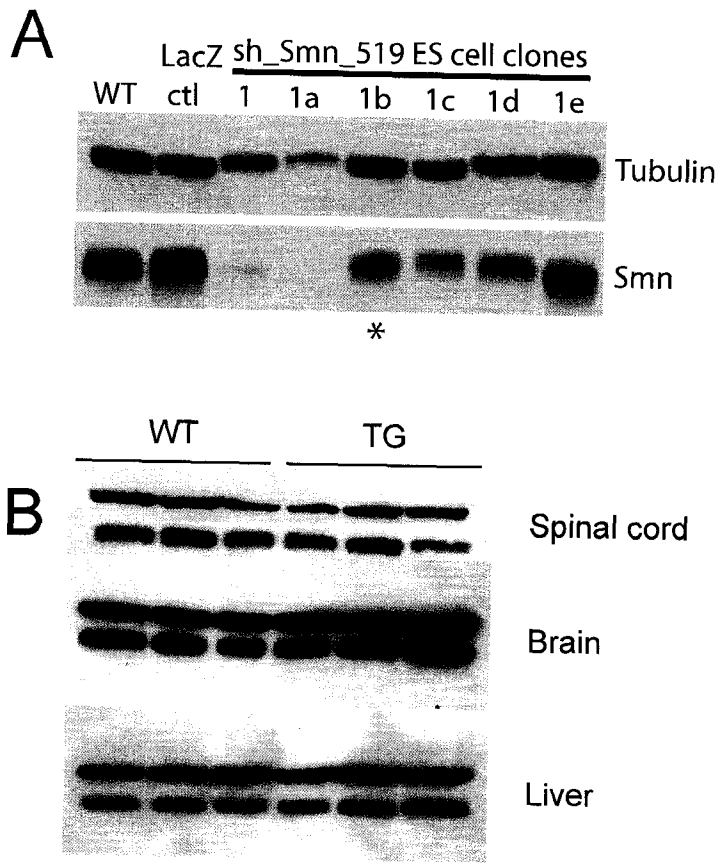
A
LacZ
sh_Smn_519 ES cell clones
WT
ctl
1
1a
1b
1c
1d
1e
Tubulin
Smn
*
B
WT
TG
Spinal cord
Brain
Liver

only one (1b) had the correct number of chromosomes. The genotype of this ES cell clone is *Smn*$^{+/-}$*;SMN2;sh-Smn_519*. This ES cell clone was used to produce chimeras by blastocyst injections. Of several mice born, one was deemed to be chimeric based on coat colour mosaicism. This mouse was bred to wild type mice and germline transmission of the shRNA transgene was confirmed. The chimera and subsequent progeny were crossed to wild type mice in the FVB background to breed out the two copies of the *SMN2* transgene to attain a greater Smn knockdown. These mice were phenotypically normal and not surprisingly we did not observe a significant knockdown of Smn (Fig. 4.11B).

4.2 DISCUSSION

The standard approach for loss of function studies in mice is to generate a knockout mouse in which the gene of interest is inactivated through homologous recombination in ES cells. A drawback of the knockout approach is that the mutant allele produced is null. Although the total loss of function of a gene can be valuable, it is not always informative, especially when it causes early embryonic lethality, as is the case when Smn is knocked out in mice (Schrank, Gotz et al. 1997). In the case of Smn, a hypomorphic allele would be much more informative, as SMA is a disorder with ranging severity and the amount of SMN protein expressed in each individual is inversely correlated with the severity of SMA (Coovert, Le et al. 1997; Lefebvre, Burlet et al. 1997; Feldkotter, Schwarzer et al. 2002). Generating a number of transgenic mouse lines with different degrees of loss of Smn expression would give us a better understanding of the pathogenesis of SMA and the dose-dependent effect. In our study, Smn hypomorphs in mice were developed using the short interference RNA (siRNA) approach.

4.2.1 Smn knockdown mice do not show an intermediate phenotype

RNA interference (RNAi) was discovered in *Caenorhabditis elegans* as a gene silencing mechanism in response to injection of long double stranded RNA (dsRNA) (Fire, Xu et al. 1998; Hannon 2002). In most mammalian cells, the introduction of long dsRNA induces a cytotoxic response due to activation of the PKR (protein kinase regulated by double-stranded RNA) system (Stark, Kerr et al. 1998; Gil and Esteban 2000). This cellular defence response can be circumvented

by the use of short interfering RNA (siRNA) or short hairpin RNAs (shRNA), composed of 21-23 nucleotide double stranded RNA molecule completely homologous to a unique target gene (Elbashir, Harborth et al. 2001; Elbashir, Lendeckel et al. 2001; Tuschl 2002; Collins and Cheng 2005; Rao and Sockanathan 2005; Coumoul and Deng 2006). RNAi gene knockdown has been successfully used to study gene functions in mouse models (Hasuwa, Kaseda et al. 2002; Kunath, Gish et al. 2003; Rubinson, Dillon et al. 2003; Tiscornia, Singer et al. 2003; van de Wetering, Oving et al. 2003; Saito, Yokota et al. 2005). In our study, we used three different methods to generate the shRNA Smn knockdown transgenic mice. In the first method, we used the conventional transgenic technique of injecting one-cell mouse embryos with one shRNA construct at a time. We produced transgenic mice, which were analyzed before birth (F_0 generation) or used to establish lines. The severity of the phenotypes observed in Smn shRNA embryos was variable and correlated roughly with the levels of Smn knockdown. The more reduced the Smn expression in these shRNA Smn knockdown embryos the more severe the abnormal morphology. Thus, in the F_0 generation the shRNA was able to reduce Smn to low enough levels to observe a severe to intermediate neurodevelopmental phenotype. When we established shRNA Smn knockdown transgenic lines, the mice had a slight reduction in Smn protein expression and no obvious phenotype. Even when the mice were bred into the Smn heterozygous background to reduce Smn levels even further, they did not display a more severe phenotype. These mice were phenotypically very similar to the Smn heterozygous mice. They showed similar loss of motor neurons at 6

months in both the spinal cord and brainstem. The degeneration of motor neurons observed in the shRNA Smn knockdown in the Smn heterozygous background echoes the pathophysiological characteristics of SMA type IV patients. These patients develop normally, and are able to stand and walk. It is only in the adult stages of life that these patients begin to show the typical SMA phenotype (Munsat and Davies 1992; Crawford and Pardo 1996). Therefore, our first attempt at creating an intermediate SMA-like mouse model using shRNA failed and we were only able to create a mild SMA-like mouse model similar to the Smn heterozygous model.

In the second method, the same microinjection technique was used, however multiple shRNA constructs were injected at one time. Our idea was that this would result in mice that express all three constructs at the same time. Targeting more regions of the Smn gene might be able to reduce Smn protein levels even further. The transgenic lines we established did not show an overt phenotype and did not have a great reduction in Smn protein expression. The lack of success with this effort may be indicative of the possibility that strong expressers of the shRNA transgenes are selected against during embryonic stages.

In the third approach, ES cell clones that expressed the shRNA construct and showed reduced levels of Smn were used to produce Smn knockdown mice. The benefit of using ES cell clones is that clones can be selected for the desired knockdown prior to generating mice. We selected ES cell clones with Smn reduction of approximately 50-60% and we produced chimeric mice which were

used to establish transgenic lines. Once again these mice did not show any overt phenotype or a great reduction in Smn protein expression, indicating that SMN must be reduced to much lower levels to observe an intermediate SMA-like phenotype.

4.2.2 Reducing Smn to 40% wild type levels does not give an intermediate SMA-like phenotype

Although, we could get a slight knockdown of Smn expression in our shRNA Smn knockdown mice, we did not achieve sufficient knockdown to observe any intermediate SMA-like phenotypes. This lack of severe SMN reduction could be due to the shRNA transgenes being turned off through epigenetic modifications. Or, mutations have occurred within the hairpin region of the shRNA sequence during replication, which could lead to a reduction in silencing efficiency (Miyagishi, Sumimoto et al. 2004). Another possible reason for the lack of Smn reduction is that Smn knockdown in the early embryo might be lethal and the only transgenic mice that survive are the low expressers. In effect, we may have been selecting against the high expressers.

While we were attempting to create Smn knockdown mice using shRNA, other members of the laboratory were creating Smn knockdown mice using a knock-in strategy. These mice have mutations within exon 7 of the *Smn* gene. Two different lines, each harbouring a different mutation, were created. The first mutation is a C to T transition at position 6 of exon 7 ($Smn^{DT/+}$) and the second is the replacement of three nucleotides within the exon splicing enhancer of exon 7

($Smn^{2B/+}$). These mice have the ability to alternatively splice *Smn*, thus producing less full-length *Smn*. From the study of these mice, it was determined that $Smn^{DT/+}$ and $Smn^{2B/+}$ express Smn at 75 and 65% levels of wild type mice, respectively. When the mice were homozygous for their mutation, Smn expression levels were reduced to 50 and 30% for $Smn^{DT/DT}$ and $Smn^{2B/2B}$, respectively. When these mice were crossed into the $Smn^{+/-}$ background to have one null *Smn* allele, the Smn expression levels were even more reduced. $Smn^{DT/-}$ and $Smn^{2B/-}$ expressed 25 and 15% of wild type Smn levels, respectively. From this series of Smn hypomorphic mice, it was determined that mice expressing greater than 50% Smn levels are phenotypically normal. Mice with 25-50% Smn protein levels are considered to be equivalent to a very mild SMA and display pathology with late-onset. Mice expressing 15% or less display early postnatal symptoms and die within the first few weeks and mice with no Smn protein are pre-implantation lethal (unpublished data). Thus, when we began our shRNA study, our hypothesis was that if you reduced Smn to levels just slightly under 50% of wild type, it would result in an intermediate phenotype. However, now after these combined studies indicate that Smn levels need to be reduced to approximately 15% of wild type levels to obtain a phenotype. Therefore, our shRNA method as we have used in mice may have limitations in that strong reduction of Smn levels in the F_0 generation would lead to embryonic lethality, and low reduction would lead to no phenotype.

Controlling the amount of shRNA expressed in mice so as to obtain the right level of Smn knockdown to yield an intermediate phenotype may require a large scale effort at generating and screening ES cell clones with Smn knockdown in the

15 to 25% range. Inclusion of an inducible system to initiate the expression of the shRNA would further allow for a more controlled effort. It has been demonstrated that an inducible system can be applied to generate conditional loss of function phenotypes *in vivo* allowing for a more controlled environment where one can decide when to reduce the expression of the gene of interest (Czauderna, Santel et al. 2003). Thus, in our case we may chose to reduce Smn after embryogenesis, therefore potentially bypassing the embryonic lethality.

5.0 Neurodevelopmental abnormalities in neural stem cells and embryos from Smn depleted mice

Spinal muscular atrophy (SMA) is a genetic disorder caused by depletion of the survival motor neuron (SMN) protein and characterized by degeneration of α-motor neurons in the spinal cord. We investigated the morphology and differentiation of neurosphere-derived neural stem cells (NSCs) generated from the brains of a hypomorphic series of SMA mice. Neurospheres from the *Smn*$^{-/-}$*;SMN2* mice, which represent a very severe model of SMA, produced NSCs with increased proliferation during growth and differentiation. These cells produced fewer Tuj1-positive neuronal cells, which displayed morphological alterations and had fewer and shorter neurites. The decrease in Tuj1-positive cells was not due to enhanced apoptosis but was accompanied by an increase in the number of nestin-positive cells. In embryos from the *Smn*$^{-/-}$*;SMN2* mouse model, we observed a significantly altered morphology of cranial nerves IX and X, which appeared to be partially fused. In addition, a subset of these embryos displayed truncated lumbar spinal nerves. These results give us insight into the most severe model of SMA in which SMN is nearly completely depleted, and suggest that SMN has a role in neurodevelopment as well as in neuromaintenance. Our work raises the possibility that SMN depletion impacts neurodevelopment and neuromaintenance to varying extents leading to SMA pathogenesis.

5.1 RESULTS

5.1.1 Smn dosage effects neuronal stem cell behaviour in neurosphere cultures

To determine the effect of Smn depletion on neural stem cell behavior, we employed a primary culture technique in which embryonic neural cells are plated at clonal density on non-adherent substrates in the presence of epidermal growth factor (EGF) and basic fibroblast growth factor (bFGF). In these cultures, some of the cells form multicellular structures called neurospheres which, when dissociated and replated, form new spheres. Furthermore, cells within the neurospheres can differentiate into neurons, astrocytes, or oligodendrocytes, demonstrating that the sphere-forming cells represent neural stem cells (NSCs) (McKay 1997; Daadi and Weiss 1999). NSCs by definition are multi-potent, self-renewing cells that can be propagated in culture. Among other roles, they can be used in the *in vitro* study of pathogenesis of human neurological disorders (Bahn, Mimmack et al. 2002; Castren, Tervonen et al. 2005).

Neurosphere cultures were established from embryonic brains (E14.5) to characterize the impact of Smn dosage on neuronal stem cell behavior. Neurospheres were grown as spherical floating clusters in the presence of EGF and bFGF. Smn protein in spheres and in differentiating NSCs was examined by western blot analysis (Fig. 5.1). The level of Smn protein is considerably increased in dissociated neural stem cells after 3 and 5 days of differentiation (Fig. 5.1). Furthermore, as expected, the levels of Smn were considerably reduced in neurospheres and NSCs from $Smn^{-/-}$;*SMN2*

Fig. 5.1. Smn protein expression in neurospheres and differentiated neural stem cells from wild type and *Smn*$^{-/-}$;*SMN2* embryos. Western blot analysis of neurospheres during growth conditions (0 days), and NSCs after 3 and 5 days of differentiation. Cell lysates were resolved on 10% SDS-PAGE. Smn levels were determined by blotting with an anti-Smn antibody (lower band); anti-actin (upper band) was used as a loading control.

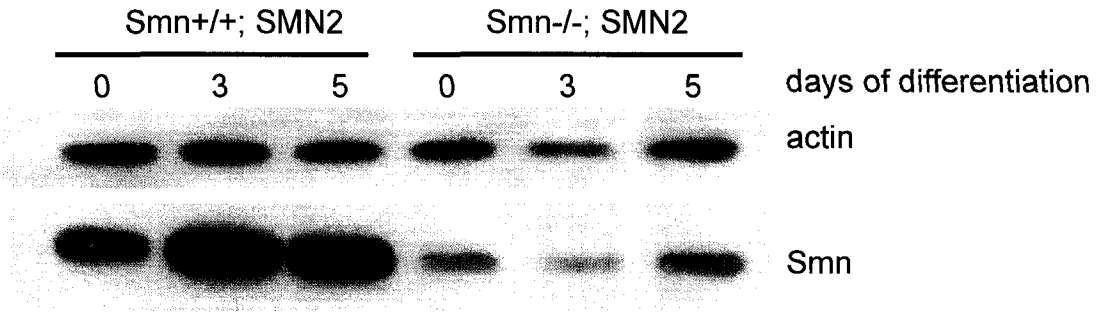
Smn+/+; SMN2
Smn-/-; SMN2
0
3
5
0
3
5
days of differentiation
actin
Smn

mice (Fig. 5.1). Since each neurosphere is believed to arise from a single NSC, the number of neurospheres generated from a fixed number of cells was taken as a measurement of NSC number. There was no difference in neurosphere number between the different genotypes. We also assessed neurosphere growth by measuring the size of the neurospheres over time. Using cultures in 25 cm^2 flasks at a low initial cell density (10^4 cells/ml), the sizes of neurospheres were determined at 72, 120, and 168 hours (Fig. 5.2A-C). The neurosphere size increased with culture time, and there was no difference in size of the neurospheres derived from the different mouse strains (ranging from the wild type to *Smn*$^{+/-}$ to *Smn*$^{-/-}$;*SMN2* mice). Although there was no significant difference in sphere size between the genotypes, when dissociated and plated in the presence of BrdU, NSCs from the brains of *Smn*$^{-/-}$;*SMN2* mice showed a significant increase in the percent of proliferating cells (Fig. 5.2D). Thus, dissociated NSCs from the severely SMN depleted mouse model are in a more proliferative state which may reflect retention in a progenitor status. To test this possibility, we analyzed the expression of nestin in these cells. Nestin is defined as a class VI intermediate filament, and is accepted as a marker of neural stem/progenitor cells (Wiese, Rolletschek et al. 2004). Dissociated cells were analyzed for nestin expression under growth conditions (Fig. 5.2E). We found that 23.1 ± 2.1% and 23.8 ± 2.4% of wild type and *Smn*$^{+/-}$ NSCs, respectively were nestin-positive. In contrast, 29.5 ± 3.4% of *Smn*$^{-/-}$;*SMN2* NSCs were nestin-positive, a significantly ($p<0.05$) higher number than that observed with cells from

Fig. 5.2. Growth of Smn depleted embryo-derived neurospheres is unaffected. (A, B, C) Sphere diameter at 3, 5, and 7 day growth, respectively. Panels on the right are representative images of neurospheres from either *Smn*$^{+/+}$*;SMN2* or *Smn-/-;SMN2* embryos. NSCs from *Smn*$^{-/-}$*;SMN2* embryos have enhanced progenitor cell numbers. (D) BrdU incorporation reveals a significant (*$P < 0.05$) increase in the number of proliferating cells in *Smn*$^{-/-}$*;SMN2* NSCs compared to all the other genotypes. Panels on the right represent examples of BrdU-positive cells (green). (E) An increase in the number of nestin-positive cells is observed in *Smn*$^{-/-}$*;SMN2* NSCs compared to all the other genotypes. Panels on the right represent examples of nestin-positive cells (green). Nuclei were counter-stained with Hoechst. Scale bar, 50 μm.

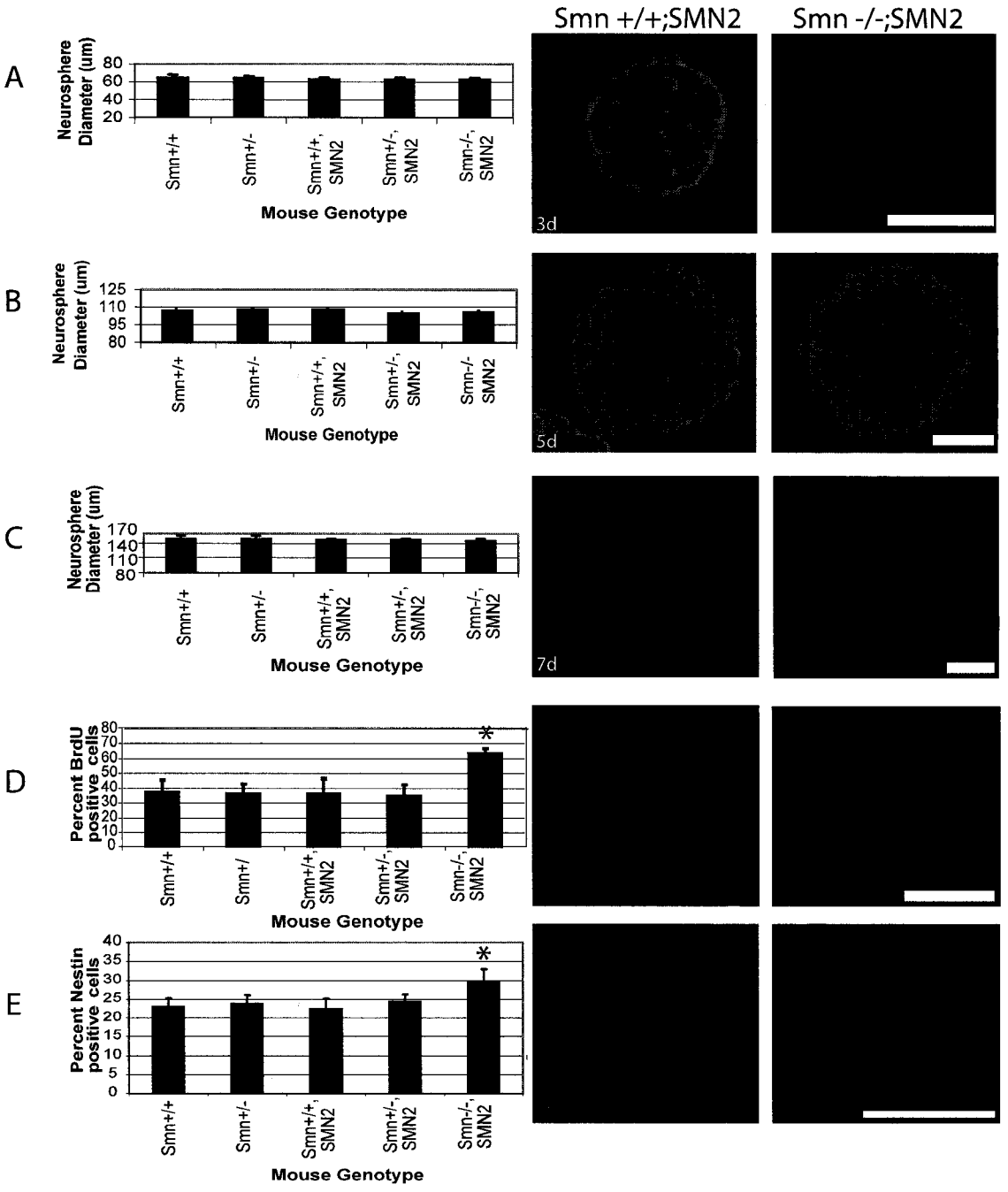
Smn +/+;SMN2
Smn -/-;SMN2
A
Neurosphere Diameter (um)
80
60
40
20
Smn+/+
Smn+/-
Smn+/+, SMN2
Smn+/-, SMN2
Smn-/-, SMN2
Mouse Genotype
3d
B
Neurosphere Diameter (um)
125
110
95
80
Smn+/+
Smn+/-
Smn+/+, SMN2
Smn+/-, SMN2
Smn-/- SMN2
Mouse Genotype
5d
C
Neurosphere Diameter (um)
170
140
110
80
Smn+/+
Smn+/-
Smn+/+, SMN2
Smn+/-, SMN2
Smn-/-, SMN2
Mouse Genotype
7d
D
Percent BrdU positive cells
80
70
60
50
40
30
20
10
0
*
Smn+/+
Smn+/
Smn+/+, SMN2
Smn+/-, SMN2
Smn-/-, SMN2
Mouse Genotype
E
Percent Nestin positive cells
40
35
30
25
20
15
10
5
0
*
Smn+/+
Smn+/-
Smn+/+, SMN2
Smn+/-, SMN2
Smn-/-, SMN2
Mouse Genotype

the other genotypes, consistent with *Smn*$^{-/-}$;*SMN2* NSCs remaining in a progenitor state.

5.1.2 Smn dosage effects multilineage differentiation of neuronal stem cells

Neural stem cells from neurospheres can undergo multilineage differentiation and give rise to neurons, astrocytes, or oligodendrocytes (Gage 2000). We compared the differentiation potential of NSCs generated from the brains of wild type, *Smn*$^{+/-}$, and *Smn*$^{-/-}$;*SMN2* mouse embryos. When the NSCs from the *Smn*$^{-/-}$;*SMN2* mice were differentiated for 5 days, they produced significantly fewer cells positive for the neuronal marker Tuj1 (10.4 ± 4.1%) than NSCs differentiated from wild type (24.4 ± 1.3%) and *Smn*$^{+/-}$ (23.5 ± 1.8%) embryos (Fig. 5.3 and 5.4A). In contrast, these NSCs produced similar numbers of myelin basic protein (MBP)-positive and glial fibrillary acidic protein (GFAP)-positive cells, thus similar numbers of astrocytes and oligodendrocytes, respectively regardless of the genotype of the mice (Fig. 5.3 and 5.4B,C). Similar results were obtained with NSCs differentiated for 3 days (see Fig. 5.5 and 5.6).

To address the reduction of Tuj1-positive cells from differentiating *Smn*$^{-/-}$;*SMN2* NSCs, we quantified cell death in these cells and compared it to that in wild type cells. There was no significant difference in cell death between NSCs from wild type, *Smn*$^{+/-}$ and *Smn*$^{-/-}$;*SMN2* embryos (Fig. 5.7A,C). Since the reduction in Tuj1-positive cells in *Smn*$^{-/-}$;*SMN2* derived NSCs cannot be explained by an increase in cell death, we looked at the possibility that Smn depletion may be preventing the NSCs from progressing to a more differentiated

Fig. 5.3. *Smn*$^{-/-}$;*SMN2* NSCs have altered differentiation properties. NSCs derived from the mild and severe SMA mouse models were assessed at 3 days of differentiation. NSCs from the *Smn*$^{+/+}$ (A), *Smn*$^{+/-}$ (B), *Smn*$^{+/+}$;*SMN2* (C), *Smn*$^{+/-}$;*SMN2* (D) and *Smn*$^{-/-}$;*SMN2* (E) mice were immunostained (in green) for nestin, MBP, GFAP, and Tuj1. Nuclei were counter-stained with Hoechst. Scale bar, 50 μm.

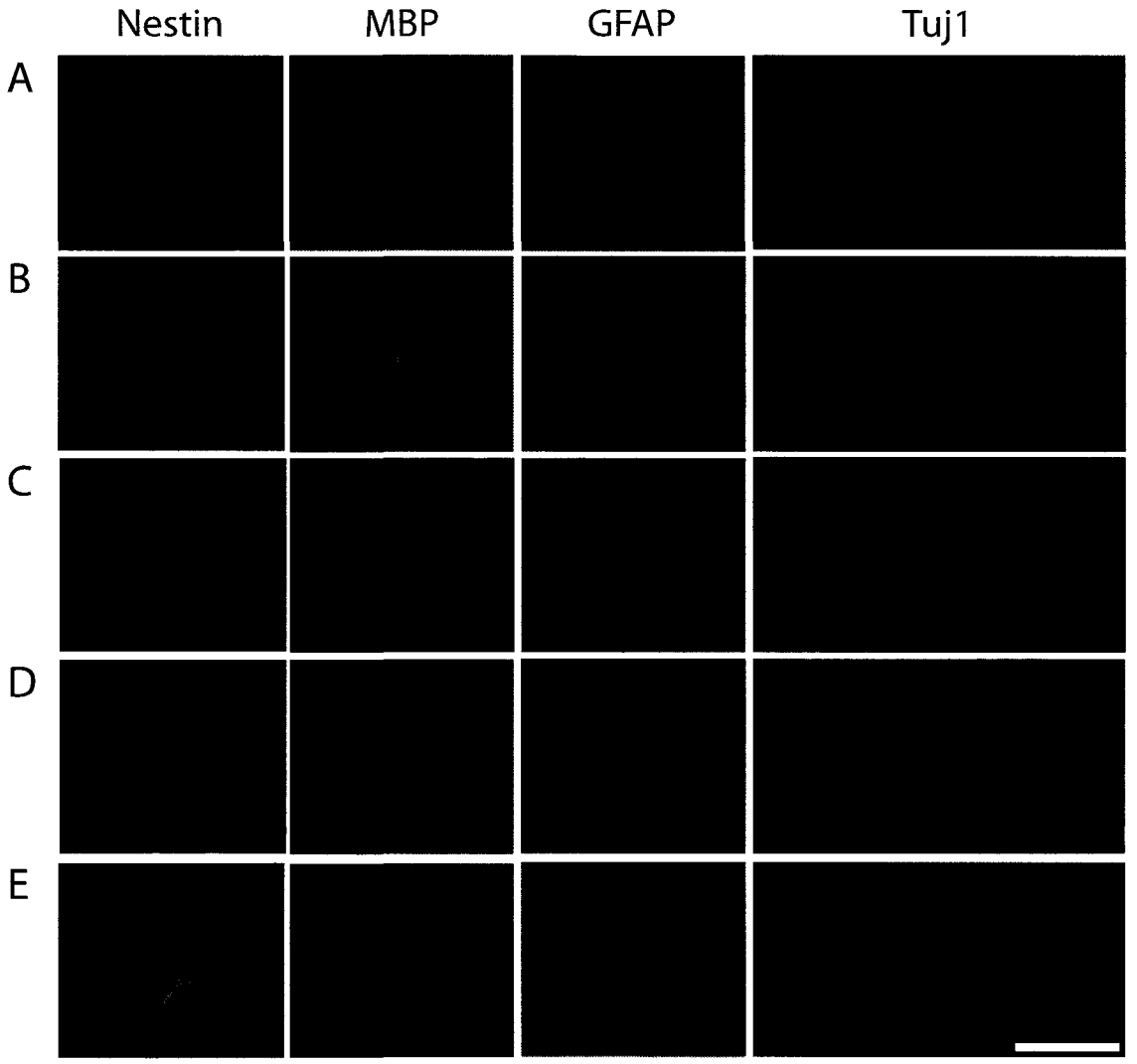
Nestin
MBP
GFAP
Tuj1
A
B
C
D
E

Fig. 5.4. Neuronal differentiation of NSCs from *Smn*$^{-/-}$;*SMN2* mice is compromised. Analysis was performed on cultures at 3 days of differentiation. (A – D) Percent of cells positive for Tuj1, MBP, GFAP, and nestin, respectively. There is a significant decrease (*$P < 0.05$) in the appearance of Tuj1-positive cells and a significant increase (*$P < 0.05$) in the percentage of nestin-positive cells in differentiating *Smn*$^{-/-}$;*SMN2* NSCs compared to the other genotypes.

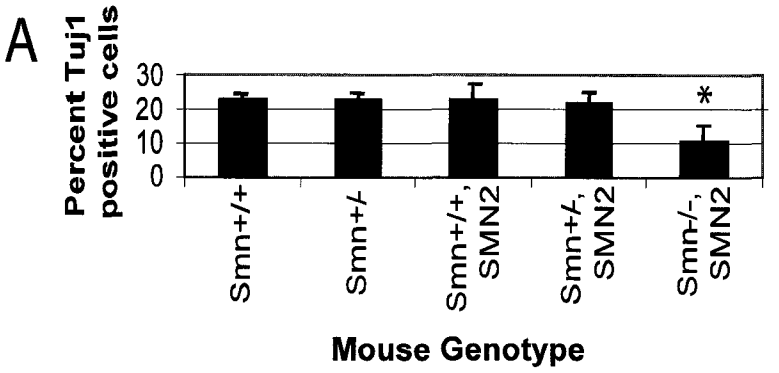
A
Percent Tuj1 positive cells
30
20
10
0
*
Smn+/+
Smn+/-
Smn+/+, SMN2
Smn+/-, SMN2
Smn-/-, SMN2
Mouse Genotype

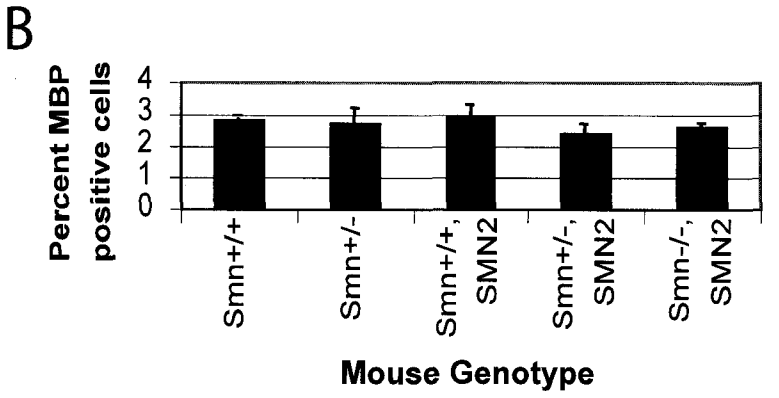
B
Percent MBP positive cells
4
3
2
1
0
Smn+/+
Smn+/-
Smn+/+, SMN2
Smn+/-, SMN2
Smn-/-, SMN2
Mouse Genotype

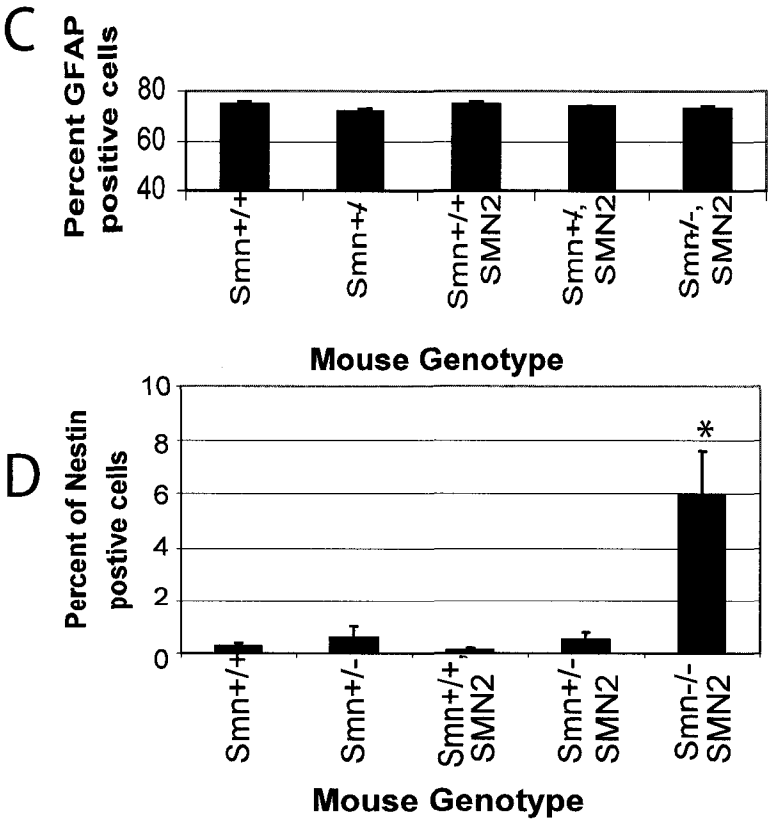
C
Percent GFAP positive cells
80
60
40
Smn+/+
Smn+/-
Smn+/+ SMN2
Smn+/-, SMN2
Smn-/-, SMN2
Mouse Genotype
D
Percent of Nestin postive cells
10
8
6
4
2
0
*
Smn+/+
Smn+/-
Smn+/+ SMN2
Smn+/- SMN2
Smn-/- SMN2
Mouse Genotype

Fig. 5.5. *Smn*$^{-/-}$;*SMN2* NSCs have altered differentiation properties. NSCs derived from the mild and severe SMA mouse models were assessed at 5 days of differentiation. NSCs from the *Smn*$^{+/+}$ (A), *Smn*$^{+/-}$ (B), *Smn*$^{+/+}$;*SMN2* (C), *Smn*$^{+/-}$;*SMN2* (D) and *Smn*$^{-/-}$;*SMN2* (E) mice were immunostained (in green) for nestin, MBP, GFAP, and Tuj1. Nuclei were counter-stained with Hoechst. Scale bar, 50 μm.

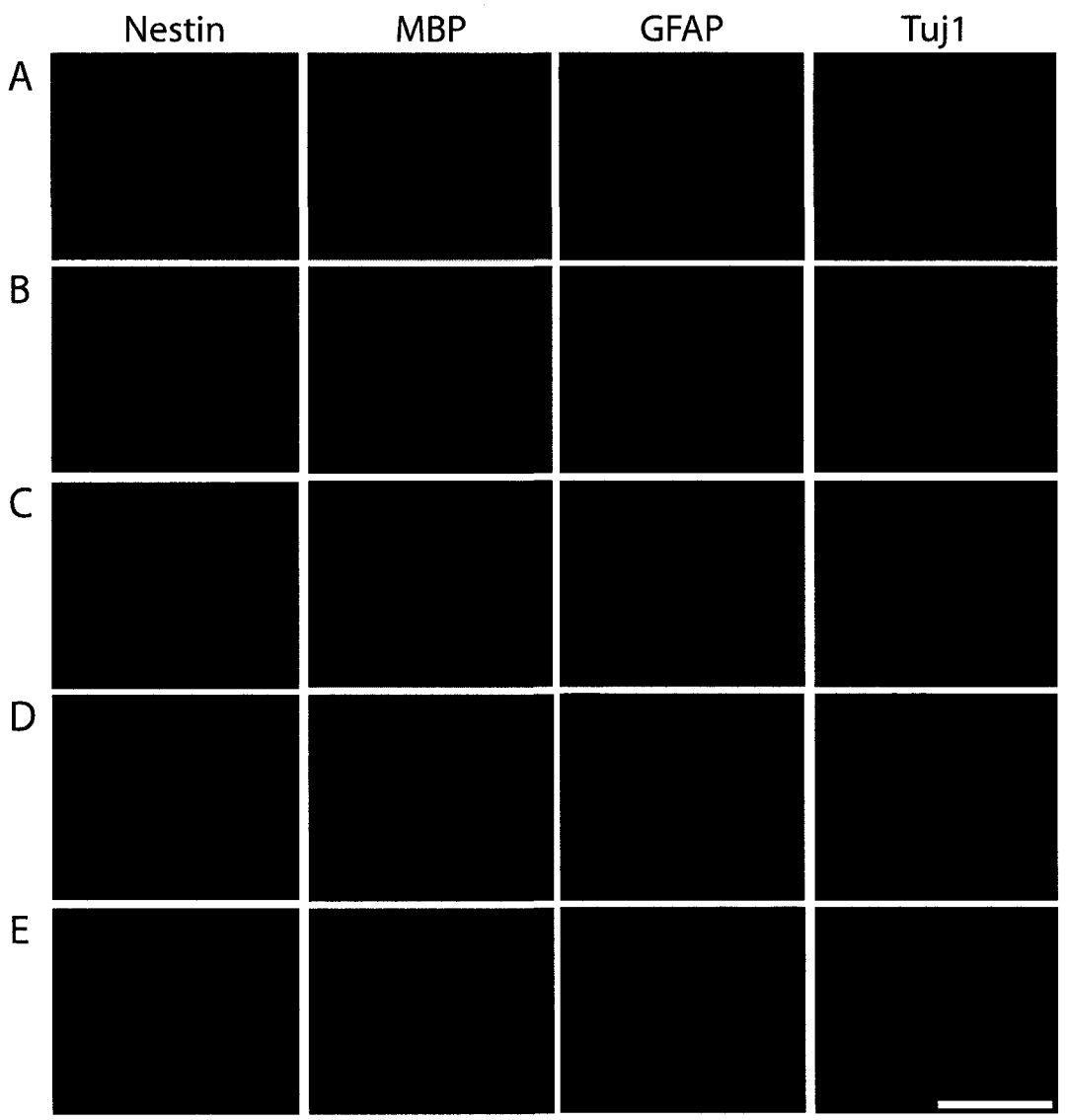
Nestin
MBP
GFAP
Tuj1
A
B
C
D
E

Fig. 5.6. Neuronal differentiation of NSCs from *Smn*$^{-/-}$;*SMN2* mice is compromised. Analysis was performed on cultures at 5 days of differentiation. (A – D) Percent of cells positive for nestin, MBP, GFAP, and Tuj1, respectively. There is a significant decrease (*P < 0.05) in the appearance of Tuj1-positive cells and a significant increase (*P < 0.05) in the percentage of nestin-positive cells in differentiating *Smn*$^{-/-}$;*SMN2* NSCs compared to the other genotypes.

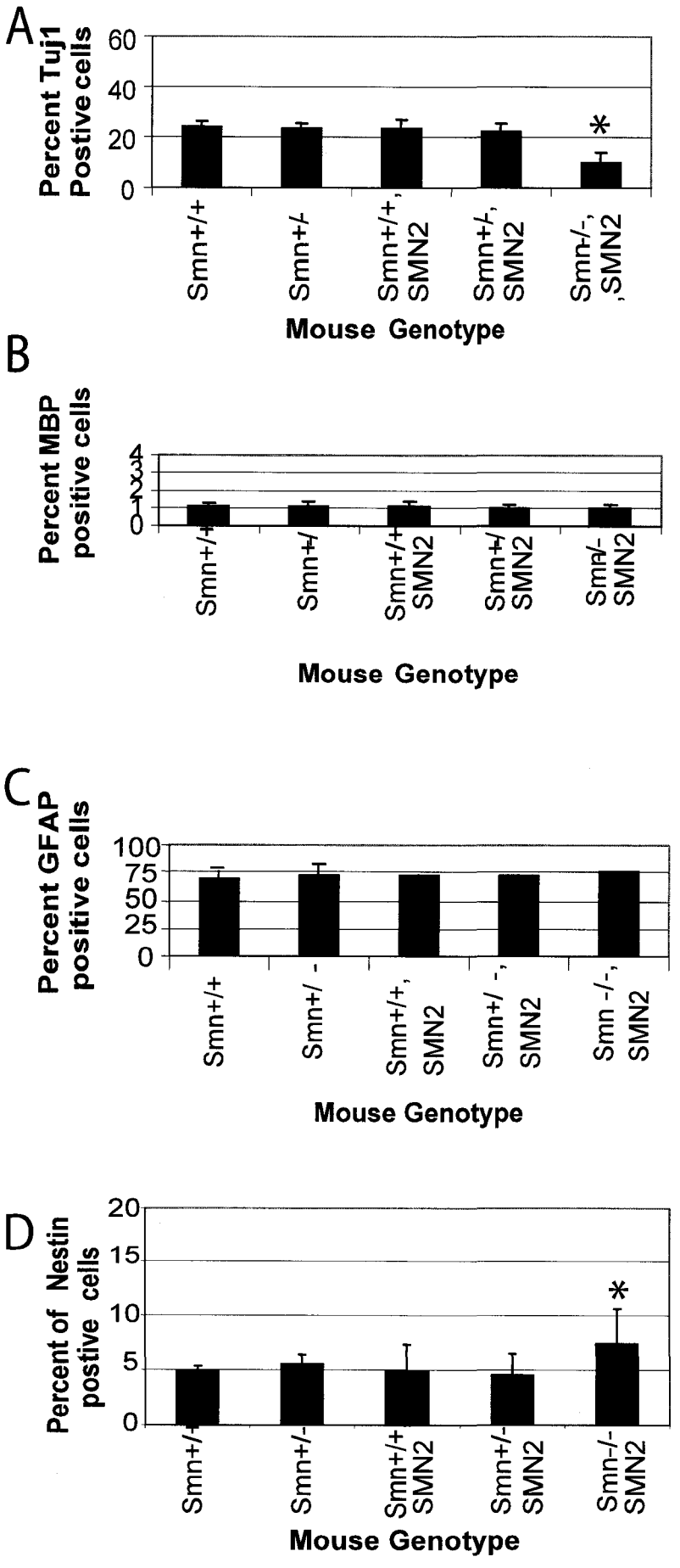
A
Percent Tuj1 Postive cells
60
40
20
0
*
Smn+/+
Smn+/-
Smn+/+, SMN2
Smn+/-, SMN2
Smn-/-, SMN2
Mouse Genotype
B
Percent MBP positive cells
4
3
1
0
Smn+/+
Smn+/-
Smn+/+ SMN2
Smn+/- SMN2
Smn-/- SMN2
Mouse Genotype
C
Percent GFAP positive cells
100
75
50
25
0
Smn+/+
Smn+/ -
Smn+/+, SMN2
Smn+/ -, SMN2
Smn -/-, SMN2
Mouse Genotype
D
Percent of Nestin postive cells
20
15
10
5
0
*
Smn+/+
Smn+/-
Smn+/+ SMN2
Smn+/- SMN2
Smn-/- SMN2
Mouse Genotype

state. To test this hypothesis, we looked at BrdU incorporation, as well as nestin staining. BrdU was added 24 hours prior to fixing the cells at 3 and 5 days of differentiation to determine the number of cells that would still be proliferating after removal from mitogens. The differentiating NSCs from *Smn*$^{-/-}$;*SMN2* embryos had significantly more BrdU positive cells at 3 and 5 days of differentiation compared to wild type and *Smn*$^{+/-}$ NSCs (Fig. 5.7B,D). *Smn*$^{-/-}$;*SMN2* NSCs had 33.2 ± 2.6% and 17.8 ± 2.3% BrdU positive cells compared to 26.7 ± 1.6% and 12.5 ± 1.0% for wild type and 26.3 ± 3.0% and 12.5 ± 0.8% for *Smn*$^{+/-}$ cells at 3 and 5 days of differentiation, respectively (Fig. 5.7B,D). There is a downward trend in proliferation over the 3 to 5 day time points, however, there was a significant increase in the percentage of S-phase cells in the *Smn*$^{-/-}$;*SMN2* genotype compared with all others.

As described above, there was a significantly higher number of nestin-positive cells in the *Smn*$^{-/-}$;*SMN2* NSCs during growth conditions (Fig. 5.2E). With continued differentiation into specialized cell types, nestin expression should be down-regulated in differentiated NSCs (Wiese, Rolletschek et al. 2004). Consistent with the extended period of proliferation, the percentage of nestin-positive cells was more than 10-fold higher in differentiating *Smn*$^{-/-}$;*SMN2* NSCs as compared to wild type or any other genotype (Fig. 5.4D). Similar results were obtained with NSCs differentiated for 3 days (see Fig. 5.6). These results indicated that Smn depleted NSCs from the *Smn*$^{-/-}$;*SMN2* mice remain in a progenitor state and very few differentiate into a neuronal phenotype.

Fig. 5.7. NSCs from *Smn*$^{-/-}$;*SMN2* mice have enhanced proliferation rates during differentiation but do not display an increase in apoptosis. (A,C) Percent of TUNEL positive cells at 3 (A) and 5 (C) days of differentiation. (B,D) BrdU incorporation reveals a significant (*$P < 0.05$) increase in the number of proliferating cells in *Smn*$^{-/-}$;*SMN2* NSCs compared to all the other genotypes at 3 (B) and 5 (D) days of differentiation.

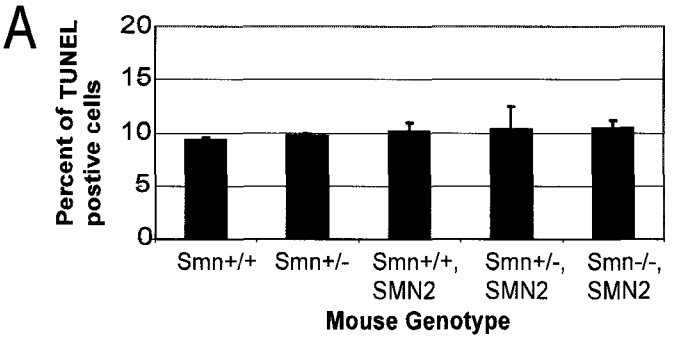
A
Percent of TUNEL postive cells
20
15
10
5
0
Smn+/+
Smn+/-
Smn+/+, SMN2
Smn+/-, SMN2
Smn-/-, SMN2
Mouse Genotype

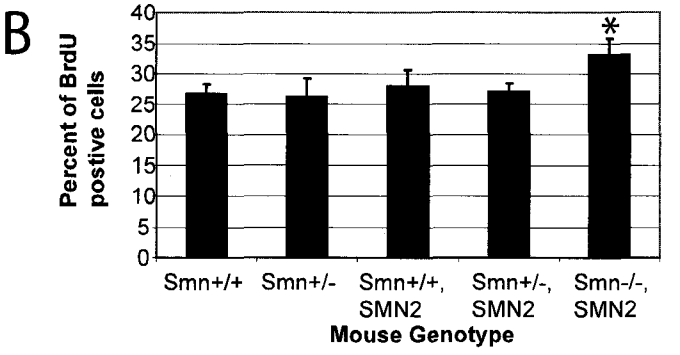
B
Percent of BrdU postive cells
40
35
30
25
20
15
10
5
0
*
Smn+/+
Smn+/-
Smn+/+, SMN2
Smn+/-, SMN2
Smn-/-, SMN2
Mouse Genotype

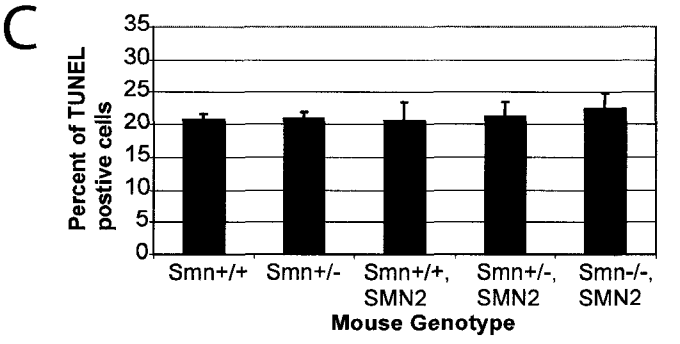
C
Percent of TUNEL postive cells
35
30
25
20
15
10
5
0
Smn+/+
Smn+/-
Smn+/+, SMN2
Smn+/-, SMN2
Smn-/-, SMN2
Mouse Genotype

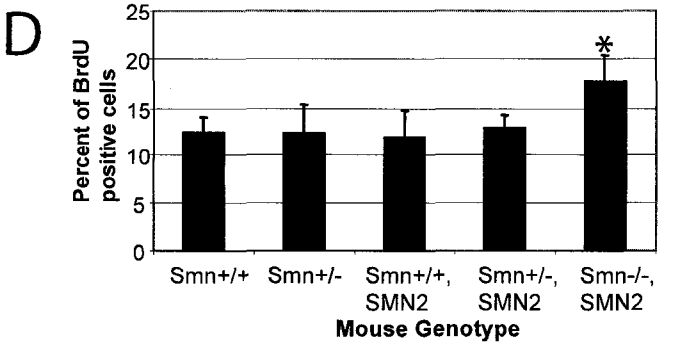
D
Percent of BrdU positive cells
25
20
15
10
5
0
*
Smn+/+
Smn+/-
Smn+/+, SMN2
Smn+/-, SMN2
Smn-/-, SMN2
Mouse Genotype

5.1.3 Neuritogenesis is affected in Smn depleted neuronal stem cells

We investigated whether the differentiation defect in the *Smn*$^{-/-}$;*SMN2* NSCs was associated with alterations in other features of neuronal differentiation by quantifying various aspects of neuritogenesis. Morphological analysis revealed that *Smn*$^{-/-}$;*SMN2* differentiated neurons contained fewer primary neurites compared with those from wild type and *Smn*$^{+/-}$ mice. The proportion of neurons that exhibit more than one primary neurite was reduced by 3-fold in dissociated cell cultures derived from NSCs generated from *Smn*$^{-/-}$;*SMN2* embryos (19.9 ± 1.8% and 76.4 ± 2.6% of Tuj1-positive cells) than in wild type (62.4 ± 1.6% and 93.7 ± 0.8% of Tuj1-positive cells) and *Smn*$^{+/-}$ (61.5 ± 1.1% and 93.6 ± 1.0% of Tuj1-positive cells) at 3 and 5 days of differentiation, respectively (Fig. 5.8A and 5.9A). Furthermore, the number of neurites per Tuj1-positive cell at 3 and 5 days of differentiation was significantly lower in *Smn*$^{-/-}$;*SMN2* (1.2 ± 0.2 and 1.5 ± 0.2, respectively) than in wild type (1.7 ± 0.1 and 5.3 ± 0.1, respectively) and *Smn*$^{+/-}$ (1.6 ± 0.5 and 5.2 ± 0.1, respectively) (Fig. 5.8B and 5.9B). Finally, the length of the longest neurite was significantly shorter in the *Smn*$^{-/-}$;*SMN2* (15.2 ± 0.6 μm and 25.4 ± 0.4 μm) than in wild type (32.4 ± 2.2 μm and 79.9 ± 1.9 μm) and *Smn*$^{+/-}$ (32.6 ± 1.3 μm and 79.1 ± 2.4 μm) at 3 and 5 days of differentiation, respectively (Fig. 5.8C and 5.9C). These results indicate that Smn depletion alters the neuronal lineage differentiation of NSCs.

Fig. 5.8. The morphology of TuJ1-positive neurons from *Smn*$^{-/-}$;*SMN2* NSCs is affected. Analysis was performed on cultures at 3 days of differentiation. (A) Percent of Tuj1-positive cells with greater than one neurite. (B) Number of neurites per Tuj1-positive cell that has at least one neurite. (C) Length of the longest neurite in Tuj1-positive cells that have at least one neurite. Only the severe *Smn*$^{-/-}$;*SMN2* SMA cultures show any significant difference in any of the above (*$P < 0.05$).

A
Percent of Cells with >1 neurite
70
60
50
40
30
20
10
0
*
Smn+/+
Smn+/ -
Smn+/+, SMN2
Smn+/ -, SMN2
Smn -/-, SMN2
Mouse Genotype

B
Number of # neurites/cell
2.5
2
1.5
1
0.5
0
*
Smn+/+
Smn+/ -
Smn+/+, SMN2
Smn+/ -, SMN2
Smn -/-, SMN2
Mouse Genotype

C
Average length of Longest Neurite
40
30
20
10
0
*
Smn+/+
Smn+/ -
Smn+/+, SMN2
Smn+/ -, SMN2
Smn -/-, SMN2
Mouse Genotype

Fig. 5.9. The morphology of TuJ1-positive neurons from *Smn*$^{-/-}$;*SMN2* NSCs is affected. Analysis was performed on cultures at 5 days of differentiation. (A) Percent of Tuj1-positive cells with greater than one neurite. (B) Number of neurites per Tuj1-positive cell that has at least one neurite. (C) Length of the longest neurite in Tuj1-positive cells that have at least one neurite. Only the severe *Smn*$^{-/-}$;*SMN2* SMA cultures show any significant difference in any of the above (*$P < 0.05$).

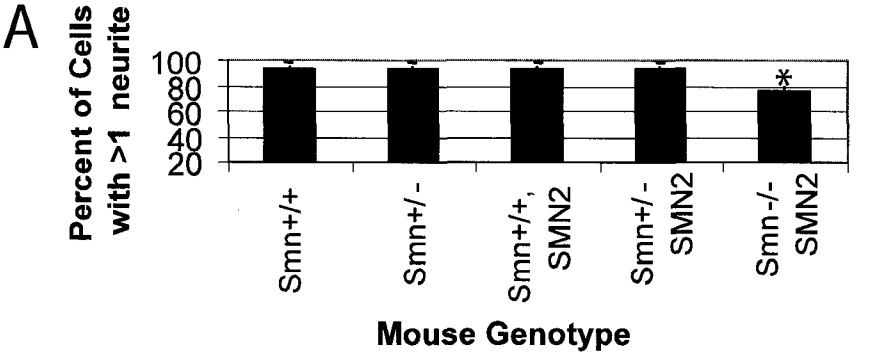
A
Percent of Cells with >1 neurite
100
80
60
40
20
*
Smn+/+
Smn+/-
Smn+/+, SMN2
Smn+/- SMN2
Smn-/- SMN2
Mouse Genotype

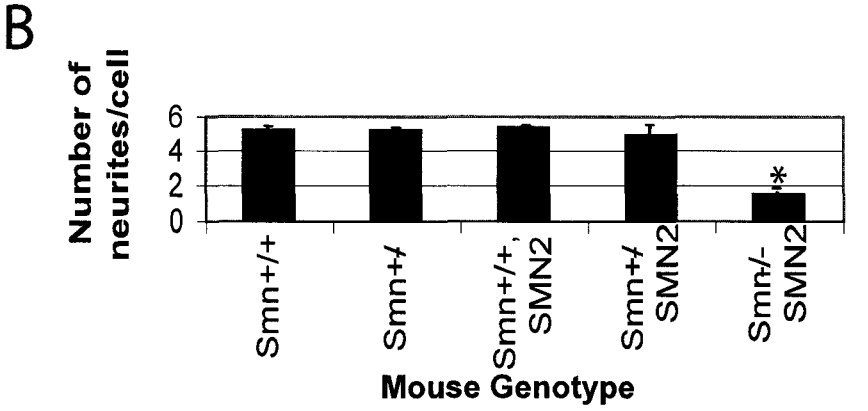
B
Number of neurites/cell
6
4
2
0
*
Smn+/+
Smn+/-
Smn+/+, SMN2
Smn+/- SMN2
Smn-/- SMN2
Mouse Genotype

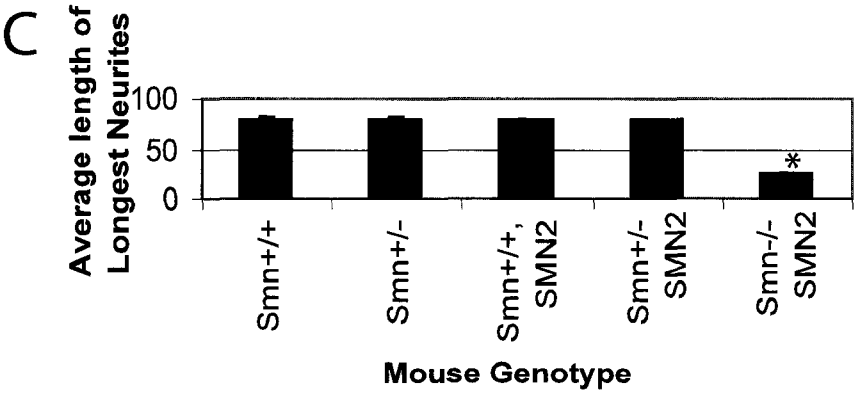
C
Average length of Longest Neurites
100
50
0
*
Smn+/+
Smn+/-
Smn+/+, SMN2
Smn+/- SMN2
Smn-/- SMN2
Mouse Genotype

5.1.4 Neuronal patterning defects and truncations of cranial and spinal nerves in the *Smn$^{-/-}$;SMN2* embryos

To assess whether Smn may have a role in specifying cranial nerve patterning and axonal growth, we analyzed axonal tracts by whole mount immunostaining at E10.5 with anti-neurofilament antibodies (2H3) (Fig. 5.10). The *Smn$^{-/-}$;SMN2* mice displayed abnormal patterning of the glossopharyngeal nerve (IX) and the vagus nerve (X) such that these nerves appeared to be partially fused in 19 out of 21 embryos examined (Fig. 5.10E and Table 5.1). The wild type and the *Smn$^{+/-}$* embryos did not show the merging of nerves IX and X, and maintained a gap between these two nerves (Fig. 5.10A,B). In addition, 7 out of 21 *Smn$^{-/-}$;SMN2* embryos also exhibited truncations in the lumbar spinal nerves (Fig. 5.10E, last panel and Table 5.1). The reduction of Smn thus affects the normal formation of some cranial nerves, most notably those containing axons of the branchiomotor neurons subtype. Furthermore, these defects were much more apparent in embryos with severe depletion of Smn.

5.1.5 Motor neuron subpopulations are born in a normal manner in the spinal cord of *Smn$^{-/-}$;SMN2* embryos

To investigate the impact of Smn knockdown on the generation of specific neuronal populations within the neural tube, we performed immunohistochemistry with antibodies specific for subpopulations of progenitors in transverse sections of the spinal cord at forelimb and hindlimb levels of the *Smn$^{+/-}$* and *Smn$^{-/-}$;SMN2* mice at E10.5 and E11.5. Islet1 is an early marker of neuronal differentiation and

Fig. 5.10. Neuronal patterning defects and truncations of cranial and spinal nerves in the *Smn*$^{-/-}$;*SMN2* embryos. Whole mount immunostaining of *Smn*$^{+/+}$ (A), *Smn*$^{+/-}$ (B), *Smn*$^{+/+}$;*SMN2* (C), *Smn*$^{+/-}$;*SMN2* (D) and *Smn*$^{-/-}$;*SMN2* (E) E10.5 embryos was performed using the anti-neurofilament antibody 2H3. Cranial nerves IX, X, and XI, as well as the spinal lumbar nerves are indicated. Note that all of the photographs represented in the left column were taken at the same magnification.

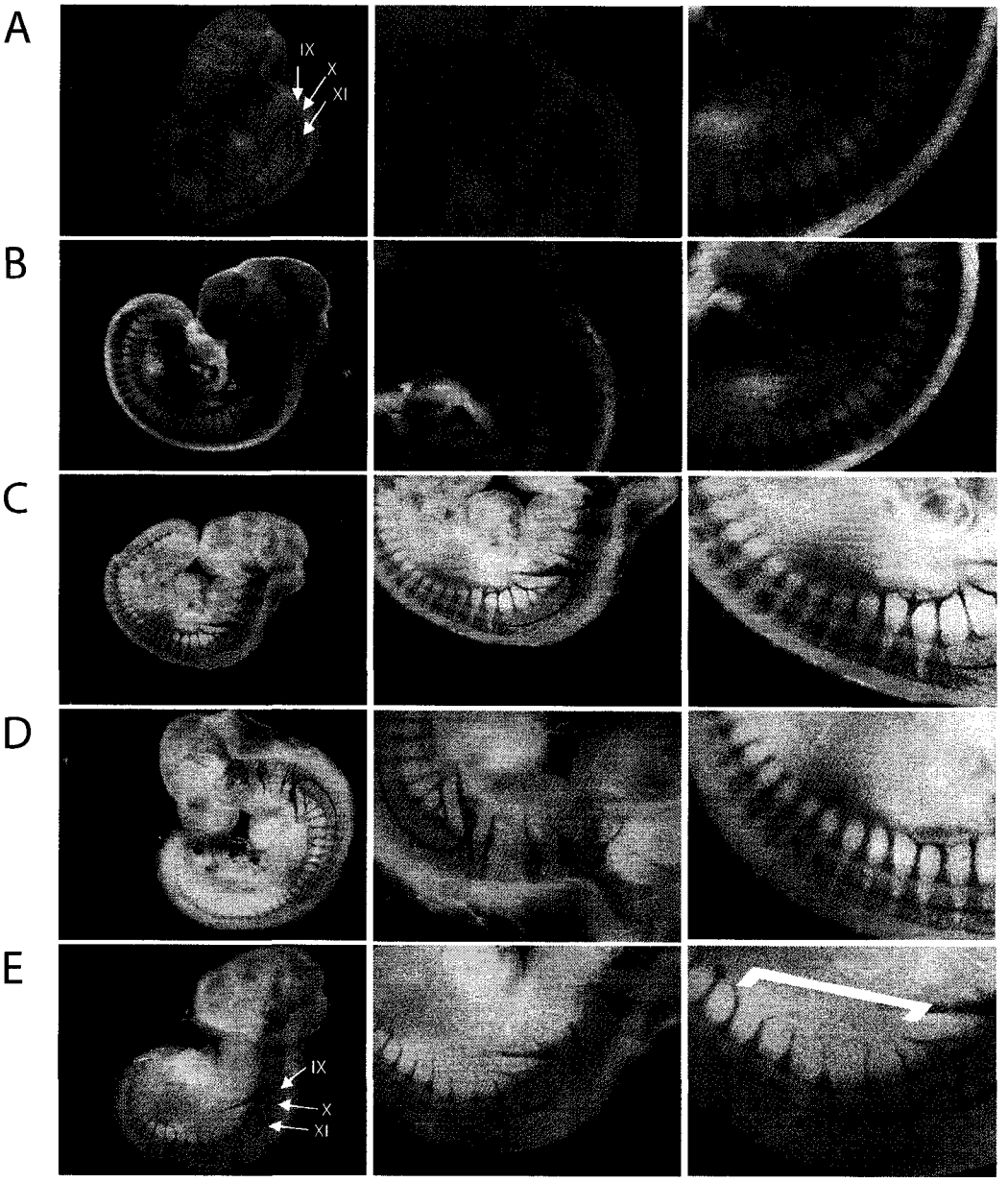
A
IX
X
XI
B
C
D
E
IX
X
XI

Table 5.1. Cranial and spinal nerve defects in E10.5 *Smn*$^{-/-}$;*SMN2* embryos.

Genotype	Total	Abnormal nerve patterning	Fused nerves IX and X	Truncated lumbar nerves
Smn$^{+/+}$	17	0	0	0
Smn$^{+/-}$	19	1	1	0
Smn$^{+/+}$;*SMN2*	23	0	0	0
Smn$^{+/-}$;*SMN2*	38	2	2	0
Smn$^{-/-}$;*SMN2*	21	17	17	7

is required for the generation of all spinal motor neurons (Karlsson, Thor et al. 1990; Ericson, Thor et al. 1992; Tsuchida, Ensini et al. 1994). Lim1 is expressed in motor neurons from the lateral motor column in the spinal cord (Tsuchida, Ensini et al. 1994; Appel, Korzh et al. 1995). Nestin is an intermediate filament protein expressed in neural stem cells (Lendahl, Zimmerman et al. 1990; Zimmerman, Parr et al. 1994; Wiese, Rolletschek et al. 2004) and HB9 is expressed by postmitotic motor neurons (Arber, Han et al. 1999; Thaler, Harrison et al. 1999; Broihier and Skeath 2002)(for normal distribution patterns of these marker proteins, see Fig. 5.11). There was no significant difference in the total number of Islet1-postive cells in the ventromedial region of the spinal cord at both the forelimb and hindlimb levels in wild type and mutant embryos (Fig. 5.12). Similar results were obtained for Lim1 and HB9, indicating that specific sub-populations of motor neurons were generated in the spinal cords of Smn-depleted embryos (Fig. 5.12), and suggesting that the nerve patterning defect and truncation we have observed (Fig. 5.10) is not due to a decrease in neuron number, nor a delay in motor neuron differentiation.

5.1.6 Assessment of neuromuscular junctions in the *Smn*$^{+/-}$ and *Smn*$^{-/-}$;*SMN2* mice

Since we have observed abnormal patterning of the glossopharyngeal nerve and the vagus nerve, and truncations in the lumbar spinal nerves in the *Smn*$^{-/-}$;*SMN2* severe mice, we investigated the formation of neuromuscular junctions. We have assessed the morphology of neuromuscular junctions at

Fig. 5.11. Motor neuron subpopulations are born in a normal manner in the spinal cord of *Smn*$^{-/-}$;*SMN2* embryos. Immunohistochemistry on transverse sections of spinal cord at forelimb (A) and hindlimb (B) level demonstrates the expression of marker genes for distinct subpopulations of neuronal progenitors in E10.5 (A) and E11.5 (B) wild type embryos.

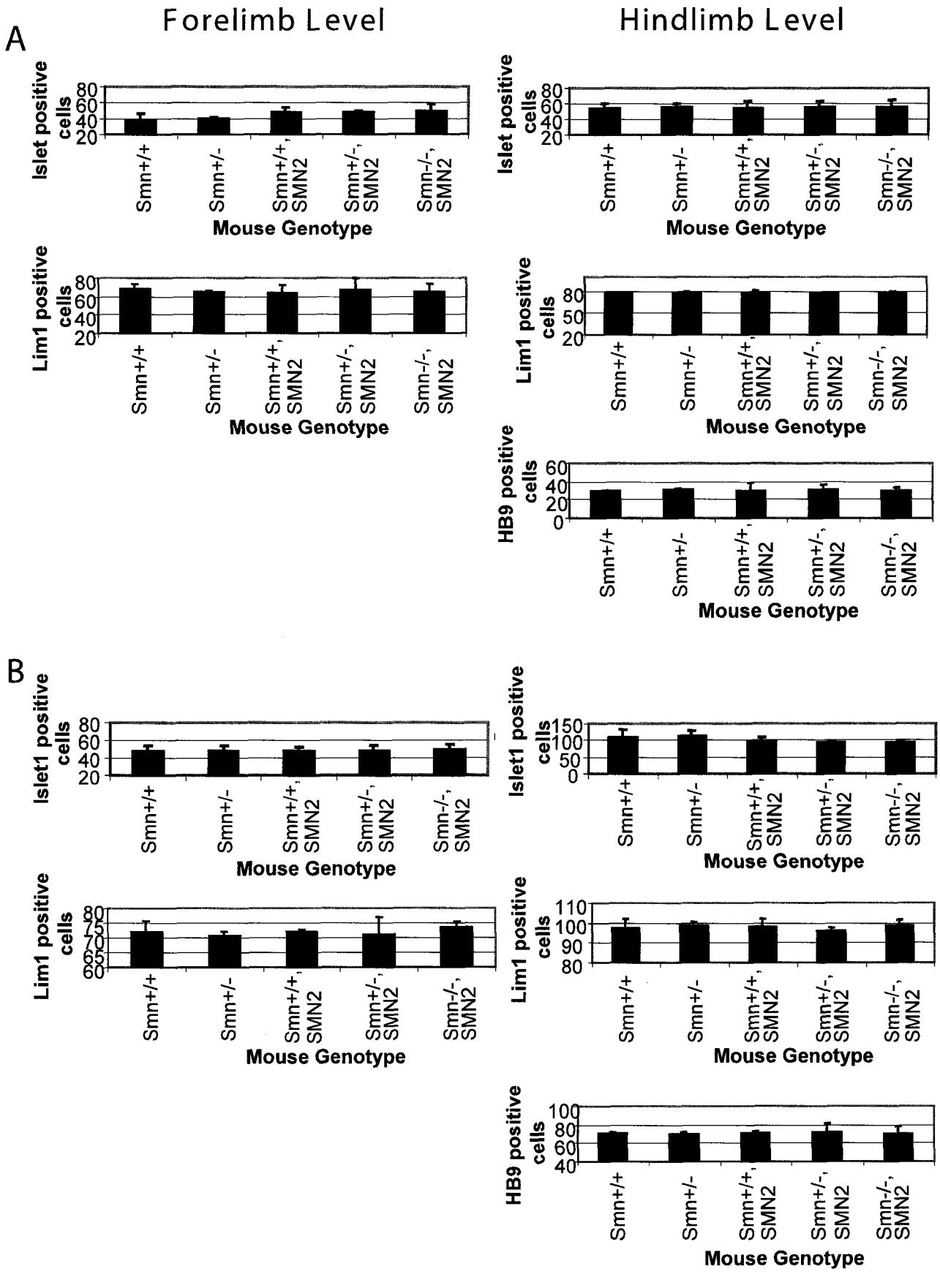
A
Forelimb Level
Hindlimb Level
Islet positive cells
Lim1 positive cells
HB9 positive cells
Smn+/+
Smn+/-
Smn+/+, SMN2
Smn+/-, SMN2
Smn-/-, SMN2
Mouse Genotype
B
Islet1 positive cells
Lim1 positive cells
HB9 positive cells
Mouse Genotype

Fig. 5.12. No difference in neuronal marker number between wild type and mutant mice. Numbers of Islet 1, Lim1, and HB9 positive cells at the forelimb (left column) and hindlimb level (right column) at E10.5 (A) and E11.5 (B). No significant differences were apparent between any of the genotypes analyzed.

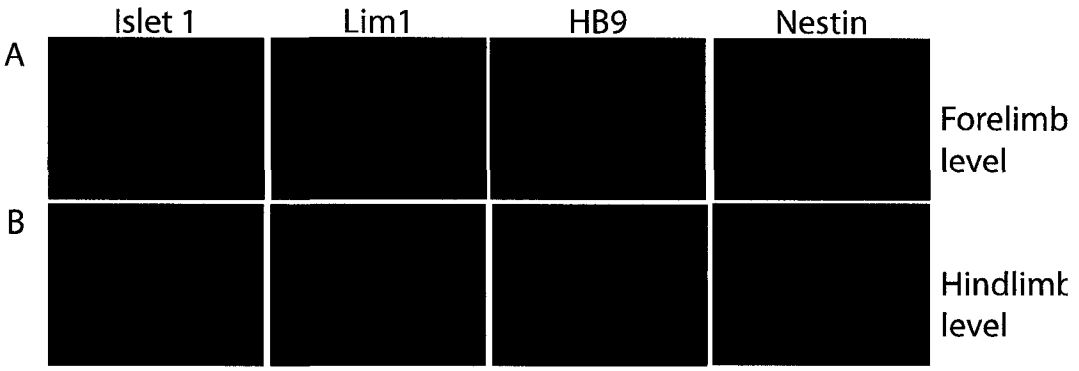
Islet 1
Lim1
HB9
Nestin
A
B
Forelimb level
Hindlimb level

E18.5 in the diaphragm and gastrocnemius muscles by performing electron microscopy. At E18.5 the neuromuscular junctions appeared as a thin layer of basal lamina between the axon and muscle. There were no differences observed between wild type and mutant muscle (for normal neuromuscular junction morphology see Fig. 5.13). We have also assessed the number of neuromuscular junctions at E18.5 in the diaphragm and gastrocnemius muscles by staining with α-bungarotoxin. There was no significant difference in the total number of neuromuscular junctions between the wild type and mutant muscle (Fig. 5.14), suggesting that the abnormalities in neuronal patterning and truncation in the *Smn*$^{-/-}$;*SMN2* severe mice do not affect neuromuscular junction formation.

Fig. 5.13. No difference in neuromuscular junction morphology between wildtype and mutant muscle. Electron micrograph of a neuromuscular junction from E18.5 wildtype diaphragm muscle at low (A) and high (B) magnification. Black scale bar, 10 um. White scale bar, 500 nm.

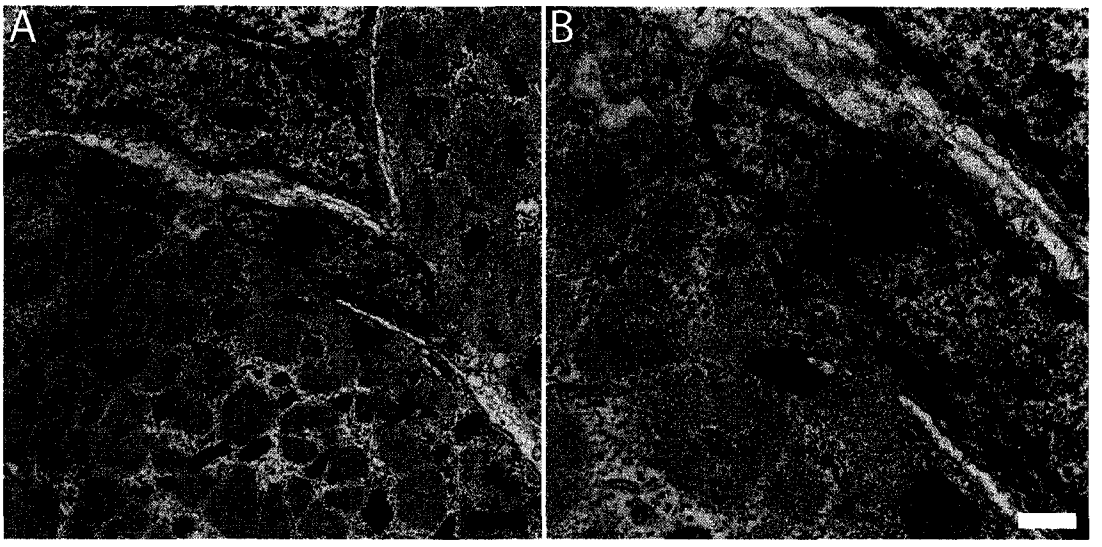
A
B

Fig. 5.14. No difference in neuromuscular junction number between wildtype and mutant muscle. Dystrophin (green) and alpha-bungarotoxin (red) staining in diaphragm (A) and gastronemius (B) muscle of wildtype E18.5 embryos. There is no significant difference in the number of neuromuscular junctions per defined area in diaphragm (C) and gastronemius (D) muscle between all genotypes. Scale bar, 50 um.

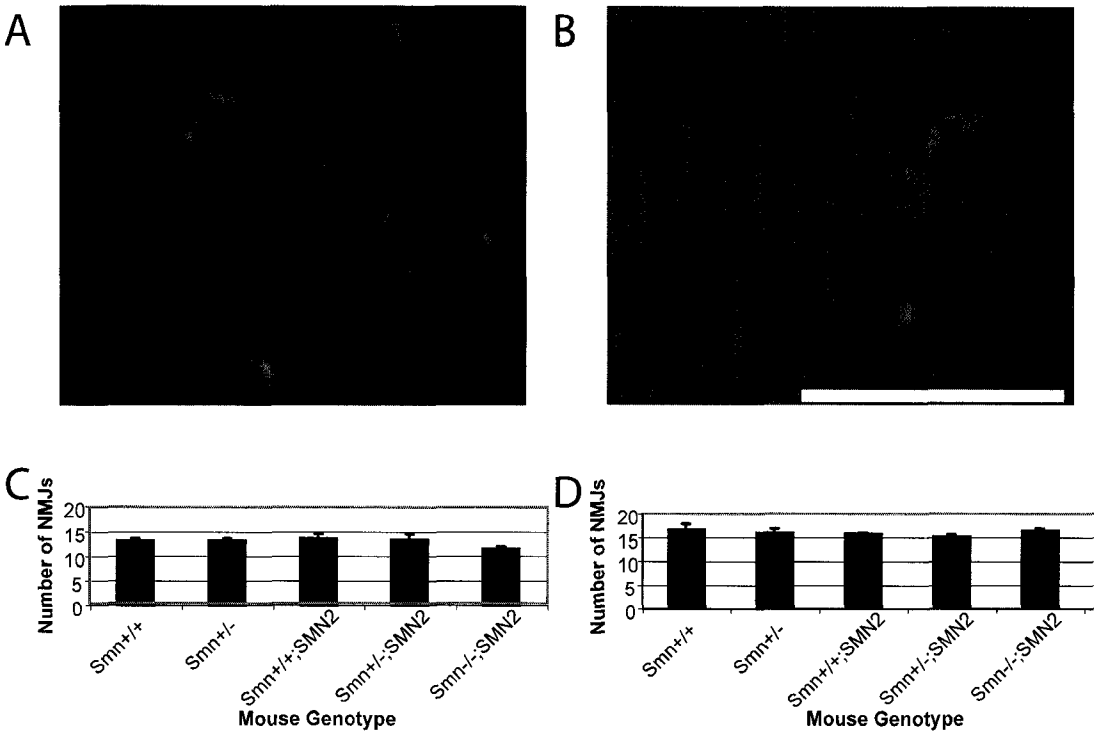
A
B
C
Number of NMJs
20
15
10
5
0
Smn+/+
Smn+/-
Smn+/+;SMN2
Smn+/-;SMN2
Smn-/-;SMN2
Mouse Genotype
D
Number of NMJs
20
15
10
5
0
Smn+/+
Smn+/-
Smn+/+;SMN2
Smn+/-;SMN2
Smn-/-;SMN2
Mouse Genotype

5.2 DISCUSSION

SMA displays a wide range of disease severity caused by a similar range of SMN dosage. Patient studies have shown that *SMN2* gene copy number is inversely correlated with SMA disease severity (Coovert, Le et al. 1997; Lefebvre, Burlet et al. 1997; Feldkotter, Schwarzer et al. 2002; Wirth, Brichta et al. 2006). Type I SMA patients generally have a low number (1-2) of *SMN2* copies (Feldkotter, Schwarzer et al. 2002), and thus have the most severe phenotype. Type II and III SMA patients usually have a higher number (3-4) of *SMN2* copies and conversely have relatively milder phenotype. The dosage effect of SMN has been recapitulated in mouse models of SMA (Hsieh-Li, Chang et al. 2000; Jablonka, Schrank et al. 2000; Monani, Sendtner et al. 2000; Monani, Pastore et al. 2003; Le, Pham et al. 2005). The work on these SMA mouse models and on cell culture systems (Rossoll, Jablonka et al. 2003; Zhang, Pan et al. 2003; Bowerman, Shafey et al. 2007) has shown that SMN has nuclear as well as cytoplasmic functions and interacts with a large number of proteins. It is not clear which of these disparate functions contribute to SMA pathophysiology.

The early, sometimes fetal, onset of the severe forms of SMA has contributed to the ongoing debate in the field as to whether this disease is a neurodevelopmental as well as a neuro-maintenance disorder. The mouse models of SMA would suggest that the severity of the neurodevelopmental deficit depends on the dosage of Smn protein available as shown in ours as well as other studies. Insight into this issue is important for timing of intervention in the treatment of different forms of SMA.

5.2.1 Neurodevelopment defect in severe SMA embryos

In this study, we have chosen to study neurodevelopment in two SMA mouse models; one (*Smn*$^{-/-}$;*SMN2*) with very severe neurological deficits reminiscent of human type I SMA and one (*Smn*$^{+/-}$) with modest motor neuron loss in which there is no overt phenotype, resembling human SMA type IV.

We have shown that axons from cranial nerves IX and X display partial fusion in the *Smn*$^{-/-}$;*SMN2* severe SMA model providing evidence that Smn depletion affects the determination and/or differentiation of at least a subset of branchial motor neurons during hindbrain development. Cranial nerves IX and X belong to the branchiomotor and visceromotor class of nerves and innervate the laryngeal and pharyngeal muscles responsible for swallowing as well as the autonomic system which impacts intestinal peristalsis as well as heart rate and respiration (Birnkrant, Pope et al. 1998; Cordes 2001). Thus, the involvement of this class of neurons not only fits well with the respiratory failure seen in SMA patients (Bach, Niranjan et al. 2000; Bach, Baird et al. 2002), but also cardiac involvement (Tanaka, Uemura et al. 1976; Kimura, Yokota et al. 1980; Ceroni, Grandi et al. 1982; Liu, Chen et al. 1999; Yasuma, Kuru et al. 2004), as well as intestinal dysmotility.

In addition to the cranial nerve abnormality, truncated lumbar nerves were observed in a subset of the most affected *Smn*$^{-/-}$;*SMN2* embryos suggesting that Smn depletion can impact axon growth/guidance in the nerves that innervate the muscles of the lower body, which are central to walking and sitting, two traits

affected in the most severe form of SMA (Munsat and Davies 1992). Importantly, the nerve patterning defect and truncation we have observed is not associated with a decrease in neuron number; normal numbers of specific sub-populations of motor neurons are generated appropriately in the spinal cords of Smn-depleted embryos.

These results are similar to those reported for the zebrafish SMA model (McWhorter, Monani et al. 2003). In the latter study, morpholino anti-sense oligonucleotides targeting *Smn* mRNA (Smn-MO) were injected into zebrafish embryos to decrease the levels of SMN protein and mimic SMA. Zebrafish embryos injected with Smn-MO had a decrease in Smn protein levels which resulted in truncated nerves and aberrant motor axon branching.

5.2.2 No abnormalities in neuromuscular junction morphology and number

Due to the abnormal patterning of the glossopharyngeal and the vagus nerves, and truncations in the lumbar spinal nerves observed in the *Smn*$^{-/-}$;*SMN2* severe mice, we investigated the formation of neuromuscular junctions. During development, the neuromuscular junction undergoes physiological and morphological maturation beginning at E15.5, extending to several weeks after birth (Dennis 1981). In our study, neuromuscular junctions of embryonic mice were examined at the fine structural level using electron microscopy. We did not observe any differences between the neuromuscular junctions in wild type and *Smn*$^{-/-}$;*SMN2* severe mice at E18.5. However, at this early stage the neuromuscular junction appears as a basal lamina between the axon and the

muscle. The characteristic junctional folds of the neuromuscular junction do not appear until 2 weeks after birth (Matthews-Bellinger and Salpeter 1983). We could not study the neuromuscular junction at that age because the *Smn*$^{-/-}$;*SMN2* severe mice do not live past birth. Furthermore, the number of neuromuscular junctions did not differ from wild type to *Smn*$^{-/-}$;*SMN2* severe mice. Thus, formation of neuromuscular junctions is not affected by a severe reduction in Smn expression.

5.2.3 Severe SMA neural stem cells are remaining in a progenitor state

In the present study, we have corroborated our findings from the *in vivo* phenotype by assessing the impact of Smn dosage on NSC differentiation *in vitro*. NSCs are multi-potent, self-renewing cells that can be propagated in culture and provide a source of cells for *in vitro* studies aimed at elucidating the mechanisms in the pathogenesis of human neurological disorders like amyotrophic lateral sclerosis (ALS), fragile X syndrome and Down syndrome (Bahn, Mimmack et al. 2002; Castren, Tervonen et al. 2005; Liu and Martin 2006; Chi, Ke et al. 2007). ALS is a fatal adult human disease caused by motor neuron degeneration with similarities to SMA. In the context of ALS, NSCs are being studied to see if they may be used to restore neurological function in patients. In this regard, it has been demonstrated that new neurons can be generated from some brain regions in mice. New upper motor neurons with long distance corticospinal projections can be generated from the endogenous NSC pool in adult mice (Chen, Magavi et al. 2004). The preservation of NSCs and neuroprogenitors in the SMA mouse models could support strategies designed to activate the neural stem cell pool for the

replacement of motor neurons that degenerate in these mice (Zang and Cheema 2002). As well, adult NSCs and neuroprogenitors in the SMA mice could be harvested for use in transplantation to reconstruct motor neuron groups and skeletal muscle. Thus studying neural stem cells in the context of SMA is an important prelude to the development of such therapies.

The absence of phenotype in terms of establishing, growing and ultimate size of spheres for the various mutant backgrounds suggests that Smn is not required for sphere growth consistent with the low levels of Smn protein observed in growing spheres compared to differentiating NSCs. Upon initiating a differentiation program on dissociated neurospheres, a decrease in Tuj1-positive neurons was observed uniquely in *Smn*$^{-/-}$*;SMN2* NSCs with no change in the number of oligodendrocytes or astrocytes and no increase in cell death. In addition, there is an increase in the number of proliferative NSCs and the number of nestin-positive cells in the Smn depleted NSCs. Nestin expression should be downregulated in differentiated NSCs (Wiese, Rolletschek et al. 2004) and BrdU incorporation should decrease as cells exit the cell cycle. Since differentiating NSCs from *Smn*$^{-/-}$*;SMN2* mice continue to express nestin and incorporate BrdU, we conclude that these cells are failing to exit the cell cycle appropriately and are remaining in a progenitor state and not differentiating as they normally do. Thus, the decrease in Tuj1-positive cells and the increase in nestin-positive and BrdU-positive cells from *Smn*$^{-/-}$*;SMN2* mice indicates that the *Smn*$^{-/-}$*;SMN2* NSCs are delayed in their differentiation into neurons.

The *Smn*$^{-/-}$;*SMN2* NSCs that do differentiate into neurons exhibit prominent morphological defects. In particular, the number of primary neurites and neurite outgrowth was reduced. Other studies have shown that the depletion of Smn leads to a reduction in neurite outgrowth. It has been demonstrated that a reduction of Smn by shRNA in PC12 cells significantly decreases the growth of neurites (Bowerman, Shafey et al. 2007; van Bergeijk, Rydel-Konecke et al. 2007). Other studies have shown a decrease in neurite length in primary neurons from Smn deficient mice (Rossoll, Jablonka et al. 2003; Jablonka, Karle et al. 2006). The reduced number of primary neurites and the short neurite length of these differentiating neurons may represent the effects of Smn depletion on the dominating neuronal population at the early stage of neuronal development.

It therefore appears that severe depletion of SMN has an impact on axonal outgrowth *in vivo* and in cell culture whereas a moderate depletion does not. It could be argued that in severe forms of SMA, in which motor neurons have defects in axon outgrowth, that the neurodevelopmental aspect is most significant and there may be faulty innervation of target muscle, ultimately leading to muscle atrophy. At the other extreme, in mild forms of SMA, motor neurons may innervate their target muscle correctly, but because of unspecified defects, post-natal denervation, and late-onset degeneration eventually occur leading to muscle atrophy. Thus, in mild SMA, the neuro-maintenance aspect would have a greater role. This model fits best with electrophysiologic results in human SMA, which show early loss of motor units (Swoboda, Prior et al. 2005) and immature muscle histology (Hausmanowa-Petrusewicz, Fidzianska et al. 1980) in severe SMA.

These results give us a better understanding of the dual role of SMN, one during development and the other during post-natal stages. Interestingly, none of the abnormalities in neuronal outgrowth or patterning seen in the severe mouse were observed in the "type IV" mild SMA *Smn*$^{+/-}$ mouse although this strain loses approximately 30% of its motor neurons by five weeks of age (Jablonka, Schrank et al. 2000; Balabanian, Gendron et al. 2007). We are thus confronted by a disconnect; in the severe SMA mouse we observe a gross phenotype and motor neuron loss and in the mild mouse only the latter. The fact that anatomic anomalies are not seen in all the axonal tracts where there is neuronal loss in the severe SMA mouse and not at all in the mild SMA model suggests that anomalies, although clearly a reflection of the underlying Smn depletion, do not themselves cause motor neuron loss. It is not clear whether the unidentified SMN role(s), which do lead to motor neuron death, are at play in the developmental stage (not withstanding our failure to detect a phenotype) or post development in neuro-maintenance or both. A better understanding of the dual role of SMN, one during neurodevelopment and the other during post-natal neuro-maintenance is important as we develop appropriate therapies for the different types of SMA.

6.0 Identification of novel interacting protein partners of SMN using Tandem Affinity Purification

Tandem Affinity Purification (TAP) has emerged as a useful tool for studying protein complexes *in vitro*. We have used this purification system to identify novel survival motor neuron (SMN) interacting proteins in C2C12 and PC12 cells. Mutations in SMN cause Spinal Muscular Atrophy (SMA), a neuromuscular disease that affects voluntary movement and causes proximal, symmetrical limb and trunk muscle weakness that progresses to paralysis, respiratory distress, and ultimately death. Both neurons and muscle are severely affected in this disease. Thus, to discover new SMN interacting partners in these relevant cell types, we fused a TAP-tag, consisting of a HIS hexamer and FLAG epitope separated by the Tobacco Etch Virus (TEV) protease cleavage site, to either the N- or C-terminal of SMN. These fusion proteins were stably expressed in C2C12 and PC12 cells at similar to endogenous levels and native SMN protein complexes were purified from cell lysates at different stages of growth and differentiation. Interestingly, the profile of SMN interacting proteins varies depending on the cell type and stage. We have identified a number of novel SMN interacting proteins in both C2C12 and PC12 cells, and from among these, we have validated Annexin II and myosin regulatory light chain (MRLC). Furthermore, we demonstrate that MRLC levels are increased and the protein is mis-localized in Smn depleted C2C12 cells. Our work has set the foundation on which to assess the importance of the various Smn interacting proteins in the context of SMA pathogenesis.

6.1 RESULTS

6.1.1 Generation of NTAP-SMN and CTAP-SMN stable cell lines

The TAP-tag vector consists of a HIS and a FLAG epitope separated by a Tobacco Etch Virus (TEV) protease cleavage site. The N-terminal TAP-tag (NTAP) has the HIS epitope on the outside and the C-Terminal TAP-tag (CTAP) has the FLAG epitope on the outside (Fig. 6.1A). Recombinant retroviruses carrying the NTAP-SMN and CTAP-SMN constructs were prepared to infect C2C12 and PC12 cells. Stable cell lines that maintain the expression of the fusion protein at similar to endogenous levels were generated (Fig. 6.1B-E). Clones N5 and C12 were selected from the C2C12 stable cell lines expressing NTAP-SMN and CTAP-SMN, respectively for all subsequent experiments. Similarly, clones N4 and C1 from the PC12 stable cell lines expressing NTAP-SMN and CTAP-SMN, respectively were selected for all subsequent experiments.

6.1.2 Purification of SMN complexes

Cell extracts from all four clones were collected at growth, one, three, five, and seven days of differentiation. The tagged SMN proteins, as well as any associated components, were recovered by tandem affinity purification. Samples were resolved by SDS-PAGE, and the gels were silver stained to reveal the protein banding pattern for the different cell types as well for the different stages of differentiation. Interestingly, in C2C12 cells the SMN complex constituents vary depending on whether the analysis is done at growth, early differentiation, or

Fig. 6.1. NTAP and CTAP-SMN constructs and clones. A. Schematic of the N-terminal (NTAP) and C-terminal (CTAP) SMN constructs. B-D. Cell lysates of C2C12 (B,C) and PC12 (D,E) clones expressing NTAP-SMN and CTAP-SMN were resolved on SDS-PAGE. SMN levels were determined by blotting with an anti-Smn antibody. The endogenous Smn protein migrates at a faster rate than the tagged fusion protein. The asterisk (*) indicates the clones that were used for the subsequent studies.

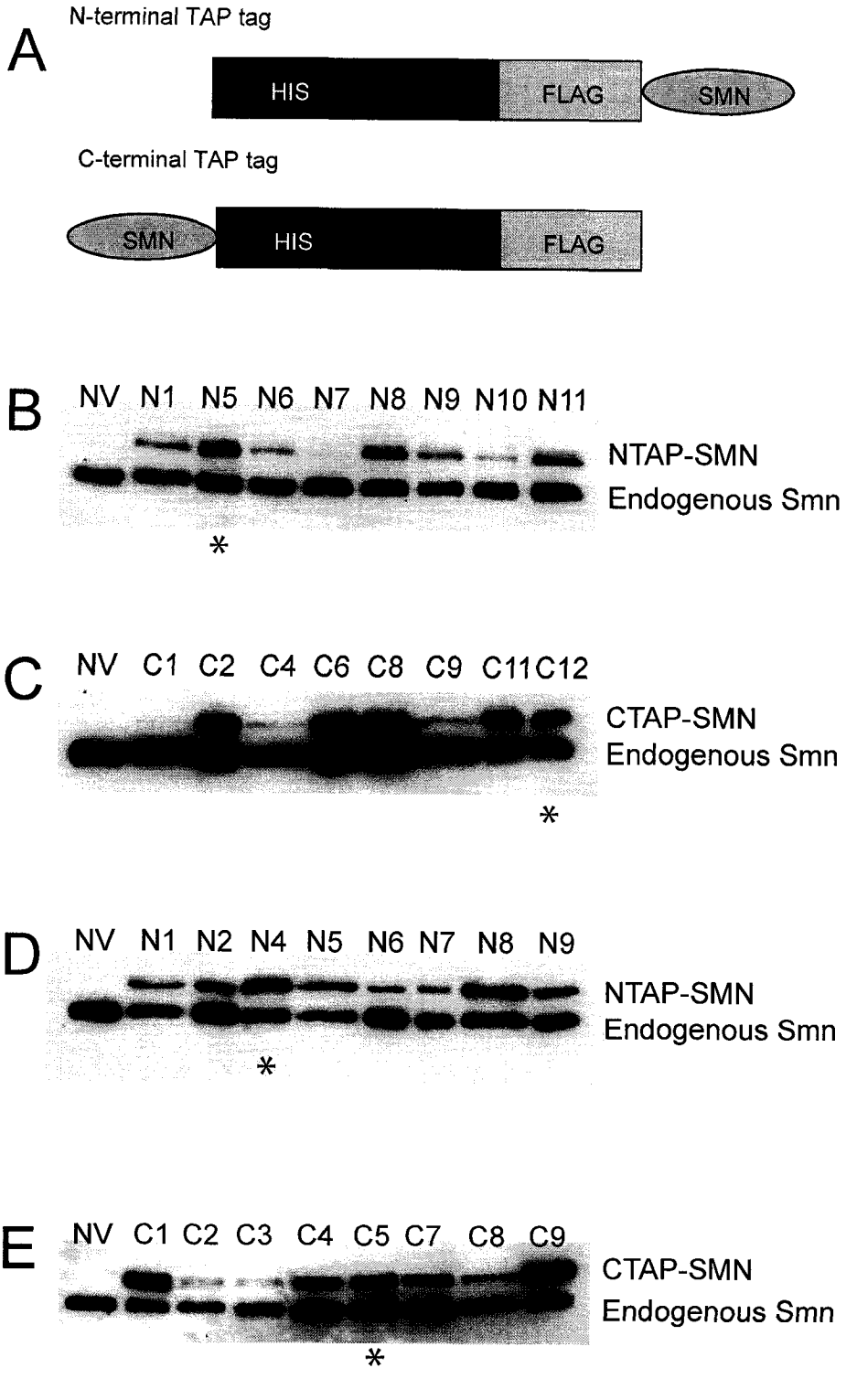
A
N-terminal TAP tag
HIS
FLAG
SMN
C-terminal TAP tag
SMN
HIS
FLAG
B
NV N1 N5 N6 N7 N8 N9 N10 N11
NTAP-SMN
Endogenous Smn
*
C
NV C1 C2 C4 C6 C8 C9 C11C12
CTAP-SMN
Endogenous Smn
*
D
NV N1 N2 N4 N5 N6 N7 N8 N9
NTAP-SMN
Endogenous Smn
*
E
NV C1 C2 C3 C4 C5 C7 C8 C9
CTAP-SMN
Endogenous Smn
*

late differentiation (Fig. 6.2 and Fig. 6.3). By contrast, in PC12 cells the Smn complex remains relatively invariant during growth and differentiation (Fig. 6.2 and Fig. 6.3). In addition, in both the C2C12 and PC12 purifications, the NTAP-SMN fusion was more efficient at purifying interacting proteins than the CTAP-SMN fusion. This difference could be due to possible interference of the TAP-tag at the C-terminal end of SMN.

6.1.3 Identification of co-purifying proteins

To identify the proteins that were co-purified with NTAP-SMN and CTAP-SMN, silver stained visible bands were excised from gels and subjected to tryptic digestion. An LTQ linear ion trap mass spectrometer was used for identification of the resulting peptides. In this manner, we not only detected known binding partners for SMN, such as Gemin2, SnrpD1, and profilin, but we have in addition identified new binding partners (summarized in Tables 6.1-6.4). There were many SMN interacting proteins that were specific to the C2C12 cell or PC12 cell sample, however some SMN interacting proteins were identified in both C2C12 and PC12 cells and these are listed in Table 6.5.

6.1.4 Validation of novel SMN interacting proteins

Of the many novel SMN interacting proteins identified, we chose to validate Annexin II and myosin regulatory light chain (MRLC) in C2C12 cells and Annexin II in PC12 cells. Annexin II was identified as an interacting protein in both C2C12 and PC12 cells, whereas MRLC was specific to C2C12 cells. As

Fig. 6.2. NTAP-SMN complex purification. NTAP-SMN complex purified from C2C12 (A) and PC12 (B) cell clones during growth, and 1, 3, 5 and 7 days of differentiation were resolved on SDS-PAGE and silver stained. The numbers indicate the bands that were excised from the gel and identified by mass spectrometry. Molecular weight markers are indicated on the left.

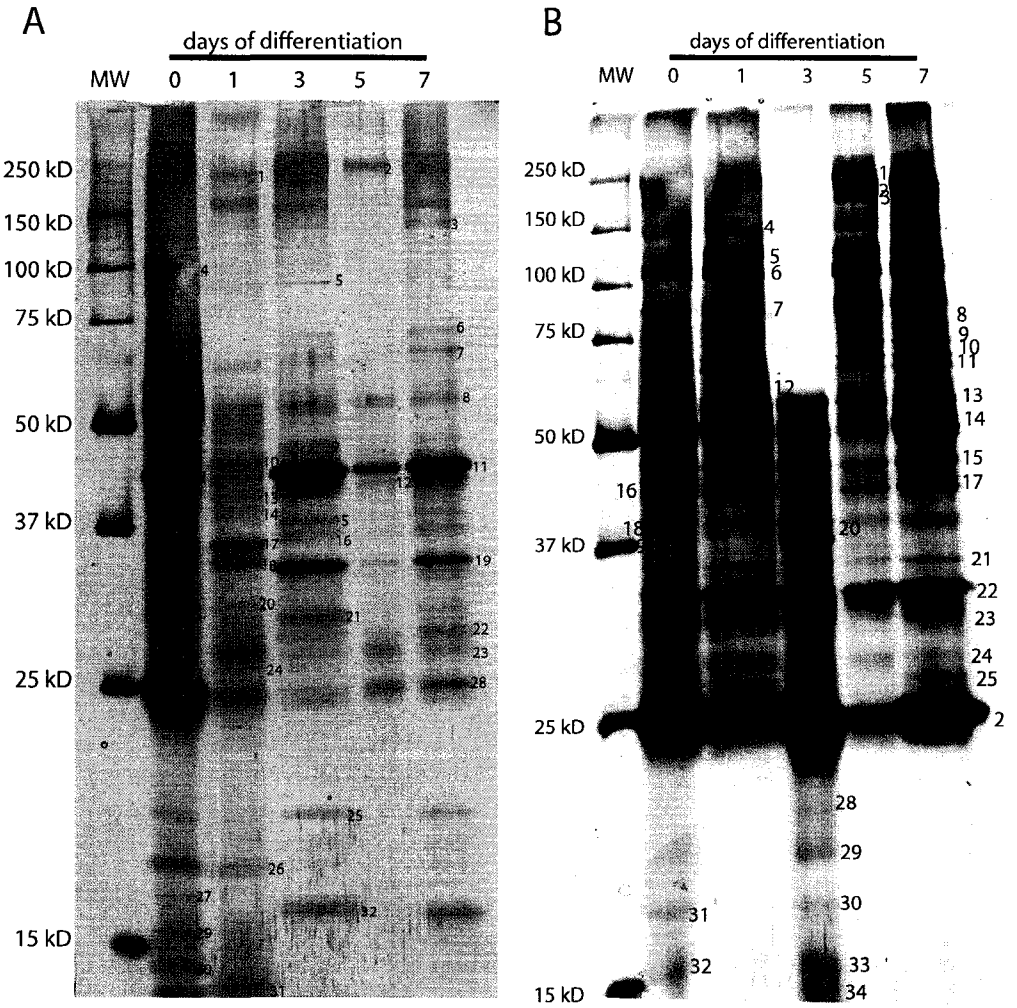
A
days of differentiation
MW
0
1
3
5
7
250 kD
150 kD
100 kD
75 kD
50 kD
37 kD
25 kD
15 kD
B
days of differentiation
MW
0
1
3
5
7
250 kD
150 kD
100 kD
75 kD
50 kD
37 kD
25 kD
15 kD

Fig. 6.3. CTAP-SMN complex purification. CTAP-SMN complex purified from C2C12 (A) and PC12 (B) cell clones during growth, and 1, 3, 5 and 7 days of differentiation were resolved on SDS-PAGE and silver stained. The numbers indicate the bands that were excised from the gel and identified by mass spectrometry. Molecular weight markers are indicated on the left.

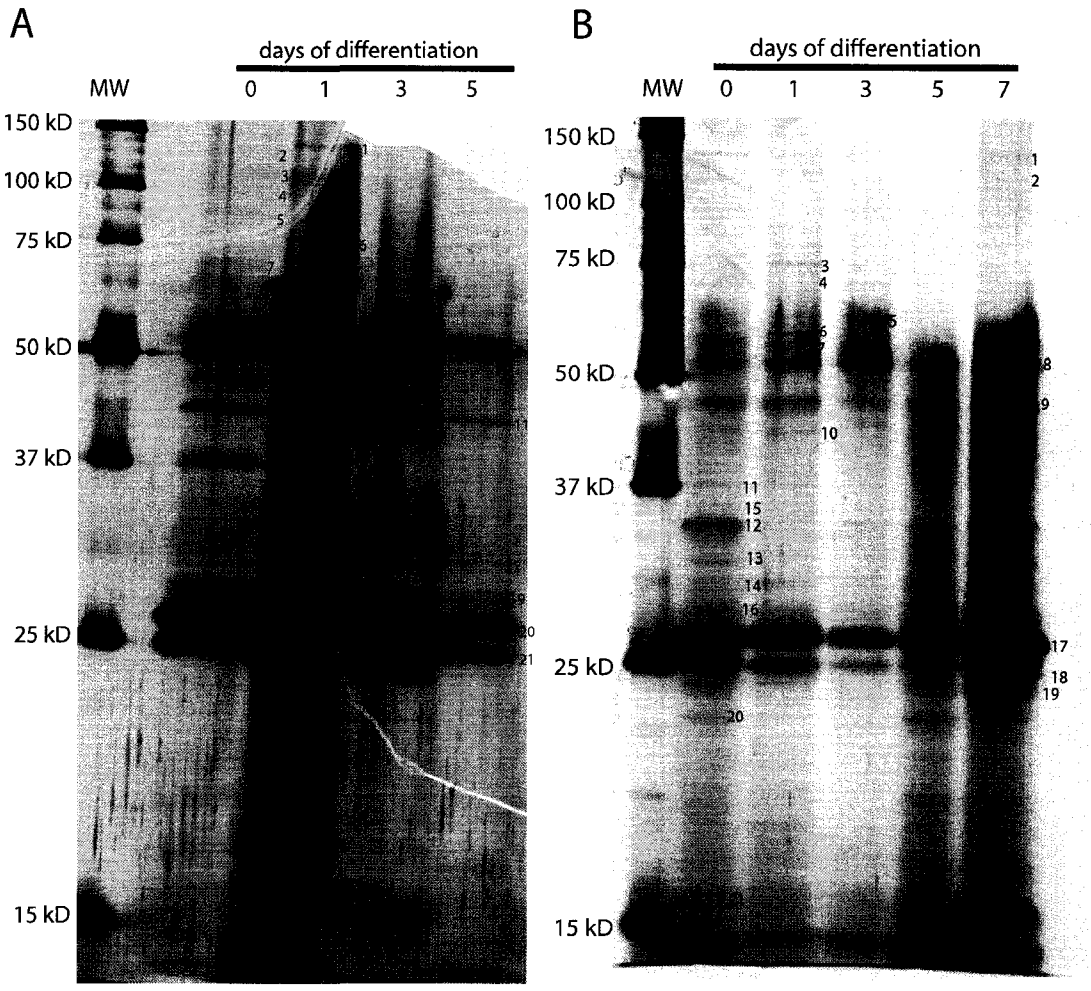
A
days of differentiation
MW
0
1
3
5
150 kD
100 kD
75 kD
50 kD
37 kD
25 kD
15 kD
B
days of differentiation
MW
0
1
3
5
7
150 kD
100 kD
75 kD
50 kD
37 kD
25 kD
15 kD

Table 6.1. Identification of Proteins recovered from the NTAP-SMN tandem affinity purification in C2C12 cells.

BAND	Protein Identification	Days of Differentiation					C2C12 CTAP-SMN *	PC12 TAP-tag SMN **
		0	1	3	5	7		
1	Fn1 NOD-derived CD11c +ve dendritic cells	+	+	+	-	-	-	-
2	Myh9 Myosin-9	-	-	+	+	+	-	-
3	Myh9 15 days pregnant adult female amnion cDNA	-	-	-	-	+	-	-
	Myh10 Myosin, heavy polypeptide 10, non-muscle	-	-	-	-	+	-	-
4	Actn4 Alpha-actinin-4	+	-	-	-	-	-	-
	Actn1 Alpha-actinin-1	+	-	-	-	-	-	-
5	Actn1 Alpha-actinin-1	+	+	+	+	+	-	-
	Actn4 Alpha-actinin-4	+	+	+	+	+	-	-
	Sfpq Splicing factor, proline- and	+	+	+	+	+	-	+
	Gsn Isoform 1 of Gelsolin precursor	+	+	+	+	+	+	-
6	Gsn Isoform 1 of Gelsolin precursor	+	+	+	+	+	+	-
	Actb Actin, cytoplasmic 1	+	+	+	+	+	+	+
	Sfpq Splicing factor, proline- and	+	+	+	+	+	-	+
7	Myh9 15 days pregnant adult female amnion cDNA	+	+	+	+	+	-	-
8	Actb Actin, cytoplasmic 1	+	+	+	+	+	+	+
	Acta1 Actin, alpha skeletal muscle	+	+	+	+	+	+	+
9	Ppm1b Protein phosphatase 1B2 53 kDa isoform	-	-	+	-	-	-	+
10	Ppm1a Protein phosphatase 2C isoform alpha	-	+	-	-	-	-	+
11	Similar to cytoplasmic beta-actin	+	+	+	+	+	-	-
	Isoform C of Lamin-A/C	+	+	+	+	+	+	-
	Smn1 Survival motor neuron protein	+	+	+	+	+	+	+
12	Actb Actin, cytoplasmic 1	-	-	+	+	+	+	+
	Acta1 Actin, alpha skeletal muscle	-	-	+	+	+	+	+
	Smn1 Survival motor neuron protein	-	-	+	+	+	+	+
13	Mapk1 Mitogen-activated protein kinase 1	+	+	-	-	-	-	+
14	Dnajb11 DnaJ homolog subfamily B member 11	+	+	-	-	-	-	-
15	Tpm2 Isoform 1 of Tropomyosin beta chain	-	-	+	+	+	-	-
	Tpm1 Isoform 1 of Tropomyosin-1 alpha chain	-	-	+	+	+	-	-
16	Tpm2 Isoform 1 of Tropomyosin beta chain	-	-	+	+	+	-	-
	Tpm1 Isoform 1 of Tropomyosin-1 alpha chain	-	-	+	+	+	-	-
17	Nono Isoform 1 of Non-POU domain-containing	+	+	-	-	-	-	+
	Sfpq Splicing factor, proline- and	+	+	-	-	-	-	+
	Fn1 Fibronectin precursor	+	+	-	-	-	-	-
18	Sfpq Splicing factor, proline- and	+	+	-	-	-	-	+
	Pspc1 Paraspeckle protein 1	+	+	-	-	-	-	+
	Nono Isoform 1 of Non-POU domain-containing	+	+	-	-	-	-	+
19	Tpm1 Isoform 2 of Tropomyosin-1 alpha chain	-	-	+	+	+	-	-
	Tpm1 Isoform 1 of Tropomyosin-1 alpha chain	-	-	+	+	+	-	-
20	Gemin 2 (SIP1)	+	+	-	-	-	-	+
21	Tpm3 Isoform 2 of Tropomyosin alpha-3 chain	-	-	+	-	-	-	-
	Tpm3 2 days neonate thymus thymic cells cDNA	-	-	+	-	-	-	-

	Tpm4 Tropomyosin alpha-4 chain	-	-	+	-	-	-	-
	Tpm1 28 kDa protein	-	-	+	-	-	-	-
22	Tpm1 28 kDa protein	-	-	+	+	+	-	-
	Tpm3 2 days neonate thymus thymic cells cDNA	-	-	+	+	+	-	-
	Tpm3 Isoform 1 of Tropomyosin alpha-3 chain	-	-	+	+	+	-	-
	similar to cytoplasmic beta-actin	-	-	+	+	+	-	-
23	Igk-C Kappa light chain C_region (Fragment)	+	+	+	+	+	+	+
24	Spin1 Isoform 1 of Spindlin-1	+	+	-	-	-	-	+
	Ppm1b Protein phosphatase 1B2 53 kDa isoform	+	+	-	-	-	-	-
25	myosin regulatory light chain	+	-	+	+	+	-	-
26	Nme2 Nucleoside diphosphate kinase B	+	+	-	-	-	+	-
	Nme1 Nucleoside diphosphate kinase A	+	+	-	-	-	+	-
27	Nme1 Nucleoside diphosphate kinase A	+	-	-	-	-	+	-
	Myl6 Isoform Smooth muscle of Myosin light	+	-	-	-	-	+	-
28	Igk-C Kappa light chain C_region (Fragment)	+	+	+	+	+	+	+
29	Snrpd2 Small nuclear ribonucleoprotein Sm D2	+	-	-	-	-	-	+
	Snrpd1 Small nuclear ribonucleoprotein Sm D1	+	-	-	-	-	-	-
30	Pdlim2 PDZ and LIM domain protein 2	+	-	-	-	-	-	-
	Igk-C Kappa light chain C_region (Fragment)	+	-	-	-	-	+	+
	Mycbp C-Myc-binding protein	+	-	-	-	-	-	+
31	Snrpf small nuclear ribonucleoprotein	+	+	-	-	-	-	+
32	Similar to myosin, light polypeptide 6	-	-	+	+	+	-	-

+ : indicates the presence of the band

- : indicates the absence of the band

* : In the C2C12 CTAP-SMN column, the '+' indicates that the band is present and the '-' indicates that the band is absent at any time point analyzed

** : In the PC12 TAP-tag SMN column, the '+' indicates that the band is present and the '-' indicates that the band is absent at any time point and in either the CTAP-SMN or NTAP-SMN purification

Table 6.2. Identification of Proteins recovered from the CTAP-SMN tandem affinity purification in C2C12 cells.

BAND	Protein Identification	Days of Differentiation				C2C12 NTAP-SMN	PC12 Tap-tag SMN
		0	1	3	5		
1	similar to Spectrin alpha chain	-	+	-	-	-	-
2	Golga3 Isoform 1 of Golgin subfamily A member 3	+	-	-	-	-	-
3	Spna2 similar to Spectrin alpha chain	+	-	-	-	-	-
4	Myo18a Isoform 2 of Myosin-XVIIIa	+	-	-	-	-	-
	Myo1c Isoform B of Myosin-Ic	+	-	-	-	-	-
5	Gsn Isoform 1 of Gelsolin precursor	+	+	-	-	+	-
	Dhx15 Putative pre-mRNA-splicing factor	+	+	-	-	-	+
6	Rrbp1 Isoform 3 of Ribosome-binding protein 1	-	+	-	-	-	-
7	Rrbp1 ribosome binding protein 1 isoform a	+	-	-	-	-	-
8	Ivns1abp influenza virus NS1A binding protein	+	+	+	+	-	-
9	Ighg1 Ig gamma-1 chain C region	+	+	+	+	+	+
10	Eef1a2 Elongation factor 1-alpha 2	+	-	-	-	-	+
11	Smn1 Survival motor neuron protein	+	+	+	+	+	+
12	Actb Actin, cytoplasmic 1	-	+	+	-	+	+
	Lmna Isoform C of Lamin-A/C	-	+	+	-	+	-
13	Acta1 Actin	-	+	-	-	+	+
14	Hnrpab S1 protein C2	+	-	-	-	-	
	Smn1 Survival motor neuron protein	+	-	-	-	+	+
15	Anxa1 Annexin A1	-	+	-	-	-	
	Acta1 Actin, alpha skeletal muscle	-	+	-	-	+	+
16	Anxa2 Annexin A2	+	-	-	-	-	+
17	Ldha L-lactate dehydrogenase A chain	-	+	+	-	-	
	Acta1 Actin, alpha skeletal muscle	-	+	+	-	+	+
18	Actb Actin, cytoplasmic 1	-	+	+	-	+	+
	Acta1 Actin, alpha skeletal muscle	-	+	+	-	+	+
19	Ighg1 Ig gamma-1 chain C region, membrane-bound	+	+	+	+	+	+
20	Igk-C Kappa light chain C_region (Fragment)	+	+	+	+	+	+
21	Igk-C Kappa light chain C_region (Fragment)	+	+	+	+	+	+
22	Not identified	-	+	-	-	-	-
23	similar to Glyceraldehyde-3-phosphate	-	+	+	-	-	+
24	Not identified	-	+	-	-	-	-
25	Nme2 Nucleoside diphosphate kinase B	-	+	-	-	+	-
	Eif5a Eukaryotic translation initiation factor	-	+	-	-	-	
26	Myl6 Isoform Smooth muscle of Myosin light	-	+	-	-	+	-
27	Lyz Lysozyme C type P precursor	-	-	+	-	-	-

+ : indicates the presence of the band

- : indicates the absence of the band

* : In the C2C12 NTAP-SMN column, the '+' indicates that the band is present and the '-' indicates that the band is absent at any time point analyzed

** : In the PC12 TAP-tag SMN column, the '+' indicates that the band is present and the '-' indicates that the band is absent at any time point and in either the CTAP-SMN or NTAP-SMN purification

Table 6.3. Identification of Proteins recovered from the NTAP-SMN tandem affinity purification in PC12 cells.

BAND	Protein Identification	Days of Differentiation					PC12 CTAP-SMN	C2C12 Tap-tag SMN
		0	1	3	5	7		
1	Eif5b eukaryotic translation initiation factor	+	+	-	+	+	+	-
2	Eif5b eukaryotic translation initiation factor	+	+	-	+	+	+	-
3	Supt16h FACT complex subunit SPT16	+	+	-	+	+	-	-
4	Ipo8 Isoform 1 of Importin-8	+	+	-	+	+	-	-
5	Ipo8 Isoform 1 of Importin-8	+	+	-	+	+	-	-
6	Ipo8 Isoform 1 of Importin-8	+	+	-	+	+	-	-
7	Sfpq Splicing factor, proline	+	+	-	+	+	-	+
8	Pfkm 6-phosphofructokinase	+	+	-	+	+	-	-
	Pfkp Isoform 1 of 6-phosphofructokinase type C	+	+	-	+	+	-	-
	Vps35 Vacuolar protein sorting-associated	+	+	-	+	+	-	-
	Sec23a Protein transport protein Sec23A	+	+	-	+	+	-	-
	Sec23b Protein transport protein Sec23B	+	+	-	+	+	-	-
	Dhx15 Putative pre-mRNA-splicing factor	+	+	-	+	+	-	+
	Ddx1 ATP-dependent RNA helicase DDX1	+	+	-	+	+	-	-
	Nin Isoform 1 of Ninein	+	+	-	+	+	-	-
9	Hspa5 78 kDa glucose-regulated protein precursor	+	+	-	+	+	-	-
	Ddx3x ATP-dependent RNA helicase DDX3X	+	+	-	+	+	-	-
	Prmt5 Protein arginine N-methyltransferase 5	+	+	-	+	+	-	-
10	Hspa8 Heat shock cognate 71 kDa protein	+	+	-	+	+	-	+
	Lmna Isoform A of Lamin-A/C	+	+	-	+	+	-	-
	Hspa9 Stress-70 protein, mitochondrial precursor	+	+	-	+	+	-	-
	Prmt5 Protein arginine N-methyltransferase 5	+	+	-	+	+	-	-
	Ddx3x similar to DEAD (Asp-Glu-Ala-Asp) box	+	+	-	+	+	-	-
	Pabpc2 poly A binding protein, cytoplasmic 2	+	+	-	+	+	-	-
11	Prmt5 Protein arginine N-methyltransferase 5	+	+	-	+	+	-	-
	Ighg1 Ig gamma-1 chain C region, membrane-bound	+	+	-	+	+	+	+
	Vgf VGF nerve growth factor inducible	+	+	-	+	+	-	-
	Ddx5 Probable ATP-dependent RNA helicase DDX5	+	+	-	+	+	-	-
	Hnrpl Heterogeneous nuclear ribonucleoprotein L	+	+	-	+	+	-	-
12	Hnrpl Heterogeneous nuclear ribonucleoprotein L	+	+	-	+	+	-	-
	Ddx5 Probable ATP-dependent RNA helicase DDX5	+	+	-	+	+	-	-
	Lmna Isoform C of Lamin-A/C	+	+	-	+	+	-	-
	Cct3 T-complex protein 1 subunit gamma	+	+	-	+	+	-	-
13	Nono Isoform 1 of Non-POU domain-containing	+	+	+	+	+	-	+
	Cct8 T-complex protein 1 subunit theta	+	+	+	+	+	-	-
	G6pdx Glucose-6-phosphate 1-dehydrogenase X	+	+	+	+	+	-	-
14	Ighg1 Ig gamma-1 chain C region, membrane-bound	+	+	+	+	+	+	+
	Serbp1 Isoform 1 of Plasminogen activator	+	+	+	+	+	-	-
	Ppm1b Protein phosphatase 1B2 53 kDa isoforms	+	+	+	+	+	-	+
	Prph1 Isoform 3u of Peripherin	+	+	+	+	+	-	-
15	Smn1 Survival motor neuron protein	+	+	+	+	+	+	+
	Eef1a1 Elongation factor 1-alpha 1	+	+	+	+	+	-	-
	Eef1a2 Elongation factor 1-alpha 2	+	+	+	+	+	+	+
	Tuba1a Tubulin alpha-1 chain	+	+	+	+	+	-	+
	Dnaja2 DnaJ homolog subfamily A member 2	+	+	+	+	+	-	-
	Prph1 Isoform 3u of Peripherin	+	+	+	+	+	-	-

16	Tufm Isoform 1 of Elongation factor Tu,	+	-	-	-	-	-	-
	Eif4a1 Eukaryotic initiation factor 4A-I	+	-	-	-	-	-	-
	U2af2 Splicing factor U2AF 65 kDa subunit	+	-	-	-	-	-	-
	Ppm1a Protein phosphatase 2C isoform alpha	+	-	-	-	-	-	+
17	Actb Actin, cytoplasmic 1	+	+	+	+	+	+	+
	Acta1 Actin, alpha skeletal muscle	+	+	+	+	+	-	+
18	Mapk1 Mitogen-activated protein kinase 1	+	+	+	+	+	-	+
	Idh3b Tumor-related protein	+	+	+	+	+	-	-
	Csnk2a1 Casein kinase II subunit alpha	+	+	+	+	+	-	-
19	Idh3g Isocitrate dehydrogenase [NAD] subunit	+	+	-	-	-	-	-
	Lancl1 LanC-like protein 1	+	+	-	-	-	-	-
	Hnrpa3 Isoform 1 of Heterogeneous nuclear	+	+	-	-	-	-	-
	Pcbp1 Poly(rC)-binding protein 1	+	+	-	-	-	-	-
20	Igk-C Kappa light chain C_region (Fragment)	-	-	+	-	-	+	+
21	Igk-C Kappa light chain C_region (Fragment)	+	+	+	-	+	+	+
	Gapdh Glyceraldehyde-3-phosphate dehydrogenase	+	+	+	-	+	-	+
	Eif2s1 Eukaryotic translation initiation factor	+	+	+	-	+	-	-
	Smn1 Survival motor neuron protein	+	+	+	-	+	+	+
22	Smn1 Survival motor neuron protein	+	+	+	+	+	+	+
	Ldha L-lactate dehydrogenase A chain	+	+	+	+	+	-	-
	Ldhb L-lactate dehydrogenase B chain	+	+	+	+	+	-	-
23	Gemin 2 (Sip1)	+	+	+	-	+	-	+
24	cytokine-like nuclear factor n-pac	+	+	-	-	-	-	-
	Spin1 Isoform 1 of Spindlin-1	+	+	-	-	-	-	+
	Mtap S-methyl-5-thioadenosine phosphorylase	+	+	-	-	-	-	-
25	Psph Phosphoserine phosphatases	+	-	-	-	-	-	-
	Nipsnap1 Protein NipSnap1	+	-	-	-	-	-	-
26	Psph Phosphoserine phosphatases	+	+	+	-	+	-	-
	Prdx4 Peroxiredoxin-4	+	+	+	-	+	-	-
27	Hspb1 Isoform A of Heat-shock protein beta-1	+	+	+	+	+	-	-
	Pfn1 Profilin-1	+	+	+	+	+	+	-
28	Igk-C Kappa light chain C_region	-	-	+	-	-	+	+
29	Not identified	-	-	+	-	-	-	-
30	Not identified	-	-	+	-	-	-	-
31	Rbm3 Putative RNA-binding protein 3	+	-	-	-	-	-	-
32	Snrpd2 Small nuclear ribonucleoprotein Sm D2	+	-	-	-	-	-	+
33	Not Identified	-	-	+	-	-	-	-
34	Phf5a PHD finger-like domain-containing protein	-	-	+	-	-	-	-
	Mycbp C-Myc-binding protein	-	-	+	-	-	-	+

+ : indicates the presence of the band

- : indicates the absence of the band

* : In the PC12 CTAP-SMN column, the '+' indicates that the band is present and the '-' indicates that the band is absent at any time point analyzed

** : In the C2C12 TAP-tag SMN column, the '+' indicates that the band is present and the '-' indicates that the band is absent at any time point and in either the CTAP-SMN or NTAP-SMN purification

Table 6.4. Identification of Proteins recovered from the CTAP-SMN tandem affinity purification in PC12 cells.

BAND	Protein Identification	Days of Differentiation					PC12 NTAP-SMN	C2C12 Tap-tag SMN
		0	1	3	5	7		
1	Eif5b eukaryotic translation initiation factor	+	+	+	+	+	+	-
	Dnahc17 Novel protein similar to dynein,	+	+	+	+	+	-	-
2	Eif5b eukaryotic translation initiation factor	-	-	-	-	+	+	-
3	Nucleolin	-	+	-	-	-	-	-
4	Nucleolin	-	+	-	-	-	-	-
5	Not Identified	+	+	+	-	-	-	-
6	Not identified	+	+	-	-	-	-	-
7	Hspa1l Heat shock 70 kDa protein 1L	+	+	-	-	+	-	-
8	Tubb2b Tubulin beta-2B chain	+	+	+	+	+	+	-
9	Eef1a2 Elongation factor 1-alpha 2	+	+	+	+	+	+	+
	Smn1 Survival motor neuron protein	+	+	+	+	+	+	+
10	Actg1 Gamma actin-like protein	+	+	-	-	+	-	-
11	Chrnb3 Isoform 2 of Neuronal acetylcholine	+	+	-	-	+	-	-
12	similar to heterogeneous nuclear	+	+	+	+	+	-	-
13	Klk1b24 Kallikrein 1-related peptidase b24	+	-	-	+	+	-	-
14	Not identified	+	+	+	+	+	-	-
15	Actb Actin, cytoplasmic 1	+	-	-	-	-	+	+
	Anxa2 Annexin A2	+	-	-	-	-	-	+
	Pfn1 Profilin-1	+	-	-	-	-	+	-
16	similar to heterogeneous nuclear	+	+	+	+	+	-	-
17	Igk-C Kappa light chain C_region	+	+	+	+	+	+	+
	Pfn1 Profilin-1	+	+	+	+	+	+	-
18	Igk-C Kappa light chain C_region	+	+	+	+	+	+	+
19	Igk-C Kappa light chain C_region	+	+	-	+	+	+	+
20	Not identified	+	-	-	+	+	-	-
21	Rps16 Rps16 protein	+	+	+	+	+	-	-
22	Ftl2 Ferritin light chain 2	+	+	+	+	+	-	-

+ : indicates the presence of the band
- : indicates the absence of the band
* : In the PC12 NTAP-SMN column, the '+' indicates that the band is present and the '-' indicates that the band is absent at any time point analyzed
** : In the C2C12 TAP-tag SMN column, the '+' indicates that the band is present and the '-' indicates that the band is absent at any time point and in either the CTAP-SMN or NTAP-SMN purification

Table 6.5. SMN interacting proteins that were identified in both the PC12 and C2C12 cells.

Protein identified	C2C12		PC12	
	Growth	Differentiation	Growth	Differentiation
Smn1	+	+	+	+
Gemin2	+	+	+	+
Small nuclear ribonucleoprotein	+	+	+	+
Elongation factor 1-alpha 2	+	-	+	+
Eukaryotic translation initiation factor	+	+	+	+
Ppm1b Protein phosphatase 1B2	-	+	+	+
Splicing factor, proline	+	+	+	+
Actb Actin, cytoplasmic 1	+	+	+	+
Acta1 Actin, alpha skeletal muscle	+	+	+	+
Isoform C of Lamin-A/C	+	+	+	+
Mapk1 Mitogen-activated protein kinase 1	+	+	+	+
Annexin A2	+	+	+	+

+ : indicates the presence of the protein
- : indicates the absence of the protein

well, Annexin II is part of a family of structurally similar proteins that bind to phospholipids and may be involved in regulation of membrane transport, membrane channel activity, and interaction of the cell membrane with the extracellular matrix (Waisman 1995; Menell, Cesarman et al. 1999). MRLC is one of three members of the hetero-hexamer that makes up the actin-based motor known as myosin II. The other two members are the myosin heavy chain and essential light chain. Modification of MRLC regulates myosin activity (reviewed by (Sweeney, Bowman et al. 1993)).

To confirm that Annexin II and MRLC are associated with Smn in C2C12 cells, we performed immunoprecipitation experiments with the endogenous proteins. Cell lysates from C2C12 cells at growth, 1 and 3 days of differentiation were used to immunoprecipitate complexes with Smn, Gemin2, MRLC and Annexin II. The associated complexes were analysed for the presence of Smn (Fig. 6.4B). As expected, control immunoprecipitates did not contain any of the proteins (Fig. 6.4A). As a further validation of any interaction, we performed the reverse immunoprecipitation with Smn in the C2C12 cell lysates from growth, and 1 and 3 days of differentiation, and the associated complexes were analysed for the presence of Smn, Gemin2, Annexin II and MRLC (Fig. 6.4C). From these experiments, we demonstrate that Gemin2 immunoprecipitates with Smn in C2C12 cells at all time points studied, and that Annexin II and MRLC immunoprecipitate with Smn in C2C12 cells only during growth and 1 day of differentiation (Fig. 6.4B,C). Similarly, we performed immunoprecipitations to confirm Annexin II association with Smn in PC12 cells. Included in the analysis

Fig.6.4. Annexin II and myosin regulatory light chain interact with Smn in cultured C2C12 cells. A. Controls for the immunoprecipitation of Smn, Gemin2, MRLC and Annexin II in C2C12 cells. Controls are lysate alone (positive control), antibodies incubated with the appropriate sepharose beads (A1), and lysate incubated with either protein A or G sepharose beads (A2). These gels were then immunoblotted for Smn. B. Immunoprecipitation of Smn, Gemin2, MRLC and Annexin II during growth, and 1 and 3 days of differentiation in C2C12 cell lysates were resolved on SDS-PAGE. Immunoblot analysis was performed using a Smn antibody. C. Immunoprecipitation of Smn during growth (0), 1 and 3 days of differentiation in C2C12 cell lysates were resolved on SDS-PAGE. Controls (lanes 3-5) are lysate incubated with protein G sepharose beads and Smn antibody with protein G sepharose beads. Immunoblot analysis was performed using Smn, Gemin2, MRLC and Annexin II antibodies, as indicated to the right of figure.

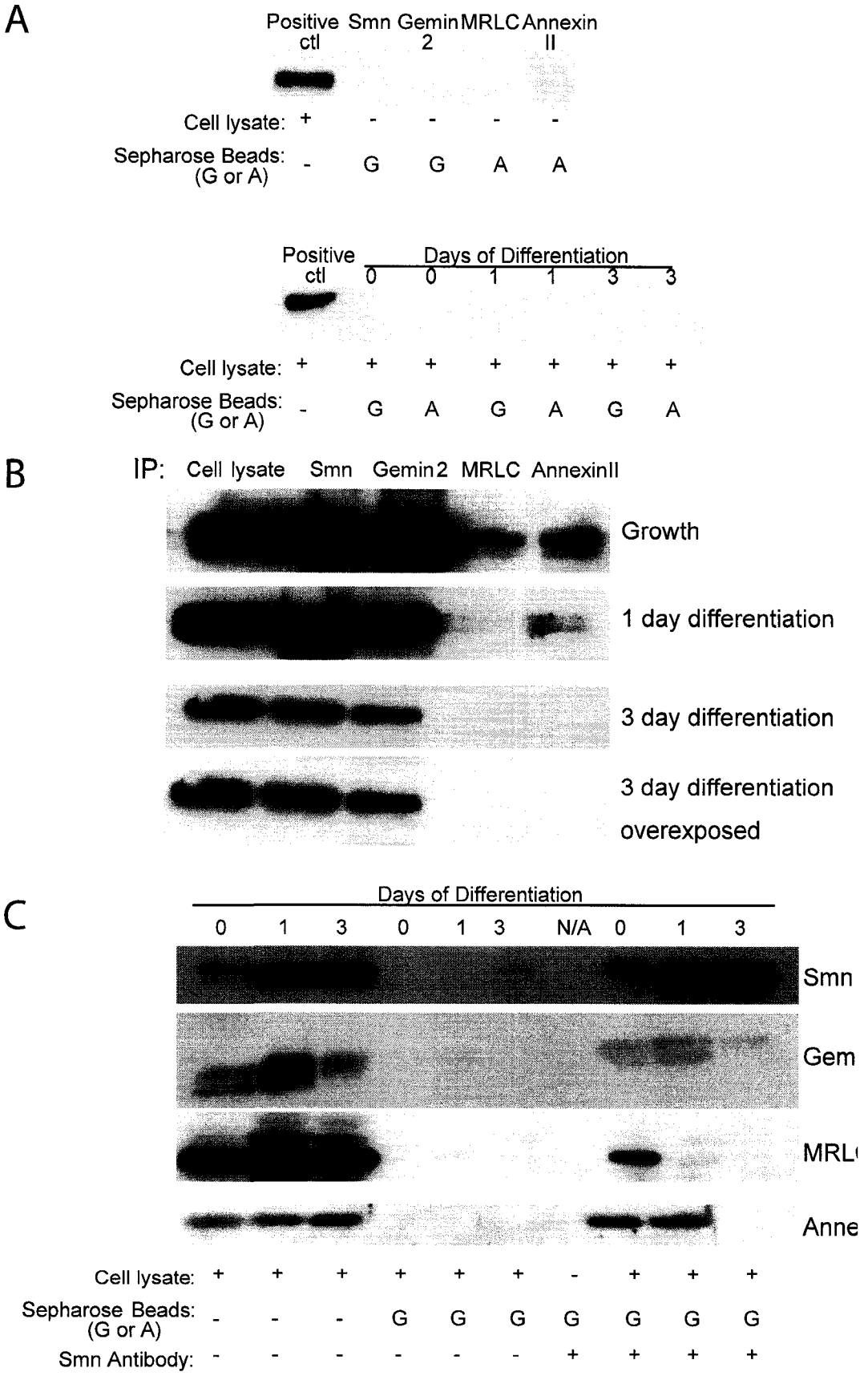
A
Positive ctl
Smn
Gemin 2
MRLC
Annexin II
Cell lysate: + - - - -
Sepharose Beads: (G or A) - G G A A
Positive ctl
Days of Differentiation
0 0 1 1 3 3
Cell lysate: + + + + + + +
Sepharose Beads: (G or A) - G A G A G A
B
IP: Cell lysate Smn Gemin2 MRLC AnnexinII
Growth
1 day differentiation
3 day differentiation
3 day differentiation overexposed
C
Days of Differentiation
0 1 3 0 1 3 N/A 0 1 3
Smn
Gem
MRL
Anne
Cell lysate: + + + + + + - + + +
Sepharose Beads: (G or A) - - - G G G G G G G
Smn Antibody: - - - - - - + + + +

were immunoprecipitations with Gemin2, nucleolin, and profilin-1, known interactors of Smn. Our results demonstrate that all four proteins immunoprecipitate with Smn in PC12 cells during growth and 3 days of differentiation (Fig. 6.5).

6.1.5 Myosin Regulatory Light Chain levels are increased and the protein is mis-localized in Smn depleted cells

Having identified Annexin II and MRLC as two Smn interacting proteins in C2C12 cells, we next performed experiments to determine if Smn depletion had any impact on these proteins. We took advantage of our previously described C2C12 cell line, 2B3, in which Smn is knocked down by approximately 90% (Shafey, Cote et al. 2005). We first assessed the levels of Annexin II and MRLC in wild type and 2B3 C2C12 cells. The level of Annexin II was unaffected in the Smn knockdown cells, however the level of MRLC is noticeably increased in the 2B3 cells (Fig. 6.6A).

We further analysed the distribution of Annexin II and MRLC to determine if these proteins are still properly localized in the 2B3 cells. Annexin II is found in the cytoplasm and around the nucleus in both the wild type and 2B3 cells (Fig. 6.6B). In contrast, MRLC localization is dramatically effected in 2B3 cells. Normally, MRLC is present in the cytoplasm of wild type C2C12 cells at relatively low levels (Fig. 6.6B). However, in 2B3 cells, in addition to being localized in the cytoplasm, MRLC is also found clustered in the nucleus, and it is present at relatively higher

levels than in the wild type cells (Fig. 6.6B). The abnormal localization is particularly obvious at 3 days of differentiation.

Fig. 6.5. Annexin II and nucleolin interact with Smn in cultured PC12 cells. A. Controls for the immunoprecipitation of Smn, Gemin2, profilin, Annexin II, and nucleolin in PC12 cells. Controls are lysate alone (positive control), antibodies incubated with the appropriate sepharose beads (A1), and lysate incubated with either protein A or G sepharose beads (A2). These gels were then immunoblotted for Smn. B. Immunoprecipitation of Smn, Gemin2, Profilin, Annexin II, and nucleolin during growth and 3 days of differentiation in PC12 cell lysates were resolved on SDS-PAGE. Immunoblot analysis was performed using an Smn antibody. C. Immunoprecipitation of Smn during growth (0) and 3 days of differentiation in PC12 cell lysates were resolved on SDS-PAGE. Controls (lanes 4-7) are lysate incubated with protein G sepharose beads and Smn antibody with protein G sepharose beads. Immunoblot analysis was performed using Smn, Gemin2, Profilin, Annexin II, and nucleolin antibodies.

A

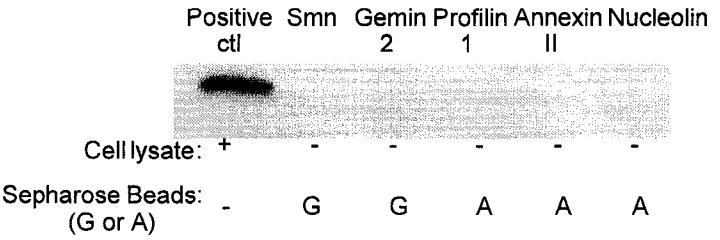
Positive ctl
Smn
Gemin 2
Profilin 1
Annexin II
Nucleolin
Cell lysate: + - - - - -
Sepharose Beads: (G or A) - G G A A A

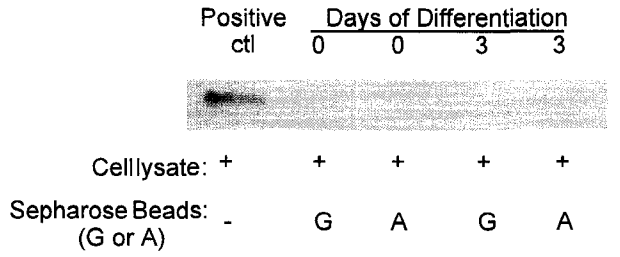
Positive ctl
Days of Differentiation
0 0 3 3
Cell lysate: + + + + +
Sepharose Beads: (G or A) - G A G A

B

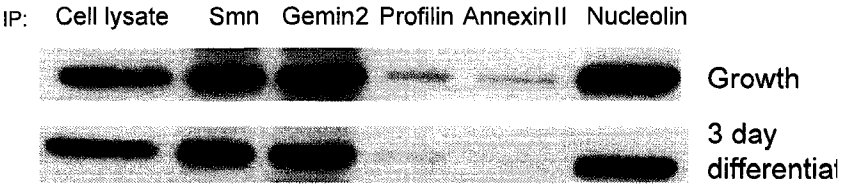
IP: Cell lysate
Smn
Gemin2
Profilin
AnnexinII
Nucleolin
Growth
3 day differentiat

C

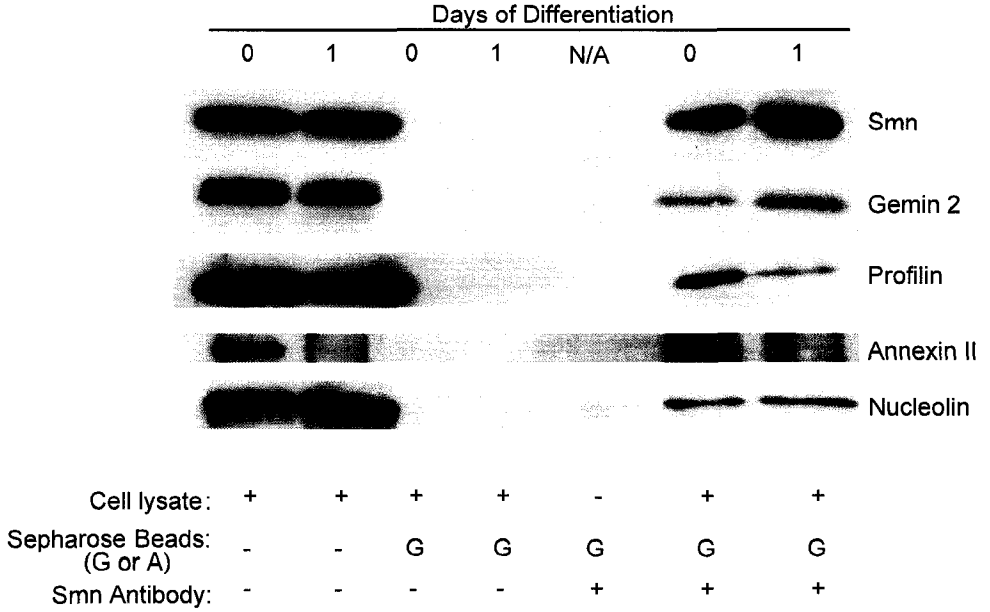
Days of Differentiation
0 1 0 1 N/A 0 1
Smn
Gemin 2
Profilin
Annexin II
Nucleolin
Cell lysate: + + + + - + +
Sepharose Beads: (G or A) - - G G G G G
Smn Antibody: - - - - + + +

Fig. 6.6. Level and localization of myosin regulatory light chain is affected in Smn-depleted C2C12 cells. A. Immunoblot analysis of Smn, Annexin II and MRLC levels in wild type and 2B3 Smn knockdown C2C12 cells. Actin was used as a loading control. B. Immunocytochemistry of Smn, Annexin II and MRLC in wild type and 2B3 Smn knockdown C2C12 cells. Magnification for MRLC is at 20X (column 3) and 63 X (column 4). Scale bar, 50 μm in column 3 and 5 μm in column 4.

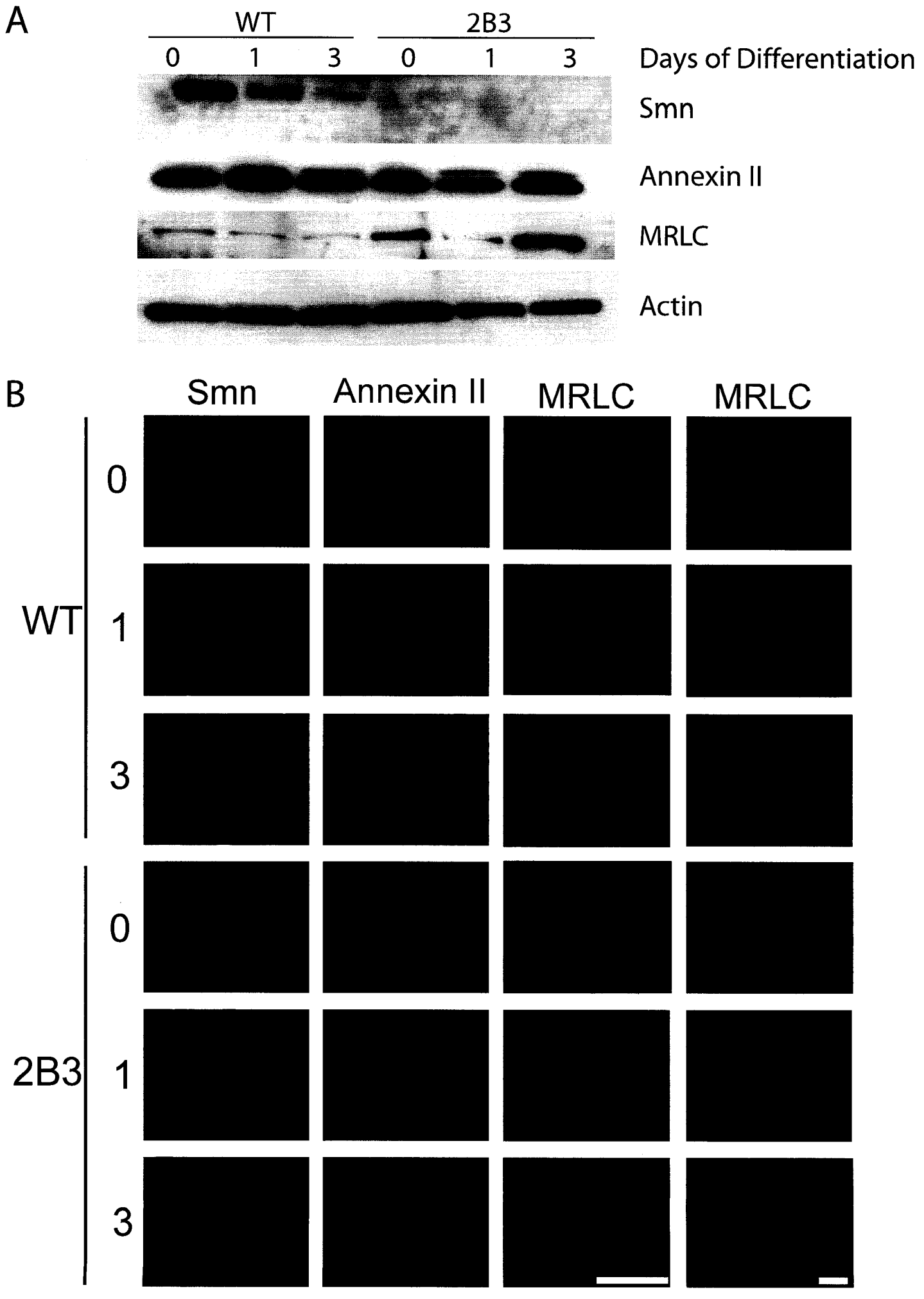
A
WT
2B3
0
1
3
0
1
3
Days of Differentiation
Smn
Annexin II
MRLC
Actin
B
Smn
Annexin II
MRLC
MRLC
WT
2B3
0
1
3
0
1
3

6.2 DISCUSSION

Previous studies have determined that mutations or deletions in the *SMN1* gene are the primary cause of SMA (Melki, Lefebvre et al. 1994; Bussaglia, Clermont et al. 1995; Lefebvre, Burglen et al. 1995; Brahe, Clermont et al. 1996; Parsons, McAndrew et al. 1996; Hahnen, Schonling et al. 1997). Understanding how SMN functions and in particular how its depletion leads to pathogenesis in SMA patients is an intense field of study. Amongst the many questions being addressed is why systemically reduced levels of functional SMN protein lead to specific degeneration of motorneurons and muscle atrophy. It is possible that in addition to the reported role in splicing and transcriptional regulation, SMN could be playing a motorneuron and/or muscle specific function through differences in the constituents that make up the SMN complex in these relevant cell types. Thus, determining whether SMN is part of diverse complexes in neurons and muscle, and if these complexes are dynamic or static should lead us to a better understanding of SMA pathophysiology. Therefore, we chose to examine whether Smn interacting proteins change during different stages of growth and differentiation of C2C12 muscle and PC12 neuronal-like cells.

6.2.1 Tandem affinity purification is a useful tool for identifying SMN interacting partners

Cellular functions are the result of the coordinated action of several proteins in macromolecular complexes. Protein complex composition can vary with time to adapt to changing cellular requirements. Therefore, the analysis of protein complex

composition can be an important step in elucidating the pathophysiology of a disease. Mass spectrometry-based proteomic tools have proven to be successful in the identification of multicomponent complexes formed under native conditions (Puig, Caspary et al. 2001; Aebersold and Mann 2003). The TAP system is an affinity purification technique originally developed in yeast that enables the purification of protein complexes under close to physiological conditions (Rigaut, Shevchenko et al. 1999; Knuesel, Wan et al. 2003; Yang, Sampson et al. 2006). This approach has emerged as a useful tool for studying protein complexes *in vitro* (Rigaut, Shevchenko et al. 1999; Knuesel, Wan et al. 2003) and *in vivo* (Yang, Sampson et al. 2006). We used this approach to study the changes in SMN complex constituents during different stages of growth and differentiation in C2C12 and PC12 cells. In C2C12 cells, there are several changes to the nature of Smn associated proteins from growth, to early differentiation, and then to late differentiation. The dynamic nature of the SMN complex in C2C12 cells indicates the possibility for a change in the role that SMN plays at different stages of muscle development and/or differentiation.

In contrast to C2C12 cells, the SMN complex appears to be relatively static in PC12 cells, with the banding pattern of the purified complex remaining essentially unchanged over time. The reason for this relatively invariant pattern in the SMN associated proteins is that for the most part the PC12 cell remains morphologically unchanged during differentiation, except for the establishment of neurite processes. Since this latter structure only makes up a minor proportion of the cell in terms of volume, any change in the SMN complex may be masked.

6.2.2 Novel SMN interacting protein partners were identified in PC12 and C2C12 cells

From our analysis, we identified many known SMN interacting proteins, including Gemin2, sm proteins, snRNPs, and profilin. We also identified many novel SMN associated proteins in both the C2C12 and PC12 cells. Some of these proteins, like Annexin II, were identified as SMN interactors in both cell lines. However, many interacting proteins are specific to one cell type, such as myosin regulatory light chain in C2C12 cells. The identification of these cell specific interactors may imply a specific role for Smn in those cell types. We have validated the interaction between Smn and Gemin2, profilin, nucleolin and Annexin II in PC12 cells and we have validated the interaction between Smn and Gemin2, Annexin II and MRLC in C2C12 cells. Of importance, these validations were performed on the endogenous proteins, and by immunoprecipitating either Smn or the interacting protein.

6.2.3 MRLC is perturbed in Smn depleted C2C12 cells

Although Annexin II levels and localization were not perturbed in Smn depleted C2C12 cells, MRLC was found to be present at elevated levels and its localization was affected. Understanding why MRLC is up regulated and mis-localized in a muscle cell may lead us to a better understanding of the specific role of Smn in muscle and how this affects SMA pathophysiology.

In our previous study, we had demonstrated that Smn deficiency in C2C12 myoblasts leads to abnormal myoblast fusion (Shafey, Cote et al. 2005), which is corroborated by findings that SMA patient derived myoblasts have fusion abnormalities (Arnold, Gueye et al. 2004), and that satellite cells derived from SMA patients cultured with normal motor neurons cause premature motor neuron disorganization and death (Guettier-Sigrist, Coupin et al. 1998). In mice, it has been shown that removal of *Smn* exon 7 specifically from muscle causes dystrophic changes (Cifuentes-Diaz, Frugier et al. 2001) and satellite cell abnormalities (Nicole, Desforges et al. 2003) that lead to paralysis and death. In *Drosophila,* Smn hypomorphs cannot fly or jump (Rajendra, Gonsalvez et al. 2007). As well, it has been shown that in *Drosophila,* Smn co-localizes with the sarcomeric actin and forms a complex with α-actinin, a thin filament cross-linker (Rajendra, Gonsalvez et al. 2007). When a hypomorphic allele of *Smn* is expressed in these flies, the expression pattern of α-actinin in the flight muscles is disrupted. Not only was α-actinin affected in these mutant flies, but the expression of myosin in the flight muscle was also disrupted (Rajendra, Gonsalvez et al. 2007). Thus, all of these studies suggest and further establish a role for Smn in muscle. The latter observation in combination with our own observation that MRLC interacts with Smn and is affected in Smn depleted C2C12 cells raises the possibility that Smn may be affecting the *Drosophila* flight muscle differentiation via interactions with MRLC and myosin.

6.2.4 MRLC perturbation may affect myoblast fusion

Myoblast fusion is a critical process for the terminal differentiation of skeletal muscle. An important regulator of this process is the small GTPase protein Rho (Nishiyama, Kii et al. 2004; Charrasse, Comunale et al. 2006). Rho GTPases are molecular switches that control a variety of cytoskeleton-dependent cell functions such as actin cytoskeleton organization, microtubule dynamics, membrane transport, cell polarity and transcriptional activity (Etienne-Manneville and Hall 2002). Rho activity, which is high in proliferating myoblasts, decreases during myogenesis (Charrasse, Comunale et al. 2006). If Rho is constitutively active, myoblast fusion is blocked (Nishiyama, Kii et al. 2004). Consistent with this, the activity of Rho's effector, the Rho-associated kinase (ROCK), is also decreased in differentiating C2C12 cells, and constitutively active ROCK blocks myoblast fusion (Nishiyama, Kii et al. 2004). Thus, the down regulation of Rho/ROCK signaling is required for proper myoblast fusion. When RhoA is in its active state, it activates ROCK, resulting in phosphorylation and activation of MRLC, which in turn regulates the assembly of stress fibers (Kimura, Ito et al. 1996; Totsukawa, Yamakita et al. 2000; Ueda, Murata-Hori et al. 2002). Here we have shown that when Smn is depleted in C2C12 myoblasts, MRLC levels are up-regulated, and the protein is mis-localized. This could be a result of improper activation of the Rho/ROCK signaling pathway. Interestingly, inappropriate activation of the Rho/ROCK pathway has been previously observed in Smn depleted PC12 cells which leads to defects in differentiation and neuritogenesis (Bowerman, Shafey et al. 2007). Thus, there is a possibility that depletion of Smn in C2C12 cells leads to improper activation of the Rho/ROCK pathway, which then leads to alteration in

MRLC levels and localization. However, the functional effect and pathophysiological significance of the changes in MRLC is yet to be determined. Further investigation on the functional relationship of MRLC and other proteins identified in our TAP-tag screen should lead to a better understanding of the mechanisms that lead to motorneuron degeneration and muscle atrophy in SMA.

Using the Tandem Affinity Purification method, we have been able to elucidate many novel SMN interacting proteins in disease relevant cell types. The discovery of these proteins will lead to a better understanding of SMN's role in the pathophysiology of SMA and may lead us to the identification of new drug targets.

7.0 OVERALL DISCUSSION

7.1 SMA is not a cell autonomous disease

It has been previously thought that SMA is primarily a motor neuron disease. However, from our studies and the studies of others, it is not clear that SMA is a cell autonomous disease. The pattern of proximal weakness in SMA is more reminiscent of a myopathic disorder rather than a neuropathic one. As well, the neuromuscular pathology of severe SMA is distinct from other motor neuron diseases. In type I SMA patients, autopsy studies have documented very large areas of rounded, small myofibers rather than angulated, atrophic myofibers that are typical of denervation (Wharton, McDermott et al. 2003). These myofibers ultrastructurally appear to be arrested in development (Fidzianska, Goebel et al. 1990), and they express abnormal amounts of developmental isoforms of myosin (Soubrouillard, Pellissier et al. 1995). These pathological observations raised the possibility that SMA is not a cell autonomous disease and that SMN deficiency results in primary abnormalities in both motor neurons and muscle, which then leads to a failure of communication between these two components of the motor unit. Several *in vitro* and *in vivo* studies support this hypothesis. In our study we demonstrated that Smn deficiency in C2C12 myoblasts leads to abnormal myoblast fusion (Shafey, Cote et al. 2005), which is corroborated by findings that SMA patient derived myoblasts have fusion abnormalities (Arnold, Gueye et al. 2004), and that satellite cells derived from SMA patients cultured with normal motor neurons causes premature motor neuron disorganization and death

(Guettier-Sigrist, Coupin et al. 1998). In mice, removal of *Smn* exon 7 specifically from muscle causes dystrophic changes (Cifuentes-Diaz, Frugier et al. 2001) and satellite cell abnormalities (Nicole, Desforges et al. 2003) leading to paralysis and death at one month of age. *Drosophila* Smn hypomorphs cannot fly or jump, suggesting a role for Smn in muscle (Rajendra, Gonsalvez et al. 2007). As well, *Drosophila* deficient in Smn show a significant disorganization of both the presynaptic terminus and the postsynaptic neurotransmitter receptors, and replacement of Smn is required in both the motor neuron and muscle to rescue the phenotype (Chan, Miguel-Aliaga et al. 2003). This observation in the *Drosophila* SMA model differs from the mouse SMA model. In the mouse model, it has been shown in a recent study that full-length SMN expression in neurons of the *Smn*$^{-/-}$*;SMN2* mice using a prion promoter rescues these mice, whereas SMN expression in skeletal muscle using a human skeletal actin promoter does not (Gavrilina, McGovern et al. 2008). However, the prion promoter used in this study expresses SMN at high levels in neurons and astrocytes, and low levels in cardiac and skeletal muscle (Gavrilina, McGovern et al. 2008). Thus, in this study, they did not increase the expression of SMN solely in neurons. There was increased SMN expression in muscle as well. As we have stated previously in Chapter 4, SMN expression in mice does not have to be increased much more than 15% of wild type levels to observe an increased lifespan with no SMA-like phenotype. Thus, the level of SMN expression increased in the muscle of the *Smn*$^{-/-}$*;SMN2* mice in combination with the increase in SMN in the neurons using the prion promoter could explain the increased survival of these mice. Thus, since skeletal muscle is

known to be a source of signals that influence motor neuron survival, growth, and maintenance (Funakoshi, Belluardo et al. 1995), it is possible that a primary abnormality of muscle contributes to the pathogenesis of SMA. If this is the case, it raises the possibility that therapy delivered directly to the muscle, a more accessible tissue than the spinal cord, could be beneficial for SMA patients.

7.2 Specific roles for SMN in neurons and muscle

It has been demonstrated that a minimal level of SMN protein is required for the survival of all cells, which is consistent with the essential housekeeping function of SMN. When flies and mice have no functional Smn present there is embryonic lethality (Schrank, Gotz et al. 1997; Miguel-Aliaga, Chan et al. 2000). However, transgenic mice that express reduced levels of full-length SMN protein are rescued from early embryonic lethality, but they develop motor neuron loss, atrophy of muscle fibers, muscle weakness, and early death (Hsieh-Li, Chang et al. 2000; Monani, Sendtner et al. 2000). The mechanism of selective disruption of motor neurons and muscle in mice and humans due to reduced levels of SMN protein remains unknown. One possibility is that overall, motor neurons and muscle have a uniquely high demand for small nuclear ribonucleoprotein assembly and messenger RNA processing. Alternatively, inefficient small nuclear ribonucleoprotein assembly could cause inappropriate splicing of one or more motor neuron or muscle-specific transcripts crucial for the survival and proper function of these cells. Another possibility is that SMN has unique functions in motor neurons and muscle that have yet to be identified. SMN has been shown to

be localyzed within axons and at the growth cone (Rossoll, Kroning et al. 2002). It has been suggested that SMN has a role in axonal messenger RNA trafficking (Rossoll, Jablonka et al. 2003), RNA editing (Rossoll, Kroning et al. 2002) and neurite outgrowth (Rossoll, Jablonka et al. 2003; Bowerman, Shafey et al. 2007; van Bergeijk, Rydel-Konecke et al. 2007). Our studies corroborate the latter theory, that SMN has unique roles in motor neurons and muscle and disruption of some of these functions leads to SMA.

7.3 Motor neuron specific role in SMA

In one of our studies, we followed the changes in the SMN complex in the PC12 neuronal-like cell and discovered that the constituents of this complex did not change from growth through differentiation. It is of course possible that changes in the complex may be occurring in some sub-cellular regions, e.g. the neurite, but not in the cell body. Since the cell body is much larger than the neurite, it would contribute to a much higher extent to the purification of Smn than would the neurite and thus, we would be unable to readily detect any changes. One way to avoid this problem would be to use a tagged TAP-tag-SMN that would only be expressed or more highly expressed in the axon/neurite. Microtubules are abundant in axons, thus fusion of a microtubule-associated protein, such as tau, might target TAP-tag-SMN to the axons. It has been previously demonstrated that tau-β-galactosidase (Callahan and Thomas 1994) and tau-GFP (Pratt, Sharp et al. 2000) are efficiently targeted to axonal processes. Thus, if we can express the

TAP-tag-SMN in axons only, we would be able to detect changes in the SMN complex in the axon during neuronal differentiation more readily.

One aspect that our study did allow us to do was to compare the differences in SMN interacting proteins in neuronal-like and muscle-like cells. Most previous studies designed to identify the components of the SMN complex have used HeLa cells (Liu and Dreyfuss 1996; Fischer, Liu et al. 1997; Liu, Fischer et al. 1997; Buhler, Raker et al. 1999; Charroux, Pellizzoni et al. 1999; Charroux, Pellizzoni et al. 2000; Meister, Buhler et al. 2000). This cell line is not the most appropriate cell line to study the relationship between the SMN complex and SMA disease because motor neurons and muscle are the primary tissues affected in SMA, and HeLa cells are a cancer cell line. Most studies have used HeLa cells because they are much easier to culture than neurons, especially primary motor neurons. However, more relevant cell types should be studied because surprisingly in our study, there were many putative SMN interacting proteins that were specific to one cell type or the other. This observation leads us to believe that there are specific roles for SMN in neurons and muscle. In the neuron, some of the specific interacting partners included Profilin, Annexin II, nucleolin, actin (cytoplasmic and skeletal), and mitogen-activated protein kinase. Some of these interacting partners could influence SMA pathogenesis due to the pathways for which they are involved. Some of these pathways include the RhoA/ROCK pathway, the Ras pathway, the myosin light chain phosphatase pathway, and the extracellular signal regulated kinase pathway.

Changes in neurite outgrowth and growth cone dynamics are intimately linked to regulation of the actin cytoskeleton (Kuhn, Meberg et al. 2000). It has been previously observed that actin expression is affected in Smn depleted PC12 cells (van Bergeijk, Rydel-Konecke et al. 2007). A change in the G-/F-actin ratio was observed, indicating that SMN has a significant effect on actin dynamics. In another study, we have demonstrated that Smn depletion leads to improper differentiation and shortened neurite length in Smn depleted PC12 cells (Bowerman, Shafey et al. 2007). Smn reduction in these mutant PC12 cells alters the expression pattern of profilin II, resulting in an increase in the neuronal-specific profilin IIa isoform. This increase in profilin IIa availability leads to an increased formation of ROCK/profilin IIa complex and an inappropriate activation of the RhoA/ROCK pathway. Thus, SMN may influence actin polymerization and stabilization by binding to profilin IIa. As well, it has been demonstrated that SMN modulates axon growth and localization of β-actin mRNA in growth cones while its knockdown affects axonal outgrowth and pathfinding (Rossoll, Kroning et al. 2002; McWhorter, Monani et al. 2003; Rossoll, Jablonka et al. 2003). Thus, SMN seems to play a key role in actin metabolism in axons and growth cones and could be doing so via a direct interaction with actin.

It is also possible that SMN could indirectly facilitate actin assembly and neurite outgrowth by interactions with some of the proteins identified in our screen, such as mitogen-activated protein kinase (MAPK), also known as extracellular signal regulated kinase (ERK). The activation of the ERK pathway is able to promote different, and sometimes opposite, cellular processes. This wide variety of

responses elicited by the activation of a single pathway has been shown to rely on the timing and strength of this activation (Marshall 1995). For instance, sustained, high activation of the ERK pathway induces cell cycle arrest that can be linked to senescence, apoptosis, or differentiation; whereas transient activation followed by a sustained but lower level of ERK activity is a common feature of cell proliferation (Qui and Green 1992; Pumiglia and Decker 1997). Thus, if SMN binding to MAPK was perturbed in SMN depleted cells, and we couldn't achieve high activation of the ERK pathway, these SMN depleted cells may not differentiate properly and may remain in a more proliferative state. If this were to occur, it could explain the lack of differentiation of our Smn depleted neural stem cells into neurons because these cells appear to be remaining in a more proliferative state. Therefore, the different interactions discovered in our tap-tag analysis suggest that there are many possible motor neuron specific roles for SMN that could contribute to SMA pathogenesis.

7.4 Muscle specific role in SMA

In our SMN tap-tag study, we followed the SMN complex through growth and differentiation in a muscle-like cell (C2C12), similar to experiments done in the neuronal-like cells. Once again, we detected SMN interacting proteins that were specific to the muscle-like cells. As above, some of these interacting partners could influence SMA pathogenesis due to the pathways for which they are involved.

We showed that depletion of Smn in C2C12 cells resulted in defects in myoblast fusion (Shafey, Cote et al. 2005). Myoblast fusion is a critical process for

the terminal differentiation of skeletal muscle. The molecular and cellular events that occur during myoblast fusion, although long studied, are still unclear. Many of the genes essential for fusion encode proteins that act on actin reorganization, suggesting that this is a central event during myoblast fusion. Earlier cell culture studies showed that the cytoskeleton is extensively reorganized in fusing myoblasts (Fulton, Prives et al. 1981), and interfering with the formation of actin filaments inhibits fusion (Sanger, Holtzer et al. 1971; Sanger and Holtzer 1972; Constantin, Cognard et al. 1995). Our study identified interactions between different forms of actin (cytoplasmic and skeletal) and α-actinin and SMN, which could explain the abnormalities observed in myoblast fusion when Smn is depleted. Others have shown that in *Drosophila,* Smn co-localizes with the sarcomeric actin and forms a complex with α-actinin, a thin filament cross-linker (Rajendra, Gonsalvez et al. 2007). When a hypomorphic allele of *Smn* is expressed in these flies, the expression pattern of α-actinin in the flight muscles was disrupted, suggesting that Smn is involved in muscle differentiation. Not only was α-actinin affected in flight muscles, but the expression of myosin was also disrupted (Rajendra, Gonsalvez et al. 2007). This observation correlates well with our study, since we found that Smn interacts with a component of myosin, myosin regulatory light chain (MRLC). Myosin is a hetero-hexamer comprised of two myosin heavy chains, two essential light chains and two regulatory light chains and is involved in muscle differentiation and contraction. Not only did we find that MRLC interacts with Smn, but that MRLC levels were increased in Smn depleted cells and that the protein localization was disrupted. Perturbation of MRLC in Smn-

depleted cells could be affecting proliferation and cell fusion of since MRLC is necessary for normal cell migration, cytokinesis, proliferation, and morphology.

One of the pathways affected by the loss of Smn could be the Rho/ROCK pathway. Rho GTPases are molecular switches that control a variety of cytoskeleton-dependent cell functions such as actin cytoskeleton organization, microtubule dynamics, membrane transport, cell polarity and transcriptional activity (Etienne-Manneville and Hall 2002). Inappropriate activation of the Rho/Rock pathway has been previously shown in Smn-depleted PC12 cells (Bowerman, Shafey et al. 2007) and this leads to defects in PC12 differentiation and axonal outgrowth. Thus, there is a possibility that depletion of Smn in C2C12 cells leads to improper activation of the Rho/ROCK pathway. As well, Rho plays a critical role in skeletal muscle differentiation. Rho activity, which is high in proliferating myoblasts, decreases during myogenesis. If Rho is constitutively active, myoblast fusion is blocked (Nishiyama, Kii et al. 2004). Consistent with this, the activity of Rho's effector, the Rho-associated kinase (ROCK), is also decreased in differentiating C2C12 cells. Constitutively active ROCK blocks myoblast fusion (Nishiyama, Kii et al. 2004). The down regulation of Rho/ROCK signaling is required for proper myoblast fusion. Therefore, it is plausible that the loss of Smn could lead to improper up-regulation of the Rho/ROCK signaling pathway and thus lead to abnormalities in myoblast fusion.

Unlike in the neuronal-like cells, we were able to see changes in the SMN complex between growth and differentiation in the muscle-like cells. This observation suggests that the SMN complex is not static, and is in fact dynamic,

and thus has specific roles during different stages of development and after during the maintenance phase.

7.5 The impact of SMN dosage on SMA pathogenesis

SMA represents a spectrum of different severities, largely due to the dosage effect of *SMN2*. The amount of SMN protein expressed in each individual is inversely correlated with the severity of SMA. Thus, SMA can be considered to be a dose-dependent disorder. It has also been clearly demonstrated from animal and cell culture SMA models that SMN protein dosage determines severity of disease. We have generated a hypomorphic series of C2C12 myoblast stable cell lines with variable Smn knockdown (Shafey, Cote et al. 2005) to gain a better understanding of the influence of SMN protein dosage in muscle. Reduction of Smn in these cells resulted in defects in cellular properties, such as myoblast fusion, but importantly, the severity of these abnormalities was directly correlated with the decrease in Smn protein dosage.

The dosage effect of SMN has been recapitulated in mouse models of SMA (Hsieh-Li, Chang et al. 2000; Jablonka, Schrank et al. 2000; Monani, Sendtner et al. 2000; Monani, Pastore et al. 2003; Le, Pham et al. 2005). The most severe models of SMA, *Smn*$^{-/-}$*;SMN2,* express approximately 5% of wild type levels of Smn protein, show a severe SMA-like phenotype and die soon after birth (Hsieh-Li, Chang et al. 2000; Monani, Sendtner et al. 2000). When a SMNΔ7 allele is added to the *Smn*$^{-/-}$*;SMN2* background to give a heterozygous *SMNΔ7;Smn*$^{-/-}$*;SMN2* the

expression levels of Smn increase slightly and the lifespan increases from 5 days to 13 days (Le, Pham et al. 2005). When an A2G missense SMN allele is added to the *Smn*$^{-/-}$*;SMN2* background, to give a heterozygous A2G*;Smn*$^{-/-}$*;SMN2* the Smn expression levels are approximately 20-25% of wild type levels and the survival has increased to 227 days (Monani, Pastore et al. 2003). Lastly, when only one allele of Smn is expressed to give 50% of wild type Smn levels, the mice show a very mild phenotype and survive to 736 days (Jablonka, Schrank et al. 2000). Thus, from these mouse models it has been demonstrated that the level of Smn protein is correlated with the severity of disease. In our study, we have assessed two extreme SMA mouse models, *Smn*$^{+/-}$ (mild) and *Smn*$^{-/-}$*;SMN2* (severe) to help us understand how the dosage of Smn impacts on overall development, as well as on neuronal development and function. The early, sometimes fetal, onset of the severe forms of SMA has contributed to the ongoing debate in the field as to whether this disease is a neurodevelopmental as well as a neuro-maintenance disorder. Based on findings from our mouse model studies and those of others, it could thus be argued that the severity of the neurodevelopmental deficit depends on the dosage of Smn protein. In the severe SMA forms, in which motor neurons show defects in axon outgrowth and fail to connect properly to their target muscle, coupled with muscle atrophy, the neurodevelopmental aspect is most significant. In contrast, in the milder forms of SMA, where motor neurons grow towards and innervate their target muscles, but eventually show abnormalities, such as unspecified defects, post-natal denervation, and late-onset degeneration, leading to muscle atrophy, the neuro-maintenance aspect would have a greater role. Thus,

the amount of SMN expressed would determine whether the disease will primarily affect development or maintenance of neurons and muscle.

7.6 Conclusion

Overall, we have shown that SMA is not a cell autonomous disease. It not only involves motor neurons, but also involves muscle. We have discovered that SMN protein dosage affects disease severity in cell culture and in mice, and furthermore that SMN dosage determines whether the defects seen in mice result from aberrant neuro-development or neuro-maintenance. These findings (Fig. 7.1) area an important and will guide future work to determine cellular targets and timing of intervention in the treatment of different forms of SMA.

Fig. 7.1 Pathogenic events occurring in SMA due to reduced SMN. We have summarized the contributions our studies have made in understanding the pathogenesis of SMA.

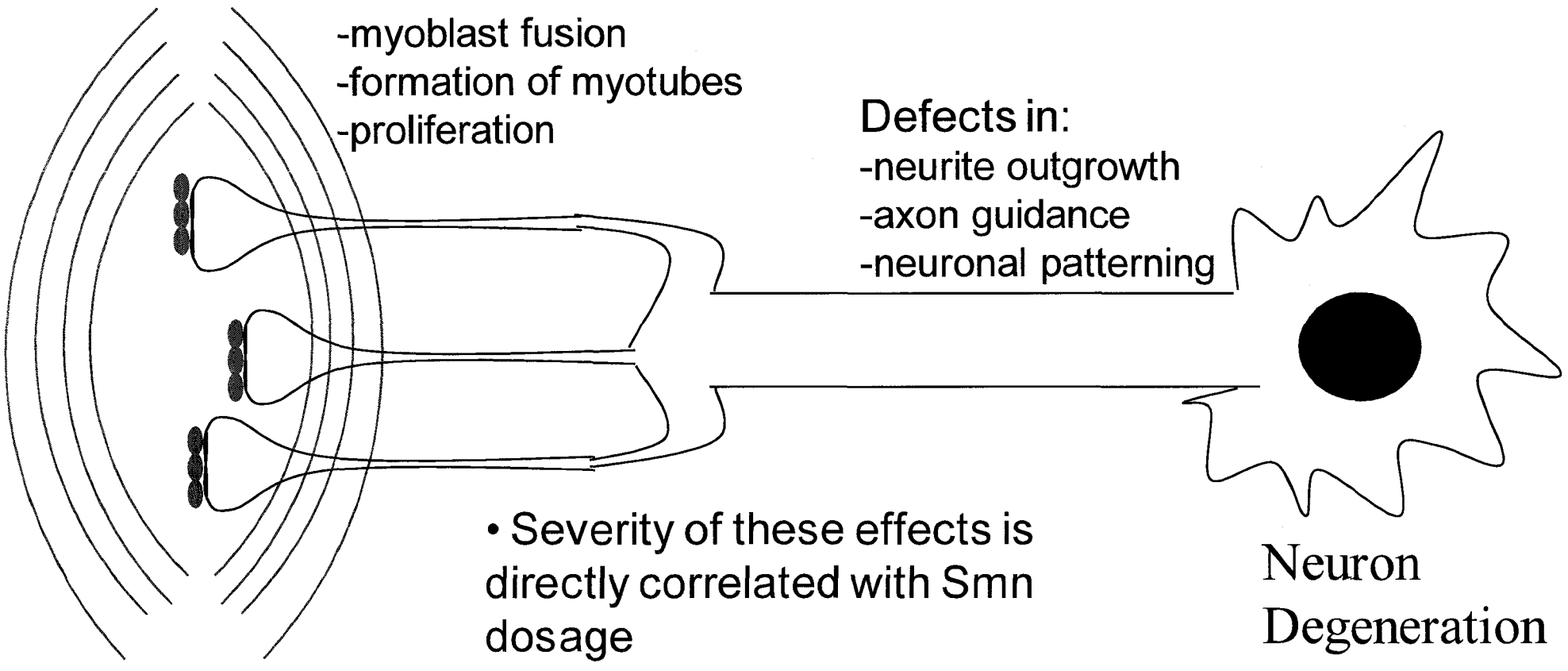

- Severity of these effects is directly correlated with Smn dosage
- Dual role of SMN:
  - (1) during development
  - (2) during post-natal stages

Adapted from Briese et. al. 2005, *Bioessays*

8.0 CONCLUDING REMARKS

Based on patient studies which showed that *SMN2* determines SMA disease severity in a dose-dependent manner, i.e. the more copies of *SMN2* through gene duplication, the milder the disease outcome (Coovert, Le et al. 1997; Lefebvre, Burlet et al. 1997; Feldkotter, Schwarzer et al. 2002; Wirth, Brichta et al. 2006), I hypothesized that altering Smn dosage will result in changes in cellular properties and ultimately determine disease severity in mouse models. Elucidating how the dosage of Smn impacts on overall development, as well as on neuronal development and function, has led us to a better understanding of the pathogenesis of SMA. The studies presented in this thesis have raised a number of additional points that are worthy to pursue experimentally in the future.

8.1 Assessment of muscle defects in SMA mice

Our studies in the C2C12 Smn knockdown cell culture model have implicated a muscle function for SMN in the context of SMA. We could more fully assess whether muscle defects are present in SMA mouse models. Histological analysis of skeletal muscle from mutant $Smn^{-/-}$;*SMN2* (severe), $Smn^{+/-}$ (mild) and wild type mice could be performed on different muscles, such as diaphragm, intercostal and several extensor (quadriceps, tibialis anterior, and extensor digitorum longus) and flexor muscles (gastrocnemius and soleus). These muscles are important for survival and ambulation, and demonstrate pathology in SMA patients. Frozen transverse sections of the above named muscles could be assessed for muscle morphology and neurogenic changes. Standard hematoxylin

and eosin staining could be used to look for atrophy, muscle fiber angulation and grouped atrophy, all of which are indicative of neurogenic changes. Fiber caliber size and the number of centrally nucleated fibers could also be determined. A drawback from using the above mouse models are that the severe mice die prior to or soon after birth, making the analysis difficult and the mild mice do not show a phenotype until much later in adulthood. Thus, we would need to use mice with a more intermediate phenotype such as the $Smn^{2B/-}$ mice mentioned previously. The muscle study would allow us to get a better understanding of the pathophysiology underlying SMA and in particular the defects in muscle biology.

8.2 Assessment of the formation of neuromuscular junctions with exogenous myotubes

Most studies on SMA focus on the functional role of SMN in motor neurons alone. Yet, as we have discussed above, there is increasing evidence for a primary muscle defect in addition to the motor neuron defect. To help determine if muscle is a primary target in SMA, we could examine the ability of neuromuscular junctions to form when Smn is depleted in either the muscle and/or the motor neuron. The ability of neuromuscular junctions to be formed between primary motorneurons deficient in Smn with wild type myotubes, Smn depleted primary motor neurons with myotubes deficient in Smn and wild type primary neurons with Smn depleted myotubes could be studied using modified Campenot chambers. With this system, it is possible to investigate critical pathways involved in the establishment and maintenance of motor neurons, and to determine where these

pathways are disrupted in SMA. We would explore the impact of genotype of the muscle and motor unit on the formation of neuromuscular junctions in this culture system. This model would be useful in determining whether Smn deficiency in the motorneuron or in the muscle causes the degeneration in SMA.

8.3 Creating Smn hypomorphs in mice using knockdown ES cell clones

We attempted to make Smn knockdown mice using a number of approaches. None of our attempts were successful at creating Smn hypomorphs. However, in our ES cell approach we used ES cells that had an Smn reduction of approximately 50-60%. We discovered that this amount of knockdown was not enough to produce a SMA phenotype. However, the benefit of using ES cell clones is that they can be selected for the desired knockdown prior to generating mice. Thus, we can generate ES cell clones with varying Smn knockdown using our shRNA constructs and select clones with a high reduction of Smn to use in subsequent blastocysts injections and chimera production. This would hopefully yield lines with sufficient Smn knockdown to result in phenotypes of ranging severity.

The Smn knockdown mouse lines could either be kept as heterozygotes (on a $Smn^{+/+}$ background) or could be crossed into the $Smn^{+/-}$ background to further amplify any knockdown of Smn protein. Generating a number of transgenic lines with different degrees of loss of expression and function, thus creating a hypomorphic series of mice with varying degrees of Smn expression would give us

a better understanding of the pathogenesis of SMA and this dose-dependent effect.

8.4 Creating inducible Smn hypomorphs in mice

Mice containing an inducible or a repressible shRNA targeting Smn would provide SMA models for testing therapeutics and characterization of the disease, and allow for the identification of critical developmental and adult stages during which SMN is essential. The goal would be to develop inducible animal models of SMA that are not only faithful to the biochemical defect of the human disease (i.e. reduced SMN) but which could also facilitate pre-clinical drug testing as well as permit determination of when SMN depletion is neuropathic, and conversely when SMN needs to be present to moderate or prevent motor neuron loss.

A number of inducible systems have been developed for the generation of animal models of diseases (Yamamoto, Hen et al. 2001; Albanese, Hulit et al. 2002; Aagaard, Amarzguioui et al. 2007; Hasanuzzaman, Kutner et al. 2007). The most popular inducible systems are the doxyclycline and tetracycline inducible systems. These transgenic mouse systems have been used to establish models to study cancer, development, memory and plasticity as well as neurodegenerative disorders, such as prion disease and Huntington's disease (Yamamoto, Hen et al. 2001; Albanese, Hulit et al. 2002; Aagaard, Amarzguioui et al. 2007; Hasanuzzaman, Kutner et al. 2007). The use of an inducible system for the study of SMA would allow us to determine when and at what level depletion of SMN is

pathogenic and if a reversal of motor neuron degeneration is possible when SMN levels are restored, and at what time this upregulation is necessary.

8.5 Further assessment of neurodevelopment

An important question is whether Smn depletion can cause neurodevelopmental problems in addition to the neuronal maintenance defects during post-natal stages. In my thesis, we investigated the morphology and differentiation of neurosphere-derived neural stem cells (NSCs) generated from the brains of *Smn*$^{+/-}$ (mild) and *Smn*$^{-/-}$;*SMN2* (severe) SMA mice. Neurospheres from the severe genotype produced NSCs with increased proliferation during growth and differentiation, which resulted in fewer Tuj1-positive neuronal cells associated with an increase in the number of nestin-positive cells. We could follow up on these observations to understand the molecular pathways that have been mis-regulated in NSCs from severe SMA mice. It has been previously demonstrated that neural precursor cell population is regulated by cell cycle genes and in particular those that regulate the G1/S transition. It is also known that the Notch-Hes pathway is necessary for self-renewing cell division and, thus, maintenance of the neural precursor population (Ishibashi, Ang et al. 1995; Hatakeyama, Bessho et al. 2004). Deletion of *Notch1*, *Hes1*, or *Hes1/Hes5* results in premature differentiation of embryonic neural precursors (Ishibashi, Ang et al. 1995; Ohtsuka, Sakamoto et al. 2001). Conversely, overexpression of activated *Notch1* or *Hes1* causes an expansion of neural precursor numbers (Ishibashi, Moriyoshi et al. 1994). We could determine if perturbation of the Notch pathway contributes to the

neurodevelopmental defect in *Smn*$^{-/-}$;*SMN2* (severe) SMA mice. To determine whether Notch signaling is affected in Smn-depleted neural precursor cells, we could examine expression of members of the Notch-signaling pathway including Notch1, Delta-like1, Hes1, and Hes5 by performing *in situ* hybridization on wild type, Smn$^{+/-}$, and *Smn*$^{-/-}$;*SMN2* embryo brain sections. Further, to determine whether there is increased Notch activation, activated Notch could be assessed by immunoblot analysis using an antibody directed against the cleaved intracellular fragment (Robey, Chang et al. 1996). We could determine if there is an enhancement of both full length (260 kD) and activated Notch1 (120 kD) in the Smn-depleted tissues. Similar analysis could be performed on neurospheres and NSCs derived from wild type and *Smn*$^{-/-}$;*SMN2* embryos. Establishing if the critical Notch-Hes pathway, which is necessary for self-renewing cell division and maintenance of the neural precursor population, is perturbed would highlight the developmental consequences of depleting SMN and would indicate that SMA pathogenesis involves a neurodevelopmental aspect, especially with regards to the severe form of the disease.

8.6 Further validation of SMN interacting proteins identified by TAP-tag SMN purification

As we have validated MRLC and Annexin II in C2C12 cells, we can validate other identified SMN interacting proteins in the same way. Identifying and validating cell-specific or stage-specific Smn-interacting proteins would help us to better understand the diverse functions that Smn is involved in and thereby

address how SMN depletion leads to pathology in SMA patients.

8.7 Conclusion

Through our multiple studies we have uncovered a tremendous amount of insight concerning SMN's specific role in motor neurons and muscle and how the dosage of SMN influences these roles. We are now able to better understand the contribution of various cell types to SMA disease pathogenesis. Moreover our suggestion that SMN has cell-specific functions and that these functions are affected by the level of SMN expressed has shed more light on the pathophysiology of SMA. Lastly, our work will aid in the identification of novel targets for SMA therapy as well as aid in determining the window of opportunity for treatment.

9.0 REFERENCES

Aagaard, L., M. Amarzguioui, et al. (2007). "A facile lentiviral vector system for expression of doxycycline-inducible shRNAs: knockdown of the pre-miRNA processing enzyme Drosha." Mol Ther **15**(5): 938-45.

Aebersold, R. and M. Mann (2003). "Mass spectrometry-based proteomics." Nature **422**(6928): 198-207.

Albanese, C., J. Hulit, et al. (2002). "Recent advances in inducible expression in transgenic mice." Semin Cell Dev Biol **13**(2): 129-41.

Andreassi, C., C. Angelozzi, et al. (2004). "Phenylbutyrate increases SMN expression in vitro: relevance for treatment of spinal muscular atrophy." Eur J Hum Genet **12**(1): 59-65.

Appel, B., V. Korzh, et al. (1995). "Motoneuron fate specification revealed by patterned LIM homeobox gene expression in embryonic zebrafish." Development **121**(12): 4117-25.

Arber, S., B. Han, et al. (1999). "Requirement for the homeobox gene Hb9 in the consolidation of motor neuron identity." Neuron **23**(4): 659-74.

Arnold, A. S., M. Gueye, et al. (2004). "Reduced expression of nicotinic AChRs in myotubes from spinal muscular atrophy I patients." Lab Invest **84**(10): 1271-8.

Azzouz, M., T. Le, et al. (2004). "Lentivector-mediated SMN replacement in a mouse model of spinal muscular atrophy." J Clin Invest **114**(12): 1726-31.

Bach, J. R., J. S. Baird, et al. (2002). "Spinal muscular atrophy type 1: management and outcomes." Pediatr Pulmonol **34**(1): 16-22.

Bach, J. R., V. Niranjan, et al. (2000). "Spinal muscular atrophy type 1: A noninvasive respiratory management approach." Chest **117**(4): 1100-5.

Bahn, S., M. Mimmack, et al. (2002). "Neuronal target genes of the neuron-restrictive silencer factor in neurospheres derived from fetuses with Down's syndrome: a gene expression study." Lancet **359**(9303): 310-5.

Balabanian, S., N. H. Gendron, et al. (2007). "Histologic and transcriptional assessment of a mild SMA model." Neurol Res **29**(5): 413-24.

Baron-Delage, S., A. Abadie, et al. (2000). "Interferons and IRF-1 induce expression of the survival motor neuron (SMN) genes." Mol Med **6**(11): 957-68.

Battaglia, G., A. Princivalle, et al. (1997). "Expression of the SMN gene, the spinal muscular atrophy determining gene, in the mammalian central nervous system." Hum Mol Genet **6**(11): 1961-71.

Bechade, C., P. Rostaing, et al. (1999). "Subcellular distribution of survival motor neuron (SMN) protein: possible involvement in nucleocytoplasmic and dendritic transport." Eur J Neurosci **11**(1): 293-304.

Bertrandy, S., P. Burlet, et al. (1999). "The RNA-binding properties of SMN: deletion analysis of the zebrafish orthologue defines domains conserved in evolution." Hum Mol Genet **8**(5): 775-82.

Birnkrant, D. J., J. F. Pope, et al. (1998). "Treatment of type I spinal muscular atrophy with noninvasive ventilation and gastrostomy feeding." Pediatr Neurol **18**(5): 407-10.

Bowerman, M., D. Shafey, et al. (2007). "Smn depletion alters profilin II expression and leads to upregulation of the RhoA/ROCK pathway and defects in neuronal integrity." J Mol Neurosci **32**(2): 120-31.

Brahe, C., O. Clermont, et al. (1996). "Frameshift mutation in the survival motor neuron gene in a severe case of SMA type I." Hum Mol Genet **5**(12): 1971-6.

Braun, S., B. Croizat, et al. (1995). "Constitutive muscular abnormalities in culture in spinal muscular atrophy." Lancet **345**(8951): 694-5.

Brazelton, T. R., F. M. Rossi, et al. (2000). "From marrow to brain: expression of neuronal phenotypes in adult mice." Science **290**(5497): 1775-9.

Brichta, L., Y. Hofmann, et al. (2003). "Valproic acid increases the SMN2 protein level: a well-known drug as a potential therapy for spinal muscular atrophy." Hum Mol Genet **12**(19): 2481-9.

Broihier, H. T. and J. B. Skeath (2002). "Drosophila homeodomain protein dHb9 directs neuronal fate via crossrepressive and cell-nonautonomous mechanisms." Neuron **35**(1): 39-50.

Brzustowicz, L. M., T. Lehner, et al. (1990). "Genetic mapping of chronic childhood-onset spinal muscular atrophy to chromosome 5q11.2-13.3." Nature **344**(6266): 540-1.

Buhler, D., V. Raker, et al. (1999). "Essential role for the tudor domain of SMN in spliceosomal U snRNP assembly: implications for spinal muscular atrophy." Hum Mol Genet **8**(13): 2351-7.

Burghes, A. H., S. E. Ingraham, et al. (1994). "Linkage mapping of the spinal muscular atrophy gene." Hum Genet **93**(3): 305-12.

Burglen, L., S. Lefebvre, et al. (1996). "Structure and organization of the human survival motor neurone (SMN) gene." Genomics **32**(3): 479-82.

Burlet, P., C. Huber, et al. (1998). "The distribution of SMN protein complex in human fetal tissues and its alteration in spinal muscular atrophy." Hum Mol Genet **7**(12): 1927-33.

Bussaglia, E., O. Clermont, et al. (1995). "A frame-shift deletion in the survival motor neuron gene in Spanish spinal muscular atrophy patients." Nat Genet **11**(3): 335-7.

Callahan, C. A. and J. B. Thomas (1994). "Tau-beta-galactosidase, an axon-targeted fusion protein." Proc Natl Acad Sci U S A **91**(13): 5972-6.

Carissimi, C., L. Saieva, et al. (2006). "Gemin8 is a novel component of the survival motor neuron complex and functions in small nuclear ribonucleoprotein assembly." J Biol Chem **281**(12): 8126-34.

Carissimi, C., L. Saieva, et al. (2006). "Gemin8 is required for the architecture and function of the survival motor neuron complex." J Biol Chem **281**(48): 37009-16.

Cartegni, L. and A. R. Krainer (2003). "Correction of disease-associated exon skipping by synthetic exon-specific activators." Nat Struct Biol **10**(2): 120-5.

Castren, M., T. Tervonen, et al. (2005). "Altered differentiation of neural stem cells in fragile X syndrome." Proc Natl Acad Sci U S A **102**(49): 17834-9.

Ceroni, M., A. Grandi, et al. (1982). "Association of cardiomyopathy with Kugelberg-Welander disease." Ital J Neurol Sci **3**(2): 143-7.

Chan, Y. B., I. Miguel-Aliaga, et al. (2003). "Neuromuscular defects in a Drosophila survival motor neuron gene mutant." Hum Mol Genet **12**(12): 1367-76.

Chang, J. G., H. M. Hsieh-Li, et al. (2001). "Treatment of spinal muscular atrophy by sodium butyrate." Proc Natl Acad Sci U S A **98**(17): 9808-13.

Charrasse, S., F. Comunale, et al. (2006). "RhoA GTPase regulates M-cadherin activity and myoblast fusion." Mol Biol Cell **17**(2): 749-59.

Charroux, B., L. Pellizzoni, et al. (1999). "Gemin3: A novel DEAD box protein that interacts with SMN, the spinal muscular atrophy gene product, and is a component of gems." J Cell Biol **147**(6): 1181-94.

Charroux, B., L. Pellizzoni, et al. (2000). "Gemin4. A novel component of the SMN complex that is found in both gems and nucleoli." J Cell Biol **148**(6): 1177-86.

Chen, J., S. S. Magavi, et al. (2004). "Neurogenesis of corticospinal motor neurons extending spinal projections in adult mice." Proc Natl Acad Sci U S A **101**(46): 16357-62.

Chen, Q., S. D. Baird, et al. (1998). "Sequence of a 131-kb region of 5q13.1 containing the spinal muscular atrophy candidate genes SMN and NAIP." Genomics **48**(1): 121-7.

Chi, L., Y. Ke, et al. (2007). "Depletion of reduced glutathione enhances motor neuron degeneration in vitro and in vivo." Neuroscience **144**(3): 991-1003.

Cifuentes-Diaz, C., T. Frugier, et al. (2001). "Deletion of murine SMN exon 7 directed to skeletal muscle leads to severe muscular dystrophy." J Cell Biol **152**(5): 1107-14.

Cifuentes-Diaz, C., S. Nicole, et al. (2002). "Neurofilament accumulation at the motor endplate and lack of axonal sprouting in a spinal muscular atrophy mouse model." Hum Mol Genet **11**(12): 1439-47.

Collins, R. E. and X. Cheng (2005). "Structural domains in RNAi." FEBS Lett **579**(26): 5841-9.

Constantin, B., C. Cognard, et al. (1995). "Myoblast fusion is not a prerequisite for the appearance of calcium current, calcium release, and contraction in rat skeletal muscle cells developing in culture." Exp Cell Res **217**(2): 497-505.

Coovert, D. D., T. T. Le, et al. (1997). "The survival motor neuron protein in spinal muscular atrophy." Hum Mol Genet **6**(8): 1205-14.

Cordes, S. P. (2001). "Molecular genetics of cranial nerve development in mouse." Nat Rev Neurosci **2**(9): 611-23.

Coumoul, X. and C. X. Deng (2006). "RNAi in mice: a promising approach to decipher gene functions in vivo." Biochimie **88**(6): 637-43.

Crawford, T. O. and C. A. Pardo (1996). "The neurobiology of childhood spinal muscular atrophy." Neurobiol Dis **3**(2): 97-110.

Czauderna, F., A. Santel, et al. (2003). "Inducible shRNA expression for application in a prostate cancer mouse model." Nucleic Acids Res **31**(21): e127.

Daadi, M. M. and S. Weiss (1999). "Generation of tyrosine hydroxylase-producing neurons from precursors of the embryonic and adult forebrain." J Neurosci **19**(11): 4484-97.

Dennis, M. J. (1981). "Development of the neuromuscular junction: inductive interactions between cells." Annu Rev Neurosci **4**: 43-68.

Detich, N., V. Bovenzi, et al. (2003). "Valproate induces replication-independent active DNA demethylation." J Biol Chem **278**(30): 27586-92.

DiDonato, C. J., T. Brun, et al. (1999). "Complete nucleotide sequence, genomic organization, and promoter analysis of the murine survival motor neuron gene (Smn)." Mamm Genome **10**(6): 638-41.

DiDonato, C. J., X. N. Chen, et al. (1997). "Cloning, characterization, and copy number of the murine survival motor neuron gene: homolog of the spinal muscular atrophy-determining gene." Genome Res **7**(4): 339-52.

DiDonato, C. J., S. E. Ingraham, et al. (1997). "Deletion and conversion in spinal muscular atrophy patients: is there a relationship to severity?" Ann Neurol **41**(2): 230-7.

DiDonato, C. J., R. J. Parks, et al. (2003). "Development of a gene therapy strategy for the restoration of survival motor neuron protein expression: implications for spinal muscular atrophy therapy." Hum Gene Ther **14**(2): 179-88.

Elbashir, S. M., J. Harborth, et al. (2001). "Duplexes of 21-nucleotide RNAs mediate RNA interference in cultured mammalian cells." Nature **411**(6836): 494-8.

Elbashir, S. M., W. Lendeckel, et al. (2001). "RNA interference is mediated by 21- and 22-nucleotide RNAs." Genes Dev **15**(2): 188-200.

Ericson, J., S. Thor, et al. (1992). "Early stages of motor neuron differentiation revealed by expression of homeobox gene Islet-1." Science **256**(5063): 1555-60.

Etienne-Manneville, S. and A. Hall (2002). "Rho GTPases in cell biology." Nature **420**(6916): 629-35.

Feldkotter, M., V. Schwarzer, et al. (2002). "Quantitative analyses of SMN1 and SMN2 based on real-time lightCycler PCR: fast and highly reliable carrier testing and prediction of severity of spinal muscular atrophy." Am J Hum Genet **70**(2): 358-68.

Ferrari, G., G. Cusella-De Angelis, et al. (1998). "Muscle regeneration by bone marrow-derived myogenic progenitors." Science **279**(5356): 1528-30.

Fidzianska, A., H. H. Goebel, et al. (1990). "Acute infantile spinal muscular atrophy. Muscle apoptosis as a proposed pathogenetic mechanism." Brain **113 (Pt 2)**: 433-45.

Fire, A., S. Xu, et al. (1998). "Potent and specific genetic interference by double-stranded RNA in Caenorhabditis elegans." Nature **391**(6669): 806-11.

Fischer, U., Q. Liu, et al. (1997). "The SMN-SIP1 complex has an essential role in spliceosomal snRNP biogenesis." Cell **90**(6): 1023-9.

Frugier, T., F. D. Tiziano, et al. (2000). "Nuclear targeting defect of SMN lacking the C-terminus in a mouse model of spinal muscular atrophy." Hum Mol Genet **9**(5): 849-58.

Fulton, A. B., J. Prives, et al. (1981). "Developmental reorganization of the skeletal framework and its surface lamina in fusing muscle cells." J Cell Biol **91**(1): 103-12.

Funakoshi, H., N. Belluardo, et al. (1995). "Muscle-derived neurotrophin-4 as an activity-dependent trophic signal for adult motor neurons." Science **268**(5216): 1495-9.

Gage, F. H. (2000). "Mammalian neural stem cells." Science **287**(5457): 1433-8.

Gangwani, L., M. Mikrut, et al. (2001). "Spinal muscular atrophy disrupts the interaction of ZPR1 with the SMN protein." Nat Cell Biol **3**(4): 376-83.

Gavrilina, T. O., V. L. McGovern, et al. (2008). "Neuronal SMN expression corrects spinal muscular atrophy in severe SMA mice while muscle specific SMN expression has no phenotypic effect." Hum Mol Genet.

Giesemann, T., S. Rathke-Hartlieb, et al. (1999). "A role for polyproline motifs in the spinal muscular atrophy protein SMN. Profilins bind to and colocalize with smn in nuclear gems." J Biol Chem **274**(53): 37908-14.

Gil, J. and M. Esteban (2000). "Induction of apoptosis by the dsRNA-dependent protein kinase (PKR): mechanism of action." Apoptosis **5**(2): 107-14.

Gilliam, T. C., L. M. Brzustowicz, et al. (1990). "Genetic homogeneity between acute and chronic forms of spinal muscular atrophy." Nature **345**(6278): 823-5.

Grondard, C., O. Biondi, et al. (2005). "Regular exercise prolongs survival in a type 2 spinal muscular atrophy model mouse." J Neurosci **25**(33): 7615-22.

Grzeschik, S. M., M. Ganta, et al. (2005). "Hydroxyurea enhances SMN2 gene expression in spinal muscular atrophy cells." Ann Neurol **58**(2): 194-202.

Guettier-Sigrist, S., G. Coupin, et al. (1998). "Muscle could be the therapeutic target in SMA treatment." J Neurosci Res **53**(6): 663-9.

Guzzo, R. M., J. Wigle, et al. (2004). "Regulated expression and temporal induction of the tail-anchored sarcolemmal-membrane-associated protein is critical for myoblast fusion." Biochem J **381**(Pt 3): 599-608.

Haddad, H., C. Cifuentes-Diaz, et al. (2003). "Riluzole attenuates spinal muscular atrophy disease progression in a mouse model." Muscle Nerve **28**(4): 432-7.

Hahnen, E., J. Schonling, et al. (1997). "Missense mutations in exon 6 of the survival motor neuron gene in patients with spinal muscular atrophy (SMA)." Hum Mol Genet **6**(5): 821-5.

Hannon, G. J. (2002). "RNA interference." Nature **418**(6894): 244-51.

Hasanuzzaman, M., R. Kutner, et al. (2007). "A doxycycline-inducible urokinase receptor (uPAR) upregulates uPAR activities including resistance to anoikis in human prostate cancer cell lines." Mol Cancer **6**: 34.

Hasuwa, H., K. Kaseda, et al. (2002). "Small interfering RNA and gene silencing in transgenic mice and rats." FEBS Lett **532**(1-2): 227-30.

Hatakeyama, J., Y. Bessho, et al. (2004). "Hes genes regulate size, shape and histogenesis of the nervous system by control of the timing of neural stem cell differentiation." Development **131**(22): 5539-50.

Hausmanowa-Petrusewicz, I., A. Fidzianska, et al. (1980). "Is Kugelberg-Welander spinal muscular atrophy a fetal defect?" Muscle Nerve **3**(5): 389-402.

Hsieh-Li, H. M., J. G. Chang, et al. (2000). "A mouse model for spinal muscular atrophy." Nat Genet **24**(1): 66-70.

Huppi, K., S. E. Martin, et al. (2005). "Defining and assaying RNAi in mammalian cells." Mol Cell **17**(1): 1-10.

Ishibashi, M., S. L. Ang, et al. (1995). "Targeted disruption of mammalian hairy and Enhancer of split homolog-1 (HES-1) leads to up-regulation of neural helix-loop-helix factors, premature neurogenesis, and severe neural tube defects." Genes Dev **9**(24): 3136-48.

Ishibashi, M., K. Moriyoshi, et al. (1994). "Persistent expression of helix-loop-helix factor HES-1 prevents mammalian neural differentiation in the central nervous system." Embo J **13**(8): 1799-805.

Iwahashi, H., Y. Eguchi, et al. (1997). "Synergistic anti-apoptotic activity between Bcl-2 and SMN implicated in spinal muscular atrophy." Nature **390**(6658): 413-7.

Jablonka, S., K. Karle, et al. (2006). "Distinct and overlapping alterations in motor and sensory neurons in a mouse model of spinal muscular atrophy." Hum Mol Genet **15**(3): 511-8.

Jablonka, S., B. Schrank, et al. (2000). "Reduced survival motor neuron (Smn) gene dose in mice leads to motor neuron degeneration: an animal model for spinal muscular atrophy type III." Hum Mol Genet **9**(3): 341-6.

Karlsson, O., S. Thor, et al. (1990). "Insulin gene enhancer binding protein Isl-1 is a member of a novel class of proteins containing both a homeo- and a Cys-His domain." Nature **344**(6269): 879-82.

Kernochan, L. E., M. L. Russo, et al. (2005). "The role of histone acetylation in SMN gene expression." Hum Mol Genet **14**(9): 1171-82.

Kimura, K., M. Ito, et al. (1996). "Regulation of myosin phosphatase by Rho and Rho-associated kinase (Rho-kinase)." Science **273**(5272): 245-8.

Kimura, S., H. Yokota, et al. (1980). "A case of the Kugelberg-Welander syndrome complicated with cardiac lesions." Jpn Heart J **21**(3): 417-22.

Knuesel, M., Y. Wan, et al. (2003). "Identification of novel protein-protein interactions using a versatile mammalian tandem affinity purification expression system." Mol Cell Proteomics **2**(11): 1225-33.

Krause, D. S., N. D. Theise, et al. (2001). "Multi-organ, multi-lineage engraftment by a single bone marrow-derived stem cell." Cell **105**(3): 369-77.

Kuhn, T. B., P. J. Meberg, et al. (2000). "Regulating actin dynamics in neuronal growth cones by ADF/cofilin and rho family GTPases." J Neurobiol **44**(2): 126-44.

Kunath, T., G. Gish, et al. (2003). "Transgenic RNA interference in ES cell-derived embryos recapitulates a genetic null phenotype." Nat Biotechnol **21**(5): 559-61.

La Bella, V., C. Cisterni, et al. (1998). "Survival motor neuron (SMN) protein in rat is expressed as different molecular forms and is developmentally regulated." Eur J Neurosci **10**(9): 2913-23.

Le, T. T., L. T. Pham, et al. (2005). "SMNDelta7, the major product of the centromeric survival motor neuron (SMN2) gene, extends survival in mice with spinal muscular atrophy and associates with full-length SMN." Hum Mol Genet **14**(6): 845-57.

Lefebvre, S., L. Burglen, et al. (1995). "Identification and characterization of a spinal muscular atrophy-determining gene." Cell **80**(1): 155-65.

Lefebvre, S., P. Burlet, et al. (1997). "Correlation between severity and SMN protein level in spinal muscular atrophy." Nat Genet **16**(3): 265-9.

Lendahl, U., L. B. Zimmerman, et al. (1990). "CNS stem cells express a new class of intermediate filament protein." Cell **60**(4): 585-95.

Lesbordes, J. C., C. Cifuentes-Diaz, et al. (2003). "Therapeutic benefits of cardiotrophin-1 gene transfer in a mouse model of spinal muscular atrophy." Hum Mol Genet **12**(11): 1233-9.

Lim, S. R. and K. J. Hertel (2001). "Modulation of survival motor neuron pre-mRNA splicing by inhibition of alternative 3' splice site pairing." J Biol Chem **276**(48): 45476-83.

Liu, Q. and G. Dreyfuss (1996). "A novel nuclear structure containing the survival of motor neurons protein." Embo J **15**(14): 3555-65.

Liu, Q., U. Fischer, et al. (1997). "The spinal muscular atrophy disease gene product, SMN, and its associated protein SIP1 are in a complex with spliceosomal snRNP proteins." Cell **90**(6): 1013-21.

Liu, Y. B., W. J. Chen, et al. (1999). "Atrial standstill in a case of Kugelberg-Welander syndrome with cardiac involvement: an electrophysiologic study." Int J Cardiol **70**(2): 207-10.

Liu, Z. and L. J. Martin (2006). "The adult neural stem and progenitor cell niche is altered in amyotrophic lateral sclerosis mouse brain." J Comp Neurol **497**(3): 468-88.

Lorson, C. L., E. Hahnen, et al. (1999). "A single nucleotide in the SMN gene regulates splicing and is responsible for spinal muscular atrophy." Proc Natl Acad Sci U S A **96**(11): 6307-11.

Lorson, C. L., J. Strasswimmer, et al. (1998). "SMN oligomerization defect correlates with spinal muscular atrophy severity." Nat Genet **19**(1): 63-6.

Lunn, M. R., D. E. Root, et al. (2004). "Indoprofen upregulates the survival motor neuron protein through a cyclooxygenase-independent mechanism." Chem Biol **11**(11): 1489-93.

MacKenzie, A. E., P. Jacob, et al. (1994). "Genetic heterogeneity in spinal muscular atrophy: a linkage analysis-based assessment." Neurology **44**(5): 919-24.

Marshall, C. J. (1995). "Specificity of receptor tyrosine kinase signaling: transient versus sustained extracellular signal-regulated kinase activation." Cell **80**(2): 179-85.

Matthews-Bellinger, J. A. and M. M. Salpeter (1983). "Fine structural distribution of acetylcholine receptors at developing mouse neuromuscular junctions." J Neurosci **3**(3): 644-57.

McAndrew, P. E., D. W. Parsons, et al. (1997). "Identification of proximal spinal muscular atrophy carriers and patients by analysis of SMNT and SMNC gene copy number." Am J Hum Genet **60**(6): 1411-22.

McKay, R. (1997). "Stem cells in the central nervous system." Science **276**(5309): 66-71.

McKinnell, I. W., J. Ishibashi, et al. (2007). "Pax7 activates myogenic genes by recruitment of a histone methyltransferase complex." Nat Cell Biol.

McWhorter, M. L., U. R. Monani, et al. (2003). "Knockdown of the survival motor neuron (Smn) protein in zebrafish causes defects in motor axon outgrowth and pathfinding." J Cell Biol **162**(5): 919-31.

Meister, G., D. Buhler, et al. (2000). "Characterization of a nuclear 20S complex containing the survival of motor neurons (SMN) protein and a specific subset of spliceosomal Sm proteins." Hum Mol Genet **9**(13): 1977-86.

Melki, J., S. Abdelhak, et al. (1990). "Gene for chronic proximal spinal muscular atrophies maps to chromosome 5q." Nature **344**(6268): 767-8.

Melki, J., S. Lefebvre, et al. (1994). "De novo and inherited deletions of the 5q13 region in spinal muscular atrophies." Science **264**(5164): 1474-7.

Melki, J., P. Sheth, et al. (1990). "Mapping of acute (type I) spinal muscular atrophy to chromosome 5q12-q14. The French Spinal Muscular Atrophy Investigators." Lancet **336**(8710): 271-3.

Menell, J. S., G. M. Cesarman, et al. (1999). "Annexin II and bleeding in acute promyelocytic leukemia." N Engl J Med **340**(13): 994-1004.

Miguel-Aliaga, I., Y. B. Chan, et al. (2000). "Disruption of SMN function by ectopic expression of the human SMN gene in Drosophila." FEBS Lett **486**(2): 99-102.

Miguel-Aliaga, I., E. Culetto, et al. (1999). "The Caenorhabditis elegans orthologue of the human gene responsible for spinal muscular atrophy is a maternal product critical for germline maturation and embryonic viability." Hum Mol Genet **8**(12): 2133-43.

Miyagishi, M., H. Sumimoto, et al. (2004). "Optimization of an siRNA-expression system with an improved hairpin and its significant suppressive effects in mammalian cells." J Gene Med **6**(7): 715-23.

Monani, U. R., C. L. Lorson, et al. (1999). "A single nucleotide difference that alters splicing patterns distinguishes the SMA gene SMN1 from the copy gene SMN2." Hum Mol Genet **8**(7): 1177-83.

Monani, U. R., M. T. Pastore, et al. (2003). "A transgene carrying an A2G missense mutation in the SMN gene modulates phenotypic severity in mice with severe (type I) spinal muscular atrophy." J Cell Biol **160**(1): 41-52.

Monani, U. R., M. Sendtner, et al. (2000). "The human centromeric survival motor neuron gene (SMN2) rescues embryonic lethality in Smn(-/-) mice and results in a mouse with spinal muscular atrophy." Hum Mol Genet **9**(3): 333-9.

Munsat, T. L. and K. E. Davies (1992). "International SMA consortium meeting. (26-28 June 1992, Bonn, Germany)." Neuromuscul Disord **2**(5-6): 423-8.

Munsat, T. L., E. L. Mancall, et al. (1994). "The AAN launches a new education program: CONTINUUM lifelong learning in neurology." Neurology **44**(4): 771-2.

Nicole, S., B. Desforges, et al. (2003). "Intact satellite cells lead to remarkable protection against Smn gene defect in differentiated skeletal muscle." J Cell Biol **161**(3): 571-82.

Nishiyama, T., I. Kii, et al. (2004). "Inactivation of Rho/ROCK signaling is crucial for the nuclear accumulation of FKHR and myoblast fusion." J Biol Chem **279**(45): 47311-9.

Ohtsuka, T., M. Sakamoto, et al. (2001). "Roles of the basic helix-loop-helix genes Hes1 and Hes5 in expansion of neural stem cells of the developing brain." J Biol Chem **276**(32): 30467-74.

Otter, S., M. Grimmler, et al. (2007). "A comprehensive interaction map of the human survival of motor neuron (SMN) complex." J Biol Chem **282**(8): 5825-33.

Owen, N., C. L. Doe, et al. (2000). "Characterization of the Schizosaccharomyces pombe orthologue of the human survival motor neuron (SMN) protein." Hum Mol Genet **9**(5): 675-84.

Pagliardini, S., A. Giavazzi, et al. (2000). "Subcellular localization and axonal transport of the survival motor neuron (SMN) protein in the developing rat spinal cord." Hum Mol Genet **9**(1): 47-56.

Parsons, D. W., P. E. McAndrew, et al. (1996). "An 11 base pair duplication in exon 6 of the SMN gene produces a type I spinal muscular atrophy (SMA) phenotype: further evidence for SMN as the primary SMA-determining gene." Hum Mol Genet **5**(11): 1727-32.

Patrizi, A. L., F. Tiziano, et al. (1999). "SMN protein analysis in fibroblast, amniocyte and CVS cultures from spinal muscular atrophy patients and its relevance for diagnosis." Eur J Hum Genet **7**(3): 301-9.

Paushkin, S., A. K. Gubitz, et al. (2002). "The SMN complex, an assemblyosome of ribonucleoproteins." Curr Opin Cell Biol **14**(3): 305-12.

Pearn, J. (1980). "Classification of spinal muscular atrophies." Lancet **1**(8174): 919-22.

Pellizzoni, L., J. Baccon, et al. (2001). "The survival of motor neurons (SMN) protein interacts with the snoRNP proteins fibrillarin and GAR1." Curr Biol **11**(14): 1079-88.

Pellizzoni, L., B. Charroux, et al. (2001). "A functional interaction between the survival motor neuron complex and RNA polymerase II." J Cell Biol **152**(1): 75-85.

Pellizzoni, L., N. Kataoka, et al. (1998). "A novel function for SMN, the spinal muscular atrophy disease gene product, in pre-mRNA splicing." Cell **95**(5): 615-24.

Pellizzoni, L., J. Yong, et al. (2002). "Essential role for the SMN complex in the specificity of snRNP assembly." Science **298**(5599): 1775-9.

Pratt, T., L. Sharp, et al. (2000). "Embryonic stem cells and transgenic mice ubiquitously expressing a tau-tagged green fluorescent protein." Dev Biol **228**(1): 19-28.

Prior, T. W., K. J. Swoboda, et al. (2004). "Homozygous SMN1 deletions in unaffected family members and modification of the phenotype by SMN2." Am J Med Genet A **130**(3): 307-10.

Puig, O., F. Caspary, et al. (2001). "The tandem affinity purification (TAP) method: a general procedure of protein complex purification." Methods **24**(3): 218-29.

Pumiglia, K. M. and S. J. Decker (1997). "Cell cycle arrest mediated by the MEK/mitogen-activated protein kinase pathway." Proc Natl Acad Sci U S A **94**(2): 448-52.

Qui, M. S. and S. H. Green (1992). "PC12 cell neuronal differentiation is associated with prolonged p21ras activity and consequent prolonged ERK activity." Neuron **9**(4): 705-17.

Rajendra, T. K., G. B. Gonsalvez, et al. (2007). "A Drosophila melanogaster model of spinal muscular atrophy reveals a function for SMN in striated muscle." J Cell Biol **176**(6): 831-41.

Rao, M. and S. Sockanathan (2005). "Molecular mechanisms of RNAi: implications for development and disease." Birth Defects Res C Embryo Today **75**(1): 28-42.

Rigaut, G., A. Shevchenko, et al. (1999). "A generic protein purification method for protein complex characterization and proteome exploration." Nat Biotechnol **17**(10): 1030-2.

Robey, E., D. Chang, et al. (1996). "An activated form of Notch influences the choice between CD4 and CD8 T cell lineages." Cell **87**(3): 483-92.

Rossoll, W., S. Jablonka, et al. (2003). "Smn, the spinal muscular atrophy-determining gene product, modulates axon growth and localization of beta-actin mRNA in growth cones of motoneurons." J Cell Biol **163**(4): 801-12.

Rossoll, W., A. K. Kroning, et al. (2002). "Specific interaction of Smn, the spinal muscular atrophy determining gene product, with hnRNP-R and gry-rbp/hnRNP-Q: a role for Smn in RNA processing in motor axons?" Hum Mol Genet **11**(1): 93-105.

Rubinson, D. A., C. P. Dillon, et al. (2003). "A lentivirus-based system to functionally silence genes in primary mammalian cells, stem cells and transgenic mice by RNA interference." Nat Genet **33**(3): 401-6.

Rubinstein, A. L. (2003). "Zebrafish: from disease modeling to drug discovery." Curr Opin Drug Discov Devel **6**(2): 218-23.

Saito, Y., T. Yokota, et al. (2005). "Transgenic small interfering RNA halts amyotrophic lateral sclerosis in a mouse model." J Biol Chem **280**(52): 42826-30.

Sanger, J. W. and H. Holtzer (1972). "Cytochalasin B: effects on cell morphology, cell adhesion, and mucopolysaccharide synthesis (cultured cells-contractile microfilaments-glycoproteins-embryonic cells-sorting-out)." Proc Natl Acad Sci U S A **69**(1): 253-7.

Sanger, J. W., S. Holtzer, et al. (1971). "Effects of cytochalasin B on muscle cells in tissue culture." Nat New Biol **229**(4): 121-3.

Scharf, J. M., D. Damron, et al. (1996). "The mouse region syntenic for human spinal muscular atrophy lies within the Lgn1 critical interval and contains multiple copies of Naip exon 5." Genomics **38**(3): 405-17.

Schrank, B., R. Gotz, et al. (1997). "Inactivation of the survival motor neuron gene, a candidate gene for human spinal muscular atrophy, leads to massive cell death in early mouse embryos." Proc Natl Acad Sci U S A **94**(18): 9920-5.

Selenko, P., R. Sprangers, et al. (2001). "SMN tudor domain structure and its interaction with the Sm proteins." Nat Struct Biol **8**(1): 27-31.

Shafey, D., P. D. Cote, et al. (2005). "Hypomorphic Smn knockdown C2C12 myoblasts reveal intrinsic defects in myoblast fusion and myotube morphology." Exp Cell Res **311**(1): 49-61.

Simard, L. R., M. Vanasse, et al. (1992). "Linkage study of chronic childhood-onset spinal muscular atrophy (SMA): confirmation of close linkage to D5S39 in French Canadian families." Genomics **14**(1): 188-90.

Singh, N. K., N. N. Singh, et al. (2006). "Splicing of a critical exon of human Survival Motor Neuron is regulated by a unique silencer element located in the last intron." Mol Cell Biol **26**(4): 1333-46.

Skordis, L. A., M. G. Dunckley, et al. (2001). "Characterisation of novel point mutations in the survival motor neuron gene SMN, in three patients with SMA." Hum Genet **108**(4): 356-7.

Skordis, L. A., M. G. Dunckley, et al. (2003). "Bifunctional antisense oligonucleotides provide a trans-acting splicing enhancer that stimulates SMN2 gene expression in patient fibroblasts." Proc Natl Acad Sci U S A **100**(7): 4114-9.

Soubrouillard, C., J. F. Pellissier, et al. (1995). "Expression of developmentally regulated cytoskeleton and cell surface proteins in childhood spinal muscular atrophies." J Neurol Sci **133**(1-2): 155-63.

Stark, G. R., I. M. Kerr, et al. (1998). "How cells respond to interferons." Annu Rev Biochem **67**: 227-64.

Sumner, C. J., T. N. Huynh, et al. (2003). "Valproic acid increases SMN levels in spinal muscular atrophy patient cells." Ann Neurol **54**(5): 647-54.

Sweeney, H. L., B. F. Bowman, et al. (1993). "Myosin light chain phosphorylation in vertebrate striated muscle: regulation and function." Am J Physiol **264**(5 Pt 1): C1085-95.

Swoboda, K. J., T. W. Prior, et al. (2005). "Natural history of denervation in SMA: relation to age, SMN2 copy number, and function." Ann Neurol **57**(5): 704-12.

Talbot, K., C. P. Ponting, et al. (1997). "Missense mutation clustering in the survival motor neuron gene: a role for a conserved tyrosine and glycine rich region of the protein in RNA metabolism?" Hum Mol Genet **6**(3): 497-500.

Tanaka, H., N. Uemura, et al. (1976). "Cardiac involvement in the Kugelbert-Welander syndrome." Am J Cardiol **38**(4): 528-32.

Thaler, J., K. Harrison, et al. (1999). "Active suppression of interneuron programs within developing motor neurons revealed by analysis of homeodomain factor HB9." Neuron **23**(4): 675-87.

Tiscornia, G., O. Singer, et al. (2003). "A general method for gene knockdown in mice by using lentiviral vectors expressing small interfering RNA." Proc Natl Acad Sci U S A **100**(4): 1844-8.

Totsukawa, G., Y. Yamakita, et al. (2000). "Distinct roles of ROCK (Rho-kinase) and MLCK in spatial regulation of MLC phosphorylation for assembly of stress fibers and focal adhesions in 3T3 fibroblasts." J Cell Biol **150**(4): 797-806.

Tsuchida, T., M. Ensini, et al. (1994). "Topographic organization of embryonic motor neurons defined by expression of LIM homeobox genes." Cell **79**(6): 957-70.

Tuschl, T. (2002). "Expanding small RNA interference." Nat Biotechnol **20**(5): 446-8.

Ueda, K., M. Murata-Hori, et al. (2002). "Rho-kinase contributes to diphosphorylation of myosin II regulatory light chain in nonmuscle cells." Oncogene **21**(38): 5852-60.

van Bergeijk, J., K. Rydel-Konecke, et al. (2007). "The spinal muscular atrophy gene product regulates neurite outgrowth: importance of the C terminus." Faseb J **21**(7): 1492-502.

van de Wetering, M., I. Oving, et al. (2003). "Specific inhibition of gene expression using a stably integrated, inducible small-interfering-RNA vector." EMBO Rep **4**(6): 609-15.

Viollet, L., S. Bertrandy, et al. (1997). "cDNA isolation, expression, and chromosomal localization of the mouse survival motor neuron gene (Smn)." Genomics **40**(1): 185-8.

Waisman, D. M. (1995). "Annexin II tetramer: structure and function." Mol Cell Biochem **149-150**: 301-22.

Wang, J. and G. Dreyfuss (2001). "A cell system with targeted disruption of the SMN gene: functional conservation of the SMN protein and dependence of Gemin2 on SMN." J Biol Chem **276**(13): 9599-605.

Wharton, S. B., C. J. McDermott, et al. (2003). "The cellular and molecular pathology of the motor system in hereditary spastic paraparesis due to mutation of the spastin gene." J Neuropathol Exp Neurol **62**(11): 1166-77.

Wielowieyski, P. A., S. Sevinc, et al. (2000). "Alternative splicing, expression, and genomic structure of the 3' region of the gene encoding the sarcolemmal-associated proteins (SLAPs) defines a novel class of coiled-coil tail-anchored membrane proteins." J Biol Chem **275**(49): 38474-81.

Wiese, C., A. Rolletschek, et al. (2004). "Nestin expression--a property of multi-lineage progenitor cells?" Cell Mol Life Sci **61**(19-20): 2510-22.

Will, C. L., C. Schneider, et al. (2001). "A novel U2 and U11/U12 snRNP protein that associates with the pre-mRNA branch site." Embo J **20**(16): 4536-46.

Williams, B. Y., S. L. Hamilton, et al. (2000). "The survival motor neuron protein interacts with the transactivator FUSE binding protein from human fetal brain." FEBS Lett **470**(2): 207-10.

Wirth, B., L. Brichta, et al. (2006). "Spinal muscular atrophy: from gene to therapy." Semin Pediatr Neurol **13**(2): 121-31.

Wirth, B., B. Voosen, et al. (1993). "Fine mapping and narrowing of the genetic interval of the spinal muscular atrophy region by linkage studies." Genomics **15**(1): 113-8.

Yamamoto, A., R. Hen, et al. (2001). "The ons and offs of inducible transgenic technology: a review." Neurobiol Dis **8**(6): 923-32.

Yang, P., H. M. Sampson, et al. (2006). "A modified tandem affinity purification strategy identifies cofactors of the Drosophila nuclear receptor dHNF4." Proteomics **6**(3): 927-35.

Yasuma, F., S. Kuru, et al. (2004). "Dilated cardiomyopathy in Kugelberg-Welander disease: coexisting sleep disordered breathing and its treatment with continuous positive airway pressure." Intern Med **43**(10): 951-4.

Yong, J., T. J. Golembe, et al. (2004). "snRNAs contain specific SMN-binding domains that are essential for snRNP assembly." Mol Cell Biol **24**(7): 2747-56.

Yong, J., L. Pellizzoni, et al. (2002). "Sequence-specific interaction of U1 snRNA with the SMN complex." Embo J **21**(5): 1188-96.

Young, P. J., P. M. Day, et al. (2002). "A direct interaction between the survival motor neuron protein and p53 and its relationship to spinal muscular atrophy." J Biol Chem **277**(4): 2852-9.

Zang, D. W. and S. S. Cheema (2002). "Degeneration of corticospinal and bulbospinal systems in the superoxide dismutase 1(G93A G1H) transgenic mouse model of familial amyotrophic lateral sclerosis." Neurosci Lett **332**(2): 99-102.

Zerres, K. and S. Rudnik-Schoneborn (1995). "Natural history in proximal spinal muscular atrophy. Clinical analysis of 445 patients and suggestions for a modification of existing classifications." Arch Neurol **52**(5): 518-23.

Zhang, H. L., F. Pan, et al. (2003). "Active transport of the survival motor neuron protein and the role of exon-7 in cytoplasmic localization." J Neurosci **23**(16): 6627-37.

Zimmerman, L., B. Parr, et al. (1994). "Independent regulatory elements in the nestin gene direct transgene expression to neural stem cells or muscle precursors." Neuron **12**(1): 11-24.

Zon, L. I. and R. T. Peterson (2005). "In vivo drug discovery in the zebrafish." Nat Rev Drug Discov **4**(1): 35-44.

10.0 CURRICULUM VITAE

Dina Shafey

Education

- **Doctor of Philosophy** 2005-2008
  Cellular Molecular Medicine
  University of Ottawa, Canada
- **Master of Science** 2003-Ph.D. transfer
  Cellular Molecular Medicine
  University of Ottawa, Canada
- **Bachelor of Science** 1999-2003
  Biochemistry and Biotechnology
  Carleton University, Canada

Awards & Distinctions

- Canadian Institute of Health Research, Doctoral: Canadian Graduate Scholarship 2007-2008
- Ontario Graduate Scholarship 2003-2007
- Excellence Scholarship, University of Ottawa 2003-2007
- Admissions Scholarship, University of Ottawa 2005-2009
- Dean's Honour list, Carleton University 2000-2003
- E.W.R Steacie Scholarship, Carleton University 2002-2003
- Department of BMI Summer Research Scholarship, University of Ottawa 2002
- Claude Bissell Scholarship, Carleton University 2001-2002
- Gerhard Herzberg Scholarship, Carleton University 2000-2001
- President's Scholarship, Carleton University 1999-2000

Work Experience

- **Graduate Student** 2003-2008
  University of Ottawa, Ottawa Health Research Institute
  As a graduate student I studied Spinal Muscular Atrophy and the role of Smn on the motor neuron/ muscle function and on mouse embryonic development. My work has resulted in publications well as numerous Conference presentations

- **Volunteer** 2001-2008
  Children's Hospital of Eastern Ontario
  As a volunteer at the Children's Hospital of Eastern Ontario, I assist the staff by providing direct client and support services.

- **Summer Research Student** June-Sept 2003
  Ottawa Health Research Institute
  As a summer research student I conducted a literature review on Spinal Muscular Atrophy to understand the key aspects of the disease before beginning my graduate studies.

- **Summer Research Student** May-Aug 2002
  CHEO Research Institute
  As a summer research student, I studied the distinct patterns of expression of the inhibitor of apoptosis protein cIAP2 during mouse embryogenesis. A publication resulted from this work.

- **Tutor in the Classroom** Nov 2001-May 2002
  Ottawa-Carleton District School Board
  As a tutor in the classroom, I taught elementary school students about conservation as it pertains to the environment and energy.

- **Summer Research Student** May-Aug 2000
  Office of the Governor General
  As a summer student at the Chancellery, working on the Caring Canadian Award, I researched the accomplishments of Canadians who had been nominated for this prestigious volunteer award.

Publications

Refereed Publications

Shafey, D., MacKenzie, A., and Kothary, R. (2007). Neurodevelopmental abnormalities in neural stem cells and embryos from severe SMA mice. Submitted to *Human Molecular Genetics.*

Bowerman, M., **Shafey, D.**, and Kothary, R. (2007). Smn depletion alters profilin II splicing and leads to upregulation of the RhoA/ROCK pathway and defects in neuronal integrity. *J Mol Neurosci.* 32(2):120-131.

Shafey, D., Korneluk, R., and Holcik, M. (2006). Distinct patterns of expression of the inhibitor of apoptosis protein cIAP2 during murine embryogenesis. *Apoptosis.* 11(7):1257-9.

Shafey, D., Côté, P., De Repentigny, R., and Kothary, R. (2005). Hypomorphic Smn knockdown C2C12 myoblasts reveal intrinsic defects in myoblast fusion and myotube morphology. *Exp Cell Res.* 311(1):49-61.

Abstracts

Shafey, D. and Kothary, Rashmi. (2007). Identification of differences in Smn interacting protein partners during different stages of C2C12 and PC12 differentiation. . Families of SMA meeting. Chicago, IL. June 2007.

Shafey, D., Hayward-McClelland, De Repentigny, R., Kaplansky, D. Mackenzie, A. and Kothary, R. (2006). Characterization of neuronal development in mild (Smn +/-) versus severe (Smn-/-;SMN2) SMA mice. Families of SMA meeting. Montreal, QC. June 2006.

Bowerman, M., **Shafey, D.,** and Kothary, R. (2006). Smn knockdown in PC12 cells: assessing a role for Smn in neuronal differentiation. Families of SMA meeting. Montreal, QC. June 2006.

Shafey, D., De Repentigny, R., Pinheiro, B., Côté, P. and Kothary, R. (2005). Establishment of a hypomorphic series of Smn knockdown mice. Families of SMA meeting. Philadelphia, PA. June 2005.

Bowerman, M., **Shafey, D.,** Beauvais, A., De Repentigny, R., and Kothary, R. (2005). Smn knockdown in PC12 cells: assessing a role for Smn in neuronal differentiation. Families of SMA meeting. Philadelphia, PA. June 2005.

Shafey, D., Côté, P, De Repentigny, Y., and Kothary, R. (2005). Establishment of a hypomorphic series of Smn knockdown C2C12 myoblasts and mice. Toronto, ON. March 2005.

Kothary, R., Côté, P, De Repentigny, Y., and **Shafey, D**. (2004). siRNA mediated knockdown of Smn in cell culture and in mice. American Society of Human Genetics. Toronto, ON. October 2004.

Shafey, D., Côté, P, De Repentigny, Y., and Kothary, R. (2004). siRNA mediated knockdown of Smn in cell culture and in mice. Families of SMA meeting. Chicago, IL. June 2004.